

Biennial Report

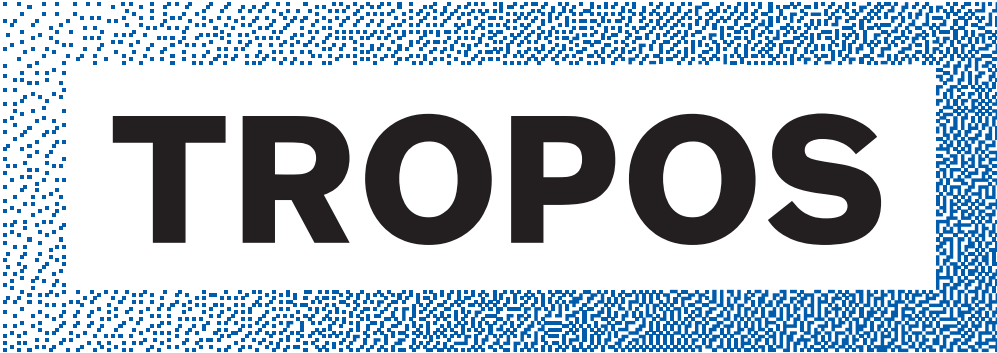
Zweijahresbericht
2014/2015

Member of the



TROPOS

Leibniz Institute for
Tropospheric Research



TROPOS

Leibniz Institute for
Tropospheric Research

Member of the



Imprint

Published by

TROPOS

Leibniz Institute for Tropospheric Research
Leibniz-Institut für Troposphärenforschung e.V. Leipzig
Member of the Leibniz Association (WGL)

Permoserstraße 15
04318 Leipzig
Germany

Phone: ++49 (341) 2717-7060

Fax: ++49 (341) 2717-99-7060

Email: info@tropos.de

Internet: <http://www.tropos.de>

Copy editors

Katja Schmieder, Konstanze Kunze, Kerstin Müller,
Heike Scherf, Beate Richter, Tilo Arnhold (Photographer)

Editorial board

Andres Macke, Hartmut Herrmann, Ina Tegen,
Frank Stratmann, Alfred Wiedensohler

Photo and illustration credits © TROPOS / as described
in the captions /

p. 1: top, middle - Tilo Arnhold / TROPOS
bottom - Maik Merkel / TROPOS

p. 27: top - Wolfram Birmili / TROPOS
middle - Maik Merkel / TROPOS
bottom - Tilo Arnhold / TROPOS

p. 119: all - Tilo Arnhold / TROPOS

Table of contents

- 3 **Introduction / Einleitung**
- 13 **Overview of the individual contributions /
Übersicht der Einzelbeiträge**
- 18 **Overview of appendices /
Überblick der Anhänge**

Articles

- 29 K. Müller et al.: Results from the SOPRAN study regarding dust and sea exchange processes
- 41 P. Seifert et al.: ACCEPT campaign: Tracing mixed-phase cloud microphysical properties with Doppler-polarimetric cloud radar and lidar
- 52 B. Wehner et al.: Results from the Melpitz Column Experiment
- 61 D. van Pinxteren et al.: Regional air quality in Leipzig: Results from a source apportionment study of size-resolved aerosol particles
- 64 S. Kecorius et al.: Spatial and temporal distribution of black carbon in the metropolitan area of Manila, Philippines
- 68 B. Stieger et al.: Chemical characterization and sources of inorganic gaseous and PM₁₀ pollutants at the Melpitz site in Central Europe
- 72 S. Henning et al.: What influences CCN properties in central Europe?
- 75 C. Engler et al.: Regional aerosol modelling in the framework of HOPE
- 78 F. Senf et al.: Satellite-based characterization of the growth phase of deep convective cells over Central Europe
- 81 J. Bühl et al.: Combined Vertical-Velocity Observations with Doppler Lidar, Cloud Radar and Wind Profiler
- 84 B. Madhavan et al.: Spatio-temporal variability of surface solar irradiance with pyranometer network
- 87 A. Mutzel et al.: Highly oxidized multifunctional organic compounds observed in tropospheric particles – a field and laboratory study
- 91 S. Richters et al.: Highly oxidized multifunctional organic compounds (HOMs) from the ozonolysis of sesquiterpenes
- 94 D. Niedermeier et al.: Can we define an asymptotic value for the ice active surface site density for heterogeneous ice nucleation?
- 97 E. H. Hoffmann et al.: Modelling of the marine multiphase DMS chemistry with the new CAPRAM DMS-Module 1.0
- 100 R. Schrödner et al.: 3-D multiphase chemistry modelling in the context of HCCT-2010
- 104 M. Jähn et al.: Large Eddy Simulations of Island Effects in the Caribbean Trade Wind Region
- 107 U. Vogelsberg et al.: Parcel model studies on iron mobilization in mineral aerosol
- 110 R. Wagner et al.: Towards understanding the interannual variability in Saharan dust emissions
- 113 J. Hofer et al.: First year activities within the Central Asian Dust Experiment (CADEX): lidar observations, chemical aerosol analysis, and dust transport modeling
- 116 S. Mertes et al.: Characterization of ice particle and cloud drop residuals sampled during the HALO cloud missions ML-CIRRUS and ACRIDICON-CHUVA

Table of contents

Appendices

- 121 Publications
 - 121 Publication statistics
 - 121 Publications
- 136 University courses
- 138 Academical degrees
 - 138 Completed academic qualifications 2014/2015
 - 142 Summary of completed academic qualifications
- 143 Awards
- 143 Guest scientists
- 146 Visits of TROPOS scientists
- 147 Meetings
- 148 International and national field campaigns
- 151 Memberships
- 154 Editorships
- 154 Reviews
- 155 Cooperations
 - 155 International cooperations
 - 159 National cooperations
- 163 Boards
 - 163 Boards of trustees
 - 163 Scientific advisory board
 - 164 Members of the TROPOS association
- 165 Organigram

Introduction / Einleitung

Overview / Übersicht



Introduction

Since 1992 the Leibniz Institute for Tropospheric Research (TROPOS) is located in the "Research Park Leipzig/Permoserstraße" close to the Helmholtz Centre for Environmental Research, the Leibniz-Institute for Surface Modification and other research establishments and related businesses. Its name identifies TROPOS as a member of the Leibniz Association.



Fig. / Abb. 1: TROPOS main building. / TROPOS-Hauptgebäude.
(Photo: Patric Seifert / TROPOS)

ciation. The institute was founded for the investigation of physical and chemical processes in the polluted troposphere.

Over the years a well-defined and globally unique research profile of TROPOS emerged. Today, the focus is on the physical and chemical interactions between atmospheric small airborne particles (aerosol particles) and cloud particles. Despite their minute absolute amount, aerosol and cloud particles are essential parts of the atmosphere because they control the budgets of energy, water and trace

Einleitung

Im Wissenschaftspark Leipzig/Permoserstraße befindet sich seit 1992 das Leibniz-Institut für Troposphärenforschung e. V. (TROPOS) in Nachbarschaft zum Helmholtz-Zentrum für Umweltforschung, zum Leibniz-Institut für Oberflächenmodifizierung sowie weiteren Einrichtungen. Sein Name weist es als Mitglied der Wissenschaftsgemeinschaft Gottfried Wilhelm Leibniz aus. Gegründet wurde es zur Erforschung physikalischer und chemischer Prozesse in der belasteten Troposphäre.

Das TROPOS hat über die Jahre ein klares und weltweit einzigartiges Forschungsprofil herausgebildet, in dessen Mittelpunkt heute die physikalischen und chemischen Wechselwirkungen zwischen atmosphärischen Schwebeteilchen (Aerosolpartikeln) und Wolkenpartikeln stehen. Trotz geringster absoluter Mengen sind diese Partikel wesentliche Bestandteile der Atmosphäre, weil sie den Energie-, Wasser- und Spurenstoffhaushalt des Erdsystems beeinflussen. Menschliche Aktivitäten können die Eigenschaften



Fig. / Abb. 3: TROPOS cloud laboratory. / TROPOS-Wolkenlabor.
(Photo: Tilo Arnhold / TROPOS)



Fig. / Abb. 2: Model of the new TROPOS chemistry laboratory. / Modell des neuen TROPOS-Chemielaborgebäudes. (Photo: Schulz & Schulz Architekten GmbH)

dieser hochdispergierten Systeme verändern und damit sowohl direkt als auch indirekt auf den Menschen zurückwirken. Beispielhaft seien hier die gesundheitliche Wirkung eingeatmeter Partikel und Nebeltröpfchen und die regionalen und globalen Klimaänderungen genannt.

Trotz dieser wichtigen Beziehungen zwischen Mensch auf der einen und Aerosol/Wolken auf der anderen Seite müssen die physiko-chemischen Prozesse von Aerosol- und Wolkenbildung und die Wechselwirkungen mit Gesundheit und Klima zu einem großen Teil noch erforscht werden. Gründe dafür sind Schwierigkeiten bei der Analyse der beteiligten kleinsten Stoffmengen und das komplexe Verhalten atmosphärischer Mehrphasensysteme, deren Einzelprozesse in der Atmosphäre nicht klar getrennt beobachtet werden können. Im gegenwärtigen Sachstand

Introduction / Einleitung



Fig. / Abb. 4: Lidar measurements during the HD(CP)² Observational Prototype Experiment (HOPE) 2013 in Melpitz. / Lidar-Messung während der HD(CP)² Observational Prototype Experiment (HOPE) 2013 in Melpitz. (Photo: Tilo Arnhold / TROPOS)

substances of the Earth System. Human activities can change these highly disperse systems and thus directly as well as indirectly feedback on human beings. This occurs for example via health effects caused by inhaled particles and fog droplets and through regional and global climate change.

Despite these strong connections between human beings, aerosols, and clouds, the important physico-chemical processes of aerosol and cloud formation and the relationships with climate and health still need to be investigated to a large extent. This is mainly due to difficulties with analyzing the very small samples and because of the complex behaviour of tropospheric multiphase systems, in which individual processes seldom can clearly be distinguished. In climate research this limitation is reflected in much larger uncertainties in predicted anthropogenic aerosol and cloud effects in comparison to the greenhouse effects of gases.

To gain rapid advances in our process understanding of the tropospheric multiphase system and to improve the application of this process understanding in the prediction of the consequences of human impacts the following tools are applied at TROPOS: Parallel to field studies in polluted regions analytical methods for aerosol and cloud investigations are developed. These tools are not only applied in field experiments but also in extensive laboratory investigations, which form a second major activity. A third approach consists of the formulation and application of numerical models that reach from process models to regional simulations of the formation, transformation and effects of tropospheric multiphase systems. This approach provides the framework for an overall process understanding of tropospheric multiphase systems.

zum globalen Klimawandel spiegelt sich diese Komplexität in den sehr viel größeren Unsicherheiten in allen zu Aerosol- und Wolkenwirkung veröffentlichten Zahlen im Vergleich zu den Treibhauseffekten der Gase wieder. Um raschen Zuwachs im Prozessverständnis troposphärischer Mehrphasenprozesse zu erreichen und dessen Anwendung auf die Vorhersage der Folgen menschlicher Eingriffe zu verbessern, werden am TROPOS folgende Arbeitsbereiche eingesetzt:

Neben Feldstudien in belasteten Regionen werden physikalische und chemisch-analytische Verfahren zur Untersuchung von Aerosolpartikeln und Wolken entwickelt. Diese Verfahren werden auch in ausgedehnten Laboruntersuchungen eingesetzt, der zweiten Hauptarbeitsrichtung des Instituts. Ein dritter Arbeitsbereich entwickelt und wendet numerische Modelle von der Prozessbeschreibung bis zur Beschreibung der regionalen Bildung, Umwandlung und Wirkung troposphärischer Mehrphasensysteme an und bildet den Rahmen für ein umfassendes Prozessverständnis atmosphärischer Multiphasensysteme.

Feldexperimente und Prozessstudien

Die Feldexperimente des Instituts dienen der Aufklärung des atmosphärischen Kreislaufs der Aerosol- und Wolkenpartikel und der damit verbundenen Prozesse. Die Komplexität dieses Systems wird dabei unter anderem dadurch bestimmt, dass in der Atmosphäre Partikel und Tropfen auftreten, deren Durchmesser sich vom Nano- bis zum Mikrometerbereich um mehr als sechs Größenordnungen unterscheidet. Außerdem kann man in den Aerosolpartikeln viele der kondensationsfähigen Stoffe des



Fig. / Abb. 5: Balloon ascent during the Melpitz Column Experiment 2015. / Ballonauftstieg während der Intensivmesskampagne Melpitz-Säule 2015. (Photo: Janine Lückerath / University of Bayreuth)

Field experiments and process studies

Field experiments elucidate the atmospheric life cycle and related processes of aerosol and cloud particles. The complexity of this system is reflected in the fact that atmospheric aerosols and cloud particle exist with diameter from nano- to micrometer spanning more than six orders of magnitude. Furthermore, many of the condensable substances of the Earth system can be found in the aerosol and a large number of them in turn effect climate and biosphere. As a result of this diversity and mass-related analytical difficulties, essential global aerosol and cloud properties are still known to a small extend only.

This uncertainty already begins with particle sources, which are research efforts of TROPOS as well. The combustion of fossil and renewable fuels is a significant aerosol source. Measurements of the institute at many urban and rural background stations show that emissions of particles and their precursor gases are followed by strong physical and chemical transformations that need to be investigated with high-resolution sensors in order to identify the underlying processes. Despite extensive legal measures air pollution still exists in Germany and Europe with its consequences for morbidity and mortality of the respective population.

Also the conurbation Leipzig and the background station Melpitz is in the focus of investigations on air pollution with emphasis on aerosol particles, often conducted in collaboration with the Saxon State Agency for Environment and Geology (LfULG). The Melpitz research station is more and more applied to specific measurement campaigns with national and international partners ("Melpitz-Column").



Fig. / Abb. 6: Pyranometer measurements during the Melpitz Column Experiment 2015. / Pyranometer-Messungen während der Intensivmesskampagne Melpitz-Säule 2015. (Photo: Janine Lückerath / University of Bayreuth).



Fig. / Abb. 7: Measuring site Weidenbrunnen at Waldstein/Fichtelgebirge at a height of 30 meters during a campaign with University of Bayreuth in July 2014. / Messstation Weidenbrunnen in Waldstein/Fichtelgebirge in 30 Metern Höhe während einer Messkampagne mit der Universität Bayreuth im Juli 2014. (Photo: Tilo Arnhold / TROPOS)

Erdsystems finden, von denen wiederum eine große Zahl Einfluss auf das Klima und die Biosphäre haben kann. Als Folge dieser Vielfalt und der mengenbedingten analytischen Schwierigkeiten sind wesentliche globale Aerosol- und Wolkeneigenschaften noch wenig bekannt.

Diese Unsicherheit beginnt schon bei den Partikelquellen, die ebenfalls Forschungsgegenstand am TROPOS sind. Die Verbrennung fossiler und nachwachsender Brennstoffe zur Energieerzeugung und im Verkehr ist eine maßgebliche Aerosolquelle. Messungen des Instituts an vielen urbanen Messstellen und kontinentalen Hintergrundstationen zeigen, dass den Emissionen von Partikeln und deren Vorläufern enorme physikalische und chemische Umwandlungen folgen, die mit hoher zeitlicher Auflösung analysiert werden müssen, um die beteiligten Prozesse aufzuklären.

Auch der Ballungsraum Leipzig mit der Hintergrundstation Melpitz steht hier immer wieder im Interesse für Untersuchungen zur Luftverschmutzung mit dem Schwerpunkt auf Partikeln, die oft in Kooperationen mit dem Sächsischen Landesamt für Umwelt und Geologie (LfULG) durchgeführt werden. Trotz sehr weitgehender gesetzlicher Regelungen existiert in Deutschland und Europa immer noch Luftverschmutzung mit ihren Folgen für Morbidität und Mortalität in der betroffenen Bevölkerung. Die Forschungsstation Melpitz wird zunehmend für fokussierte Messkampagnen mit nationalen und internationalen Partnern genutzt („Melpitz-Säule“).

Die am höchsten belasteten Regionen über Nordamerika, Europa, Asien mit dem Schwerpunkt China, Afrika, über dem indischen Subkontinent und Südamerika sind bei weitem noch nicht hinreichend bezüglich ihrer Aerosolbelastungen und den daraus

Introduction / Einleitung



Fig. / Abb. 8: The downtown of Manila on a heavily polluted day. / Die Downtown von Manila an einem stark verschmutzten Tag. (Photo: Wolfram Birmili / TROPOS)

Even the strongest polluted regions over North America, Europe, Asia with priority on China, Africa, the Indian subcontinent, and South America are far from being sufficiently characterized in terms of aerosol burdens and ensuing climate effects. The institute thus focuses its participation in international field campaigns and dedicated long-term studies in Asia, South America and the marine troposphere over the northern and southern Atlantic.

Investigations on mineral dust and marine aerosol particles and its impact on the radiation budget, cloud formation processes and the atmospheric ice nucleation remain a core component of the institute's research. To this end, investigations in the Central Asian and the Mediterranean region will be intensified.

In the framework of the European infrastructure IAGOS the aerosol distribution in the upper troposphere is measured and analysed using a commercial

resultierenden Klimawirkungen untersucht. Auf diese Regionen konzentrieren sich daher in internationale Zusammenarbeit die Feldexperimente des TROPOS, u. a. in Form von Messkampagnen und Langzeitmessungen in Asien, Südamerika und der maritimen Troposphäre über dem südlichen und nördlichen Atlantik. Untersuchungen zum Mineralstaub und marinens Aerosolpartikeln und deren Wirkungen auf den Strahlungshaushalt, die Wolkenbildung und die atmosphärische Eisbildung bleiben ein Kernbestandteil der Arbeiten am TROPOS. Hierzu werden vermehrt Untersuchungen im zentralasiatischen und mediterranem Raum vorgenommen. Durch Nutzung eines kommerziellen Verkehrsflugzeuges der Lufthansa werden im Rahmen der Europäischen Forschungsinfrastruktur IAGOS auch Aerosolverteilungen in der oberen Troposphäre auf regelmäßig beflogenen interkontinentalen Routen gemessen und analysiert.

Am TROPOS werden verschiedene bodengebundene Fernerkundungsverfahren gekoppelt, um so zu einem synergetischen Bild der vertikalen Verteilung von Aerosolen und Hydrometeoren sowie deren Prozessierung zu gelangen. Das hierzu entwickelte Leipzig Aerosol and Cloud Remote Observation System (LACROS) wird darüberhinaus zu einem Prototyp-Instrument eines europäischen Messnetzes erweitert.

Auf kleineren Skalen werden Untersuchungen zur Partikelbildung und Wechselwirkung zwischen Aerosolpartikeln und Wolken und der Einfluss turbulenter Mischungsprozesse auf die Wolkenentwicklung mit Hilfe der hubschraubergetragenen Messplattform ACTOS durchgeführt. Zusätzlich werden Bergstationen zu Prozessstudien genutzt, die sich dem Verständnis von Einzelprozessen, wie der Partikelneubildung, der physiko-chemischen Veränderung der Aerosolpartikel beim Wolkendurchgang und dem



Fig. / Abb. 9: Measurement station "Leipzig-Mitte" of the Saxon State Office for Environment, Agriculture and Geology (LfULG) in Leipzig's city centre. / Messstation „Leipzig-Mitte“ des Sächsischen Landesamt für Umwelt, Landwirtschaft und Geologie (LfULG). (Photo: Wolfram Birmili / TROPOS)



Fig. / Abb. 10: German research vessels POLARSTERN and METEOR met in the Atlantic Ocean. / Deutsche Forschungsschiffe POLARSTERN und METEOR begegnen sich im tropischen Atlantik. (Photo: Dominik Nachtsheim / PoE)

Lufthansa aircraft operated on frequent intercontinental routes.

At TROPOS different ground-based remote sensing methods are coupled in order to achieve a synergistic picture of the vertical distribution of clouds and aerosols as well as their processing. The Leipzig Aerosol and Cloud Remote Observation System (LACROS), that has been developed to this end, will be further extended towards a European network prototype instrument.

On smaller scales, investigations concerning new particle formation, the interactions between aerosol particles and clouds, and the influences of turbulent mixing processes on cloud development are carried out with help of the helicopter-borne measurement platform ACTOS. In addition, process studies are conducted at suitable locations such as mountain observatories to investigate particle nucleation, particle processing through clouds, and the influence of aerosols particles on the development and freezing of clouds.

TROPOS leads several regional, national and European measurements networks to monitor atmospheric aerosols and cloudiness. In the framework of the Global Atmospheric Watch (GAW) programme of the WMO TROPOS hosts the World Calibration Centre for physical in-situ aerosol measurement (WCCAP) to assure high quality standards at national and international observatories.

Field campaigns are supported and complemented by analyses based on meteorological satellites. In particular satellite products provide the spatio-temporal development of clouds and their interaction with radiation, as well as transport paths of aerosols. Especially the geostationary European weather satellite Meteosat is applied to this end.

Einfluss von Aerosolpartikeln auf die Entwicklung und das Gefrieren von Wolken widmen.

TROPOS ist maßgeblich an regionalen, nationalen und Europäischen Messnetzen zur Erfassung des atmosphärischen Aerosols und der Bewölkung beteiligt. Das Institut betreibt im Rahmen des Global Atmospheric Watch (GAW) Programmes der WMO das Weltkalibrierzentrum für physikalische Aerosolmessungen (WCCAP) mit dem Ziel der Qualitätssicherung von in-situ Messungen an nationalen und internationalen Messstationen.

Feldexperimente werden durch Analysen, basierend auf meteorologischen Satelliten, unterstützt und erweitert. Insbesondere werden mit Satellitenprodukten die raumzeitliche Entwicklung von Wolken und deren Strahlungsantrieb untersucht, ebenso wie die Transportwege von Aerosolen. Hierzu dient insbesondere der geostationäre europäische Wettersatellit METEOSAT.



Fig. / Abb. 11: The TROPOS aerosol chamber (LEAK) during the Long Night of the Sciences 2014. / Die TROPOS-Aerosolkammer (LEAK) zur Langen Nacht der Wissenschaften 2014. (Photo: Tilo Arnhold / TROPOS)

Introduction / Einleitung



Fig. / Abb. 12: Two Counterflow Virtual Impactor systems for the collection of large particles in lab applications (left) and of hydrometeors in atmospheric clouds aboard the German research aircraft HALO (right). / Zwei Gegenstrom-Impaktor Systeme zur Sammlung großer Partikel in Laboranwendungen (links) und von Hydrometeoren in atmosphärischen Wolken auf dem deutschen Forschungsflugzeug HALO (rechts). (Photo: Tilo Arnhold / TROPOS)

Laboratory experiments

In atmospheric research, physico-chemical models for the description of the most relevant process are continuously developed. These models are based on process parameters that need to be determined in laboratory experiments under controlled environmental conditions.

In the “Experimental Aerosol and Cloud Micro-physics Department” laboratory experiments cover the development of a large number of methods to characterize atmospheric particles in ground-based or airborne field measurement campaigns. This work includes for example the improvement of aerosol size spectrometers as well as collection systems for the physical and chemical characterization of cloud droplets and the interstitial aerosol that means those aerosol particles that are suspended in the gas phase inside the cloud along with the cloud particles.

Optical measurement techniques are developed and applied to determine the extinction coefficient of aerosol particles. Multi-wavelength lidar systems and a wind lidar are further developed in the laboratory and applied in the field to determine aerosol properties, aerosol fluxes and meteorological parameters such as temperature, relative humidity and wind. The amount of black carbon and mineral aerosol components in the aerosol samples are quantified with spectral absorption measurements.

The “Experimental Aerosol and Cloud Micro-physics Department” and the “Atmospheric Chemistry Department” are jointly carrying out process-oriented laboratory studies. Research at the Leipzig Aerosol Cloud Simulator LACIS addresses the activation

Laborexperimente

In der Atmosphärenforschung werden kontinuierlich physikalisch-chemische Modelle zur Beschreibung der wesentlichen Prozesse entwickelt. Grundlage derartiger Modelle sind stets Prozessparameter, die in Laborexperimenten unter bekannten Umgebungsbedingungen ermittelt werden.

In der Abteilung „Experimentelle Aerosol- und Wolkenmikrophysik“ werden in Laborexperimenten zahlreiche Messmethoden entwickelt, die zur Partikelcharakterisierung in boden- und luftgestützten Feldmesskampagnen eingesetzt werden. Diese Arbeiten beinhalten z. B. die Weiterentwicklung von Aerosolgrößenspektrometern sowie Sammelsysteme zur physikalischen und chemischen Charakterisierung von Wolkentröpfchen und dem interstitiellen Aerosol, also denjenigen Aerosolpartikeln, die innerhalb von Wolken neben den Wolkenpartikeln selbst in der Gasphase suspendiert sind.

Optische Messmethoden werden zur Bestimmung des Extinktionskoeffizienten von Partikeln entwickelt und angewendet. Mehrwellenlängenlidare und ein Windlidar werden zur Bestimmung von Aerosoleigenschaften, Aerosolflüssen und meteorologischen Parametern wie Temperatur, Feuchte und Wind im Labor weiterentwickelt und im Feld eingesetzt. Die Anteile „schwarzen Kohlenstoffs“ und mineralischer Aerosolkomponenten in Aerosolproben werden durch spektrale Absorptionsmessungen bestimmt.

Prozessorientierte Laboruntersuchungen werden gemeinsam von den Abteilungen „Experimentelle Aerosol- und Wolkenmikrophysik“ und „Chemie der Atmosphäre“ durchgeführt. Die Arbeiten am Strömungsreaktor LACIS betreffen die Aktivierung von

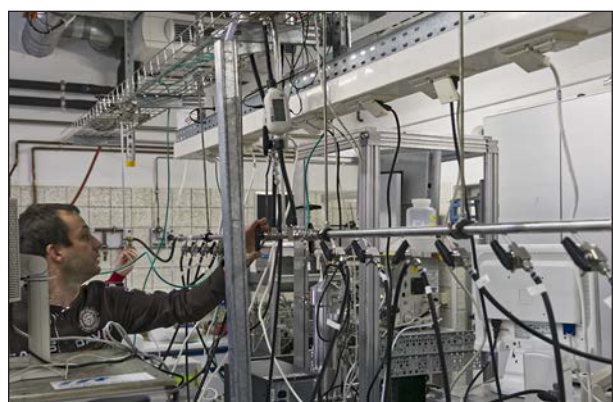


Fig. / Abb. 13: Inter comparison measurements for quality insurance with particle mobility size spectrometer in one of the TROPOS WCCAP laboratories (World Calibration Center for Aerosol Physics). / Vergleichsmessungen zur Qualitätssicherung mit Partikelgrößenspektrometern in einem der Labore des Weltkalibrierzentrums für Aerosolphysik (WCCAP) des TROPOS. (Photo: Tilo Arnhold / TROPOS)

of cloud droplets and primarily the heterogeneous formation of ice. These investigations aim at a better understanding of the underlying fundamental processes, the identification of critical and controlling parameters, and the development of parameterizations to characterize droplet and ice formation processes for applications in dynamical models.

In the "Atmospheric Chemistry Department" gas phase reactions of various radicals are being investigated in flow reactors and in the Leipzig Aerosol Chamber (LEAK). These reactions are important for ozone and particle formation caused by anthropogenic or biogenic volatile hydrocarbons. The formed particles are investigated in collaboration with the "Experimental Aerosol and Cloud Microphysics Department" determining hygroscopic growth and cloud droplet activation behaviour. In a single drop experiment, investigations on phase transfer parameters of trace gases and radicals are being conducted. The determination of phase transfer parameters and reactive uptake coefficients hereby is being extended to previously not considered chemical species and complex surfaces.

In the field of liquid phase mechanisms reactions of primarily radical oxidants are investigated with time-resolved optical detection techniques. These reactions proceed within haze particles, fog and cloud droplets as well as in deliquescent aerosol particles.

For the understanding of the oxidation of organic trace gases in the tropospheric multiphase system, a large number of reactions with various radicals are being studied as well as reactions of halogenated oxidants. The latter species are of interest for the emission of reactive halogen compounds from sea salt particles, the so-called halogen activation.



Fig. / Abb. 14: The samples of the surface film are collected from a zodiac for the ensuing laboratory investigations (Polarstern expedition PS83, 2014, from Cape Town to Bremerhaven). / Probenahme des Oberflächenfilms vom Schlauchboot aus für anschließende Laboruntersuchungen (Polarstern-Expedition PS83, 2014 von Kapstadt nach Bremerhaven). (Photo: Tilo Arnhold / TROPOS)



Fig. / Abb. 15: Laboratory technician at the laminar flow reactor of TROPOS. / Laborantin am Laminar-Strömungsrohr des TROPOS. (Photo: Tilo Arnhold / TROPOS)

Wolkentröpfchen und schwerpunktmäßig die heterogene Eisbildung. Ziele dieser Untersuchungen sind die Erlangung eines besseren Prozessverständnisses auf fundamentaler Ebene, die Identifikation kritischer und kontrollierender Parameter und die Entwicklung geeigneter Parametrisierungen zur Beschreibung von Tröpfchen- und Eisbildung in dynamischen Modellen.

In der Abteilung Chemie der Atmosphäre werden Gasphasenreaktionen verschiedener Radikale in Strömungsreaktoren und der Leipziger Aerosolkammer (LEAK) untersucht. Diese Reaktionen sind von Interesse für die Ozon- und Partikelbildung, verursacht durch anthropogene oder biogene flüchtige Kohlenwasserstoffe. Die erzeugten Partikel werden in Zusammenarbeit mit der Abteilung „Experimentelle Aerosol- und Wolkenmikrophysik“ hinsichtlich ihres Feuchtwachstums- und Aktivierungsverhaltens untersucht.

In einem Einzeltropfenexperiment werden Untersuchungen bzgl. der Phasentransferparameter für Spurengase und Radikale durchgeführt. Die Bestimmung von Phasentransferparametern und reaktiven Aufnahmekoeffizienten wird dabei auf bisher nicht betrachtete chemische Spezies und komplexe Oberflächen ausgeweitet.

Im Bereich von Flüssigphasenmechanismen werden Reaktionen von vorwiegend radikalischen Oxidantien mit zeitaufgelösten optischen Nachweistechniken untersucht. Diese Reaktionen laufen in den Tröpfchen von Wolken, Regen und Nebel sowie in wässrigen Aerosolpartikeln ab.

Hier werden zum Verständnis der Oxidation organischer Spurengase im troposphärischen Mehrphasensystem eine Vielzahl von Reaktionen verschiedener Radikale sowie Reaktionen von halogenhaltigen Oxidantien untersucht. Letztere Spezies sind von Interesse bei der Freisetzung von

Introduction / Einleitung

The liquid phase laboratory for the investigation of tropospheric liquid phase processes is an important centre for these research activities. The process studies result in the improvement of chemical mechanisms, which can be applied to the self-developed model mechanism CAPRAM.

In the field of analytic measurement technology laboratory experiments are dedicated to improve and test methods for the chemical characterization of organic aerosol components. These methods are mostly based on mass spectrometric processes, which are deployed in various coupling techniques.

In the field of sampling techniques the "Atmospheric Chemistry Department" closely collaborates with the "Experimental Aerosol and Cloud Micro-physics Department" on the development of the specific segregation of aerosol particles of a distinct size and their chemical analysis and also on the development of inlet systems and reactors.

Modeling

For the description of complex atmospheric processes, model systems of varying dimensions, complexity, and scales are developed, tested and

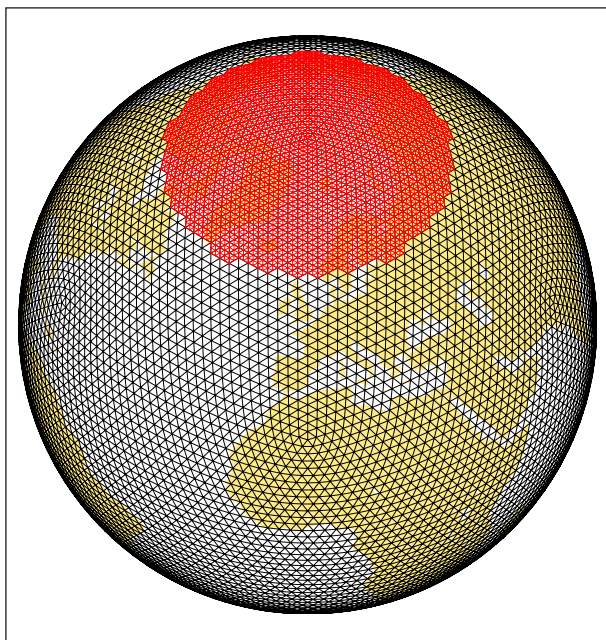


Fig. / Abb. 16: Model grid of the new weather prediction and climate model ICON (ICOsaheiral Non-hydrostatic) with Arctic nest as used for the global and Arctic focused simulations of aerosol transport and aerosol-cloud-radiation interactions within (AC)3. / Modellgitter des neuen Wettervohersage- und Klimamodells ICON (ICOsaheiral Non-hydrostatic) mit einem Nest über der Arktis, wie es für die globalen und Arktis fokussierten Simulationen des Aerosoltransports und der Aerosol-Wolken-Strahlungs-Wechselwirkungen in (AC)3 verwendet werden wird. (Graphic: created with ICON tools developed by DWD/MPI-M)

Halogenverbindungen aus maritimen Seesalzpartikeln, der so genannten Halogenaktivierung.

Das Flüssigphasen-Laserlabor zur Untersuchung der troposphärischen Flüssigphasenprozesse ist ein wichtiges Zentrum dieses Forschungsbereiches. Aus den Prozessuntersuchungen resultieren Verbesserungen chemischer Mechanismen, die in der Modellierung mit dem eigenen Mechanismus CAPRAM angewendet werden.

In der analytischen Messtechnik werden in Laborexperimenten Verfahren zur besseren chemischen Charakterisierung der organischen Bestandteile von Aerosolpartikeln entwickelt und getestet. Diese Techniken beruhen zumeist auf massenspektrometrischen Verfahren, die in verschiedenen Kopplungstechniken eingesetzt werden. Im Bereich der Probenahmetechniken gibt es auch hier eine enge Kooperation mit der Abteilung „Experimentelle Aerosol- und Wolkenmikrophysik“ zur Entwicklung einer gezielten Abscheidung von Partikeln bestimmter Größe und deren chemischer Analyse aber auch zur Entwicklung von Einlasssystemen und Reaktoren.

Modellierung

Zur Beschreibung der komplexen atmosphärischen Vorgänge werden Modellsysteme verschiedener Dimension, Komplexität und Skalenbereiche entwickelt, überprüft und angewendet, auch in Kombination mit Daten aus Feldmessungen und aus satellitengestützten Fernerkundungen.

Ein Forschungsschwerpunkt ist die Beschreibung von Kreisläufen, Wechselwirkungen und Phasenübergängen zwischen Aerosolpartikeln, Gasen und Wolken, um so unser Verständnis klimarelevanter Prozesse in troposphärischen Mehrphasensystemen zu verbessern.

Chemie-Transportmodellierung wird durch das am TROPOS entwickelte 3D-Modellsystem COSMO-MUSCAT realisiert. Seine Eignung zur Simulation des Ausbreitungsverhaltens von Partikeln und Gasen auf regionaler Skala wurde in mehreren internationalem Modellvergleichen und bei der Bearbeitung von Fragen zur Luftqualität gezeigt. In mehreren Projekten wird die Dynamik primärer und sekundärer Aerosolpartikel simuliert und deren Wechselwirkung mit Strahlung und Wolken untersucht. Für weitere Anwendungsmöglichkeiten wird zusätzlich eine „urbanierte“ Version von COSMO-MUSCAT entwickelt, die eine horizontale Gitterauflösung bis zu wenigen 100 m nutzt. Damit werden auch Untersuchungen zum Einfluss der regionalen Klimavariabilität auf Spurenstoffhaushalte durchgeführt.

Mit ASAM (All Scale Atmospheric Model) steht ein noch in der Weiterentwicklung befindliches

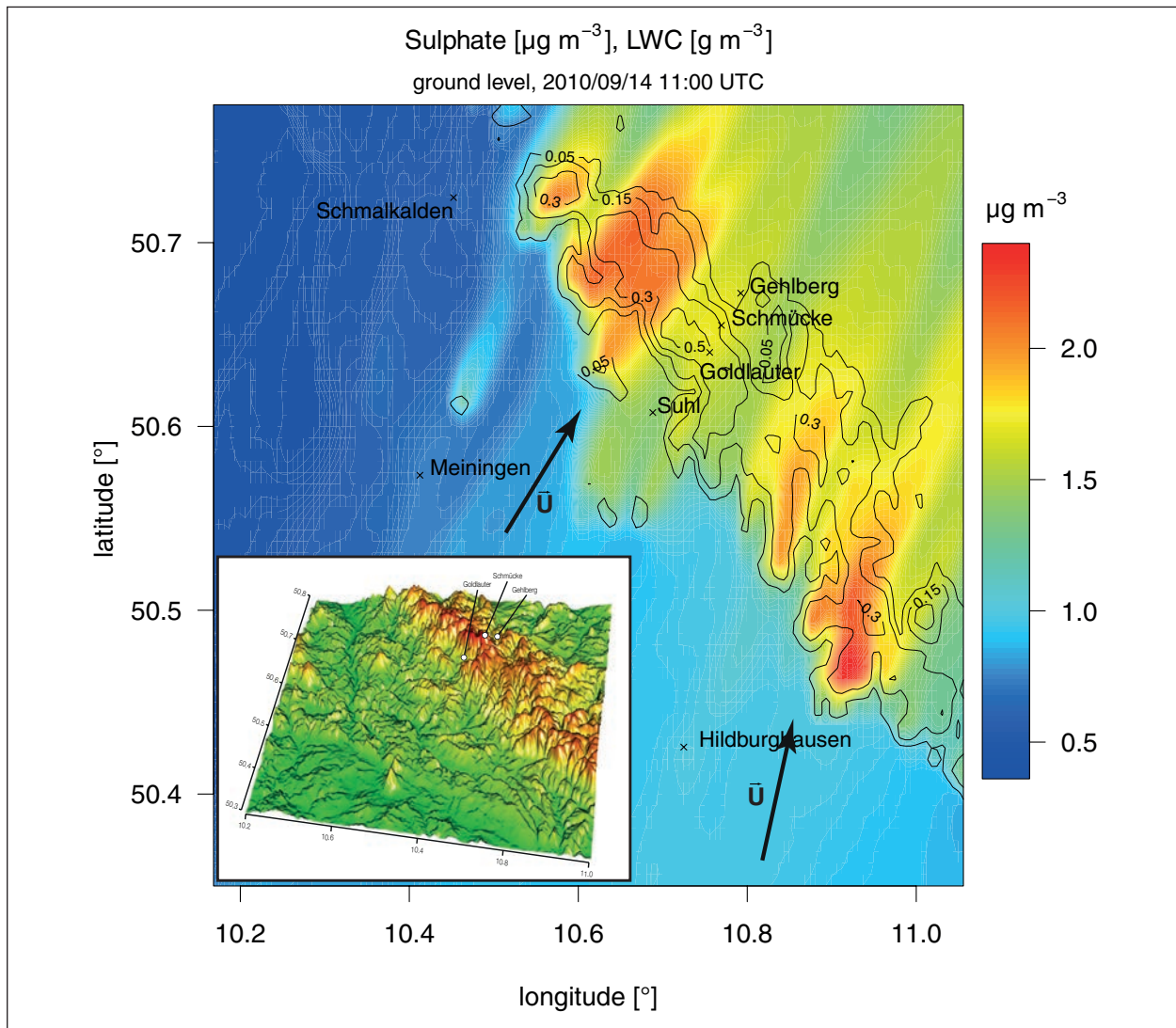


Fig. / Abb. 17: Model domain of the HCCT simulations and calculated sulphate concentrations for 14/09/2010 (11:00 o'clock). / Modellgebiet für die HCCT-Simulationen und berechnete Sulfat-Konzentrationen für den 14.09.2010 (11:00 Uhr). (Graphic: simulated with the chemistry-transport model COSMO-MUSCAT).

applied, also in combination with data from field and satellite measurements.

One focus of research is the description of cycles, interactions and phase transfer between aerosol particles, gases and clouds. The aim is an improvement in understanding of climate-relevant processes in the tropospheric multiphase system.

Chemistry-transport modeling is realized with the three-dimensional modeling system COSMO-MUSCAT that has been developed at TROPOS. Its appropriateness for the simulation of particle and gas distribution on regional scale was demonstrated in international model intercomparison studies and in applications on air quality issues.

Several projects investigate the dynamics of primary and secondary particles and their interaction with radiation and clouds. For further studies an

Modell zur Verfügung, dessen dynamischer Kern für Anwendungen vom mikroskaligen bis zum globalen Maßstab eingesetzt werden kann. In einem kartenhaften Gitter wird die Darstellung von Orographie und Hindernissen mit angeschnittenen Zellen realisiert. Das Modell wird gegenwärtig für die Untersuchung von Grenzschichtprozessen auf der Large-Eddy-Skala genutzt.

Daneben wurden und werden ein- und zweidimensionale Prozessmodelle entwickelt bzw. weiterentwickelt. SPECS (SPECtral bin cloud microphysicS) dient zur Beschreibung von Wolkenprozessen. Es erlaubt eine explizite und sehr genaue Berechnung der Prozesse Kondensation, Kollision oder Gefrieren. SPACCIM (SPectral Aerosol Cloud Chemistry Interaction Model) ist ein Paketmodell zur gekoppelten großenaufgelösten Beschreibung von Mikrophysik

Introduction / Einleitung

additional “urbanized” version of COSMO-MUSCAT is being developed using a horizontal grid resolution up to a few 100 m. It will be applied for studies of the influence of regional climate variability on the budgets of trace elements.

The model ASAM (All Scale Atmospheric Model) indicates future developments, applicable from the micro to the global scale. It realizes cut cells in a Cartesian grid for the description of orography and obstacles. Currently it is mainly used for simulations of boundary layer processes on the Large Eddy scale.

Besides this, one- and two-dimensional process models were also developed and will be developed further. SPECS (SPECtral bin cloud microphysicS) can be used for the investigation of cloud processes with a detailed description of condensation, collision or freezing. SPACCIM (SPectral Aerosol Cloud Chemistry Interaction Model) is a parcel model, which combines the size-resolved description of microphysics with a complex multiphase chemistry. Both modules can be applied for process modeling as one-dimensional box model version as well as coupled with the mesoscale model COSMO for the investigation of real situations. The process modeling studies are realized in connection with field studies and laboratory experiments.

The model simulation of the complex atmospheric systems is numerically highly demanding. The models need to be sufficiently accurate and numerically efficient to be used productively on existing computer systems. Ongoing developments within the Modeling Department thus aim at the improvement of the numerical methods and parallelisation strategies.

und Mehrphasenchemie. Beide Module können sowohl als Boxmodell zur Prozessmodellierung als auch gekoppelt an das mesoskalige COSMO-Modell zur Untersuchung von realen Situationen verwendet werden. Die Prozessmodellierungen werden im Zusammenhang mit Feldstudien sowie mit Laborexperimenten durchgeführt.

Die modelltechnische Behandlung des komplexen atmosphärischen Systems ist numerisch sehr aufwändig. Die zu entwickelnden Modelle müssen hinreichend genau sein und numerisch sehr effizient den jeweils zur Verfügung stehenden Rechnerarchitekturen angepasst werden. Zur Optimierung der verwendeten numerischen Verfahren und Parallelisierungsstrategien liefert die Abteilung Modellierung ebenfalls wesentliche Beiträge.

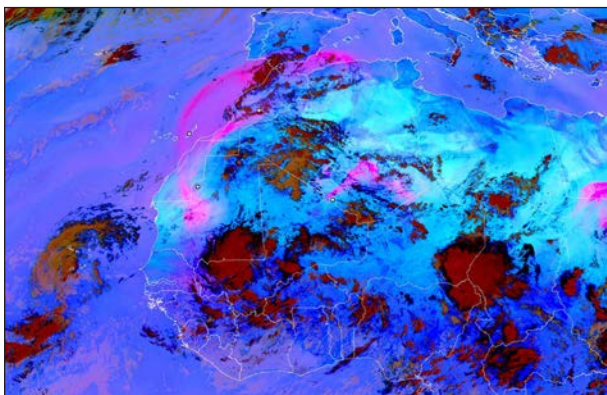


Fig. / Abb. 18: “Ring of Dust”: Pronounced Saharan dust plumes on August 6, 2015 as seen from Meteosat thermal channels. / „Staubring“: Ausgeprägte Staubwolken am 6. August 2015 aus Sicht der thermischen Kanäle des Meteosat. (Graphic: EUMETSAT / Imperial College London)

Overview of the individual contributions / Übersicht der Einzelbeiträge

Overview of the individual contributions

The biannual report presented here introduces selected work at TROPOS by means of three extended and 18 short contributions for the time period 2014 to 2015. All extended contributions have a focus on measurement campaigns, but demonstrate different strategic approaches to capture the tropospheric multiphase system. The short contributions range from physical and chemical characterization of regional air pollution to CCN measurements at the research station Melpitz to modelling of the spatial and temporal aerosol distribution to satellite- and ground-based observations of convective cloud systems and their radiative forcing to laboratory studies of fundamental mechanisms of particle and ice formation and applications in dynamical and physical/chemical process modelling at various scales to the role of long-range transport on local aerosol layers to large scale cloud observations on the new research aircraft HALO.

Extended contributions

Thanks to long-term and prospective integrative projects it is possible to obtain quantitative findings on the complex system of aerosols and clouds in focus regions. For nearly 10 years TROPOS performs measurement campaigns and continuous observations on mineral dust and maritime aerosol in the area of the Cape Verde islands. On that basis **Müller et al.** arrived at reliable statistics of the strong seasonal variability of the deposition and composition of African mineral dust. The here shown synopsis demonstrates the successful cooperation of all departments and working groups at the Institute on a central topic. For example, it is demonstrated how combined in-situ observations, modelling and remote sensing can provide the relation between regional deposition, long-range transport and dust activation. Together with partner institutes from the Leibniz Association, the Max-Planck and the Helmholtz-Society TROPOS participates on the extension and the operation of a long-term research infrastructure on ocean/atmosphere feedback mechanisms in that region.

A counterpoint to long-term structured investigations lies in dedicated short-term measurement campaigns to retrieve specific processes by means of an optimal synergy of different innovative instrumentations. As an example for that **Seifert et al.** show how ice formation, number concentration, shape and orientation of ice particles in mixed-phase clouds can be retrieved from combined measurements of Doppler- and intensity spectra with scanning radar and lidar systems. This prototype experiments set the

Übersicht der Einzelbeiträge

Der vorliegende Zweijahresbericht stellt in drei längeren und 18 Kurzbeiträgen einige ausgewählte Arbeiten des TROPOS im Zeitraum 2014 bis 2015 vor. Die Langbeiträge haben ihren Fokus auf Messkampagnen, demonstrieren hier aber unterschiedliche strategische Ansätze zur Erfassung des troposphärischen Multiphasensystems. Die Kurzbeiträge reichen von der physikalischen und chemischen Charakterisierung regionaler Luftverschmutzung über CCN-Messungen an der Forschungsstation Melpitz über Modellierung der raumzeitlichen Aerosolverteilung über satelliten- und bodengebundenen Fernerkundung von konvektiven Wolkensystemen und deren Strahlungsantrieb über Laborstudien grundlegender Mechanismen der Partikel- und Eisbildung und deren Umsetzung in dynamischen und physikalisch/chemischer Prozessmodellierungen auf unterschiedlichen Skalen über die Rolle von Ferntransporten auf lokale Aerosolschichtungen bis zu großräumigen Wolkenmessungen auf dem neuen Forschungsflugzeug HALO.

Langbeiträge

Dank langfristig und perspektivisch angelegter integrativer Projekte ist es möglich, quantitative Erkenntnisse im komplexen Aerosol/Wolkensystem in Schwerpunktregionen zu erhalten. TROPOS führt seit fast 10 Jahren Messkampagnen und Dauermessungen zum Mineralstaub und maritimen Aerosol im Bereich der Kapverdischen Inseln durch. Auf dieser Basis können **Müller et al.** verlässliche Statistiken zur starken saisonalen Variabilität der Deposition und Zusammensetzung des afrikanischen Mineralstaubes ermitteln. Die hier vorgestellte Synopsis demonstriert die erfolgreiche Kooperation aller Abteilungen und Arbeitsgruppen am Institut zu einem zentralen Thema. Zum Beispiel werden durch in-situ Beobachtung, Modellierung und Fernerkundung die Zusammenhänge zwischen regionaler Deposition, Ferntransport und Staubquellenaktivierung hergestellt. Mit Partnerinstituten aus der Leibniz-Gemeinschaft, der Max-Planck- und der Helmholtz-Gesellschaft ist TROPOS an der Erweiterung und dem Betrieb einer langfristigen Forschungsinfrastruktur zu Ozean/Atmosphäre-Wechselwirkungsmechanismen in der Region beteiligt.

Einen Kontrapunkt zu langfristigen Untersuchungen stellen fokussierte kurzzeitige Messkampagnen zur Erfassung bestimmter Prozesse durch eine optimale Synergie verschiedener innovativer Instrumentierungen dar. Als Beispiel hierfür zeigen **Seifert et al.**, wie dank kombinierter Messungen von Doppler- und Intensitätsspektren mit abtastenden

Overview of the individual contributions / Übersicht der Einzelbeiträge

basis for further field studies on retrieving the role of ice nucleating particles on ice formation in mixed phase clouds in natural or anthropogenic affected areas.

The extended contribution by **Wehner et al.** represents a combination of the two approaches above. Here, detailed physical and chemical long-term observations of the surface-near aerosol at the research station Melpitz are combined with temporary measurement campaigns and modelling studies to infer the tropospheric aerosol column ("Melpitz-Column"). The campaign took place in summer 2015 and was focused on the boundary layer. Exemplarily noteworthy is the remarkable coincidence in the (closer to cloud top) in-situ observed and the (closer to cloud bottom) remotely sensed turbulence characteristics. In the future the Melpitz-Column will continue to serve for topical measurement campaigns with national and international partners, and will be extended towards a contribution to the European research infrastructure ACTRIS (Aerosols, Clouds, and Trace gas Research InfraStructure).

Short Contributions

TROPOS applies the size resolved aerosol characterization also locally to investigate air quality in the urban region of Leipzig. In comparison with the continuous observations in Melpitz local sources can be distinguished from the rural background aerosol. This way, **van Pinxteren et al.** found on the basis of a three-year measurement campaign that situations with strong pollution are nearly half caused by local street traffic, so that corresponding reduction measures may show largest effects here. This can be achieved for instance by means of establishing low emission zones, as TROPOS could prove exemplarily for the city of Leipzig. Other regions on this world are often ruled by increasing catastrophic air pollution as **Kecorius et al.** showed exemplarily for the subtropical mega city Manila. Here, the traffic-induced load of particulate matter is nearly ten times larger than in Leipzig. For the first time, mobile sensors have been applied during the four-month Manila-campaign, in order to resolve the high spatial variability of the soot burden. Since 2010, the high temporal variability of inorganic compounds in the gas and particle -phase is continuously monitored at the research station Melpitz. **Stieger et al.** combined hourly measurements with backward trajectories to more precisely localize source regions of the long-range advected pollutants. In order to investigate the influence of natural and anthropogenic aerosol on cloud formation, number concentration and hygroscopicity of cloud condensation nuclei (CCN) have been observed and

Radar- und mit Lidarsystemen auf die Eisbildungsprozesse sowie auf Anzahl, Form und Orientierung von Eispartikeln in Mischphasenwolken geschlossen werden kann. Derartige Prototyp-Experimente legen den Grundstein für weitere Feldstudien zur Erfassung der Rolle von Eiskeimen auf die Eisbildung in Mischphasenwolken in natürlichen oder anthropogen beeinflussten Regionen.

Der Langbeitrag von **Wehner et al.** stellt eine Kombination der beiden oben genannten Ansätze dar. Hier werden detaillierte physikalische und chemische Langzeitbeobachtungen des bodennahen Aerosols an der Forschungsstation Melpitz mit temporären Messkampagnen und Modellstudien zur Erfassung der troposphärischen Aerosol-Säule kombiniert („Melpitz-Säule“). Die Kampagne fand im Sommer 2015 mit dem Fokus auf Grenzschichtaerosol statt. Exemplarisch herausgestellt ist die bemerkenswerte Übereinstimmung der (mehr am Wolkenoberrand) direkt gemessenen und der (mehr am Wolkenunterrand) fernerkundeten Turbulenzcharakteristik. Die „Melpitz-Säule“ wird auch in Zukunft zu thematischen Messkampagnen mit nationalen und internationalen Partnern genutzt und als Teil der Europäischen Forschungsinfrastruktur ACTRIS (Aerosol, Clouds, and Trace gas Research InfraStructure) weiter ausgebaut.

Kurzbeiträge

TROPOS nutzt die gräßenau gelöste Aerosolcharakterisierung auch lokal zur Untersuchung der Luftbelastung im städtischen Raum Leipzigs und kann im Vergleich mit den Dauermessungen in Melpitz lokale Quellen vom ländlichen Hintergrund-Aerosol trennen. So fanden **van Pinxteren et al.** auf Basis einer dreijährigen Messkampagne, dass Situationen mit starker Belastung fast zur Hälfte durch lokalen Straßenverkehr verursacht werden und hier Reduktionsmaßnahmen die größte Wirkung zeigen können. Dies gelingt z.B. durch die Einführung von Umweltzonen, was das TROPOS am Beispiel der Stadt Leipzig nachgewiesen hat. In anderen Regionen der Welt herrschen allerdings oftmals zunehmend katastrophale Luftbelastungen, wie **Kecorius et al.** am Beispiel der subtropischen Megastadt Manila zeigen konnten. Tatsächlich ist die verkehrsbedingte Feinstaubbelastung dort etwa zehnmal höher als in Leipzig. Auf der viermonatigen Messkampagne in Manila kamen erstmals mobile Sensoren zum Einsatz, um die hohe räumliche Variabilität der Rußbelastung aufzulösen. Die hohe zeitliche Variabilität organischer Bestandteile in der Gas- und Partikelphase wird seit 2010 kontinuierlich an der TROPOS-Forschungsstation Melpitz erfasst. **Stieger et al.**

Overview of the individual contributions / Übersicht der Einzelbeiträge

statistically analysed over several years. Results have been related to the aerosol chemical composition. On this basis, **Henning et al.** could prove a seasonal cycle of the CCN properties together with their dependency on origin and history of the advected air masses.

TROPOS significantly contributes to the experimental and modelling activities of the joint project "High Definition Clouds and Precipitation for improving Climate Prediction" (HD(CP)²), and coordinated the intensive field campaign "HD(CP)² Observational Prototype Experiment" (HOPE) in Jülich and Melpitz in spring and fall 2013. As a pilot study to future modeling studies on aerosol/cloud-interactions **Engler et al.** computed the aerosol size distributions (from which in turn CCN and ice nucleating particle concentration can be obtained) from prognosticated aerosol mass distributions. Comparisons with observed aerosol size distributions during HOPE-Melpitz indicate that the model is missing an aerosol source.

In the framework of the Hans Ertel Centre for Weather Research **Senf et al.** analysed a comprehensive data set of the geostationary satellite Meteosat to characterize dynamical and microphysical processes, which are responsible for the formation and intensity of thunderstorms over Germany. Objectives of this work are improved forecasts of convective extrem events as well as more precise weather warnings.

In addition to satellite remote sensing ground-based remote sensing is able to detect the microphysical processes during the formation and evolution of clouds with a higher resolution.

Bühl et al. demonstrate how the spatial distribution of the microphysical properties together with their dynamical forcing can be simultaneously obtained from Doppler-lidar, cloud-radar and wind-profiler measurements. The way aerosols and clouds determine the spatiotemporal variability of the solar irradiance at the surface has been determined for the first time by **Madhavan et al.** from a dense network of pyranometers, which was in operation during both the HOPE-Melpitz and the HOPE-Jülich campaign. The resulting statistics not only are relevant for climate studies on radiative forcing, but are also of large value for yield investigations of solar power plants.

One of the strengths of TROPOS is the coupled investigation of processes in the field, model and the laboratory. **Mutzel et al.** detected the recently discovered highly oxidized multifunctional organic compounds (HOM) in the particle phase both in the Leipziger Aerosol Kammer (LEAK) and at the TROPOS research station Melpitz. They also

kombinierten stündliche Messwerte mit Rückwärtstrajectorien, um so die Quellregionen antransportierter Schadstoffe genauer zu lokalisieren. Um den Einfluss der natürlich und anthropogen erzeugten Aerosole auf die Wolkenbildung zu untersuchen, wurde in Melpitz über mehrere Jahre die Anzahl und Hygroskopizität von Wolkenkondensationskernen (CCN) erfasst, statistisch ausgewertet und mit der chemischen Zusammensetzung in Verbindung gebracht. Auf dieser Basis konnten **Henning et al.** einen Jahresgang der CCN-Eigenschaften und deren Abhängigkeit vom Ursprung und von der Historie der antransportierten Luftmassen nachweisen.

TROPOS trägt maßgeblich zu den experimentellen und modellierenden Arbeiten des Verbundprojektes „High Definition Clouds and Precipitation for improving Climate Prediction“ (HD(CP)²) bei und koordinierte dort auch die Intensivmesskampagnen „HD(CP)² Observational Prototype Experiment“ (HOPE) in Jülich und Melpitz im Frühling und Herbst 2013. Als Vorstudie zu zukünftigen Modellstudien zu Aerosol/Wolken-Wechselwirkungen berechneten **Engler et al.** aus prognostizierten Aerosolmassen die zugehörigen Aerosolgrößenverteilungen, die wiederum in CCN- und Eisnukleationskern- (IN) -Konzentrationen umgerechnet werden können. Vergleiche mit gemessenen Aerosolgrößenverteilungen während HOPE-Melpitz weisen auf eine fehlende Aerosolquelle im Modell hin.

Senf et al. werten im Rahmen des Hans-Ertel Zentrums für Wetterforschung des Deutschen Wetterdienstes einen umfangreichen Datensatz des geostationären Satelliten Meteosat aus, um die für die Entstehung und Intensität von Gewittern verantwortlichen dynamischen und mikrophysikalischen Prozesse über Deutschland zu charakterisieren. Ziele dieser Arbeit sind verbesserte Vorhersagen von konvektiven Extremereignissen sowie genauere Unwetterwarnungen. In Ergänzung zur Satellitenfernerkundung kann die bodengebundene Fernerkundung die mikrophysikalischen Prozesse bei der Bildung und Entwicklung von Wolken mit höherer Auflösung erfassen. So zeigen **Bühl et al.** wie man aus Doppler-Lidar, Wolkenradar und Windprofilmessungen gleichzeitig die räumliche Verteilung der wolkenmikrophysikalischen Eigenschaften und deren dynamische Antriebsfelder erhält. Wie sich Aerosole und Wolken auf die raumzeitliche Variabilität der solaren Einstrahlung am Boden auswirken, bestimmen erstmalig **Madhavan et al.** aus einem dichten Pyranometer-Netz, welches sowohl bei HOPE-Melpitz, als auch bei HOPE-Jülich zum Einsatz kam. Die hier gewonnenen Statistiken sind nicht nur für Klimastudien zum Strahlungsantrieb, sondern auch für

Overview of the individual contributions / Übersicht der Einzelbeiträge

identified HOM as a central element in the particle phase chemistry of aerosols. In a further study **Richters et al.** investigated the HOM formation from the ozonolysis of biogenic emitted sesquiterpenes as aerosol precursor compounds, and managed to quantify the total molar HOM yields.

Another central mechanism next to the formation and growth of aerosol and cloud particles that is intensively researched at TROPOS is the heterogeneous formation of ice. At the Leipzig Aerosol and Cloud Interaction Simulator (LACIS) **Niedermeier et al.** investigated the immersion freezing behaviour of feldspar. In combination with a stochastic model they arrived at an upper limit for the ice activity of mineral dust, which may play an important role in the modelling of the atmospheric ice formation.

A classical example for a climate-relevant connection of chemical and physical processes is the oxidation of dimethylsulfide (DMS) in the formation and processing of aerosol particles. **Hoffmann et al.** developed a complex multiphase chemistry mechanism for the marine DMS-halogen chemistry, and managed to prove the importance of multiphase processes in the DMS reduction as well as in the formation of their oxidation products.

Bridging specific laboratory studies and field experiments can be achieved by means of most realistic three-dimensional modelling studies. **Schrödner et al.** integrated highly complex chemical mechanisms into the chemistry transport model COSMO-MUSCAT and achieved a realistic modelling of the effect of clouds on tropospheric oxidants and on the secondary aerosol mass. Comparisons with corresponding measurements from the HCCT-2010 (Hill Cap Cloud Thuringia 2010) campaign have shown general agreements, but also pointed to gaps in the mechanism modelling. In a more atmospheric dynamically motivated comparison **Jähn et al.** demonstrated good matches in the development of convective structures from lidar observations and from Large Eddy Simulations over the area of the Caribbean Island Barbados, where the intensive measurement campaign SALTRACE (Saharan Aerosol Long-range Tranport and Aerosol-Cloud interaction Experiment) took place. These inter-comparisons significantly contribute to a better process understanding of the boundary layer development, entrainment of aerosol from the free troposphere and cloud formation.

In contrast to spatially high resolved three-dimensional atmospheric models one-dimensional air parcel models can optimally resolve chemical and physical processes. By means of the chemical air parcel model SPACCIM **Vogelsberg et al.** investigated the dissolution of mineral aerosol compounds (especially mineral iron) exemplarily for two major dust storm events. The

Ertragsuntersuchungen von Solarkraftanlagen von großer Bedeutung.

Eine der Stärken des TROPOS ist die gekoppelte Untersuchung von Prozessen im Feld, im Modell und im Labor. Die kürzlich entdeckten hochoxidierten multifunktionellen organischen Verbindungen (HOMs) konnten **Mutzel et al.** sowohl in der Leipziger Aerosol Kammer (LEAK) als auch an der TROPOS-Forschungsstation Melpitz in der Partikelphase nachweisen und als zentrales Element in der Partikelphasenchemie von Aerosolen identifizieren. In einer weiteren Studie untersuchten **Richters et al.** speziell die HOM-Bildung aus der Ozonolyse biogen emitierter Sesquiterpene als Aerosolvorläuferverbindungen und konnten die HOM-Ausbeuten quantifizieren. Neben Bildung und Wachstum von Aerosol- und Wolkenpartikeln ist die heterogene Eisbildung ein weiterer grundlegender Mechanismus, der am TROPOS intensiv erforscht wird. **Niedermeier et al.** untersuchten am Leipzig Aerosol Cloud Interaction Simulator (LACIS) das Immersionsgefrierverhalten von Feldspatpartikeln und konnten in Kombination mit einem stochastischen Modell eine Obergrenze der Eisaktivität von Mineralstäuben ermitteln, welche in der Modellierung der atmosphärischen Eisbildung eine wichtige Rolle spielen kann.

Ein klassisches Beispiel für eine klimarelevante Verknüpfung chemischer und physikalischer Prozesse ist die Oxidation von Dimethylsulfat (DMS) in der Neubildung und Prozessierung von Aerosolpartikeln. **Hoffmann et al.** entwickelten einen komplexen Multiphasenchemiemechanismus zur marinen DMS-Halogen-Chemie und konnten so die große Bedeutung von Multiphasenprozessen für den DMS-Abbau sowie die Bildung von dessen Oxidationsprodukten nachweisen.

Die Brücke zwischen dezidierten Laborexperimenten und Feldarbeiten kann durch möglichst realitätsnahe dreidimensionale Modellstudien geschlagen werden. **Schrödner et al.** integrierten hochkomplexe chemische Mechanismen in das Chemietransportmodell COSMO-MUSCAT und erreichten so eine realistische Modellierung des Einflusses von Wolken auf troposphärische Oxidantien und die sekundäre Aerosolmasse. Vergleiche mit entsprechenden Messungen des Experiments HCCT-2010 (Hill Cap Cloud Thuringia 2010) zeigen generelle Übereinstimmungen, wiesen aber auch auf Lücken in der Mechanismen-Modellierung hin. In einem mehr atmosphärendynamisch motivierten Vergleich wiesen **Jähn et al.** gute Übereinstimmungen in der Entwicklung konvektiver Strukturen aus Lidarbeobachtungen und Large-Eddy-Simulationen über dem Gebiet der Karibikinsel Barbados nach, auf der die

Overview of the individual contributions / Übersicht der Einzelbeiträge

relations between the soluble iron content and total dust mass found in laboratory could be reproduced in the model.

The influence of large scale and regional dynamics on Saharan dust processes has been investigated by **Wagner et al.** from a combination of satellite data analysis and regional modelling. This work emphasizes the complex relations between dust source activation and circulation- and precipitation patterns in North Africa. From there, the so-called “global dust belt” reaches in easterly direction to Central Asia. Here, mineral dust contributes to the glacier retreat by reducing the surface albedo. For the first time, the characteristics of surface-near and vertical dust distribution over Tajikistan have been retrieved by TROPOS in the framework of the long-term measurement campaign CADEX (Central Asian Dust Experiment). From Lidar measurements **Hofer et al.** identified typical mechanisms of long-range-transport and deposition of mineral dust.

Besides remote sensing and surface-near measurements TROPOS contributes to airborne aerosol and cloud observation techniques for several years as for example on board the German research aircraft HALO. **Mertes et al.** applied the HALO-CVI (Counterflow Virtual Impactor) to investigate characteristic differences in the formation of natural and anthropogenic influenced cirrus and tropical convective clouds.

Intensivmesskampagne SALTRACE (Saharan Aerosol Long-range Transport and Aerosol-Cloud interaction Experiment) zum atlantischen Ferntransport des afrikanischen Aerosols stattfand. Diese Vergleiche tragen erheblich zu einem besseren Prozessverständnis von Grenzschichtentwicklung, Einmischung des Aerosols aus der freien Troposphäre und Wolkenbildung bei.

Im Gegensatz zu räumlich hoch aufgelösten dreidimensionalen Atmosphärenmodellen können eindimensionale Luftpaketmodelle chemische und physikalische Prozesse optimal auflösen. **Vogelsberg et al.** untersuchten mit dem chemischen Luftpaketmodell SPACCIM chemische Lösungsprozesse mineralischer Aerosolbestandteile (insbesondere mineralischen Eisens) am Beispiel markanter Saharastaubsturmergebnisse. Die in Labormessungen gefundene Relation zwischen Eisenlöslichkeit und Gesamteisengehalt konnte im Modell reproduziert werden.

Den Einfluss der großräumigen und regionalen Dynamik auf Saharastaubprozesse untersuchten **Wagner et al.** aus der Kombination von Satelliten-datenanalyse und regionaler Modellierung. Die Arbeit unterstreicht die komplexen Zusammenhänge zwischen der Aktivierung von Staubquellen und Zirkulations- und Niederschlagsmustern in Nordafrika. Von Afrika erstreckt sich der sogenannte „globale Staubgürtel“ in östliche Richtung bis Zentralasien. Mineralstaub trägt dort über die Reduzierung der Bodenalbedo zum Rückgang der Gletscher bei. In Tadschikistan erfasst TROPOS erstmalig die Charakteristika der bodennahen und vertikalen Staubverteilung im Rahmen der Langzeitmesskampagne CADEX (Central Asian Dust Experiment). **Hofer et al.** konnten mit Lidarmessungen typische Mechanismen des Ferntransports und der Deposition von Mineralstaub nachweisen. Neben Fernerkundung und bodennahen Direktmessungen ist TROPOS seit mehreren Jahren an der Entwicklung von flug-getragenen Aerosol- und Wolkenmessverfahren u.a. auf dem neuen deutschen Forschungsflugzeug HALO und nun auch an den ersten HALO-Wolkenmesskampagnen beteiligt. **Mertes et al.** untersuchten mit dem HALO-CVI (Counterflow Virtual Impactor) charakteristische Unterschiede in der Bildung natürlicher und anthropogen beeinflusster Cirruswolken und tropischer konvektiver Wolken.

Overview of appendice / Überblick der Anhänge

Overview of appendices

Knowledge transfer and public visibility

TROPOS research for the expert public. On account of the application oriented fundamental research of the Institute its scientific knowledge is mainly transferred through scientific publications and conference contributions (see list, p. 121).

During the reporting period TROPOS was involved in two significant conferences. TROPOS hosted the “15th Eletctromagnetic and Light Scattering Conference” (ELS 2015) and co-organized the “15th EuCheMS International Conference on Chemistry and the Environment” (ICCE 2015).

140 researchers from 22 countries attended the triennial top-level conference of light scattering experts ELS. The ELS reveals a variety of topics from basic research and theory of light propagation, remote sensing of surfaces, aerosols and clouds through to biomedical applications.

ICCE is the mayor European conference of environmental chemistry. 500 participants from 50 countries met for presentations and discussions on current development in the areas of (environmental) toxicology, analytic chemistry, microbiology and geosciences.

Emphasis is also to be laid on the “Leipzig Dust Days” in 2014 and 2015, which were initiated by TROPOS to show the variety of disciplines in the research area desert dust and to establish partnerships. Current research topics, results and questions were presented.

TROPOS plays a leading role within the European research infrastructure ACTRIS (Aerosols, Clouds, and Trace gases Research InfraStructure Network) and organised the first workshop of work package 2 in ACTRIS “Remote sensing of vertical aerosol distribution” with 100 participants. (see list, p. 147).

Results of TROPOS research contribute to environmental policy advice. For example for the Land of Saxony and the Federal Environmental Agency (UBA) practise oriented investigations regarding the behaviour and the future development of air pollutants are conducted. In the framework of projects in collaboration with the Environmental Agency and the Saxon State Office for the Environment, Agriculture and Geology (LfULG) measurement data of fine and ultrafine particles are collected, evaluated and provided for further interpretation of the concentration and chemical composition of this particles.

In the field of clean air policy advice TROPOS also contributes with its own studies, which are used

Überblick der Anhänge

Wissenstransfer und Außenwirkung

TROPOS-Forschung für Fachpublikum. Auf Grund der Ausrichtung des Institutes als anwendungsorientiertes Grundlagenforschungsinstitut erfolgt die Verwertung hauptsächlich in Fachpublikationen und Konferenzbeiträgen (siehe Liste, S. 121). Von den wissenschaftlichen Tagungen, an deren Organisation TROPOS beteiligt war, stechen im Berichtszeitraum zwei heraus: TROPOS organisierte die „15. Eletctromagnetic and Light Scattering Conference“ (ELS 2015) in Leipzig und hat die „15. EuCheMS International Conference on Chemistry and the Environment“ (ICCE 2015), ebenfalls in Leipzig, mitorganisiert.

An der alle drei Jahre stattfindenden Spitzen-tagung der Lichtforschung ELS haben rund 140 Forschende aus 22 Ländern teilgenommen. Die Konferenz bildete ein Themenspektrum von der Grundlagenforschung zur Theorie der Lichtausbreitung, Fernerkundung von Oberflächen, Aerosolen und Wolken bis hin zu biomedizinischen Anwendungen ab.

Die ICCE ist die größte europäische Tagung der Umweltchemie. 500 Teilnehmende aus 50 Ländern trafen sich bei Vorträgen und Foren zu aktuellen Entwicklungen in der (Umwelt-)Toxikologie, der Analytischen Chemie, der Mikrobiologie und der Geowissenschaften.

Herauszuhoben sind ebenfalls die vom TROPOS organisierten „Leipziger Staubtage“ 2014 und 2015, an denen aktuelle Forschungsthemen und Fragestellungen zum Thema Wüstenstaub vorgestellt wurden, um die Vielfalt der Fachbereiche zum Forschungsbereich zu zeigen und neue Verbindungen zu knüpfen.

TROPOS spielt eine führende Rolle im Netzwerk der europäischen Forschungsinfrastruktur ACTRIS



Fig. / Abb. 1: Conference ELS-XV at TROPOS in Leipzig, 2015. / ELS-XV-Konferenz in Leipzig 2015. (Photo: Tilo Arnhold / TROPOS)

Overview of appendix / Überblick der Anhänge

for air directive discussions and the implementation of clean air strategies. In addition the institute uses national forums for the presentation of research results.

TROPOS research results for the public at large. TROPOS seeks dialogue with the public using print media, radio and TV. The disseminations of press releases have been significantly increased and shall be maintained at this level in 2014 and 2015. 20 press releases have been published during the reporting period per year. Subsequently 135 publications in 2014 and 129 publications in 2015 were registered.

TROPOS is part of the public relations work of the German Climate Consortium (DKK), the "Klimanavigator" and the Leibniz Association.

The 2013 launched website was further enhanced and addresses research partners as well as the public. The section "Discover" aims to present TROPOS research for the interested public. Focal points, for example are "Focus dust" or "Low emission zone Leipzig". To illustrate scientific work scientists create picture reports from their measurement campaigns around the world, for example on campaigns in the Antarctic, the Phillipines, Tadzhikistan or with the research vessel Polarstern but also reports from the Melpitz measurements station or Fichtelgebirge. Therefore the section "Measurement campaigns" was created in the menu point "Current issues".

Together with 60 other institutions TROPOS was part of the "Science Night" on 27 June, 2014, when laboratories, lecture halls, institutes, clinics, repositories, and archives gave an insight into their work. For the first time all three Leibniz institutes of Leipzig presented a joint program of short lectures.

For the first time as well a tour and presentation of the Cloud Laboratory was combined with a concert



Fig. / Abb. 2: Discussion group "DKK-Klima-Frühstück", 11.02.2015 in Berlin. / Gesprächskreis „DKK-Klima-Frühstück“, 11.02.2015 in Berlin. (Photo: Tilo Arnhold / TROPOS)

(Aerosols, Clouds, and Trace gases Research InfraStructure Network) und führte im November 2015 den von 100 Teilnehmenden besuchten Workshop zum Workpackage 2 „Fernerkundung von vertikaler Aerosolverteilung“ durch (siehe Liste, S. 147).

Die Forschungsergebnisse des TROPOS dienen auch als ein Beitrag zur Politikberatung im Umweltbereich. So werden für das Land Sachsen und das Umweltbundesamt (UBA) praxisrelevante Untersuchungen zum Verhalten und zur künftigen Entwicklung von Schadstoffen in der Atmosphäre durchgeführt. Außerdem werden im Rahmen von Auftragsprojekten für das UBA und das Sächsische Landesamt für Umwelt und Geologie (LfULG) über längere Zeiträume Messdaten zu den Konzentrationen feiner und ultrafeiner Aerosolpartikel sowie zur chemischen Partikelzusammensetzung in der Atmosphäre erhoben, ausgewertet und diesen Institutionen zur weiteren Nutzung zur Verfügung gestellt.

Im Bereich der Luftreinhaltung trägt TROPOS zur Politikberatung auch durch eigene Forschungsergebnisse bei, die in der Richtliniendiskussion und bei der Erstellung von Luftreinhalteplänen verwendet werden.

Das Institut nutzt zusätzlich nationale Innovations- und Forschungsforen für die Präsentation und Darstellung seiner Forschung.

TROPOS-Forschung für die breite Öffentlichkeit. TROPOS sucht den Dialog mit der Öffentlichkeit auch über Printmedien sowie Hör- und Fernsehfunk. Die Veröffentlichung von Pressemitteilungen war im vorigen Berichtszeitraum intensiviert worden und konnte 2014/15 auf diesem Niveau gehalten werden. Im aktuellen Berichtszeitraum wurden pro Jahr je rund 20 Pressemitteilungen verfasst. Dadurch entstanden im Jahr 2014 135 Medienveröffentlichungen. Im Jahr 2015 waren es 129 Veröffentlichungen.

TROPOS ist an den Öffentlichkeitsaktionen des Deutschen Klimakonsortiums (DKK), des Klimanavigators und der Leibniz-Gemeinschaft aktiv beteiligt.

Der 2013 erneuerte Internetauftritt wurde weiter ausgebaut. Das Internetangebot richtet sich neben Forschenden zugleich an die breite Öffentlichkeit. Die Rubrik „Entdecken“ hat daher zum Ziel, die Forschung für alle Interessierten zu erläutern. Schwerpunkte waren dabei beispielsweise „Staub im Fokus“ und die „Umweltzone in Leipzig“. Um Wissenschaft anschaulicher zu machen, kommen auf www.tropos.de zunehmend Forschende zu Wort, die auch selbst von den Messkampagnen in aller Welt berichten. Dazu wurde unter „Aktuelles“ die Rubrik „Messkampagnen“ auf- und ausgebaut, in der z. B. Berichte und Fotos von Expeditionen mit dem FS Polarstern, aus der Antarktis, den Philippinen oder

Overview of appendice / Überblick der Anhänge



Fig. / Abb. 3: TROPOS was awarded the second time with the audit „berufundfamilie“ certificate on 29.06.2015. / Das TROPOS wurde am 29.06.2015 zum zweiten Mal mit dem Zertifikat audit „berufundfamilie“ ausgezeichnet. (Photo: berufundfamilie)

in the framework of the cultural event “Music and Architecture”. Other educational events, for example the open day at the measurement station Melpitz, round off the activities for the public at large.

Selected topics and activities during the reporting period. In addition to the institute's competence in urban air quality (particulate matter and low emission zones) especially climate relevant expertise about cloud formation processes or the impact of dust in the atmosphere became more important.

TROPOS provided the scientific proof of the positive low emission zone effect in January 2014. Subsequently researchers on that subject were on high demand for interviews on particulate matter questions. This applies to the Aerosol Group on the one hand and also to atmospheric chemistry investigations on e.g. heating with wood and the effect of combustion on the air quality as well as modelling the expansion of pollutants (the so called stench in the Erzgebirge region).

For the second time the German Climate Consortium organised a press breakfast with the contribution of TROPOS and the Jülich Research Centre in February 2015, this time on the topic “Clouds as the greatest uncertainty in the climate system”. The subject-specific background knowledge is still asked by journalists.

To address policy maker on the federal level TROPOS contributed to various events in Berlin, for example to: the “Klimadialog” (i.e. climate dialogue) of Deutsche Umwelthilfe (German environmental aid association) in January 2014 on the topic “Climate effect of soot – political and administrative frameworks” or the event “Clean Air now” of Verkehrsclub Deutschland (VDC, German Transport Club) in May 2014.

Tadschikistan genauso gezeigt werden wie aus dem Fichtelgebirge oder aus Melpitz bei Leipzig.

Zusammen mit 60 anderen Institutionen beteiligte sich TROPOS an der alle zwei Jahre stattfindenden „Langen Nacht der Wissenschaften“ am 27. Juni 2014, die Einblicke in Labore, Hörsäle, Institute, Kliniken, Magazine und Archive bot und damit auch in die Labore des TROPOS. Erstmals präsentierten an diesem Abend die drei Leipziger Leibniz-Institute ein gemeinsames Vortragsprogramm.

Ebenfalls zum ersten Mal öffnete TROPOS im Mai 2015 kulturinteressierten LeipzigerInnen im Rahmen von „Musik trifft Architektur“ seine Tür, einem Konzert mit Vortrag und Führung zum Wolkenlabor. Eine Vielzahl weiterer Führungen und andere Veranstaltungen wie z.B. der Tag der offenen Tür an der Feldstation Melpitz rundeten die Aktivitäten für die breite Öffentlichkeit ab.

Ausgewählte Themen und Aktivitäten im Berichtszeitraum. Neben der Kompetenz des TROPOS zur urbanen Luftqualität (Feinstaub und Umweltzonen) gewann besonders klimarelevantes Wissen über Prozesse wie Wolkenbildung oder die Auswirkungen von Staub in der Atmosphäre an Bedeutung.

So lieferte TROPOS beispielsweise im Januar 2014 die entscheidenden Belege für die Wirksamkeit der Leipziger Umweltzone. Die Forschenden des Institutes waren daraufhin bei den Medien gefragte Experten zum Thema Feinstaub. Neben der Expertise der Aerosolgruppe gehören dazu auch die atmosphärenchemischen Untersuchungen zu den Auswirkungen von „Heizen mit Holz“ auf die urbane Luftqualität sowie die Modellierung der Ausbreitung von Schadstoffen (der so genannte „Katzenstreck-Gestank“ im Erzgebirge).

Das Deutsche Klimakonsortium organisierte zum zweiten Mal mit dem TROPOS und dem FZ Jülich gemeinsam im Februar 2015 ein Pressefrühstück in Berlin. Zum Thema „Wolken - die großen Unbekannten im Klimasystem“ wird auch nach Monaten noch Hintergrundwissen von Journalisten nachgefragt. Um politische Entscheidungsträger auf Bundesebene zu erreichen, beteiligte sich das Institut zusammen mit Partnern an Informationsveranstaltungen in Berlin – so zum Beispiel zusammen mit dem IASS, dem FZ Jülich und dem UBA am „Klimadialog“ der Deutschen Umwelthilfe im Januar 2014 zum Thema „Wie stark wärmt Ruß wirklich und welche politischen und administrativen Rahmenbedingungen bestehen?“ oder an der Veranstaltung „Clean Air now“ des Verkehrsclubs Deutschland (VCD) im Mai 2014.

Besonders bei den audiovisuellen Medien ist die Wolkenforschung nach wie vor sehr beliebt.

Overview of appendice / Überblick der Anhänge

A still very popular topic among actors of audio-visual media is cloud research. So ZDF for example reported about a cloud measurement campaign in the Artic and about the Cloud Laboratory, 3 sat about investigations on board research vessel Polarstern or MDR about new methods on thunderstorm forecast and the “Melpitz Column” campaign. A media partnership with “Sächsische Zeitung” could be installed for future reporting on the Transregio project “Arctic Amplification”, which was approved by DFG in 2015.

In 2015 various activities with regard to the Leibniz Year 2016 were initiated by the local authority of Leipzig, the Leibniz Institutes, and the Leibniz Association to draw public attention to the scientific achievements of Gottfried Wilhelm Leibniz.

Equal opportunities and promotion of young researchers

Already during recruiting processes measures for the absolutely non-discriminatory collaboration are applied at the institute and are improved constantly. TROPOS intends to further increase the proportion of international researchers.

Following the so-called Leibniz cascade model TROPOS also intends to increase the proportion of women, especially in post-doc and leading positions. Therefore, a stage-model was implemented in 2012, which was defined according to the current structure of employees at the institute. Particularly worth mentioning here is the approvement of the Leibniz SAW proposal “Dust at the interface” within funding line “Women in leading scientific positions” from Dr. habil. Kerstin Schepanski in 2015 and the participation of Dr. Heike Kalesse in the Leibniz Mentoring Programme for women in 2015. Three young female researchers of TROPOS represented the Leibniz Association at the “Science and Technology in Society Forum 2015” (STS Forum) in Kyoto, where policy makers and company representatives discussed society relevant questions of sustainability in the 21st century.

Audit “berufundfamilie”: An important prerequisite for equal opportunities and career orientation is the reconciliation of career and family, especially for the promotion of young researchers.

In 2011 the TROPOS efforts in this direction were internally and externally manifested in the certificate for the “career and family audit”. As a result of a re-auditing procedure TROPOS received the certificate for the audit once again on 29 June, 2015. The preparations for the re-audit 2014 were started in 2013. According the evaluation on the implementation of the “DFG research-oriented equal opportunity standards”



Fig. / Abb. 4: The awarding ceremony of the Paul-Crutzen-Prize 2015 to Dr. Sebastian Scheinhardt. / Verleihung des Paul-Crutzen-Preises 2015 an Dr. Sebastian Scheinhardt. (Photo: Tilo Arnhold / TROPOS)

So berichtete beispielsweise das ZDF über eine Wolkenkampagne in der Arktis und das Leipziger Wolkenlabor, 3sat über Untersuchungen auf dem Forschungseisbrecher „Polarstern“ oder das MDR-Fernsehen über neue Methoden zur Gewitterfrüherkennung und die Messkampagne zur Melpitz-Säule. Die deutsche Ausgabe des „National Geographic“ widmete der Wolkenforschung im April 2015 eine Titelstory mit TROPOS-Beteiligung.

Mit der Sächsischen Zeitung konnten die Weichen für eine Medienpartnerschaft für eine umfangreiche Berichterstattung zu dem 2015 von der DFG bewilligten Transregio „Arktische Verstärkung“ gestellt werden. Außerdem wurde mit der Leibniz-Gemeinschaft und der Stadt Leipzig beschlossen, das Leibniz-Jahr 2016 auch entsprechend in Leipzig zu begehen und so die Öffentlichkeit auf die Forschung im Namen von Gottfried Wilhelm Leibniz aufmerksam zu machen.

Chancengleichheit und Nachwuchsförderung

Am TROPOS werden Maßnahmen zur absolut diskriminierungsfreien Zusammenarbeit am Institut bereits im Einstellungsverfahren angewendet und fortlaufend verbessert.

Das Institut ist weiterhin bestrebt, den Anteil an internationalen Wissenschaftlerinnen und Wissenschaftlern zu erhöhen.

TROPOS will den Anteil von Frauen, vor allem in wissenschaftlichen Führungspositionen, weiter erhöhen und verfolgt dabei das so genannte Kaskadenmodell nach den Empfehlungen der Leibniz-Gemeinschaft, wobei ein an die momentane institutsspezifische Stellsituations angepasstes Stufenmodell im Jahr 2012 definiert wurde. Speziell erwähnt sei hier die Förderung für Frau Dr. habil. Kerstin Schepanski im Leibniz-Wettbewerbsverfahren SAW unter

Overview of appendice / Überblick der Anhänge

for which the Leibniz Association has agreed in 2008, TROPOS is among the first 18 institutes rated as excellent and thus placed in position 13 of 89 institutes.

Promotion of young researchers. TROPOS actively promotes young researchers in the bachelor and master education at the Leipzig University as well as during and after doctoral research projects. The institute is involved in the development and implementation of the new Bachelor and Master programmes and is exclusively responsible for four modules and partially responsible for further two modules.

Highly qualified scientists of the Institute contribute to teaching activities in cooperation with the Leipzig University as joint appointments. In addition to Meteorology students also Chemistry and Physics students are trained at TROPOS (see list, p. 138).

The institute offers young researchers an individualized realization of their dissertation projects supported by the supervision committee in the framework of the structured doctoral training programme.

TROPOS scientists give lectures at the Universities of Jena, Beijing, Jinan, and Shanghai, Helsinki and Stockholm, in international summer and winter schools, training courses and networks (see list, p. 136).

In 2012 the Leipzig Graduate School on "Aerosol, Clouds and Radiation: Mineral dust" was formed on the subject of characteristics and effects of mineral dust aerosol particles. This structured doctoral training program in collaboration with the Leipzig University is member of the Research Academy Leipzig (RAL).

Create future. TROPOS is a partner within the MINT-Individual network to inspire and generate interest in technical and natural science studies, and especially shows career perspectives in tropospheric research. Students get to know research work in a playful manner and have the possibility to directly talk to scientists from the MINT field. In the framework of this initiative the institute regularly participates in the Girls' Day (girls future day). In 2014 and 2015 interested female students could gain insight into laboratories and career opportunities as scientists and other professions at TROPOS. In total 12 practical trainings employees of the institute supervised pupils and five educational events for pupils and students were performed during the reporting period

Two BELL projects (Besondere Lernleistung, i.e. special learning performance) were supervised.

As in the last years TROPOS will continue to finance an apprentice position.

der Förderlinie „Frauen in Leitungspositionen“ sowie die Aufnahme von Frau Dr. Heike Kalesse in das Leibniz-Mentoring-Programm für Frauen in 2015.

Drei TROPOS Nachwuchswissenschaftlerinnen nahmen als Vertreterinnen der Leibniz-Gemeinschaft am „Science and Technology in Society Forum 2015“ (STS Forum) in Kyoto teil, auf dem Wissenschaftlerinnen, politische Entscheidungstragende und Unternehmensbeauftragte Fragen der Nachhaltigkeit im 21. Jahrhundert diskutierten.

TROPOS ist laut Auswertung zur Umsetzung der „Forschungsorientierten Gleichstellungsstandards der DFG“ im Jahr 2014, denen sich die Leibniz Gemeinschaft 2008 verpflichtet hat, in der Spitzengruppe von 18 Instituten mit der Bewertung „herausragend“ und damit auf Platz 13 von 89 Leibniz-Instituten.

Audit „berufundfamilie“: Eine Voraussetzung für die Chancengleichheit ist die Vereinbarkeit von Beruf und Familie für den wissenschaftlichen Nachwuchs und somit eine bessere Karriereplanung. Mit der Zertifizierung zum Audit „berufundfamilie“ am 25. Mai 2011 wird das Engagement des TROPOS für die Vereinbarkeit von Beruf und Familie nach innen und außen dokumentiert und seit dem angewendet. Am 29.06.2015 wurde TROPOS nach vorherigem Reauditierungsverfahren zum zweiten Mal mit dem Zertifikat zum Audit „berufundfamilie“ ausgezeichnet

Nachwuchsförderung. TROPOS fördert aktiv den wissenschaftlichen Nachwuchs in der Bachelor- und Masterausbildung, während der Promotionsvorhaben und darüber hinaus.

Das Institut ist eng in die Entwicklung und in die Durchführung der neuen Bachelor- und Masterstudiengänge an der Universität Leipzig eingebunden



Fig. / Abb. 5: The Leibniz delegation during the "Science and Technology in Society (STS) Forum" 2015 in Kyoto, Japan. / Die Leibniz-Delegation während des „Science and Technology in Society (STS) Forum“ 2015 in Kyoto, Japan. (Photo: Leibniz Association)

Overview of appendix / Überblick der Anhänge

Cooperations and networking

Numerous grown networks within the Leibniz Association, with Universities, with Max Planck Institutes, with institutes of the Helmholtz Society, and collaborations at the international level demonstrate the actual level of TROPOS networking in the field of interdisciplinary aerosol and cloud research. Similar alike TROPOS is networked on the European and global level and actively develops research programmes (see list, p. 155).

Technological developments at TROPOS lead to international standards in the experimental direct and indirect acquisition of aerosols and hydrometeors from ground up to the high atmosphere as well as in model-based descriptions of the complex multiphase system.

TROPOS uses its national cooperation through several pathways (see list, p. 159). Examples are e.g.:

1. the CARIBIC project in cooperation with Lufthansa that was ensured for another 10 years after running already for 10 years,
2. the TROPOS participation in the DFG research group INUIT investigating the atmospheric ice nucleation together with eight partners,
3. the DFG priority programmes, and the implementation and use of the new HALO aircraft platform,
4. the cooperation with the Federal Environmental Agency for the characterization of aerosol particles,
5. the DWD projects (Deutscher Wetterdienst) for the development of LIDAR measurement devices and ceilometer measurement networks,
6. the contribution to the DWD Hans Ertel Centre for weather research, subject 1 "Atmospheric dynamics and predictability",



Fig. / Abb. 6: The TROPOS delegation during a CADEX meeting (Central Asia Dust Experiment) in Dushanbe, Tadzhikistan, 2015. / Die TROPOS-Delegation während eines CADEX-Treffens in Duschanbe, Tadschikistan, 2015. (Photo: Julian Hofer / TROPOS)

und ist für vier Module exklusiv und für zwei weitere Module teilweise verantwortlich.

Hochqualifizierte Mitarbeiterinnen und Mitarbeiter beteiligen sich als gemeinsame Berufungen an der Lehre der Universität Leipzig. Neben Studierenden der Meteorologie werden am TROPOS auch Chemie- und PhysikstudentInnen ausgebildet (siehe Liste, S. 138).

Das Institut bietet jungen WissenschaftlerInnen individuell abgestimmte und von einem Betreuungsteam begleitete Realisierung ihrer Promotionen im Rahmen der strukturierten Doktorandenausbildung. MitarbeiterInnen des TROPOS halten Kurse an den Universitäten von Jena, Peking, Jinan und Shanghai, Helsinki und Stockholm und in internationalen Sommerschulen, Ausbildungskursen und -netzwerken (siehe Liste, S. 136).

Die im Juli 2012 gegründete Leibniz-Graduierschule „Wolken, Aerosole und Strahlung am Beispiel des Mineralstaubs“ hat die DoktorandInnenausbildung am TROPOS gemeinsam mit der Universität Leipzig auf eine solide Grundlage gestellt und ist in der „Research Academy Leipzig“ (RAL) verortet.

Zukunft schaffen. TROPOS ist Partner im Netzwerk MINT-Individual und unterstützt den Weg zum naturwissenschaftlichen Studium und zeigt berufliche Perspektiven im Bereich der Atmosphärenforschung. SchülerInnen lernen die Forschungsarbeit auf spielerische Art kennen und kommen mit ForscherInnen aus dem MINT-Bereich ins Gespräch. Im Rahmen der MINT-Initiative, die zum Ziel hat, Jugendliche für einen Beruf in den Fächern Mathematik, Informatik, Naturwissenschaften und Technik zu begeistern, beteiligt sich TROPOS auch am Girls' Day, dem Mädchen-Zukunftstag. In den Jahren 2014 und 2015 konnten sich an diesem Tag interessierte Schülerinnen in den Laboren über Ausbildungsmöglichkeiten informieren. Insgesamt wurden in beiden Jahren 12 Schülerpraktika durchgeführt, fünf Bildungs- und Informationsveranstaltungen für Schulkinder und zwei für Studierende. Zwei BELL-Arbeiten (besondere Lernleistungen) wurden betreut.

TROPOS wird auch in den nächsten Jahren mindestens einen Lehrlingsausbildungsplatz aus Haushaltssmitteln finanzieren.

Bedeutende Kooperationen und Vernetzung in der Forschung

Zahlreiche bisher gewachsene Vernetzungen innerhalb der Leibniz-Gemeinschaft, mit Universitäten, mit Max-Planck-Instituten, mit Instituten der Helmholtz-Gemeinschaft sowie auf internationaler

Overview of appendice / Überblick der Anhänge



Fig. / Abb. 7: ACTRIS workshop in Leipzig 2015. / ACTRIS-Workshop in Leipzig 2015. (Photo: Tilo Arnhold / TROPOS)

7. the coordination and active participation in the BMBF project “Clouds and precipitations for advancing climate prediction” with permanent measurements at the “supersites” Leipzig/Lindenberg and the evaluation of results of an intensive measurement campaign 2013 in Jülich and Melpitz, and the provision and evaluation of satellite observation data,
8. the national cooperation for the chemical analysis within the maritime context (MPI Jena, GEOMAR),
9. the cooperation with the Leibniz Institute for Baltic Sea Research Warnemünde (IOW) and the Centre for Tropical Marine Ecology in Bremen (ZMT) for the investigation of exchange processes between the polluted ocean and the polluted atmosphere,
10. the cooperation within the newly established Leibniz research networks, currently these networks are “Crises in a Globalised World” and “Infectious Diseases”,
11. the aerosol particle research community (observing and modelling research) consisting of partners who worked together on SAMUM

Ebene zeigen den derzeitigen Stand der Vernetzung des TROPOS in der interdisziplinären Aerosol- und Wolkenforschung. Ähnlich ist TROPOS auf der europäischen und weltweiten Ebene vernetzt und entwickelt hier aktiv Forschungsprogramme (siehe Liste, S. 155).

Technologische Entwicklungen am TROPOS führen zu internationalen Standards in der experimentellen direkten und indirekten Erfassung von Aerosolen und Hydrometeoren vom Boden bis zur hohen Atmosphäre sowie in der modellmäßigen Beschreibung des komplexen Multiphasensystems.

Die inländischen Kooperationen (siehe Liste, S. 159) des Institutes werden über mehrere Pfade intensiv genutzt:

1. durch das seit über 10 Jahren laufende und durch einen Kooperationsvertrag mit der Lufthansa für weitere 10 Jahre gesicherte CARIBIC-Projekt,
2. durch die Beteiligung an der DFG-Forschergruppe INUIT zum Thema der atmosphärischen Eisnukleation, in der das TROPOS mit acht nationalen Partnern zusammenarbeitet,
3. über die laufenden DFG-Schwerpunktprogramme und über den Aufbau und die Nutzung der neuen Flugzeugplattform HALO,
4. über das Umweltbundesamt zur deutschlandweiten Aerosolcharakterisierung,
5. über Projekte des DWD zur Lidarentwicklung und Ceilometer-Messnetzen,
6. über einen Beitrag zum Hans Ertel Zentrum für Wetterforschung des Deutschen Wetterdienstes im Themenbereich 1 „Atmosphärendynamik und Vorhersagbarkeit“;
7. über die Koordination und aktive Beteiligung an der nationalen BMBF-Förderung „Wolken und Niederschlag im Kontext der Klimaforschung“ mit kontinuierlichen Messungen an den „Supersites“ Leipzig/Lindenberg und der Auswertung einer Intensivmesskampagne in 2013 in Jülich und Melpitz, und der Bereitstellung und Auswertung von Satellitenbeobachtungen,
8. über Kooperationen auf nationaler Ebene bezüglich chemischer Untersuchungen mit maritimem Bezug (MPI Jena, GEOMAR),
9. über Kooperationen mit dem Leibniz-Institut für Ostseeforschung Warnemünde und dem Zentrum für Maritime Tropenökologie zur Untersuchung von Austauschprozessen zwischen dem belasteten Ozean und der belasteten Atmosphäre,
10. über Kooperationen im Leibniz-Forschungsverbund (LFV), „Krisen einer Globalisierten Welt“ und dem LFV „Infektionskrankheiten“,

Overview of appendice / Überblick der Anhänge

- measurement campaigns and during SALTRACE projects,
- 12. the application for the further development of the national infrastructure ACTRIS in the framework of the BMBF National Roadmap,
- 13. the contribution to the collaborative research project TR 172 "Arctic Amplification" on the detection of the arctic aerosol cloud and radiation system,
- 14. the Leibniz Competition cooperation on the role of aerosol particles on the interaction between ocean and atmosphere,
- 15. the continuous studies of the marine troposphere on board the Polarstern research vessel.

In the framework of the Leibniz Competition funds TROPOS establishes collaborations within the Leibniz Association or with university institutes. TROPOS has built numerous international cooperations (see list, p. 155). The ground-based remote sensing and in-situ measurement activities of the institute are integrated into the long-term orientated Infrastructure ACTRIS and into ESA policy advice. The in-situ measurements of aerosol particles are part of the EMEP and WMO GAW networks. The collaboration with partners from Eastern Europe is being established (see list, p. 155).

- 11. über die im Rahmen der SAMUM-Kampagnen und während der SALTRACE-Projektarbeiten aufgebaute Gemeinschaft an Aerosolforschern (beobachtende und modellierende Einrichtungen),
- 12. über die Einreichung eines Antrages zur Weiterentwicklung und Nutzung der nationalen Infrastruktur ACTRIS im Rahmen der Nationalen Roadmap des BMBF,
- 13. über die Beteiligung am Sonderforschungsbereich TR 172 „Arctic Amplification“ zur Erfassung des arktischen Aerosol-, Wolken- und Strahlungssystems,
- 14. über Kooperationen im Leibniz-Wettbewerb zur Rolle des Aerosols in der Wechselwirkung zwischen Ozean und Atmosphäre,
- 15. über kontinuierliche Studien der marinen Troposphäre auf dem Forschungsschiff Polarstern.

Im Rahmen des Wettbewerbsfonds der Leibniz-Gemeinschaft werden die Kooperationsmöglichkeiten innerhalb der Leibniz-Gemeinschaft und mit Universitätsinstituten ausgebaut. Durch Kooperationsvereinbarungen ist das Institut mit zahlreichen internationalen Einrichtungen verbunden (siehe Liste, S. 155). Die bodengebundenen Fernerkundungs- und in-situ-Messungen sind international eingebunden in die langfristigen ACTRIS-Arbeiten und in Beratungstätigkeiten für die ESA. Die in-situ Aerosolaktivitäten sind international in den EMEP- und WMO-GAW-Netzwerken eingebunden. Die Zusammenarbeit mit Osteuropäischen Partnern zur Umweltbelastung und Aerosolferntransporten im europäischen Raum ist angebahnt und wird weiter ausgebaut (siehe Liste, S. 155).

Articles



Results from the SOPRAN study regarding dust and sea exchange processes

Konrad Müller, Khanneh Wadinga Fomba, Manuela van Pinxteren, Thomas Müller, Nicole Niedermeier, Bernd Heinold, Kerstin Schepanski, Hartmut Herrmann, Ina Tegen, Alfred Wiedensohler

In den verschiedenen Teilen des Verbundprojektes SOPRAN sind Mobilisierung, Transport, und Deposition des Saharastaubes sowie die Wechselwirkung mit dem Ozean untersucht worden. Durch Langzeitexperimente gelang es sehr gut, saisonale und interannuale Variationen im Transport von Saharastaub in den tropischen Nordostatlantik aufzuklären. Wechselwirkungen des Staubes mit anthropogenen und natürlichen Aerosolbestandteilen sowie die Depositionsflüsse in den Ozean konnten über lange Zeit untersucht werden. Die Bioverfügbarkeit von Eisenmetallen aus dem Staub konnte partikelgrößenselektiv bestimmt werden. Staubquellregionen wurden aus SEVIRI-Aufnahmen identifiziert. Das COSMO-MUSCAT-Modell diente zur Ermittlung der Staubemissionsflüsse sowie des Staubtransports. Ebenso wurden trockene und nasse Deposition über dem tropischen Nordostatlantik modelliert und mit den Messungen am CVAO sowie mit Satellitendaten verifiziert.

Mit der chemischen Charakterisierung des ozeanischen Oberflächenfilms während verschiedener Schiffskampagnen und vor der Insel Sao Vicente wurden erste Schritte realisiert, die Wechselwirkung von Aerosol und Ozean besser zu verstehen. Dicarbonylverbindungen, Amine und Aminosäuren sind als wichtige Stoffklassen identifiziert worden, die im Oberflächenfilm angereichert werden und auch in Aerosolpartikeln präsent sind.

Auch in Zukunft wird die Station CVAO dazu dienen, Aerosol-Ozean Wechselwirkungen zu untersuchen. Neue Projekte hierzu laufen bereits an.

Introduction

With the construction of the CVAO (Cape Verde Atmospheric Observatory) the BMBF funded SOPRAN project started in 2006. At this now permanent research site a continuous observation of the marine aerosol influenced by Saharan dust, West African anthropogenic emissions, and ocean-air exchange processes started in 2007. Beside our investigations the MPI-BGC Jena and the University of York are partners at the CVAO who are investigating marine gas-phase processes and permanent gas concentrations. Nearby in the open Atlantic the CVOO (Cape Verde Oceanic Observatory) was installed from GEOMAR Kiel to investigate oceanic processes influenced by the deposition of Saharan dust.

The emission, transport, processing, deposition of Saharan dust and its impact on oceanic processes were the goals of the project. The TROPOS scientists provided important contributions to all parts. For the first time a long time series of physical and chemical

aerosol measurements in the tropical Northeast Atlantic took place and produced a unique data base for model development and validation. External project partners used these data. During seven intensive field campaigns the size-selective PM collection by a BERNER-type five-stage low-pressure impactor and the parallel physical characterization of the aerosol was the basis for the important new findings that the tropical marine aerosol is influenced by the Saharan dust transports.

The general aim of one sub-project included a better understanding of sea-air exchange processes in terms of organic material. Sources transport and formation pathways of organic compounds in the marine compartments shall be elucidated. The investigation of the surface microlayer (SML) as a source of organic aerosol components over the Atlantic Ocean was carried out with SML samples taken at Sao Vicente and during several research-vessel cruises as well as from fine aerosol particles collected at the CVAO.

Results

Long-term aerosol measurements at the CVAO – physical characterization.

To better understand the mineral dust cycle including its pathways and atmospheric life time, information about mass concentrations and mass deposition fluxes of mineral dust in the remote ocean regions are necessary [Mahowald et al., 2005]. Direct measurements of mass deposition of mineral dust into the ocean are sparse. Literature values arise from global and regional model outputs [e.g., Ginoux et al., 2001 and Schepanski et al., 2009] and from sample measurements [Ginoux et al., 2001].

Within SOPRAN, a new method was employed to obtain mass deposition fluxes of mineral dust into the ocean. This method combines measurements of particle number size distributions (PNSD) from a mobility particle size spectrometer (MPSS) and an aerodynamic particle size spectrometer (APS), hygroscopic measurements with a humidity - differential mobility sizer - aerodynamic particle sizer (H-DMA-APS) and measurements of wind velocity and wind direction with a 3D sonic anemometer.

While the highly hygroscopic sea salt particles grow at 85% relative humidity (RH) compared to 30% RH (dry state), mineral dust particles are hydrophobic and show almost no size change at 85% RH compared to 30% RH. Thus, number fractions of mineral dust from four discrete particle diameters between 550 and 900 nm (volume equivalent diameter at dry state) particles are calculated from the humidified size distribution of the H-DMA-APS and are applied to the PNSD to obtain dust number size distributions [Niedermeier et al., 2014]. The resulting dust number concentrations of mineral dust calculated from the dust number size distribution are converted into dust mass concentrations (M_{dust}). Comparisons of dust mass concentrations with gravimetrically determined mass concentrations from samples of a Berner impactor show a high correlation of $R^2=0.98$. However, gravimetrically determined mass concentrations show a 30% higher mass concentration.

Covariance calculations from the highly time resolved measurements of the sonic anemometer are used to obtain turbulence parameters like friction velocity, Obukhov-length and roughness length. Together with the wind velocity, these turbulence parameters are used in a parameterization [Zhang et al., 2001] to obtain a size resolved deposition velocity v_d .

The mass deposition flux of mineral dust (F) is calculated with $F=\sum M_{dust} v_d$ summing over the PNSD particle diameters. Figure 1a) shows the

mass deposition flux of mineral dust for the months December 2011 to March 2012. The median values for each month lie between 15 and 18 ng/m²s, except for February with values of about 1.5 ng/m²s. The mean values indeed show less variation and have values around 30 ng/m²s for all four months (24, 27, 35 and 34 ng/m²s for Dec, Jan, Feb and Mar, respectively). There is a high variability within one month covering two orders of magnitude. For each of the shown months, there is one event when the mass concentration exceeds 100 ng/m²s, which is marked with a star. 10-day Hysplit back trajectories were calculated for each event and are shown in Fig. 1b). For the four months shown, air masses always arrived from the same source regions (Mali, Mauritania, Algeria and Morocco). Consequently, physical and chemical dust properties should be similar for these periods. In February, the air masses circulated over Algeria and Mali, thus picking up large amounts of mineral dust and leading to the highest observed mass deposition flux of 550 ng/m²s.

The method described above provides mass deposition fluxes with a high time resolution. Measurements of the spectral light absorption of mineral dust with a seven-wavelength absorption photometer (Aethalometer, model AE31) allow to determine dust concentrations [Niedermeier et al., 2014]. This method has the disadvantage that it is not size resolved, thus a representative deposition velocity for the whole size range of mineral dust must be derived.

Figure 2 shows the annual cycle of Aethalometer mass concentrations for the years 2012 and 2013, deposition velocities assumed for the whole aerosol population, and mass deposition fluxes calculated from this input. The dotted line shows the It is clearly seen that the highest mass concentrations are observed in the winter months from November to December, which is the dust season at the Cape Verde Islands. But although outside the dust season, mass concentrations of mineral dust in the summer months (June to August) show values up to 5 µg/m³. There is little variation in the deposition velocity with a mean value of 0.99 ± 0.13 mm/s. The evaluation of two more years (2014 and 2015) will show, whether a constant deposition velocity can be assumed to simplify flux calculations. The mass deposition flux of mineral dust follows the mass concentration in shape due to the deposition velocities around 1 mm/s. Highest values in the winter months reach values larger than 30 ng/m²s and thus show similar results as from the method explained above. From these measurements, the yearly mass deposition flux into the North Atlantic Ocean reaches around 125 ng/m²s.

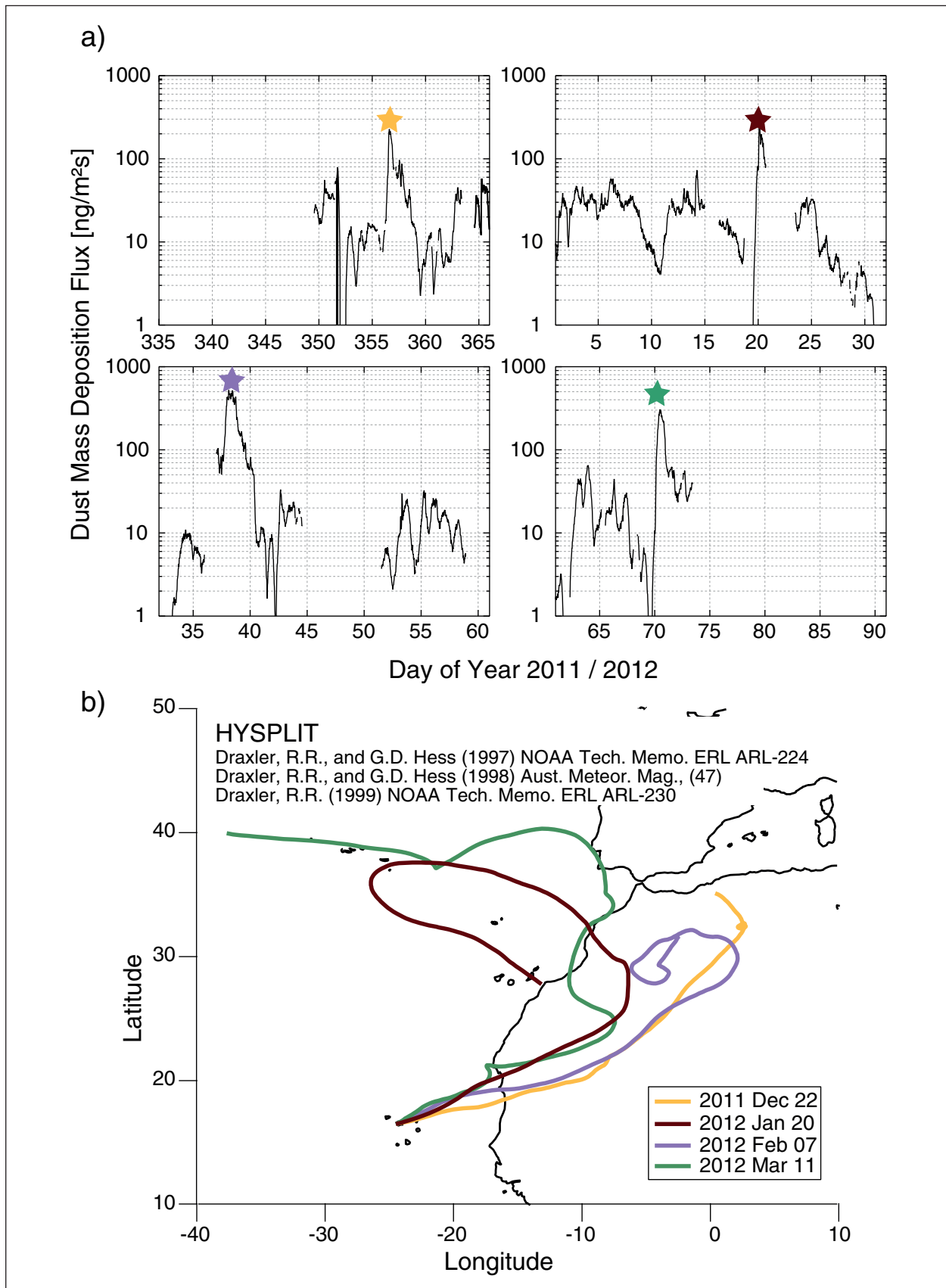


Fig. 1: Mass deposition fluxes obtained from particle number size distribution and hygroscopic measurements combined with micrometeorological measurements for December 2011 to March 2012 (a) and 10-day back trajectories from Hysplit simulations for events with mass deposition fluxes exceeding $100 \text{ ng}/\text{m}^2\text{s}$ (b). Colors of the stars indicating dust events match with the colors of the back trajectories.

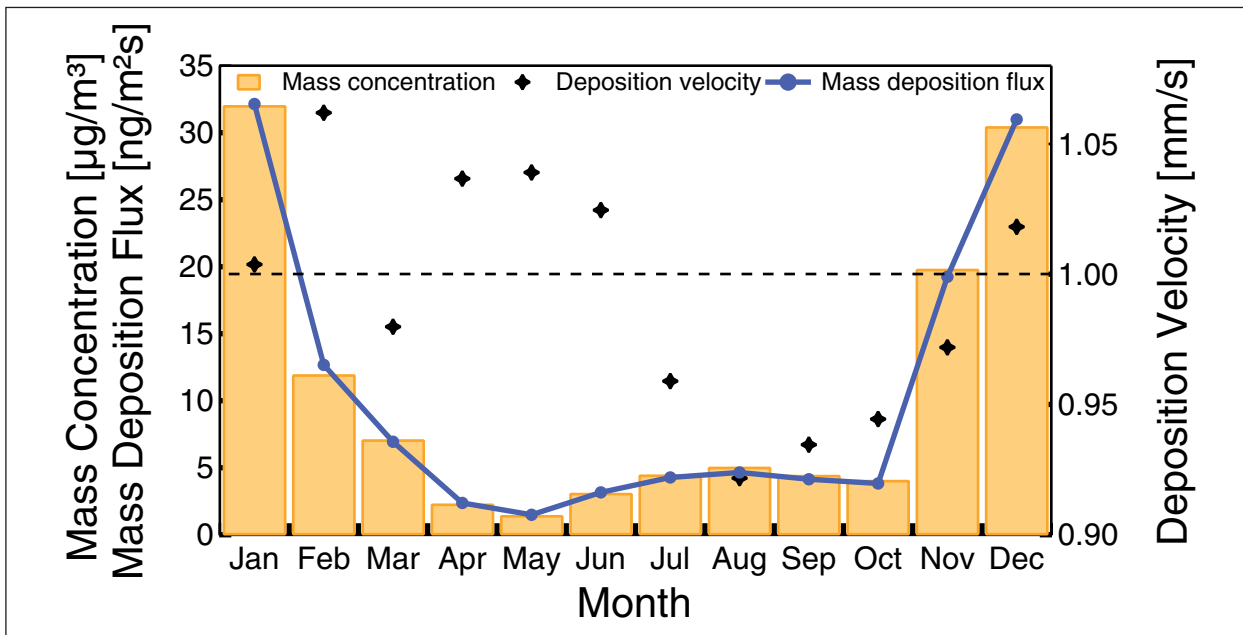


Fig. 2: Annual cycle of Aethalometer mass concentrations, deposition velocities and mass deposition fluxes of mineral dust.

Long-term aerosol measurements at the

CVAO – chemical characterization. From December 2006 on a quasi-continuous sampling of PM₁₀ aerosol is carried on using DHA-80 (DIGITEL-AG, Hegnau, Switzerland). Not only a strong seasonality was observed but also an enormous inter-annual variability of the chemical constitution of aerosol (Fig. 3). The transport of Saharan dust to the CVAO shows maxima during the “Harmattan” season from end of November to beginning of March. One of the important findings about these dust events was the parallel increase of OC, EC, and secondary anthropogenic ionic constituents in the particles within the dust events. Ground based long-term investigation of PM at the CVAO is an important step towards understanding the role of aerosols in ocean atmosphere interactions especially in the tropical Northeast Atlantic.

At the standard collection height of 32 m at the CVAO, the long term mean of sea salt and total PM₁₀ aerosol were 11 µg/m³ and 47 µg/m³, respectively, of which Saharan dust made up 55% of the PM₁₀ mass. Secondary ionic species, elemental carbon, organic matter and water completed the particle constitution. Seasonal variations were found for aerosol mass, dust, nss-sulfate, EC, OM and ammonium. The highest sulfate concentrations were strongly connected to Saharan dust events but not all dust events were responsible for the elevated sulfate concentrations. When air mass containing dust did not have contact with anthropogenic SO₂ pollution sources, the nss-sulfate was not elevated and vice

versa. During the dust season marine sources of nss-sulfate played a minor role. The averaged nss-sulfate concentration in winter marine air masses was $0.47 \pm 0.31 \mu\text{g}/\text{m}^3$ while for the dust days the averaged nss-sulfate concentration was $2.46 \pm 1.05 \mu\text{g}/\text{m}^3$. The strong increase in sulfate concentrations during the dust events is indicative of anthropogenic activities in Africa that influences the aerosol constitution. Marine precursors could explain about $40 \pm 20\%$ of the observed nss-sulfate during the non-dust periods. Nitrate concentrations, however, never showed a strong seasonal trend as shown on Fig. 3. A slight increase in the nitrate concentrations (about 20%) was often observed in the summer except during 2008 where a strong decline in nitrate concentrations from January to December was found. Ammonium and oxalate were often correlated with chlorophyll A, which suggests that ammonia and oxalic acid had also marine precursors in this environment. A distinct seasonality was observed for the halogenide depletion with the minimum in winter due to the occurrence of Saharan dust events and the lower irradiation intensity in non-dust periods. Chloride depletion varied between 10% and 35%. The observed strong annual and seasonal variation of the aerosol constitution provides useful information about the type of atmospheric nutrient deposition and the ocean responds to this deposition over the past years. Such investigations are valuable as they provide relevant background knowledge for understanding the role of the atmosphere and the ocean in the long-term global climate.

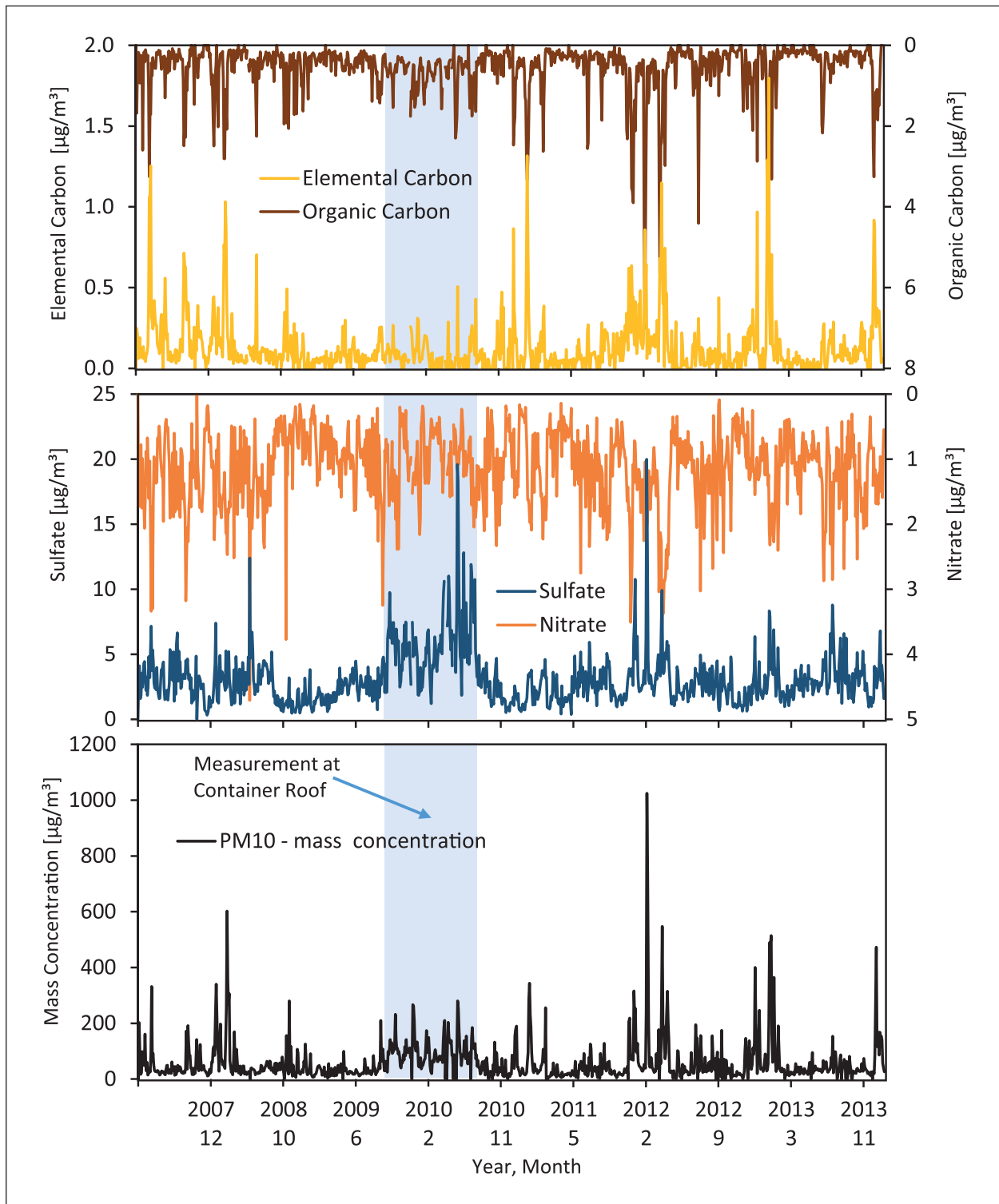


Fig. 3: Time series of PM₁₀ mass concentration, nitrate, sulfate, elemental and organic carbon on filter samples from the CVAO tower (2007-2013).

Aerosol iron and trace metals at the CVAO.

Measurements of trace metals and of important macronutrients such as iron were performed on aerosol particles collected at the CVAO. Iron, amongst others, is a key nutrient for marine organisms such as plankton and its supply to the open oceans is

mainly through atmospheric deposition of mineral dust. Saharan dust being the major source of mineral dust is thus the main source of mineral nutrients to the north-eastern Atlantic Ocean. The quantification of atmospheric iron provides useful information on the assessment of the role of mineral nutrient on the

bio productivity of marine organisms in this region. Though the total amount of iron deposited to the ocean is required, the most essential factor, however, is the amount of soluble iron that is made bioavailable to microorganism upon deposition onto the oceans. The soluble composition is known to vary depending on aerosol composition and atmospheric chemical processes. Different studies have suggested that processes involving organic complexation combined with photochemistry [Hand et al., 2004; Zhuang et al., 1992; Schroth et al., 2009] and cloud processes [Deguillaume et al., 2005; Hand et al., 2004; Desboeufs et al., 2001] in the atmosphere modify iron solubility of desert dust [Boyd, 2007; Chen and Siefert, 2004]. These processes often relate to the photochemical reduction of iron (III) to iron (II), due to the higher solubility of iron (II) compounds in comparison to the iron (III) compounds. Thus, evaluation of the various forms of soluble iron provides a more detailed understanding in the role of atmospheric processes towards iron solubility and bioavailability.

During intensive campaigns lasting up to six weeks, both sized resolved and bulk aerosol PM₁₀ samples were collected at the CVAO to determine the concentration of total and soluble iron and other trace metals. The measurements were performed with total-reflection x-ray fluorescence and ion chromatography techniques for the total and soluble trace metal content, respectively [Fomba et al., 2015]. Figure 4 shows the size distribution of iron during a winter field campaign in 2012 at the CVAO. The iron mass concentration varied between 0.06 and 32 µg/m³ with an average concentration of about 3.2 µg/m³ observed. The average aerosol mass concentration

during the period of Saharan dust storms was about 780 µg/m³. Iron was mainly observed in the coarse mode aerosol particles mainly due to the high influence of Saharan dust especially during the period of the 2nd to the 10th of February where a Saharan dust storm was observed. A similar size distribution was found for all other trace metals of crustal origin such as Al, Mn, Ti, and Ca. For trace metals such as V, Zn, Pb and As they were mainly found in the fine mode aerosol particles due to their predominantly anthropogenic origin [Fomba et al., 2013]. During days of Saharan dust storms their size distribution, however, shifted toward the coarse mode due to likely condensation on larger particles.

Soluble iron was investigated in different pH solutions including acetate buffer solution at pH 4.5 to mimic atmospheric relevant conditions regarding to cloud water and pH 5.5 in deionized water. The solubility shows a strong dependency on the solution's pH with higher soluble iron observed at lower pH. Iron solubility varied from 0.02 to 0.9% and from 0.02 to 2.5% in deionized water and acetate puffer, respectively. Figure 5 shows the temporal variation of the soluble iron content in both deionized water and acetate butter solutions. High soluble iron was observed during periods of less Saharan dust. During periods of Saharan dust storms iron solubility tends to be lower, especially at higher pH. A comparison of iron solubility data with anthropogenic trace metals such as Pb and Ni revealed that higher soluble iron content was related to days of elevated concentrations of Pb and Ni in the aerosol sample. The higher soluble composition was, therefore, caused by the influence of iron form anthropogenic activities such

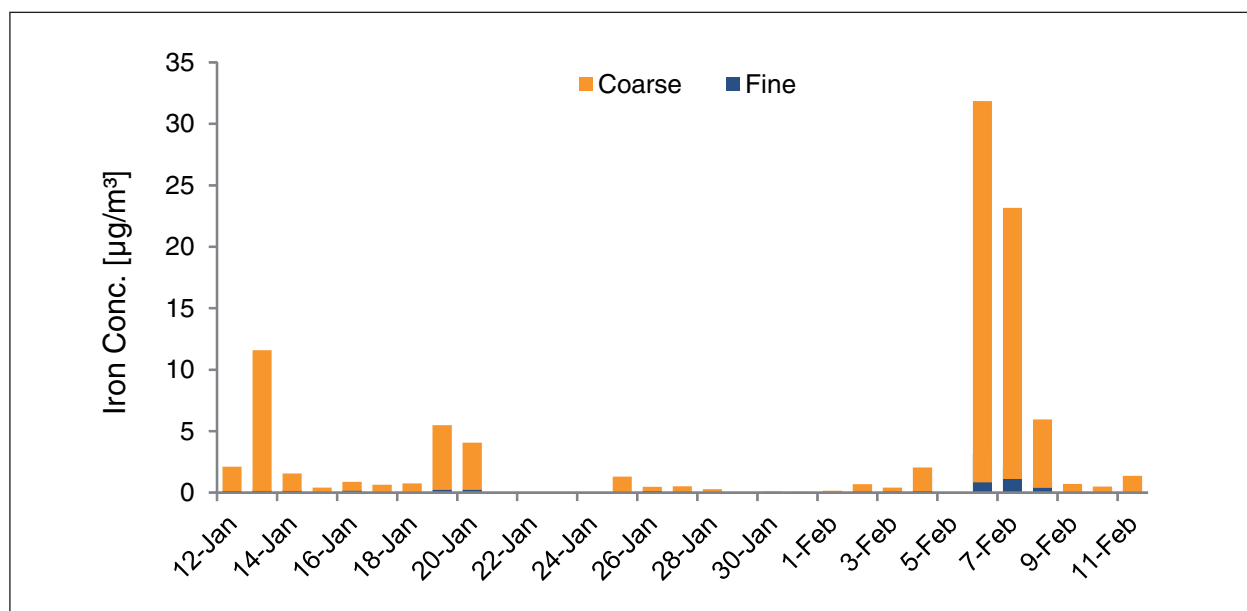


Fig. 4: Size resolved aerosol iron distribution during winter 2012 intensive field campaign.

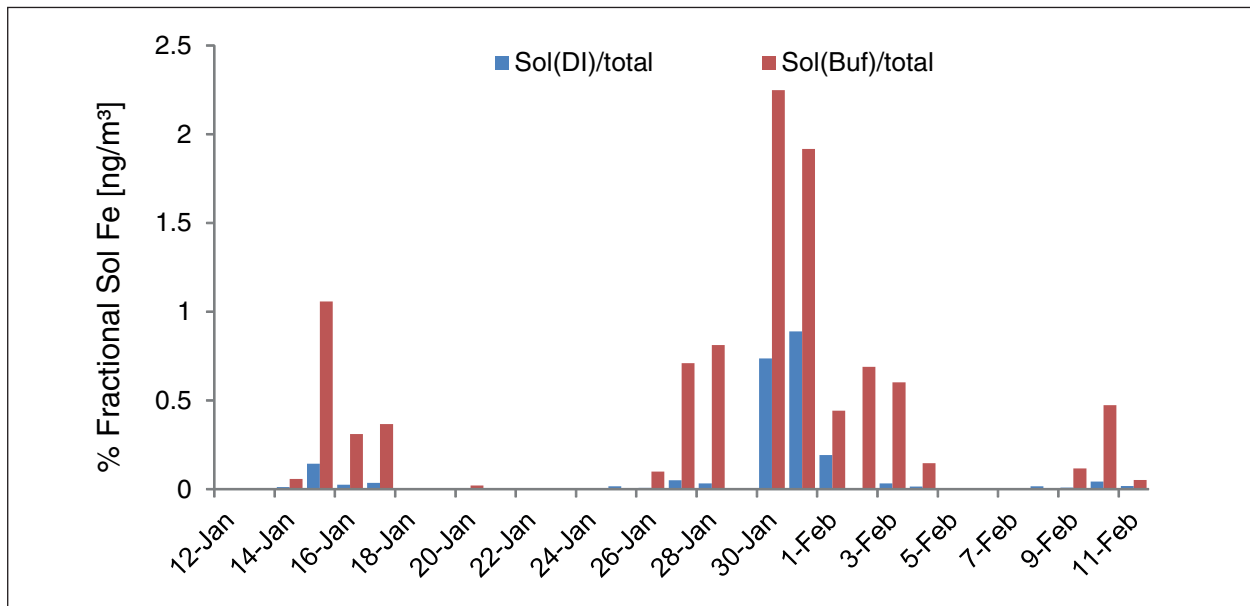


Fig. 5: Temporal variation of fractional soluble iron trace metal concentration in pH 5.5 (deionized water) and pH 4.5 (acetate buffer) during winter 2012.

as combustion sources. However, soluble iron was mainly found in the iron (III) state with less than 10% of the soluble iron present in the iron (II) state. The pH dependence of trace metals such as Mn, Zn and Cu was similar to that of iron with higher soluble content observed at lower pH.

SOPRAN-Modelling. The mineralogical and microphysical properties of Saharan dust that is transported to the tropical Atlantic depends on the source region, while the modification of dust surfaces by heterogeneous chemical processes depends on the transport pathway of the dust particles. Satellite retrievals can be used to localize dust sources and to quantify dust loads over ocean surfaces and to estimate dust deposition. However, for quantification of dust fluxes and clarification of transport trajectories numerical models of the dust cycle are needed. While global-scale dust models provide information about averages and spatiotemporal variability of dust patterns, regional scale models that are driven by forecast or re-analysis fields are suitable to investigate dust transport for specific meteorological situations. Due to inherent uncertainties in such models they must be validated with in-situ observations.

Active dust sources are identified from infrared (IR) dust index images calculated from brightness temperatures obtained from SEVIRI (Spinning Enhanced Visible and InfraRed Imager, flying on-board the geostationary Meteosat Second Generation satellite) observations [Schepanski et al., 2012]. The seasonal cycle of dust source activations over North Africa (Fig. 6) is characterized by different

meteorological conditions: In the northern hemisphere winter (December - February), dust source activation (DSA) is dominantly driven by nocturnal low-level jets (LLJs) that provide surface wind speeds sufficiently high for dust entrainment during their degradation by the onset of turbulence after sunrise. In particular dust sources located in the Bodélé depression and dry desert valleys (wadis) in the foothill regions of the Saharan mountains are activated at 30-50% of the days. In spring (March - May) dust emission is still dominated by LLJs, but in the northern Sahara Mediterranean cyclones cause substantial dust emission as well. Continental scale dust fronts initiated by density currents result in large dust outbreaks over the tropical North Atlantic with low, near surface transport height within the lowest 2 km of the atmosphere. Dust source activation activity during summer (June - August) is shifted toward the Western Sahara. In addition to LLJ favouring DSA, Haboobs and cold downdrafts initiated by deep convection result in DSA in summer. In general, the lowest DSA frequencies occur in fall.

While the satellite retrievals allow a localization of dust source regions and characterization of seasonal changes, dust emission fluxes and transport are computed with the regional model system COSMO-MUSCAT [e.g., Tegen et al., 2013]. The model system consists of the regional-scale meteorological model COSMO of the German Weather Service (Deutscher Wetterdienst, DWD) and the MultiScale Chemistry Aerosol Transport Model (MUSCAT) [Wolke et al., 2012]. For the dust model application the domain includes the major part of the Sahara desert and

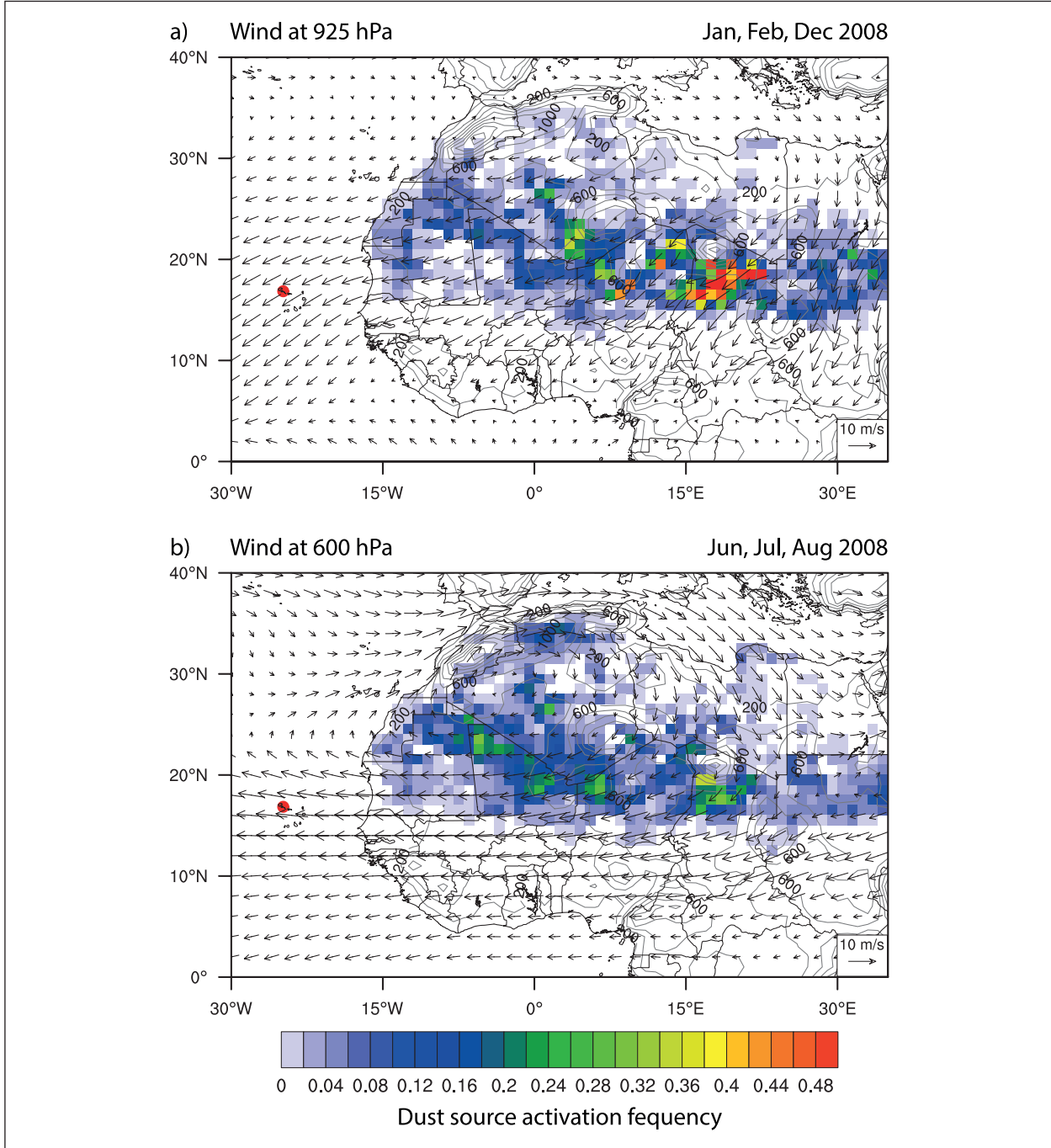


Fig. 6: Spatial distribution of dust source regions inferred from MSG SEVIRI IR dust index images for winter (a) and summer (b) 2008. The color bar shows dust source activation frequency in a grid cell representing a dust source. Contour lines represent the orography given at 200 m intervals. Overlaid wind vectors taken from the ERA-Interim re-analysis data set illustrate the seasonal mean wind indicating main transport directions. As dust is transported at lower levels during winter compared to summer, winds at 925 hPa are shown for winter, and winds at 600 hPa are shown for summer as being representative for the main dust transport direction. The Cape Verde Atmosphere Observation (CVAO) station is indicated by a red circle.

parts of the Tropical Atlantic including the Cape Verde islands. The model operates with 28 km horizontal grid resolution and 40 vertical layers. Dust emission, transport, and deposition are simulated using meteorological fields from COSMO, considering the direct dust radiative effect on atmospheric dynamics.

The location of potential dust sources derived from Meteosat Second Generation satellite observations are used to mask out areas where DSA is not observed. The model transports dust as a passive tracer in five independent size classes between 0.1 μm and 25 μm radius. Dry and wet deposition

processes depending on particle size, density and relevant meteorological parameters cause removal of dust particles.

Saharan dust transport and deposition into the tropical North Atlantic Ocean were simulated for individual events and for the full time period from January 2007 until February 2009. The model results were evaluated with in situ aerosol measurements, satellite dust indices and sun photometer measurements that are routinely taken at the Aerosol Robotic Network (AERONET) stations. Model results show generally a good agreement with the observations, but fail to reproduce dust emissions in the vicinity of mountainous terrain [Tegen et al., 2013]. The model results provide spatiotemporal context to the measurements of microphysical and chemical properties at the CVAO [Niedermeier et al., 2014].

Dust fluxes towards the ocean surfaces are controlled by dry and wet deposition processes. Dry deposition of dust particles is caused by gravitational settling and turbulent mixing on to the surface, while wet deposition is caused by the removal of atmospheric dust by precipitation. Deposition fluxes depend on the particle size, their density and meteorological conditions along the transport trajectory into the area where dust is deposited. After long-range transport from the Saharan sources the size distribution does not vary with time to a large extent, highlighting the importance of meteorological processes for dust deposition. In the Cape Verde region, dry deposition processes of dust dominate during most of the year. This is most pronounced in the northern hemisphere winter, as Saharan dust transport in the winter months occurs in the boundary layer below 2 km height. The dust layer often extends down to the surface, which enhances dry deposition fluxes by turbulent mixing processes. In contrast, in the northern hemisphere summer, dust transport occurs above the marine boundary layer at 3–5 km height and dry deposition events over the ocean are related to the sporadic occurrence of sinking of air masses containing dust. During the northern hemisphere summer season deposition fluxes in the Cape Verde region are lower than in the winter months, when dry deposition fluxes can reach 200 mg/m² per month. The comparison of dry dust deposition fluxes in the month of January in several years is illustrated in Fig. 7 for the years 2007 to 2009. Dust deposition at the Cape Verde station can be influenced by the dust transport patterns as well as the location and strengths of activated dust sources.

Regional models provide a spatiotemporal context to measurements at individual stations. Dust transport direction can be reproduced well in models that rely on meteorological fields from re-analyses

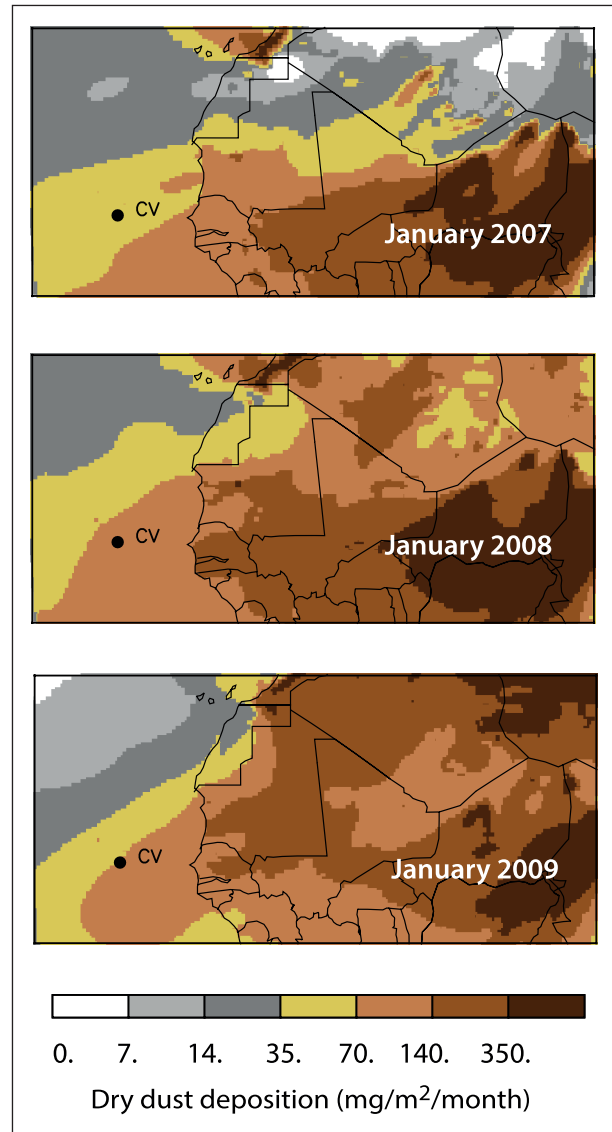


Fig. 7: COSMO-MUSCAT model results of dust dry deposition flux in the Western Sahara and the tropical north Atlantic in January in the years 2007, 2008 and 2009. The symbol 'CV' indicates the location of the CVAO.

such as COSMO-MUSCAT. However, the simulation of the location of dust source regions and the correct placement and magnitude of dust emission fluxes remains problematic in large-scale models. Higher resolved models and better descriptions of soil properties will help to determine the location and processes of dust emissions. This will also support evaluations of connections between mineral properties of soils in dust source regions and the deposition of minerals that serve as micronutrients in the tropical North Atlantic Ocean.

Oceanic export of organic matter. In several marine field campaigns aerosol particles and the sea surface microlayer (SML) - that is the direct interface

between ocean and atmosphere - were sampled and analysed for the chemical composition. Appropriate sample preparation methods were developed aiming at an enrichment of the target analytes and an elimination of the matrix [van Pinxteren et al., 2012]. The results of sea water analysis (SML and bulk water) from the southern Baltic Sea suggest that different compound groups within the broad chemical class of nitrogen containing organic compounds and carbohydrates show very different behavior with respect to water concentrations and enrichment in the SML. Generally amines and amino acids tend to be enriched in the SML, whereas for dissolved carbohydrates a trend towards depletion was observed. The characteristics of the different compound classes were found to be in strong correlation to bacterial activity and meteorological conditions [van Pinxteren et al., 2012].

Two atmospheric relevant organic compounds were studied in more detail during SOPRAN III; the alpha-dicarbonyls glyoxal (GLY) and methylglyoxal (MGLY). These compounds have attracted increasing attention over the past years because of their potential role in secondary organic aerosol formation. To date, there are few available field data of these compounds in the marine area. During SOPRAN III

measurements of GLY and MGLY in seawater and marine aerosol particles sampled during a transatlantic Polarstern cruise could be achieved. The results show that GLY and MGLY are present in the SML and corresponding bulk water with concentrations in the nmol range. Significant enrichment (factor of 4) of GLY and MGLY in the SML was found implying photochemical production of the two carbonyls however, a clear connection to global radiation was not observed. On aerosol particles, both carbonyls are strongly connected to each other, suggesting similar formation mechanisms. Both carbonyls show a very good correlation with particulate oxalate, supporting the idea of a secondary formation of oxalic acid via GLY and MGLY. A slight correlation of the two carbonyls in the SML and in the aerosol particles was found at co-located sampling areas. In summary, the results of GLY and MGLY in marine aerosol particles and in the oceanic water gave first insights towards interaction processes of these alpha dicarbonyls between ocean and atmosphere [van Pinxteren and Hermann, 2013].

A detailed chemical investigation and qualitative classification of main sources of submicron aerosol particles was performed during the RV MARIA S. MERIAN cruise MSM 18/3 that passed through equatorial upwelling areas (Fig. 8). Chemical analysis

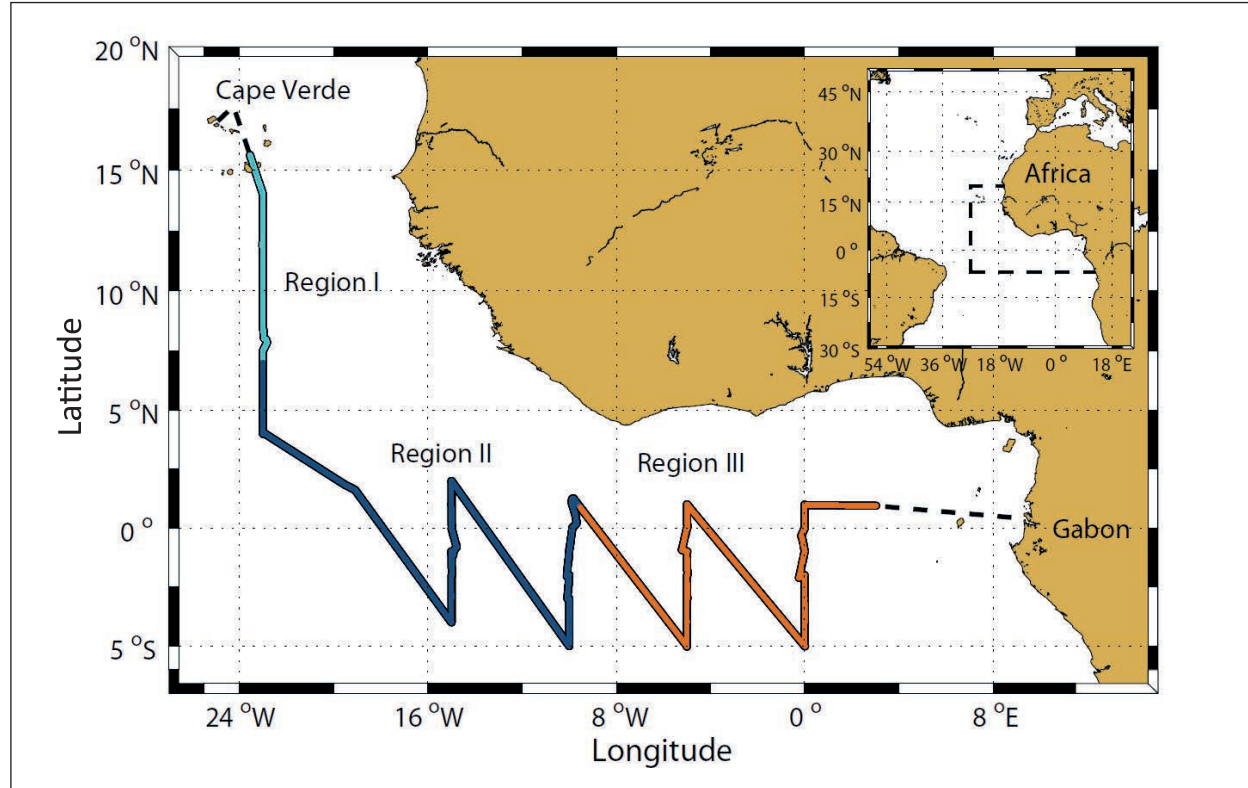


Fig. 8: Cruise track of the MERIAN MSM 18/3 cruise from Cape Verde to Gabon. The light blue line represents Region I (mainly marine-influenced aerosol particles), the dark blue line represents Region II (marine- and biomass burning-influenced aerosol particles) and the brown line represents Region III (strongly biomass burning-influenced aerosol particles).

included the determination of important secondary organic aerosol compounds (methane sulfonic acid, amines, carbonyl compounds and oxalic acid) as well as n-alkanes and related compounds. The combination of the chemical information with meteorological and biogeochemical parameters resulted in the identification of three main regimes being dominated by varying marine and anthropogenic (biomass burning) influences. The high concentrations of water-insoluble organic carbon along the cruise suggest upwelling influences on the local aerosol composition; however, due to strong external influences from biomass burning, a quantitative effect couldn't be ascertained from these measurements. Altogether, this cruise served as a case study for elucidating marine and anthropogenic influences on the chemical composition of aerosol particles in the equatorial ocean [van Pinxteren et al., 2015].

In the very last part of the SOPRAN III project, aerosol particles were studied in the joint SOPRAN laboratory campaign in the wind-wave-channel AEOLOTRON in Heidelberg. 20.000 litre of seawater were filled in the AEOLOTRON and - during different wind and light conditions - the produced particles were sampled with a filter sampler. The dependence of the transfer of organic matter from the ocean to the atmosphere regarding environmental parameters could therefore be studied under controlled conditions. Data analysis is still in progress and will help to determine differences in aerosol composition regarding ambient and laboratory produced aerosol particles.

Summary and outlook

The CVAO has evolved to an important research site for chemical and physical, aerosol, and environmental studies in the tropical marine atmosphere. SOPRAN was the first long-term project to characterize marine and Saharan dust aerosols simultaneously by physical and chemical techniques at the CVAO and during ship cruises. Laboratory experiments completed the program. Interactions between the ocean, the surface microlayer, and the atmosphere were investigated and modelled. Seasonal and interannual variations of dust concentration and deposition were observed. The size class selective dust characterization delivered interesting findings in view of the solubility of metals and the distribution of marine organic aerosol components. The experimental data verified the COSMO-MUSCAT modelled dust transport and deposition. One important task for the future modelling will be directed to a better source region and strength characterization.

The chemical aerosol characterization will be continued to describe further oceanic nutrients transports and deposition to the ocean. The investigation of the interaction of the SML and the atmosphere will be an important field of further activities. A new joint project (MarParCloud) will start this year to investigate the formation of cloud condensation and ice nuclei from SML organic emissions. The research sites at Mindelo and the CVAO will be used for several further research activities by TROPOS.

References

- Boyd, P. W. (2007), Biogeochemistry: Iron findings, *Nature*, 446(7139), 989-991, doi: 10.1038/446989a.
- Chen, Y. (2004), Seasonal and spatial distributions and dry deposition fluxes of atmospheric total and labile iron over the tropical and subtropical North Atlantic Ocean, *J. Geophys. Res.*, 109(D9), doi:10.1029/2003jd003958.
- Deguillaume, L., M. Leriche, K. Desboeufs, G. Mailhot, C. George, and N. Chaumerliac (2005), Transition Metals in Atmospheric Liquid Phases: Sources, Reactivity, and Sensitive Parameters, *Chem. Rev.*, 105(9), 3388-3431, doi:10.1021/cr040649c.
- Desboeufs, K. V., R. Losno, and J. L. Colin (2001), Factors influencing aerosol solubility during cloud processes, *Atmos. Environ.*, 35(20), 3529-3537.
- Fomba, K. W., K. Müller, D. van Pinxteren, and H. Herrmann (2013), Aerosol size-resolved trace metal composition in remote northern tropical Atlantic marine environment: case study Cape Verde islands, *Atmos. Chem. Phys.*, 13(9), 4801-4814, doi:10.5194/acp-13-4801-2013.
- Fomba, K. W., D. van Pinxteren, K. Müller, Y. Iinuma, T. Lee, J. L. Collett, and H. Herrmann (2015), Trace metal characterization of aerosol particles and cloud water during HCCT 2010, *Atmos. Chem. Phys.*, 15(15), 8751-8765, doi:10.5194/acp-15-8751-2015.
- Ginoux, P., M. Chin, I. Tegen, J. M. Prospero, B. Holben, O. Dubovik, and S. J. Lin (2001), Sources and distributions of dust aerosols simulated with the GOCART model, *J. Geophys. Res. Atmos.*, 106(D17), 20255-20273.
- Hand, J. L. (2004), Estimates of atmospheric-processed soluble iron from observations and a global mineral aerosol model: Biogeochemical implications, *J. Geophys. Res.*, 109(D17), doi:10.1029/2004jd004574.
- Mahowald, N. M., A. R. Baker, G. Bergametti, N. Brooks, R. A. Duce, T. D. Jickells, N. Kubilay, J. M. Prospero, and I. Tegen (2005), Atmospheric global dust cycle and iron inputs to the ocean, *Global Biogeochem. Cy.*, 19(4).
- Niedermeier, N., A. Held, T. Müller, B. Heinold, K. Schepanski, I. Tegen, K. Kandler, M. Ebert, S. Weinbruch, K. Read, J. Lee, K. W. Fomba, K. Müller, H. Herrmann, and A. Wiedensohler (2014), Mass deposition fluxes of Saharan mineral dust to the tropical northeast Atlantic Ocean: an intercomparison of methods, *Atmos. Chem. Phys.*, 14(5), 2245-2266, doi:10.5194/acp-14-2245-2014.
- Schepanski, K., I. Tegen, and A. Macke (2012), Comparison of satellite based observations of Saharan dust source areas, *Remote Sens. Environ.*, 123, 90-97, doi:10.1016/j.rse.2012.03.019.

- Schroth, A. W., J. Crusius, E. R. Sholkovitz, and B. C. Bostick (2009), Iron solubility driven by speciation in dust sources to the ocean, *Nat. Geosci.*, 2(5), 337-340, doi:10.1038/ngeo501.
- Tegen, I., K. Schepanski, and B. Heinold (2013), Comparing two years of Saharan dust source activation obtained by regional modelling and satellite observations, *Atmos. Chem. Phys.*, 13(5), 2381-2390, doi:10.5194/acp-13-2381-2013.
- van Pinxteren, M., B. Fiedler, D. van Pinxteren, Y. Iinuma, A. Körtzinger, and H. Herrmann (2015), Chemical characterization of sub-micrometer aerosol particles in the tropical Atlantic Ocean: marine and biomass burning influences, *J. Atmos. Chem.*, 72(2), 105-125, doi:10.1007/s10874-015-9307-3.
- van Pinxteren, M., and H. Herrmann (2013), Glycoxal and methylglyoxal in Atlantic seawater and marine aerosol particles: method development and first application during the Polarstern cruise ANT XXVII/4, *Atmos. Chem. Phys.*, 13(23), 11791-11802.
- van Pinxteren, M., C. Müller, Y. Iinuma, C. Stolle, and H. Herrmann (2012), Chemical Characterization of Dissolved Organic Compounds from Coastal Sea Surface Micro layers (Baltic Sea, Germany), *Environ. Sci. Technol.*, 46(19), 10455-10462.
- Wolke, R., W. Schröder, R. Schrödner, and E. Renner (2012), Influence of grid resolution and meteorological forcing on simulated European air quality: A sensitivity study with the modeling system COSMO-MUSCAT, *Atmos. Environ.*, 53, 110-130, doi:10.1016/j.atmosenv.2012.02.085.
- Zhuang, G. S., Z. Yi, R. A. Duce, and P. R. Brown (1992), Link between Iron and Sulfur Cycles Suggested by Detection of Fe(II) in Remote Marine Aerosols, *Nature*, 355(6360), 537-539.

Funding

The three phases of SOPRAN were supported by the German BMBF und the contract numbers FKZ 03F0462J, 03F0611J, and 03F0662J.

Cooperation

Leibniz Institute for Baltic Sea Research (IOW), Warnemünde, Germany
GEOMAR – Helmholtz Centre for Ocean Research, Kiel, Germany
Alfred Wegener Institute, Helmholtz Centre for Polar and Marine Research, Bremerhaven, Germany
Max Planck Institute for Chemistry, Mainz, Germany
University of Hamburg, Institute of Oceanography, Germany

ACCEPT campaign: Tracing mixed-phase cloud microphysical properties with Doppler-polarimetric cloud radar and lidar

Patric Seifert¹, Alexander Myagkov¹, Johannes Bühl¹, Linda Forster², Lukas Pfitzenmaier³, Heike Kalesse¹, Ronny Engelmann¹, Holger Baars¹, Albert Ansmann¹, Ulla Wandinger¹, Yann Dufournet³, Marcel Brinkenberg⁴, Matthias Bauer-Pfundstein⁵

¹ Leibniz Institute for Tropospheric Research (TROPOS), Leipzig, Germany

² Ludwig-Maximilians-Universität, München, Germany

³ Delft University of Technology, Delft, The Netherlands

⁴ Royal Netherlands Meteorological Institute, De Bilt, The Netherlands

⁵ Metek GmbH, Elmshorn, Germany

Die Untersuchung heterogener Eisbildungsprozesse bei Temperaturen zwischen -40 und 0 °C ist in vielfacher Hinsicht von großem Interesse. Zum einen ist bisher noch unvollständig erfasst, welche Prozesse und Partikel unter verschiedenen atmosphärischen Bedingungen für die heterogene Eisbildung verantwortlich sind. Zum anderen sind Fernerkundungsmethoden zur Erfassung und Charakterisierung der von heterogenen Eisbildung beeinflussten Mischphasenwolken bisher nur spärlich verfügbar und existierende Methoden mit großen Unsicherheiten verbunden.

Zur Evaluierung neuer unter Mitwirkung des TROPOS entwickelter und angewendeter Fernerkundungstechniken wurde im Herbst 2014 das ACCEPT (Analysis of the Composition of Clouds with Extended Polarization Techniques) Feldexperiment in Cabauw, NL, in Kooperation mit nationalen und internationalen Partnern durchgeführt. Zentraler Bestandteil der Kampagne war der erstmalige Einsatz eines in Kooperation von TROPOS und Metek GmbH entwickelten hybrid-mode 35-GHz Wolkenradars vom Typ MIRA-35, das die Bestimmung von Form und Orientierung von neugebildeten Eiskristallen erlaubt. Kenntnis der Partikelform ist eine wichtige Grundlage für die Interpretation mikrophysikalischer Abläufe im Lebenszyklus von Mischphasenwolken und für die Bestimmung von Partikelgrößenverteilungen aus mit Wolkenradaren gemessenen Doppler-Spektren, die Information über die Fallgeschwindigkeit der beobachteten Hydrometeore enthalten. Basierend auf den ACCEPT Messungen wurde die Langzeitstabilität der Messungen des neuen Wolkenradars demonstriert und gezeigt, dass die Form der in dünnen unterkühlten Flüssigwasserwolken gebildeten Eiskristalle mit Labormessungen vergleichbar ist. Die Informationen zur Partikelform wurden zudem verwendet, um die mikrophysikalischen Prozesse in Eiskristallen auf ihrem Weg entlang eines Fallstreifens zu dokumentieren und eine Anzahlgrößenverteilung von Eiskristallen aus einem mit einem Wolkenradar gemessenem Dopplerspektrum zu ermitteln. Die erzielten Ergebnisse demonstrieren die Eignung der entwickelten Techniken für zukünftige Schließungsexperimente zwischen Eiskeim- und Eiskristallkonzentrationen.

Introduction

Mixed-phase clouds are frequently observed in the atmospheric temperature range between -40 and 0 °C where water droplets and ice crystals can coexist. The formation and composition of these mixed-phase clouds, i.e., the partitioning of liquid water and ice, plays a crucial role in the formation of precipitation and in the cloud radiative effect. To which extent liquid water or the ice phase contributes to the

composition of a mixed-phase cloud strongly depends on environmental conditions, such as temperature and humidity, and on the properties of the available ice nucleating particles (INP) which are required to initialize the formation of a crystal at temperatures between -40 and 0 °C, the so-called heterogeneous freezing range.

On the one hand, it is of great interest to characterize the initialization of the ice phase in the heterogeneous freezing range. This has been done

at TROPOS either by means of laboratory studies with the Leipzig Aerosol and Cloud Interaction Simulator (LACIS) or based on remote-sensing observations with lidar or cloud radar or both. From the laboratory-based studies the relationship between the microphysical properties of INP and their ice formation activity can be derived in detail [Hartmann et al., 2013; Augustin-Bauditz et al., 2014]. From such investigations it is meanwhile well known that each aerosol type contributes to heterogeneous ice formation with different efficiency, depending on the particle chemical composition and size as well as atmospheric temperature and humidity. The effect of regionally and seasonally varying aerosol conditions on the heterogeneous formation of ice in the atmosphere has been investigated at TROPOS by means of remote-sensing observations with lidar. It was found by Seifert et al. [2010] that ice forms more frequently at temperatures above -20 °C when Saharan dust is present at cloud level. In the presence of volcanic ash all clouds observed at temperatures below -15 °C contained ice [Seifert et al., 2011]. By contrasting lidar observations at southern and northern mid-latitudes Kanitz et al. [2011] concluded that heterogeneous ice formation is much less efficient in the southern hemisphere which is likely caused by the considerably lower aerosol concentrations available there. A variation of heterogeneous ice formation efficiency caused by different aerosol conditions was also observed in the region of the Amazon Basin [Seifert et al., 2015]. There, ice formation was found to be much more efficient during the dry season when aerosol particles related to biomass burning are present throughout the troposphere which is not the case during the wet season. In addition, the lidar-based observations confirmed that ice formation at temperatures above -25 °C in general occurs via the liquid-phase, i.e., heterogeneous ice nucleation is initialized within or on the surface of supercooled liquid droplets [Ansmann et al., 2008].

On the other hand, the evolution of the ice phase after the initial heterogeneous formation of ice crystals is of strong interest in order to examine how the properties of INP relate to the cloud microphysical properties under different atmospheric conditions. First approaches to quantify heterogeneous ice formation based on remote-sensing observations at TROPOS have been presented recently by Bühl et al. [2013] who demonstrated that heterogeneous ice formation in shallow clouds with top temperatures above -10 °C in general produces low ice water contents in the order of 10^{-8} to 10^{-6} kg/m³. Nevertheless, a multitude of processes can occur during the mixed-phase cloud life cycle, each of them affecting shape, size, and number concentration of the formed

ice crystals. In order to characterize the evolution of a mixed-phase cloud, observational techniques are required to constrain the retrieval of the mentioned quantities. E.g., to derive the relationship between the concentrations of INP concentration and formed ice crystals, secondary ice formation and ice multiplication processes need to be absent which potentially can be validated based on observed shape, size, and number of the ice crystals.

Combined active remote sensing with lidar and cloud radar as it is comprised within the Leipzig Aerosol and Cloud Remote Observations System (LACROS) operated by TROPOS is a promising approach to obtain new insights into mixed-phase clouds. To demonstrate this potential, the mobile components of LACROS were deployed in the Analysis of the Composition of mixed-phase Clouds with Extended Polarization Techniques (ACCEPT) field experiment at the Cabauw Experimental Site for Atmospheric Research (CESAR), The Netherlands, in Fall 2014. The ACCEPT experiment was an initiative of TROPOS that was realized within a consortium of Delft University of Technology (Delft, The Netherlands), Ludwig-Maximilians Universität München (Munich, Germany), Metek GmbH (Elmshorn, Germany), and the Royal Netherlands Meteorological Institute (KNMI, De Bilt, The Netherlands).

Within this article, we provide first an overview on motivation and implementation of the ACCEPT field campaign, followed by a presentation of the attempts taken by TROPOS to shed light on the microphysical properties of shallow mixed-phase cloud layers.

ACCEPT field experiment

Motivation. The synergy of cloud radars with other active and passive sensors, in particular lidars and microwave radiometers, provides a great potential for the development of novel retrieval techniques to get reliable and robust estimations of cloud properties. Hereby, lidar provides information on the location of liquid layers within optically thin clouds. Such layers can influence the size, shape, and density of ice crystals falling through them, for instance via riming. Thus, the information about the exact location of supercooled water layers is important for the investigation of the evolution of ice phase in mixed-phase clouds. Cloud radars feature Doppler capabilities, which provide a Doppler spectrum that contains the information of the fall-velocity spectrum of observed cloud hydrometeors convolved by contributions of atmospheric motions for every detected range gate. Based on the cloud radar Doppler spectra and known size-terminal-velocity relations for different particle habits, the number size distribution of cloud

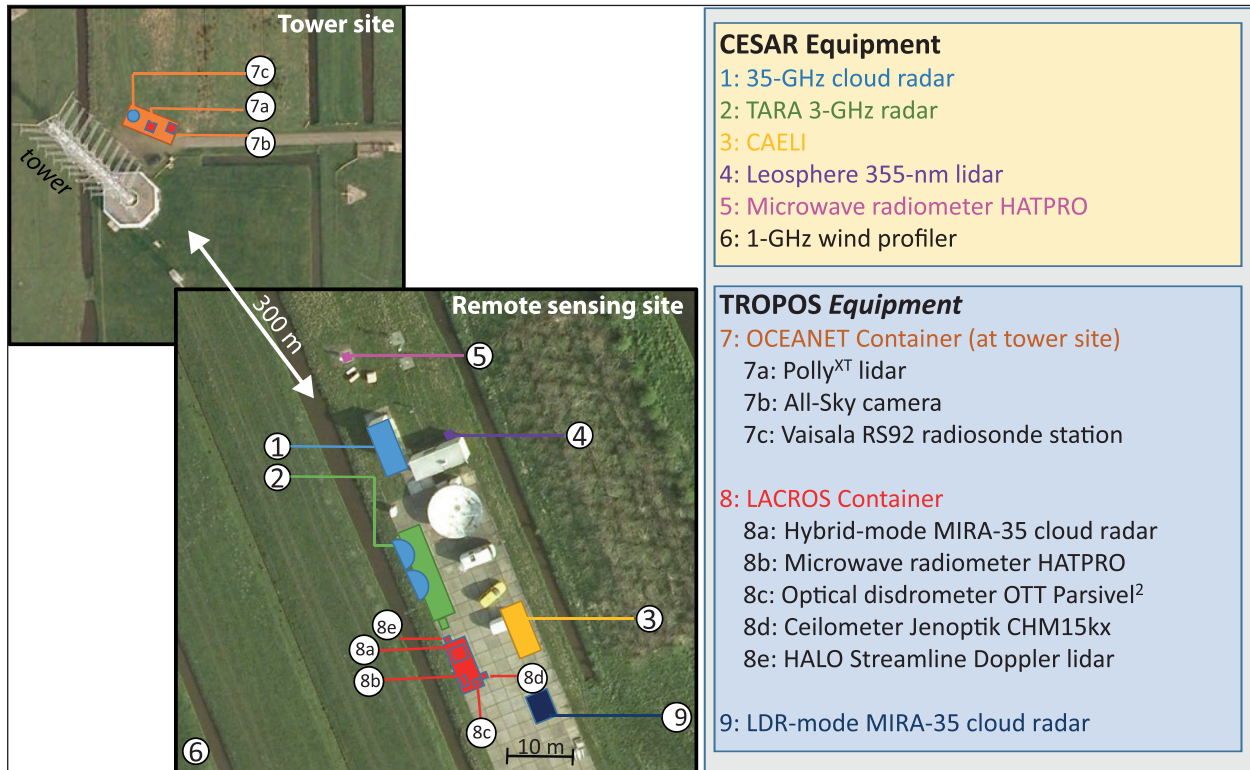


Fig. 1: Instrumental setup at the CESAR observatory during the ACCEPT field experiment.

hydrometeors can be derived. One of the important issues within this approach is an accurate estimation of ice crystal habit [Shupe et al., 2008]. It is widely considered that the ice particle shape is the largest source of error in existing size and number concentration retrievals based on combined lidar and radar vertical observations. Information about the shape of ice crystals is a prerequisite for the determination of size and mass of ice crystals, because the shape determines the relationship between measured particle fall velocity and the unknown particle size. Additionally, the accurate estimation of the particle number size distribution implies mitigation of air motion influence from radar Doppler spectra, which is another problem to solve.

In order to improve techniques for phase detection and estimation of crystal shape at all stages, from cloud formation to the precipitation of ice particles TROPOS started the initiative to realize the ACCEPT field experiment to bring together state-of-the-art cloud remote sensing instruments at one location.

Beside technical aspects concerning the cloud radar evaluation, the measurement campaign included the following broad list of scientific objectives, concerning shallow mid- and high-level cloud layers:

- Analyse the effects of ambient temperature and humidity on the shape and size of formed ice crystals.

- Develop radar-based algorithms for the detection of liquid layers in mixed-phase clouds.
- Investigate the evolution of microphysical properties of ice phase in multi-layered mixed-phase clouds.
- Study the impact of increased concentrations of ice nuclei on microphysical properties of ice crystals.
- Demonstrate the potential of size-distribution-retrieval based on combined lidar and cloud radar observations.
- Evaluate the inter-calibration of the deployed radar systems.

Experiment. The ACCEPT field experiment was conducted between 7 October and 17 November 2014 at the CESAR observatory (51.971° N, 4.927° E) in the Netherlands. The instruments deployed during ACCEPT at the CESAR site are shown in Fig. 1. A photograph of the site setup is shown in Fig. 2. Core instrumentation provided by TROPOS were the vertically pointing linear-depolarization-ratio (LDR) mode 35-GHz cloud radar MIRA-35 (9 in Fig. 1), the Humidity and Temperature Profiler (HATPRO) Microwave radiometer (8b in Fig. 1), the HALO photonics Streamline Doppler lidar (8e in Fig. 1), and the multi-wavelength Raman polarization lidar Polly^{XT} (7a in Fig. 1). In addition, TROPOS rented a newly developed 35-GHz cloud radar from Metek GmbH



Fig. 2: Photograph of the instrumental setup during the ACCEPT field experiment as seen eastward from location 6 in Fig. 1.

(8a in Fig. 1) that was operating in the so-called simultaneous transmit simultaneous receive (STS_R) mode, which is in the following referred to as hybrid-mode MIRA-35. This cloud radar was developed and implemented in the frame of the European Union project ITaRS (Initial Training for Atmospheric Remote Sensing) within a cooperation between TROPOS and Metek GmbH and is described in more detail below.

The reason for choosing CESAR site for the ACCEPT field experiment can be seen in the extensive list of already available instruments. At the CESAR observatory, the 3-GHz radar TARA (2 in Fig. 1) is operated to retrieve particle shape of large precipitation particles. At this frequency, the signal is not contaminated by reflection from supercooled water droplets and is not attenuated, providing direct information on ice crystal properties even for optically thick clouds. However, at such a frequency, freshly formed particles cannot be detected because the instrument is not sensitive to them. Therefore, TARA provides complementary information to the 35-GHz cloud radar observations of TROPOS that are obtained at a much shorter wavelength and thus allow to detect and characterize even freshly formed ice particles in optically thin clouds but suffer from attenuation and sensitivity to liquid water that affect the radar output for optically thicker clouds.

In addition, co-located measurements of the 5° off-zenith pointing polarization-lidar Polly^{XT} of TROPOS enable the detection of layers of horizontally aligned planar crystals causing specular reflections which affect only the signal measured with the zenith-pointing CAELI (3 in Fig. 1) operated by KNMI at the CESAR site.

In addition to the instruments operated at CESAR and the ones deployed by TROPOS and Metek GmbH, an ice halo imaging camera and Sun-Sky Automatic Radiometer (SSARA) were set up and operated by Ludwig-Maximilians-Universität (LMU), Munich, Germany. These instruments were located on a roof platform at KNMI in De Bilt, 30 km northeast of CESAR observatory. That location was chosen in order to relate the properties of halos produced in ice clouds observed with passive

methods at the KNMI site to the remotely sensed particle properties above the CESAR site. A good overlap of the observations was expected for afternoon times when, due to the position of the Sun, the halos seen from De Bilt are actually formed approximately above the CESAR site.

Observations of particle habit with hybrid-mode cloud radar MIRA-35

The principle of particle shape detection with scanning cloud radar is illustrated in Fig. 3 that shows the apparent axis ratio of a spherical and oblate particle observed as a function of the elevation angle of the radar antenna. The elevation dependency of the axis ratio translates into an elevation dependency of polarimetric variables such as differential reflectivity (ZDR) and correlation coefficient (ρ_{HV}). Tracking the angular changes in ZDR and ρ_{HV} it is possible not only to classify the particle shape but also to quantitatively characterize the orientation of observed ice crystals.

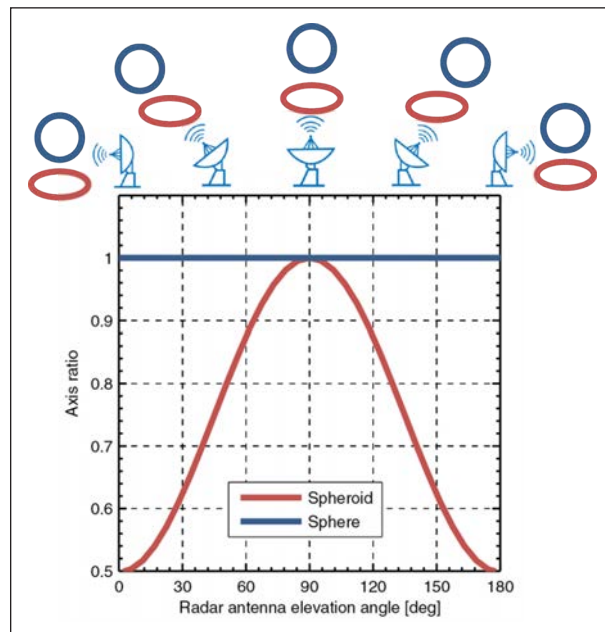


Fig. 3: Axis ratio of spheres (blue) and oblate particles (red) for different radar elevation angles.

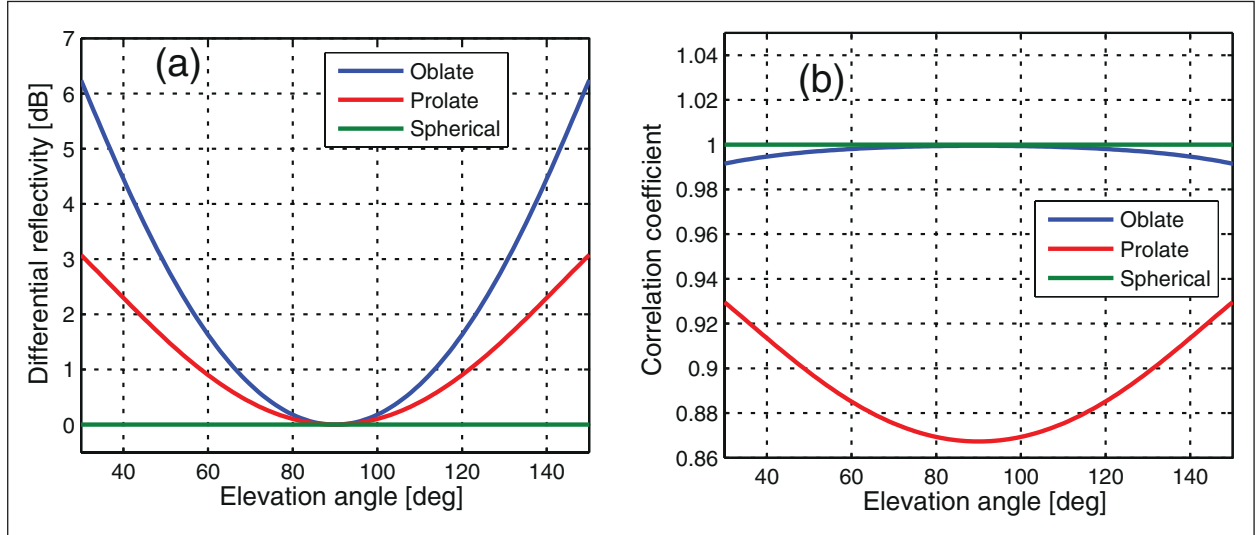


Fig. 4: Elevation dependencies of modeled (a) ZDR and (b) ρ_{HV} for strongly oblate (axis ratio $\ll 1$), strongly prolate (axis ratio $>>1$), and spherical (axis ratio of 1) solid ice particles. Particles are assumed to be oriented near horizontally with the degree of orientation of 0.99. The figure is based on look-up tables given in Myagkov et al. [2015b].

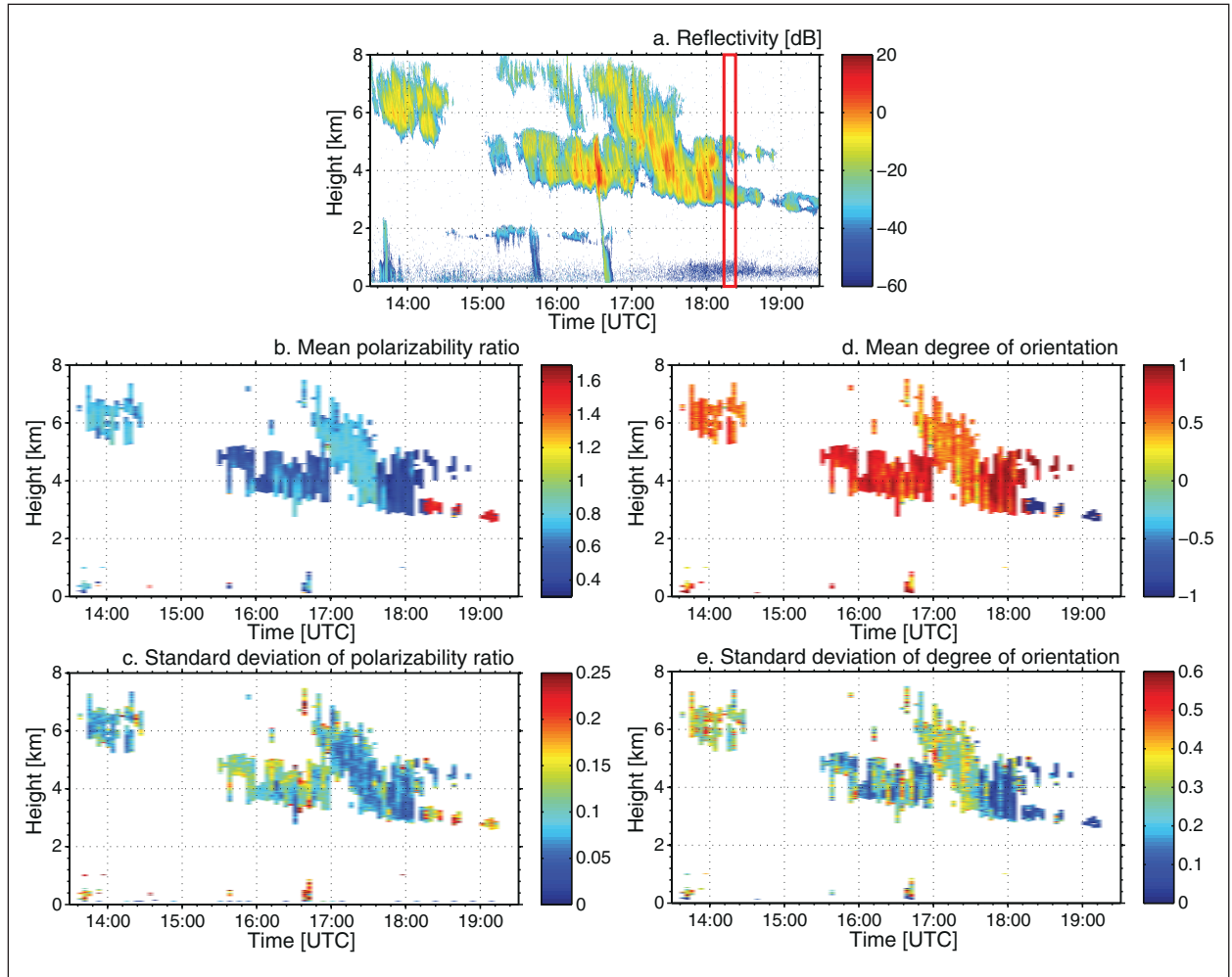


Fig. 5: Height-time cross-sections of (a) equivalent radar reflectivity factor Z_r , mean (b) and standard deviation (c) of polarizability ratio ρ_e , mean (d) and standard deviation (e) of degree of orientation ρ_o , taken during the ACCEPT field experiment on 20 October 2014. The equivalent radar reflectivity factor Z_r was measured by a collocated vertically pointed 35-GHz cloud radar MIRA-35.

In order to measure ZDR and ρ_{HV} which are widely used in polarimetric weather radars but still rarely registered with cloud radars a new cloud radar with scanning ability was developed based on a typical LDR-mode cloud radar of type MIRA-35 [Görsdorf et al., 2015]. The new radar was built and tested in collaboration between TROPOS and METEK GmbH within the ITaRS project. Technical details on the hybrid-mode cloud radar are given by Myagkov et al. [2015a]. During the ACCEPT campaign elevation scans were performed between 60° off-zenith and the zenith direction to observe the elevation dependencies of differential reflectivity ZDR and the correlation coefficient ρ_{HV} . The applicability of the two parameters for the shape determination is described in Fig. 4 that illustrates differences in modeled polarimetric variables for oblate, prolate, and spherical solid ice particles. Summarizing, ice particles of different habits have distinct polarimetric scattering signatures that are utilized in the retrieval.

The retrieval algorithm involves two steps. First, using modeled and measured elevation dependences of ZDR and ρ_{HV} ice particles are classified as either oblate, e.g., plate-like crystals or dendrites, or prolate, such as columnar shaped crystals. Second, at a certain altitude mean and standard deviation of the two parameters polarizability ratio ρ_e and degree of orientation ρ_a are estimated from ZDR and ρ_{HV} for every elevation angle in the range from 30 to 60°, where 90° elevation corresponds to the zenith direction. The polarizability ratio ρ_e depends on shapes and dielectric properties of scatterers, while the degree of orientation ρ_a characterizes the width of the orientation angle distribution of all particles in the observed volume. It is assumed that the mean orientation of ice particles is horizontal.

In Fig. 5 the application of the algorithm to a complex cloud system observed during the ACCEPT field campaign is presented. Amongst other smaller features, three different main ice particle habits can be distinguished within this measurement. Between 13:30 and 14:30 and from 17:00 to 17:45 UTC rather isotropic particles, i.e. having either a shape close to spherical or low apparent ice density, occurred that have a polarizability ratio of close to unity and a degree of orientation of close to zero. This indicates a preferred horizontal orientation. Between 15:30 and 17:00 the polarizability was low and the degree of orientation rather high, pointing to the presence of horizontally aligned plate-like crystals. It can in addition be noted that the polarizability ratio in this time range increases from cloud top to cloud base, indicating that the particles become less dense and/or turn more spherical, as it is the case during aggregation of snow flakes.

Prolate ice crystals, e.g., columnar or needle-shaped ice particles occurred between 18:10 and 19:10 UTC. During this time period, the polarizability ratio was very high whereas the degree of orientation was low, indicating that the particles were oriented along their long axis.

The shape of ice crystals at the top of mixed-phase clouds

A direct verification of the shape and orientation retrieval developed by Myagkov et al. [2015] based on in-situ measurements of ice crystals was not possible for the ACCEPT campaign, due to the absence of respective observations. Nevertheless, an indirect validation was performed on the basis of existing shape-temperature relationships obtained in laboratory studies summarized by Fukuta and Takahashi [1999]. The authors present the axis ratio and apparent density of ice crystals that formed at liquid water saturation as a function of temperature. The respective dataset is shown in Fig. 6. The apparent density accounts for the reduction of density due to inclusions of air in the spheroid defined by the axis ratio.

From the given relationships of axis ratio and apparent density, the corresponding value of the polarizability ratio ρ_e can be calculated, as is shown in Fig. 7. This enables an intercomparison between the polarizability ratios obtained from the laboratory studies and the ones measured during the ACCEPT campaign. This was done based on 22 cloud layers observed during the campaign periods. Strict selection criteria were applied to the dataset. E.g., only cloud layers were analysed where the ice formed within supercooled liquid layers and the datapoint closest to the cloud top region was used for comparison in order to minimize possible influences of effects

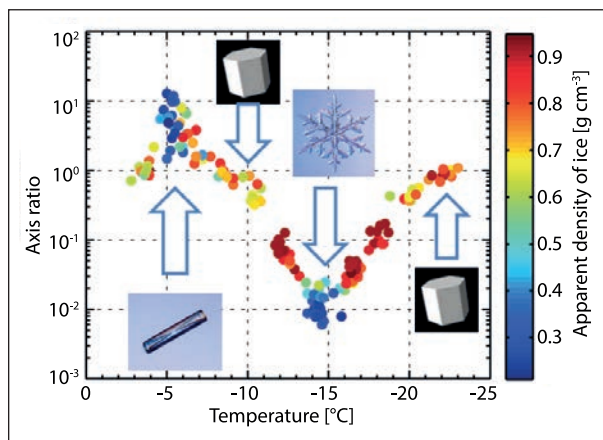


Fig. 6: Axis ratio of ice crystals formed in a cloud chamber at liquid water saturation as a function of apparent density and temperature.

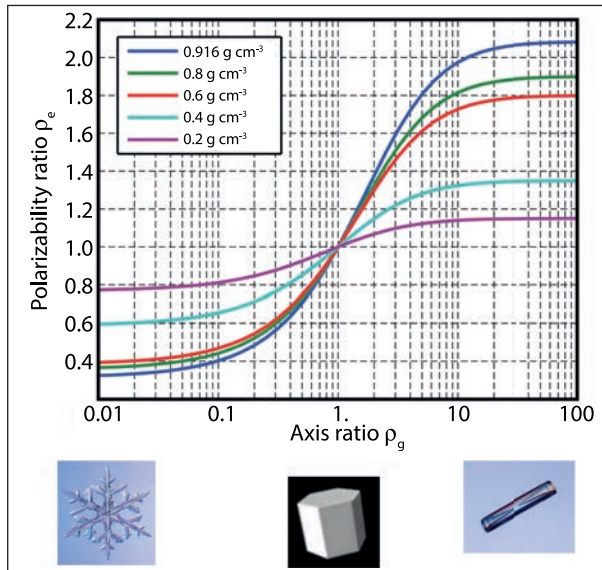


Fig. 7: Polarizability ratio as a function of geometrical axis ratio and apparent density.

such as crystal sublimation, aggregation, riming or splintering.

The result of the intercomparison is shown in Fig. 8. Whereas the blue circles depict the laboratory measurements, red circles show the measurements during the ACCEPT campaign with corresponding error bars. At all temperatures, a striking agreement between the polarizability ratios derived during ACCEPT and from the laboratory studies is visible. In addition the approximate primary shapes derived from the cloud-radar observations are depicted for different temperature regions. Prolate, e.g., needle-shaped

crystals, dominate at temperatures between -3 and -7 °C. Rather isometric particles occur at -8 to -10 °C. Between -13 and -17 °C oblate crystals such as dendrites are formed whereas crystals are rather isotropic at temperatures below -20 °C.

The intercomparison highlights that the shape of crystals that are formed in shallow supercooled liquid layers agrees very well to the pristine shapes of ice crystals formed at comparable temperatures in the laboratory.

Assessing ice particle growth processes from Doppler spectra

To gain insight into microphysical processes occurring in different layers in mixed-phase clouds, we can analyze the temporal evolution of the radar Doppler spectrum from cloud top to cloud base. As already highlighted by Marshall [1953] and shown for a snow fall case study by Kalesse et al. [2015], in situations when vertical wind shear is observed, we should track the evolution along slanted fall streaks instead of considering vertical profiles. The slope of the fall streaks is determined from the horizontal wind profile (obtained from azimuthal scans of the hybrid-mode MIRA-35) and the mean Doppler velocity profile of the vertically-pointing MIRA-35 for which data is presented in this section.

For the time period around 16:15-16:45 UTC shown in Fig. 5, a typical slanted range spectrogram (i.e., the cloud radar Doppler spectrum evolution along a fall streak) is shown in Fig. 9a. Ice particles generated near cloud top at a temperature of -15 °C are falling through a liquid layer which was detected by the Polly^{XT} Raman lidar between 4.2-4.6 km height. Below liquid base an increase in Doppler velocity (V_d) is observed. Looking at a single Doppler spectrum below the supercooled-liquid layer shown in Fig. 9b we do see a bimodal distribution with a slower and a faster ice mode. Velocities in the faster mode are on the order of 1.5 m s⁻¹ which point towards riming. The temperature range in the supercooled-liquid layer was -8 to -10 °C, which is where riming often occurs. However, it should be noted that the Doppler velocities shown are not corrected for up- and downdrafts which could shift the whole Doppler spectrum by a considerable amount up- or downward.

The shown example of a Doppler spectrum highlights the information content of radar Doppler spectra analysis: While the first moments of the Doppler spectrum (radar reflectivity Z_e and mean Doppler velocity) are dominated by the largest ice particles ($Z_e \sim D^6$), the spectrum itself reveals the presence of multiple particle populations.

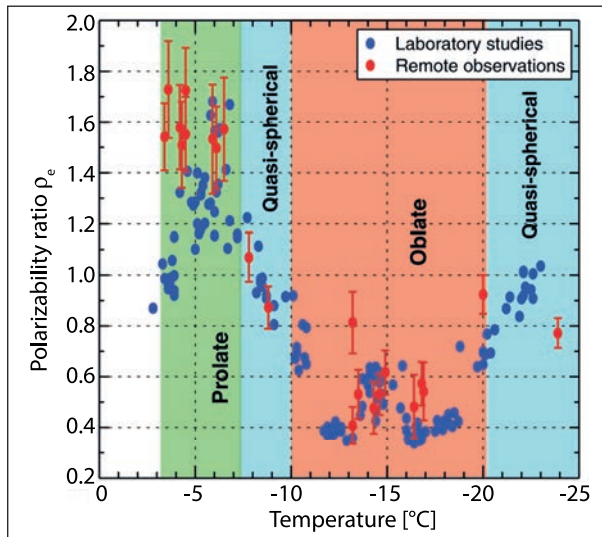


Fig. 8: Temperature dependence of polarizability ratios for ice crystals grown in the free-fall chamber (blue filled circles) and for ones located close to tops of mixed-phase clouds, retrieved from hybrid-mode MIRA-35 (red filled circles).

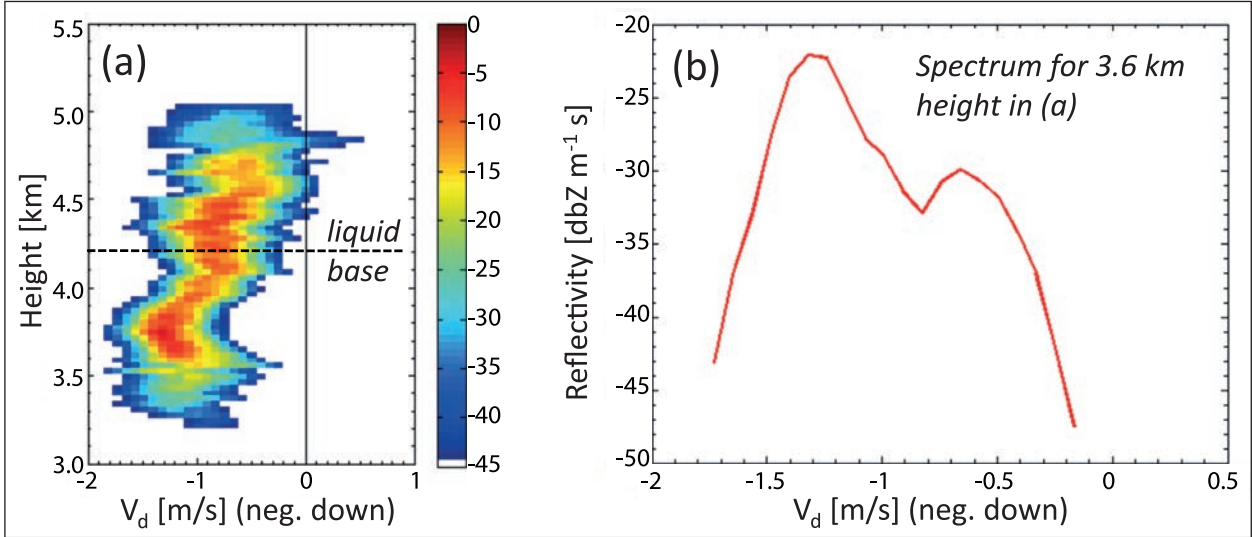


Fig. 9: (a) Slanted-range spectrogram along an ice virga falling from a liquid layer as observed on 20 October 2014 at around 16:30 (see Fig. 5). (b) Doppler spectrum taken from (a) at a height of 3.6 km. Two falling-particle modes are visible, indicating the presence of multiple particle types.

During the time of observation of the spectra shown in Fig. 9, the retrieved ice particle shape is oblate (dendrites). Figure 10a nevertheless shows an increase of polarizability ratio towards cloud base indicating that the shape becomes less oblate and/or the ice particles become less dense. When riming occurs, the ice particle shape is getting less oblate, however ice particle density increases. Figure 10b shows that the degree of orientation changes from about 0.2 in the upper part of the cloud, indicating horizontal orientation of the dendrites, to about 0.5 in the lower part of the cloud meaning the particles

are more randomly oriented there. Here, it should be noted that the shown degree of orientation relates to the one presented in Myagkov et al. [2015] by the relation $(1-p_a)/2$.

Determination of the ice crystal size distribution

The results presented in the previous sections are a prerequisite for the retrieval of particle size distributions from cloud radar Doppler spectra. In Fig. 11 a zoom into the time period from 15:35 to

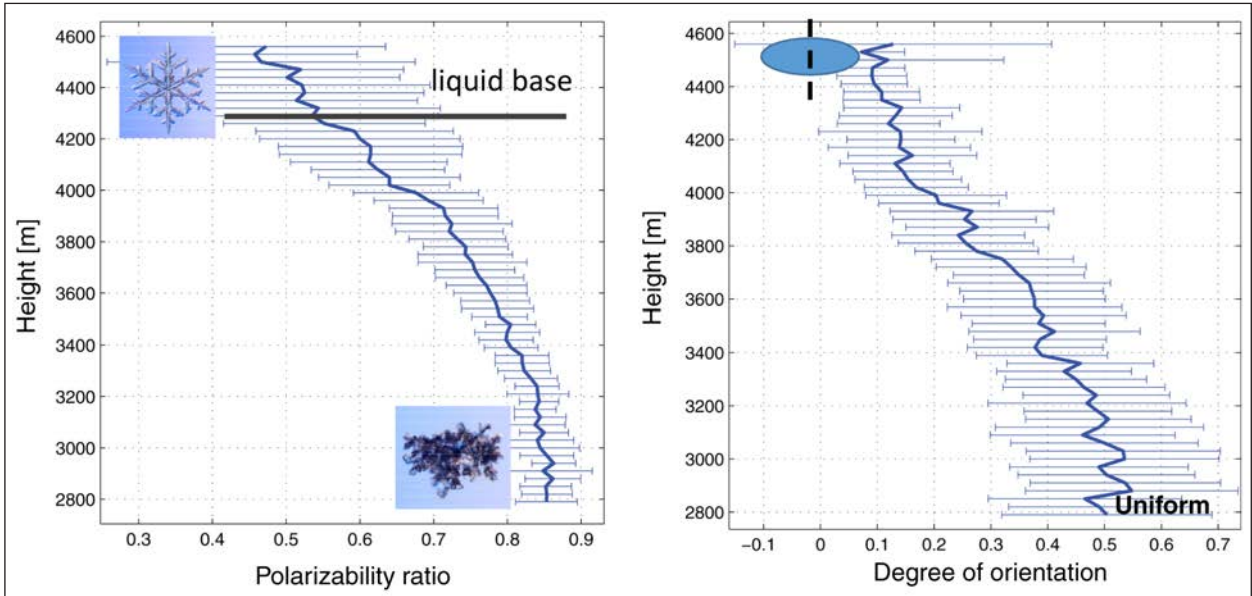


Fig. 10: Evolution of particle shape and orientation along a virga precipitating from a supercooled liquid layer as observed on 20 October 2014 at approximately 16:30 UTC (see Fig. 5). Shown are vertical profiles of (a) polarizability ratio (indicating particle axis ratio) and (b) degree of orientation (indicating alignment of particles).

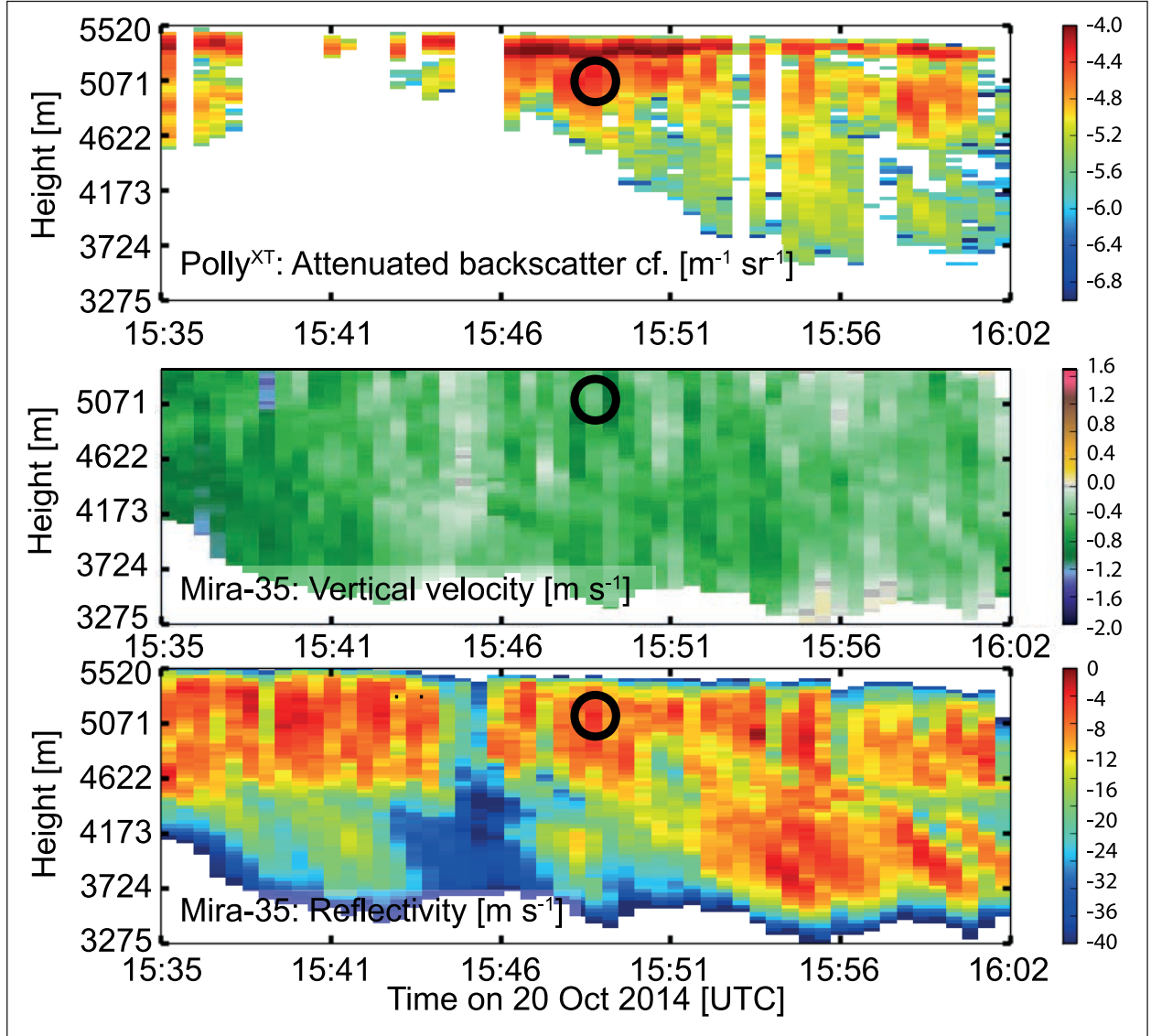


Fig. 11: Measured parameters from lidar Polly^{XT} and cloud radar MIRA-35 on 20 October 2014. The black circle denotes the region for which the ice microphysical properties are presented in Fig. 12.

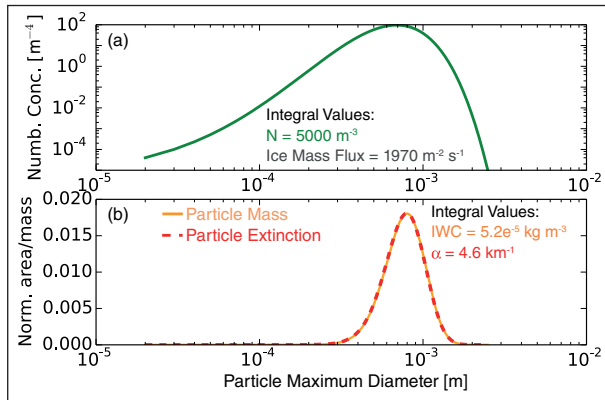


Fig. 12: Microphysical properties of ice crystals obtained for the region encircled in Fig. 11. (a) Number size distribution and resulting particle flux. (b) Weighting function for extinction coefficient alpha (red) and ice water content IWC (yellow).

16:02 of the measurement shown in Fig. 5 is presented. In Fig. 12a the retrieved number size distribution for the black circle in Fig. 11 is shown. The retrieval method was formulated by Bühl [2015]. The number size distribution is fixed to a gamma distribution. Width and mean size are derived from the shape of the cloud radar Doppler spectrum. Consecutively, the spectrum is normalized in a way that the computed radar reflectivity coefficient corresponds with the measured one, assuming stellar crystals as measured with the hybrid-mode MIRA-35 during the analysed time period (see Fig. 5). In Fig. 12b, the basic particle properties mass and particle extinction are plotted. It is interesting to see that both quantities show nearly the same dependency on particle maximum diameter, probably, due to the extremely oblate shape of the stellar ice crystals.

The total optical extinction coefficient is computed to validate the resulting number concentration. In the example shown here, a number concentration of 5000 m^{-3} is derived. The resulting flux of ice particles is $1970 \text{ m}^2 \text{ s}^{-1}$. It is worth noting again that such a retrieval is only possible with exact knowledge about particle shape, which has been in our case measured directly with the new scanning hybrid-mode cloud radar.

Summary

Based on remote sensing observations performed during the ACCEPT field experiment we demonstrate the potential of different retrieval techniques to obtain insights into the microphysical properties of mixed-phase clouds. Focus of the experiment was set on the operation of and observations with the newly developed hybrid-mode 35-GHz cloud radar MIRA-35. It was demonstrated that the new system provides a continuous, valuable dataset that enabled for the first time to derive the shape and orientation of freshly formed, pristine ice crystals. Only based on this information, Doppler spectra of ice crystals observed with cloud radar can be converted

into ice crystal number size distribution, taking into account in addition the potential bias of the Doppler spectra by atmospheric motion. In addition knowledge on the general shape of ice crystals in a volume of air simplifies the interpretation of multi-modal Doppler spectra which contain valuable information about the life cycle of a mixed-phase cloud which is subject to effects of aggregation, riming, splintering, sublimation or other processes. Another considerable improvement for the analysis of the evolution of cloud hydrometeors is the virgae tracking technique that allows to follow single parcels of air from the source at cloud top toward the ground.

The obtained expertise in the microphysical characterization of mixed-phase clouds will enable future closure studies of ice nucleating particle concentrations and the number of formed ice crystals. Also, considering the strong hemispheric contrast in heterogeneous ice formation efficiency reported by Kanitz et al. [2011], observations of the microphysical properties of mixed-phase clouds at southern and northern mid-latitudes should be aspired in order to investigate if and - if yes - how the differences in ice formation efficiency affect cloud evolution.

References

- Ansmann, A., M. Tesche, D. Althausen, D. Müller, P. Seifert, V. Freudenthaler, B. Heese, M. Wiegner, G. Pisani, P. Knippertz, and O. Dubovik (2008), Influence of Saharan dust on cloud glaciation in Southern Morocco during the Saharan Mineral Dust Experiment, *J. Geophys. Res. - Atmos.*, 113(D4), D04210, doi:10.1029/2007JD008785.
- Augustin-Bauditz, S., H. Wex, S. Kanter, M. Ebert, D. Niedermeier, F. Stolz, A. Prager, and F. Stratmann (2014), The immersion mode ice nucleation behavior of mineral dusts: A comparison of different pure and surface modified dusts, *Geophys. Res. Lett.*, 41, 1-8, doi:10.1002/2014GL061317.
- Bühl, J. (2015), Combined lidar and radar observations of vertical motions and heterogeneous ice formation in mixed-phase layered clouds - Field studies and long-term monitoring, Universität Leipzig.
- Bühl, J., A. Ansmann, P. Seifert, H. Baars, and R. Engelmann (2013), Toward a quantitative characterization of heterogeneous ice formation with lidar/radar: Comparison of CALIPSO/CloudSat with ground-based observations, *Geophys. Res. Lett.*, 40, 4404–4408, doi:10.1002/grl.50792.
- Fukuta, N., and T. Takahashi (1999), The growth of atmospheric ice crystals: A summary of findings in vertical supercooled cloud tunnel studies, *J. Atmos. Sci.*, 56(12), 1963-1979.
- Görsdorf, U., V. Lehmann, M. Bauer-Pfundstein, G. Peters, D. Vavrik, V. Vinogradov, and V. Volkov (2015), A 35-GHz polarimetric Doppler radar for long-term observations of cloud parameters—description of system and data processing, *J. Atmos. Ocean. Tech.*, 32(4), 675-690, doi:10.1175/JTECH-D-14-00066.1.
- Hartmann, S., S. Augustin, T. Clauss, H. Wex, T. Šantl-Temkiv, J. Voigtlander, D. Niedermeier, and F. Stratmann (2013), Immersion freezing of ice nucleation active protein complexes, *Atmos. Chem. Phys.*, 13, 5751-5766, doi:10.5194/acp-13-5751-2013.
- Kalesse, H., W. Szyrmer, S. Kneifel, P. Kollias, and E. Luke (2015), Fingerprints of a riming event on cloud radar Doppler spectra: observations and modeling, *Atmos. Chem. Phys. Discuss.*, 15(20), 28619-28658, doi:10.5194/acpd-15-28619-2015.
- Kanitz, T., P. Seifert, A. Ansmann, R. Engelmann, D. Althausen, C. Casciccia, and E. G. Rohwer (2011), Contrasting the impact of aerosols at northern and southern midlatitudes on heterogeneous ice formation, *Geophys. Res. Lett.*, 38, L17802, doi:10.1029/2011GL048532.
- Marshall, J. S. (1953), Precipitation trajectories and patterns, *J. Meteor.*, 10(1), 25-29, doi: 10.1175/1520-0469(1953)010<0025:PTAP>2.0.CO;2.
- Myagkov, A., P. Seifert, M. Bauer-Pfundstein, and U. Wandinger (2015), Cloud radar with hybrid mode towards estimation of shape and orientation of ice crystals, *Atmos. Meas. Tech. Discuss.*, 8(9), 9105-9163, doi:10.5194/amtd-8-9105-2015.
- Myagkov, A., P. Seifert, U. Wandinger, J. Bühl, and R. Engelmann (2016), Shape-temperature relationships of pristine ice crystals derived from polarimetric cloud radar observations during the ACCEPT campaign, *Atmos. Meas. Tech. Discuss.*, 2016, 1-37, doi:10.5194/amt-2015-365.
- Seifert, P., A. Ansmann, S. Gross, V. Freudenthaler, B. Heinold, A. Hiebsch, I. Mattis, J. Schmidt, F. Schnell, M. Tesche, U. Wandinger, and M. Wiegner (2011), Ice formation in ash-influenced clouds after the eruption of the Eyjafjallajökull volcano in April 2010, *J. Geophys. Res. - Atmos.*, 116, D00U04, doi:10.1029/2011JD015702.
- Seifert, P., A. Ansmann, I. Mattis, U. Wandinger, M. Tesche, R. Engelmann, D. Müller, C. Pérez, and K. Haustein (2010), Saharan dust and heterogeneous ice formation: Eleven years of cloud observations at a central European EARLINET site, *J. Geophys. Res. - Atmos.*, 115, D20201, doi:10.1029/2009JD013222.

Seifert, P., C. Kunz, H. Baars, A. Ansmann, J. Bühl, F. Senf, R. Engelmann, D. Althausen, and P. Artaxo (2015), Seasonal variability of heterogeneous ice formation in stratiform clouds over the Amazon Basin, *Geophys. Res. Lett.*, 42(13), 5587-5593, doi:10.1002/2015GL064068.

Shupe, M. D., J. S. Daniel, G. de Boer, E. W. Eloranta, P. Kollias, E. P. Luke, C. N. Long, D. D. Turner, and J. Verlinde (2008), A focus on mixed-phase clouds, *Bull. Amer. Meteor. Soc.*, 89(10), 1549-1562, doi:10.1175/2008BAMS2378.1.

Funding

European Union (EU), Brussels, Belgium
German Research Foundation (DFG), Bonn, Germany

Cooperation

Ludwig-Maximilians-Universität, München, Germany
Delft University of Technology, Delft, The Netherlands
Royal Netherlands Meteorological Institute, De Bilt, The Netherlands
Metek GmbH, Elmshorn, Germany

Results from the Melpitz Column Experiment

Birgit Wehner, Holger Baars, Johannes Bühl, Sebastian Dusing, Bernd Heinold, Michael Jähn, Konrad Müller, Patric Seifert, Holger Siebert, Gerald Spindler

Im Frühjahr 2015 fand das Feldexperiment ‚Melpitz Säule‘ an der TROPOS-Forschungsstation Melpitz, ca. 40 km nordöstlich von Leipzig statt. Zusätzlich zu den Langzeitmessungen von Aerosolpartikeln und meteorologischen Parametern, die dort kontinuierlich am Boden durchgeführt werden, kamen mehrere luftgetragene Systeme sowie bodengebundene Fernerkundung der LACROS (Leipzig Aerosol and Cloud Remote Observations System) Station zum Einsatz, um die atmosphärischen Prozesse in der gesamten Säule zu erfassen. Weiterhin ermöglicht diese komplexe Instrumentierung einen Vergleich der verschiedenen Systeme, wie z.B. Fernerkundung und luftgetragene in-situ Messungen. Dazu werden für diese Kampagne vor allem Aerosoldaten, gemessen mit der hubschraubergetragenen Plattform ACTOS (Airborne Cloud and Turbulence Observation System), mit den optischen Parametern des Raman Lidars Polly^{XT} verglichen. Zudem werden in einer früheren Kampagne von ACTOS durchgeführte hochaufgelöste Messungen und gegen die zeitgleich durchgeführte Vertikalwindmessung eines Dopplerlidars evaluiert.

Die Einordnung der chemischen Messungen in die lange Zeitreihe zeigt, dass der Zeitraum der Melpitz Säule verglichen mit anderen Jahren oder auch Jahreszeiten eine sehr saubere Periode darstellt. Ein Indikator dafür sind die geringen Konzentrationen von Kohlenstoff (EC/OC), die ein Maß für die anthropogene Verschmutzung sind und in Melpitz vor allem von der Anströmrichtung abhängen.

Begleitend wurden Ausbreitungssimulationen mit dem regionalen Chemie-Transport-Modell COSMO-MUSCAT durchgeführt. Die Transportmodellierung dient dazu, einen raumzeitlichen Zusammenhang der gemessenen Aerosoleigenschaften zu möglichen Quellen und Senken herzustellen. Zum anderen können Effekte der Partikelalterung und Mischungsprozesse sowie Aerosol-Strahlungswchselwirkungen analysiert werden.

Mithilfe von hochaufgelösten Large-Eddy-Simulationen für das Gebiet rund um Melpitz sollen weitere Informationen bezüglich der zeitlich und räumlich variablen Grenzschichtstrukturen und Turbulenzentwicklung gewonnen werden. Die meteorologischen Einflüsse auf Partikelneubildungsereignisse und nachfolgende Transportprozesse stehen hierbei ebenfalls im Fokus der Analyse.

Introduction

The Campaign Melpitz Column was performed from May 4 until July 10, 2015. During this time a very complex setup of aerosol and boundary layer measurements was installed at the TROPOS measurement site Melpitz. Besides a detailed aerosol characterization on ground and ground-based remote sensing, several platforms performing airborne measurements were applied to investigate the aerosol distribution in the whole column (Fig. 1). The combination of several unmanned aerial systems (UAS), the helicopter-borne platform ACTOS (Airborne Cloud and Turbulence Observation System), research aircraft, and a tethered balloon within one campaign is unique and provides

a dataset that is subject to ongoing investigations. First selected results will be presented here together with results from a former study in Melpitz in 2013. On the other hand, ground-based measurements of aerosol particle composition have been performed over several years and these long time series help to put the Melpitz Column campaign into a longer time frame.

In addition to the measurements, regional modeling of aerosol transport and large eddy simulations have been performed which complement the Melpitz Column 2015 field experiments by providing additional information on sources and transport processes of tropospheric aerosol as well as the boundary layer development.

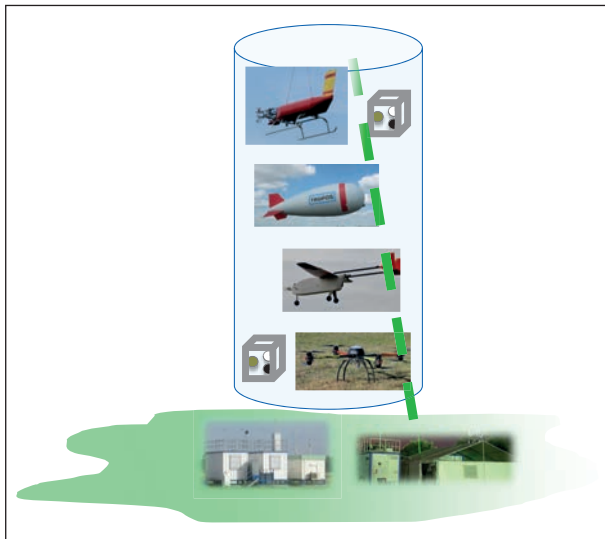


Fig. 1: Schematic of the Melpitz Column Experiment including ground-based, remote sensing and airborne measurements.

Overview on cloud and aerosol conditions

During the Melpitz Column campaign ground-based remote-sensing instruments of the Leipzig Aerosol and Cloud Observations System (LACROS) was operated continuously on site.

The instrumentation comprised active and passive remote sensing that spans from optical to microwave frequencies. Main instruments operated

during the Melpitz Column campaign were the multiwavelength Raman-polarization lidar Polly^{XT}, a 35-GHz cloud radar Mira-35, a Doppler wind lidar, and a microwave radiometer. Data of LACROS is routinely processed within Cloudnet [Illingworth et al., 2007]. One of the derived products is the aerosol and cloud target classification which is shown in Fig. 2 for the whole campaign period. It can be seen that low clouds, cirrus and precipitation occurred rather frequent. The in-situ flights of UAV and ACTOS were performed mainly during periods with little amounts of clouds as it was the case from 14 to 18 June, and the period after 24 June, with the exceptions of 27 and 29 June.

Comparison Remote Sensing – Airborne in-situ Measurements

Comparison Raman Lidar – in-situ aerosol measurements. The helicopter-borne platform ACTOS performed 12 measurement flights above the TROPOS research site Melpitz while the Raman Lidar Polly^{XT} [Engelmann et al., 2015] measured continuously at the site. ACTOS is equipped with instruments to measure basic meteorology with high time resolution [Siebert et al., 2006], aerosol parameter [Wehner et al., 2015], and for the first time also optical aerosol properties: extinction (at 630 nm) and absorption (at 450 nm, 525 nm and 624 nm). Selected profiles of

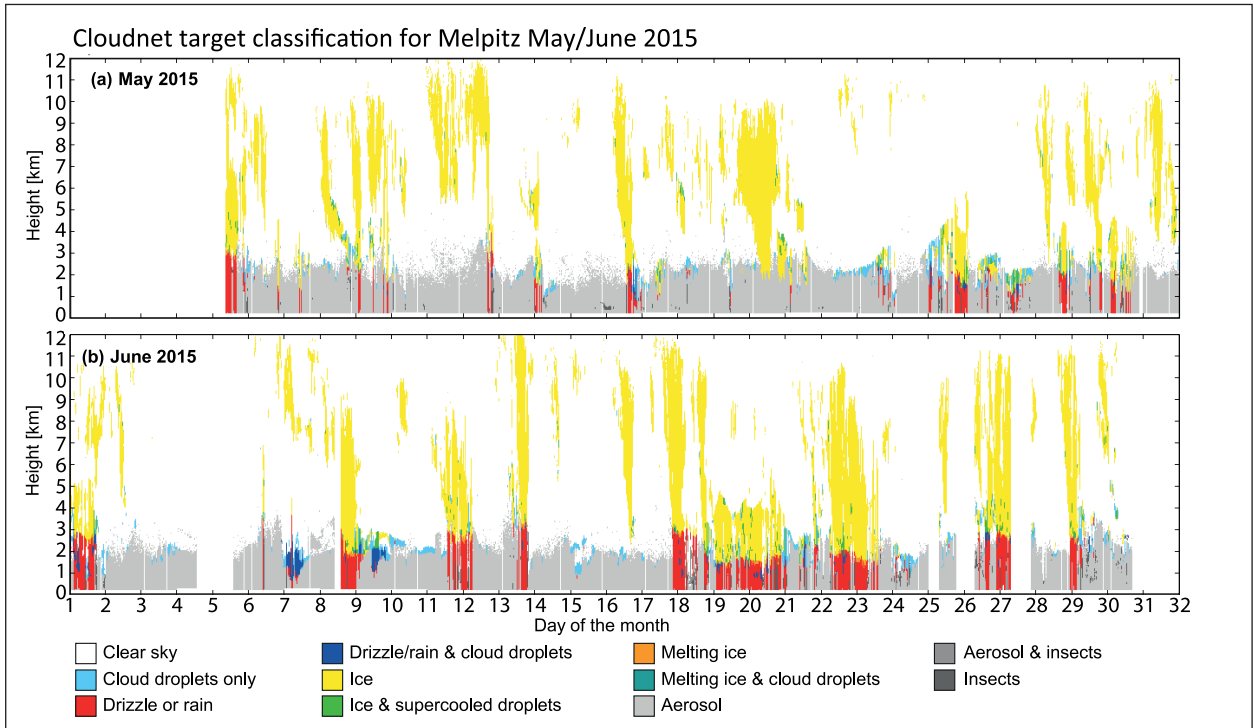


Fig. 2: Overview on the temporal evolution of the vertical structure of clouds, aerosol, and precipitation during the Melpitz Column Experiment by means of the Cloudnet target classification based on the remote sensing observations of the LACROS instrument suite.

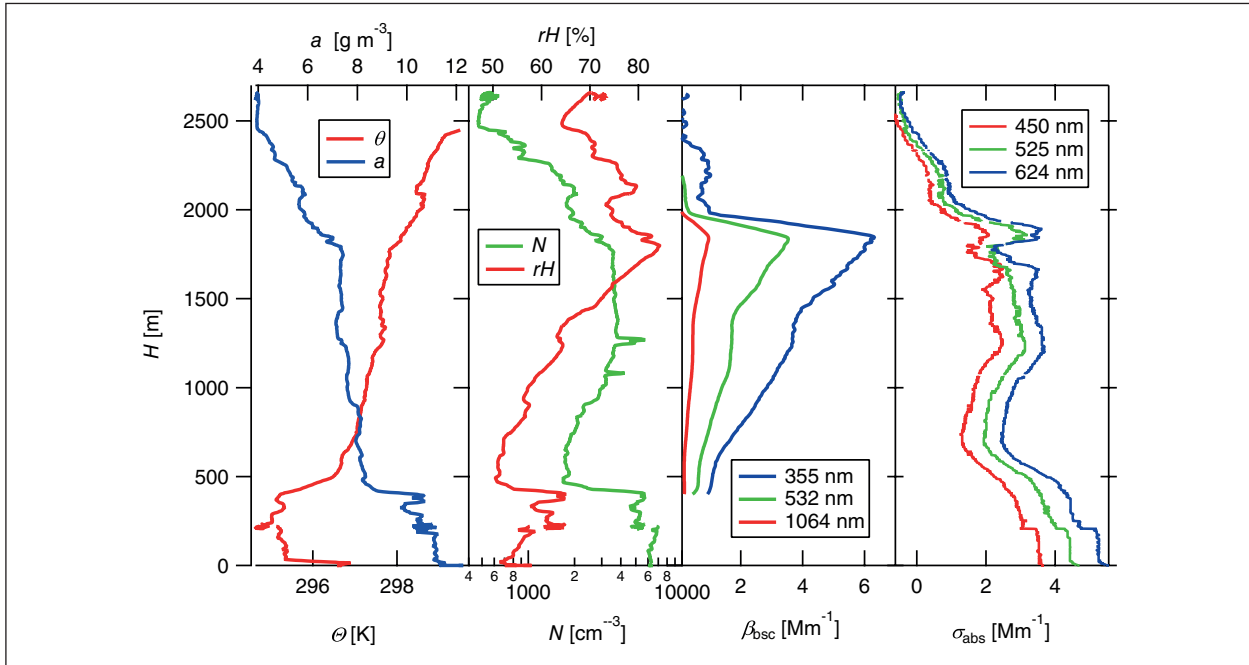


Fig. 3: Vertical profiles measured using ACTOS and Raman Lidar Polly^{XT} on June 26 2015. Presented parameters are: potential temperature (θ), absolute humidity (a), total particle number concentration (N) (all from ACTOS) particle backscatter coefficient β_{bsc} (from Polly^{XT}), and absorption coefficient σ_{abs} (from ACTOS) measured on June 26, 2015 are presented in Fig. 3.

potential temperature θ , absolute humidity a , relative humidity rH , total particle number concentration N (all from ACTOS) particle backscatter coefficient β_{bsc} (from Polly^{XT}), and absorption coefficient σ_{abs} (from ACTOS) measured on June 26, 2015 are presented in Fig. 3.

The profiles show a first temperature inversion between 400 and 500 m connected with significant decrease in N , a , and rH , while the decrease in σ_{abs} is smoother. The lidar measurements start in this height and represent the backscatter coefficient under ambient conditions in contrast to the in-situ measurements where the aerosol was dried below 40% rH before entering the measurement instruments. Figure 3 shows an increase in β_{bsc} similar to the increase in rH , caused by the associated hygroscopic growth of aerosol particles.

Aerosol particle number size distributions have also been measured in-situ in different heights. From these measurements optical properties such as backscatter and extinction will be calculated using Mie-theory in the next step and compared directly with the lidar measurements. This is a direct possibility to validate lidar-based retrievals of aerosol microphysical properties with parallel in-situ measurements.

Mean cloud turbulence observed by airborne in-situ and remote sensing. During the HOPE campaign in September 2013, several measurement flights in the Melpitz area have been performed. Here, we present an intercomparison between an ACTOS

flight in a stratocumulus (Sc) layer with observations performed by a vertically pointed Doppler lidar. The Sc layer was in a height of 1800 m and approximately 200 m thick. Both observations were spatially collocated; the 10 km-long flight path was about 500 m away from the Melpitz station where the remote sensing field was located.

The analysis focuses on a description of mean turbulence based on observations of the vertical wind velocity w . The ACTOS record comprises data sampled during a 20 km long flight path compared with a 12 km long record from the wind lidar. ACTOS observations are perpendicular to the mean flow whereas Lidar observations are along the mean wind by definition.

The upper panel of Fig. 4 shows w ranging from -1 to +1 m s^{-1} , which are typical values for Sc fields. The lower panel shows the probability density function PDF(w) which roughly follows a Gaussian function and agrees remarkably well for both observations with a similar standard deviation for both observations of $\sigma_w = 0.3 \text{ m s}^{-1}$. Both PDFs are roughly Gaussian as predicted for homogeneous and isotropic turbulence.

Figure 5 shows the power spectral density functions $F(k)$ of the vertical wind. For wavenumbers $k > 10^{-2} \text{ m}^{-1}$ both spectra show a clear power law behavior with a $-5/3$ -slope. Classical turbulence theory predicts $F(k) = \alpha \varepsilon^{2/3} k^{-5/3}$ for the inertial sub-range ($\alpha = 0.5$) from which the energy dissipation rate ε can

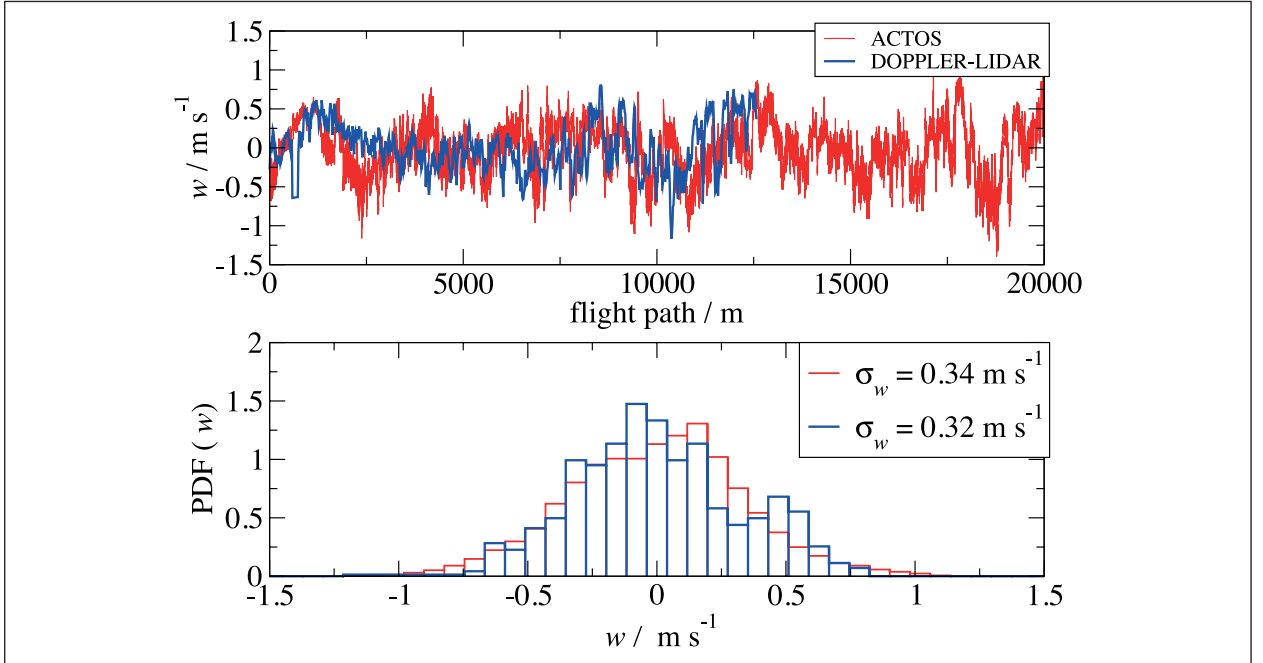


Fig. 4: Upper panel: Vertical wind velocities w along the 2 km long flight path of ACTOS (red curve) and along the mean wind passing the Doppler lidar (blue curve). Lower panel: the corresponding probability density functions PDF(w) with the standard deviations σ_w .

be estimated. The energy dissipation is widely used as a key parameter describing the turbulence intensity of a flow. Both systems yield almost the same value of $\varepsilon = 10^{-4} \text{ m}^2 \text{s}^{-3}$, typical for Sc [Siebert et al., 2010].

Due to the high spatial collocation of the airborne in-situ and remote-sensing observations,

this experiment provides high confidence that both systems sample the same areas of the cloud layer. The good agreement of the results indicates that both devices are suitable to characterize the dynamics and mean turbulent statistics of stratiform boundary layer clouds.

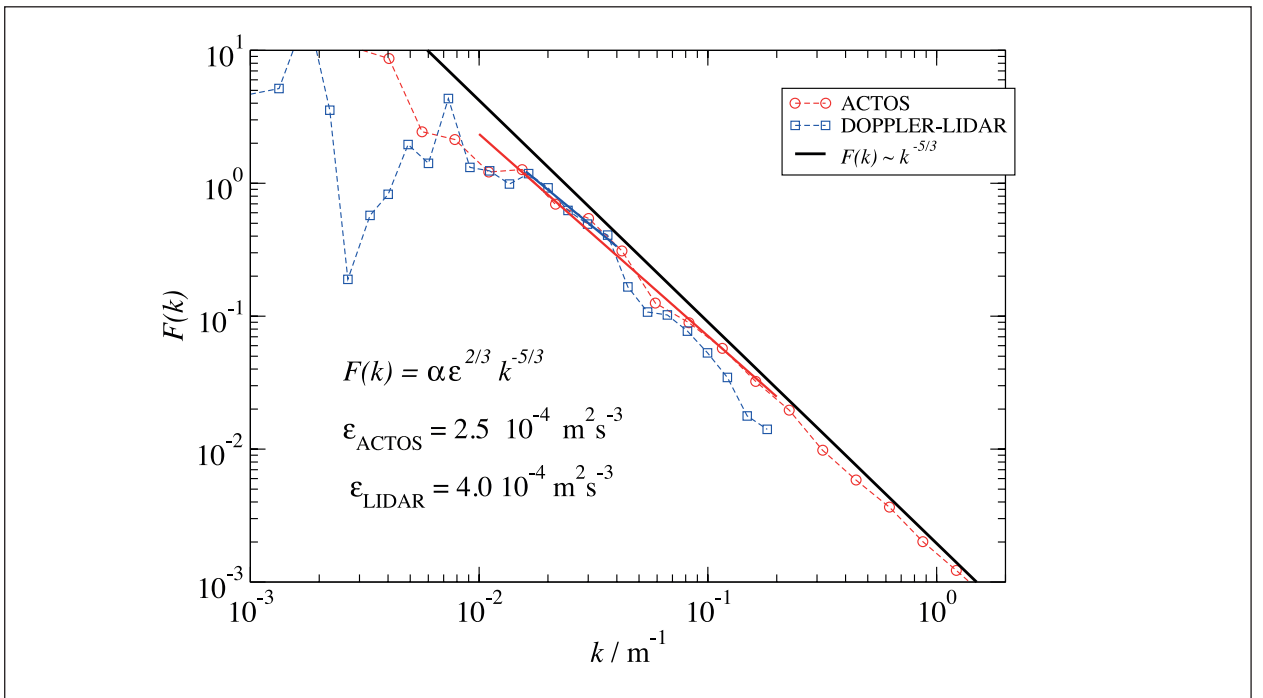


Fig. 5: Power spectral densities $F(k)$ based on ACTOS (red) and Lidar (blue) observations. A $-5/3$ -slope is included as reference for inertial subrange scaling, the estimated energy dissipation rates are presented.

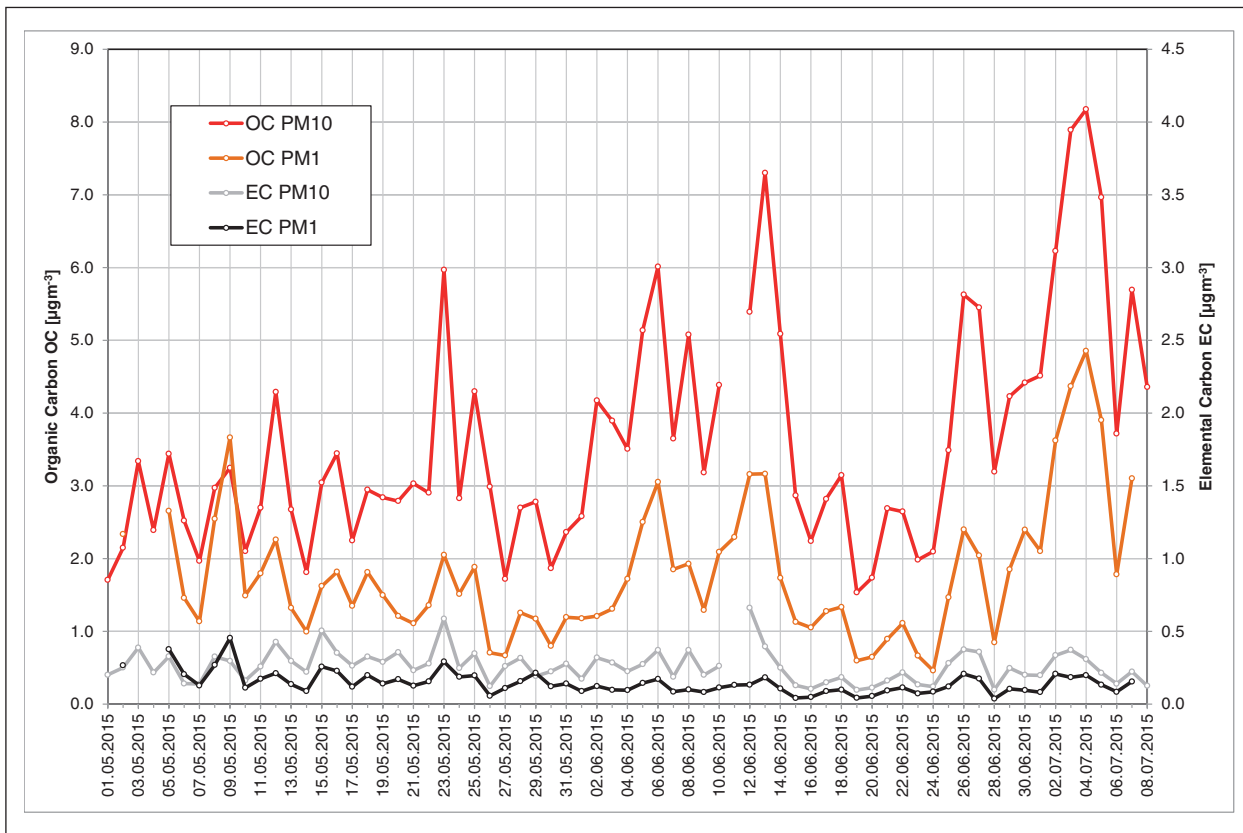


Fig. 6: Daily mean concentration of OC and EC in PM_{10} and PM_1 , (thermo-optical detection) at Melpitz site (1st of Mai until 8th of July 2015).

Thermo-optical OC and EC measurements at ground in a long-term context

High-Volume (HV) samples were taken on quartz fibre filters, daily for PM_{10} , $\text{PM}_{2.5}$ and PM_1 , at the Melpitz site [Spindler et al., 2013]. The organic carbon (OC) and the elemental carbon (EC) content (in sum total carbon, TC) at the filters were quantified using an off-line thermo-optical method [TO, Karanasiou et al., 2015]. Figure 6 shows the daily concentration of OC and EC in PM_{10} and PM_1 at the Melpitz site around the timeframe of the Melpitz Column period. The OC concentration in PM_{10} was found in the range 1.5 to 8.2 $\mu\text{m m}^{-3}$ and the EC concentration was in the range 0.1 and 0.7 $\mu\text{m m}^{-3}$, respectively.

The daily OC/EC ratio for PM_{10} varies in the range between 6.0 and 34.8, with a typical summer mean of 15.1 for a location in the middle European background influenced by air mass inflow from West. The OC/EC mean ratio for PM_1 is about 13.7 because the EC-content relatively to OC in the smaller particles is slightly higher.

During the Melpitz Column campaign the concentration of elemental carbon in PM_{10} is relatively low (0.26 $\mu\text{g m}^{-3}$). Figure 7 shows the daily EC concentration is shown together with the daily mean sector of air mass inflow since 2012 in Fig. 7. The

EC-concentrations are higher in winter, when the temperatures are low and emissions from anthropogenic burning processes are higher as in summer. The air mass inflow influences the EC-concentrations additionally. Continental, mostly dry air masses, show at one hand higher concentrations due to lower wind velocities as marine air masses with higher turbulence and enclosed rain showers. On the other hand, the emissions in the source regions in direction East or West are completely different [Spindler et al., 2012 and 2013]. Source regions with emissions from combustion processes especially individual coal fired ovens and forest fires are located in a sector east of Melpitz and EC can arrive via long-range transport. During the Melpitz Column campaign (8th May – 8th July 2015), 82% of the days show an air mass inflow from West, only 8% of days show an air mass inflow East and 10% of days could not be accessed. For the time January 2012 until November 2015 60% are West and 19% are East days and 21% could not be accessed. That demonstrates that the Melpitz Column campaign was much less influenced by continental air masses as it is for Melpitz over a longer timeframe. The method for calculating the daily mean sector for air mass inflow using 96-backward-trajectories is described in Spindler et al. [2013].

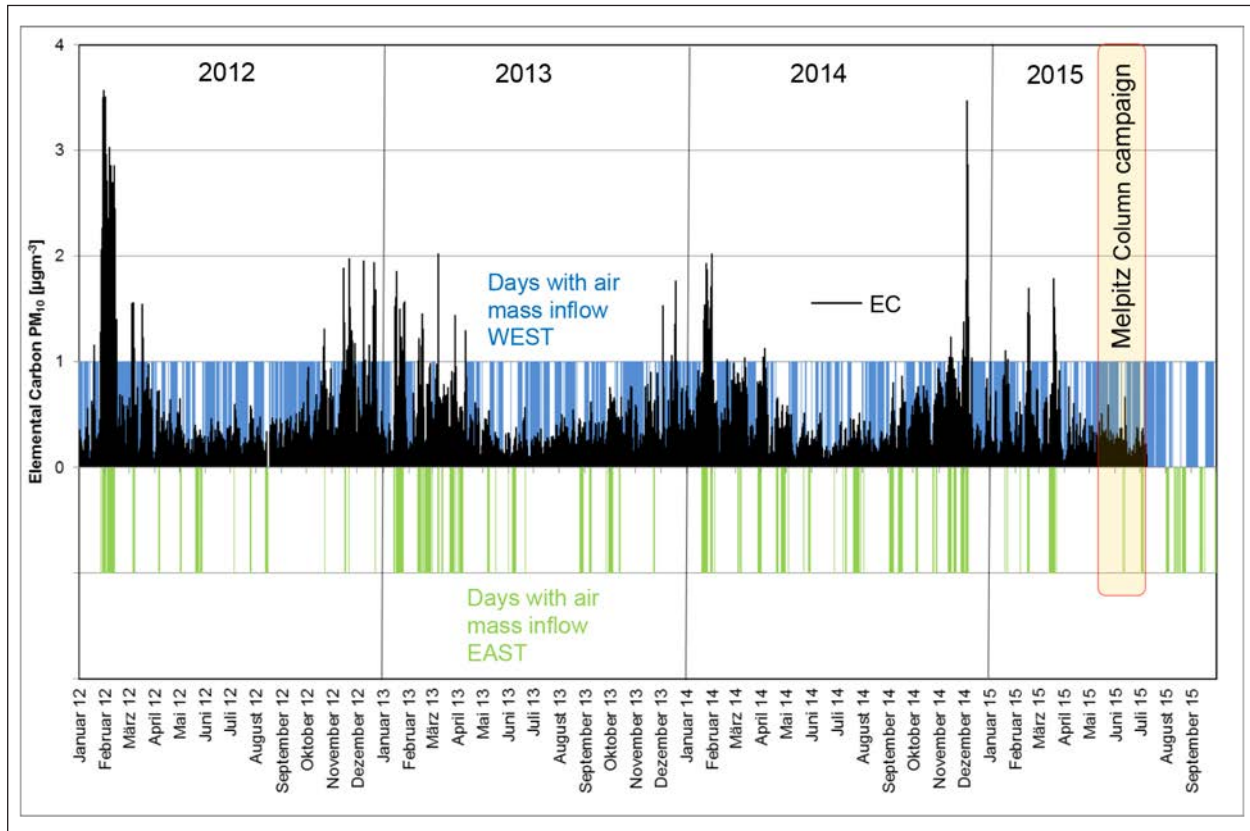


Fig. 7: Daily mean concentration of EC in PM_{10} (thermos-optical detection) at Melpitz site (1st January 2012 until 30th of September 2015). Days with an mean air mass inflow West or East are shown a blue or green bars, respectively. The time frame of the Melpitz Column campaign (1st of May until 8th of July is marked).

Regional and micro scale modelling with COSMO-MUSCAT and ASAM

Regional modelling of aerosol transport and large eddy simulations, respectively, complement the Melpitz Column 2015 field experiments by providing additional information on sources and transport processes of tropospheric aerosol as well as the boundary layer development:

Regional aerosol transport modelling. Aerosol transport simulations have been performed for the field experiment Melpitz Column 2015 using the coupled model system COSMO-MUSCAT (COnsortium for Small-scale Modeling – MUltiScale Chemistry Aerosol Transport). The model system, which describes the dynamics and transformation of tropospheric aerosol and relevant trace gases, has been developed at TROPOS for predicting air pollution dispersion at local and regional scale and process studies [e.g., Wolke et al., 2012].

The modelled period spans from 1 May to 3 July 2015. The simulations are run with 7 km horizontal grid spacing on a model domain covering Central Europe. Future model runs will include a

second, one-way nested domain centred on the Melpitz field site with 1.5 km grid spacing. Operational forecasts from the European Centre for Medium-Range Weather Forecasts (ECMWF) are used to initialize and force boundaries of the 7 km run, and Monitoring Atmospheric Composition and Climate (MACC) aerosol forecasts provide the input for atmosphere-chemical boundary conditions. The inner nest will then be driven with the initial and boundary conditions provided by the 7 km run.

The regional aerosol transport modelling will help interpret the aerosol measurements by putting them into a broader spatio-temporal context and may prove the representativeness of ground-based observations. Once thoroughly evaluated with operational and field campaign observations, the COSMO-MUSCAT results will be used to study the relative importance of local sources and long-range transport to the local aerosol conditions (See Fig. 8 for an example of the modelled aerosol distribution). In addition, the impact of aerosol-ageing and mixing processes on particle properties will be investigated. The initial simulations use a mass-based approach for the description of aerosol processes in MUSCAT. At a later stage, the extended version of the modal aerosol model M7 could be

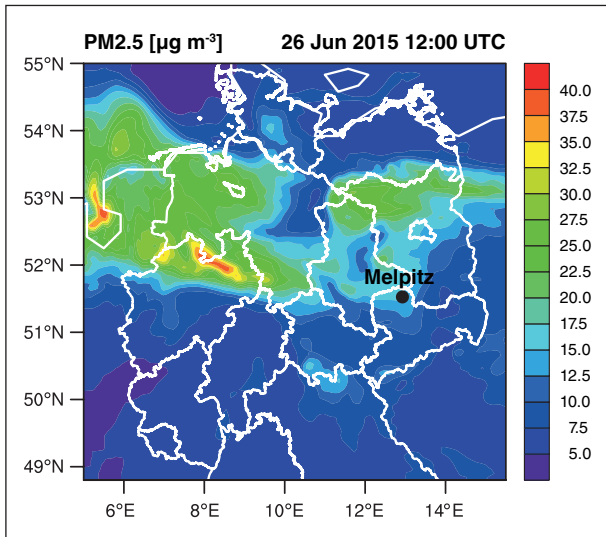


Fig. 8: Map of the fine particulate matter (PM2.5) concentration at surface level as computed with COSMO-MUSCAT for 26 June 2015, 12:00 UTC.

utilised to study the sensitivity of the results against a more detailed aerosol modelling. It is also planned to quantify the direct radiative forcing of (carbon-containing) aerosol and related dynamical effects. Since, however, ground-based in-situ measurements and remote sensing at Melpitz show below average levels of total particulate matter and, in particular, black carbon ('soot') concentrations throughout May and June 2015, it will be interesting to investigate whether

the observed aerosol conditions can be reproduced by the model and what the implications are for the radiation budget.

Large eddy simulations of boundary layer processes and turbulence. The large amount of available data gained during Melpitz Column 2015 is a very good opportunity for performing high-resolution large eddy simulations (LES). Since the results of LES are very sensitive to the forcing, especially surface fluxes, high-quality input data is necessary to obtain reliable modelling results. In this framework, simulations will be performed with the fully compressible, non-hydrostatic model ASAM (All Scale Atmospheric Model). The model utilizes a new physics package, including a multi-layer soil model and a land-use model with 9 different land classes. Radiative forcing (direct, diffuse and terrestrial irradiance) will be directly used from the thermopile pyranometers of TROPOS' MORDOR (MOBILE RaDiation ObserveRvatory) system. Hourly resolved soil parameters like temperature and humidity are available from the nearby DWD (Deutscher Wetterdienst, German Weather Service) station "Klitzschen bei Torgau," which is only 3 km away from the field site and thus can be considered as representative for the Melpitz area. Figure 9 shows the land use map for a $40 \times 40 \text{ km}^2$ domain with Melpitz located at the domain centre. The nearest city, which is described by the land class "urban area," is Torgau northeast of

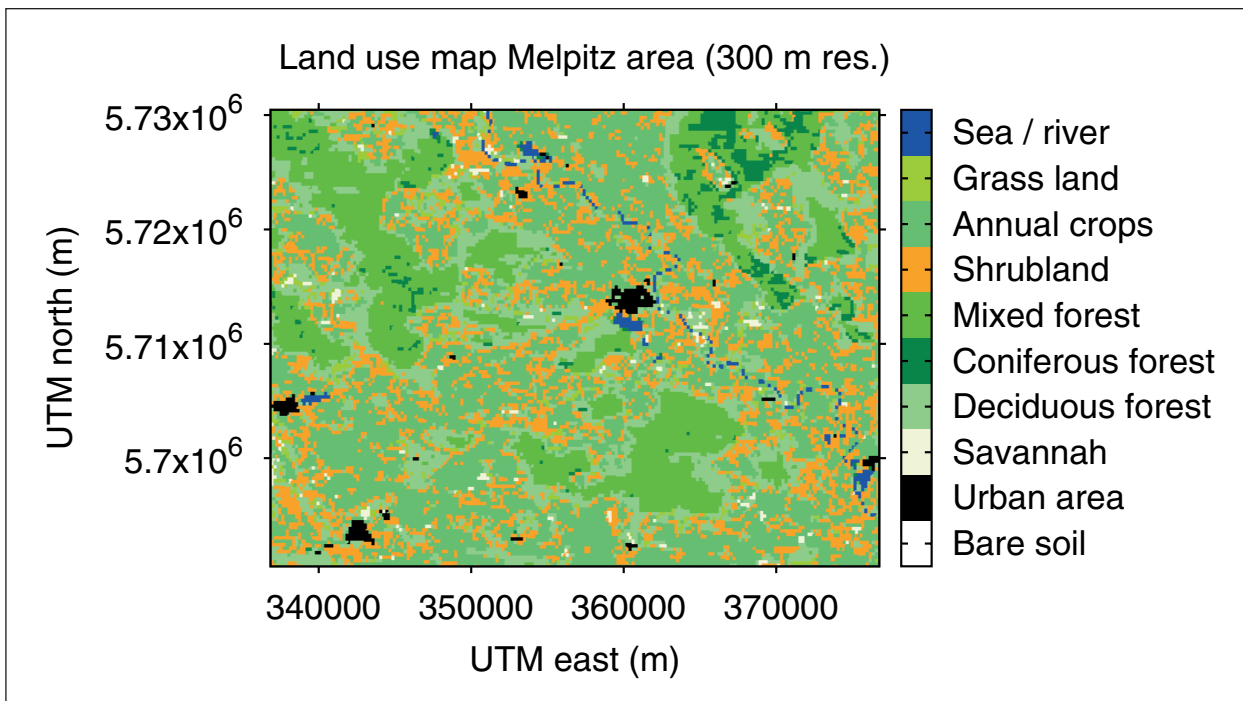


Fig. 9: Land use map in UTM coordinates (Universal Transverse Mercator) for a domain of $40 \times 40 \text{ km}^2$ around Melpitz. The land classes shown as labels are the same as used in ASAM for the surface parameterization.

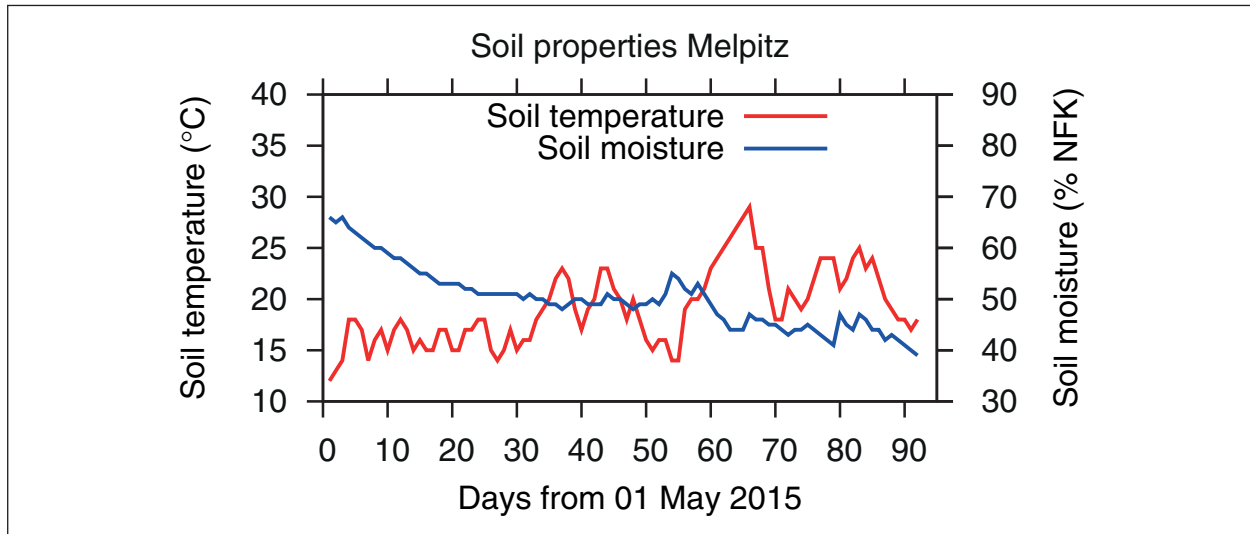


Fig. 10: Time series of daily averaged soil properties during the campaign time (May-July 2015). The soil moisture is expressed as percent plant useable water (% nFK).

Melpitz. The Elbe river flows in northwest direction passing Torgau. The surrounding area is characterized by a mixture of shrubland, annual crops and different forest types. These different land use types are related to different surface parameters like roughness length, plant cover, leaf area index, root depth etc. All these parameters influence the calculation of the surface fluxes in the LES model. Thus it is very likely that the boundary layer development will show a distinct dependence on wind direction due to the surface heterogeneity.

Not only land use, but also soil parameters have to be taken into account. Figure 10 shows the temporal variation of daily averaged soil temperature (expressed as the temperature in 5 cm depth) and soil moisture (in 60 cm depth under grass). Depending on the meteorological situation, the difference between maximum and minimum values during the campaign time are about 17 K for soil temperature and 25% for soil moisture, respectively. The COSMO-MUSCAT output serves as input data for the LES runs. To capture large-scale changes in the atmospheric state, which cannot be resolved by LES directly, a nudging term derived from the COSMO output every three hours is applied to the tendency equations of momentum, temperature and moisture.

After acquiring a consistent picture of the boundary layer structure from the LES modelling results, another focus of the analysis lies on new particle formation (NPF) events. Especially the connection of the spatiotemporal distribution of meteorological parameters to NPF events will be examined. Additionally, a tracer analysis can point out subsequent particle transport processes within the atmospheric boundary layer.

Summary

The field campaign Melpitz Column was successfully performed at the TROPOS field site Melpitz from May to beginning of July 2015. A very complex setup of ground-based instruments was installed to provide a detailed physical and chemical characterization of aerosol particles. In addition, several airborne platforms have been used to provide in-situ measurements of aerosol properties and meteorological parameters in the column during an intensive period within the campaign. Also vertical measurements have been performed continuously using remote sensing instrumentation of the LACROS facility, such as the Raman Lidar Polly^{XT} and a wind lidar. In-situ aerosol measurements will be used to calculate optical properties which will be directly compared with particle backscatter measured by the lidar. The comparison of the vertical wind velocity measured by ACTOS and a Doppler lidar within a cloud shows a good agreement which provides high confidence that both systems sample the same areas of the cloud layer. The good agreement of the results indicates that both devices are suitable to characterize the dynamics and mean turbulent statistics of stratiform boundary layer clouds.

The long-term measurements of chemical particle composition, i.e. the measurements of carbon concentration (EC/OC) being an indicator for anthropogenic pollution show that the period of Melpitz Column was relatively clean compared to former years and seasons. The EC/OC concentration in Melpitz is mainly determined by the air mass origin. During Melpitz Column clean westerly air mass were dominating.

In parallel simulations using the chemistry-transport model COSMO-MUSCAT have been performed. The regional aerosol transport modelling will help to interpret the aerosol measurements by putting them into a broader spatio-temporal context and may prove the representativeness of ground-based observations. In addition, particle aging and mixing can be analysed as well as aerosol-radiation interaction.

Highly resolved large-eddy simulations for the area around Melpitz will be used to obtain further information on the temporal and spatial variation of the boundary layer structures and turbulence. Furthermore, the influence of the meteorology on new particle formation events and following aerosol transport will be one focus of the analysis. Data analysis and modelling will be continued in the future.

References

- Engelmann, R., T. Kanitz, H. Baars, B. Heese, D. Althausen, A. Skupin, U. Wandinger, M. Komppula, I. S. Stachlewska, V. Amiridis, E. Marinou, I. Mattis, H. Linné and A. Ansmann (2015), EARLINET Raman Lidar PollyXT: the neXT generation, *Atmos. Meas. Tech. Discuss.*, 8(7), 7737-7780.
- Illingworth, A. J., R. J. Hogan, E. J. O'Connor, D. Bouniol, J. Delanoë, J. Pelon, A. Protat, M. E. Brooks, N. Gaussiat, D. R. Wilson, D. P. Donovan, H. K. Baltink, G. J. van Zadelhoff, J. D. Eastment, J. W. F. Goddard, C. L. Wrench, M. Haefelin, O. A. Krasnov, H. W. J. Russchenberg, J. M. Piriou, F. Vinit, A. Seifert, A. M. Tompkins and U. Willén (2007), Cloudnet, *Bull. Amer. Meteor. Soc.*, 88(6), 883-898.
- Karanasiou, A., M. C. Minguillón, M. Viana, A. Alastuey, J.-P. Putaud, W. Maenhaut, P. Panteliadis, G. Močnik, O. Favez, and T. A. J. Kuhlbusch (2015) Thermal-optical analysis for the measurement of elemental carbon (EC) and organic carbon (OC) in ambient air a literature review. *Atmos. Meas. Tech. Diss.*, 8, 9649-9712, doi:10.5194/amt-8-9649-2015.
- Siebert, H., H. Franke, K. Lehmann, R. Maser, E. W. Saw, D. Schell, R. A. Shaw, M. Wendisch (2006), Probing Finescale Dynamics and Microphysics of Clouds with Helicopter-Borne Measurements, *Bull. Amer. Meteor. Soc.*, 87(12), 1727–1738.
- Siebert, H., R. A. Shaw, and Z. Warhaft (2010), Statistics of small-scale velocity fluctuations and internal intermittency in marine stratocumulus clouds. *J. Atmos. Sci.*, 67:262 – 273.
- Spindler, G., T. Gnauk, A. Grüner, Y. Linuma, K. Müller, S. Scheinhardt, and H. Herrmann (2012), Size-segregated characterization of PM₁₀ at the EMEP site Melpitz (Germany) using a five-stage impactor: a six year study, *J. Atmos. Chem.*, 69, 127-157, doi:10.1007/s10874-012-9233-6.
- Spindler, G., A. Grüner, K. Müller, S. Schlimper, and H. Herrmann (2013), Long-term size-segregated particle (PM₁₀, PM_{2.5}, PM₁) characterization study at Melpitz - influence of air mass inflow, weather conditions and season, *J. Atmos. Chem.*, 70(2), 165-195, doi:10.1007/s10874-013-9263-8.
- Wehner, B., F. Werner, F. Ditas, R. A. Shaw, M. Kulmala and H. Siebert, Observations of new particle formation in enhanced UV irradiance zones near cumulus clouds, *Atmos. Chem. Phys.*, 15(20), 11701-11711, 2015.
- Wolke, R., Schröder, W., Schrödner, R., and Renner, E. (2012), Influence of grid resolution and meteorological forcing on simulated European air quality: A sensitivity study with the modeling system COSMO-MUSCAT. *Atmos. Environ.*, 53, 110-130, doi:10.1016/j.atmosenv.2012.02.085.

Funding

- European Union (EU), Brussels, Belgium
 German Federal Ministry of Education and Research (BMBF), Bonn, Germany
 German Research Foundation (DFG), Bonn, Germany
 Saxon State Agency of Environment, Agriculture and Geology (LfULG), Dresden, Germany

Cooperation

- Technical University Braunschweig, Germany
 University of Tübingen, Germany
 University of Bayreuth, BayCEER, Germany
 Technical University Darmstadt, Germany
 Deutscher Wetterdienst (DWD), Germany
 Paul Scherrer Institute, Villigen, Switzerland

Regional air quality in Leipzig: Results from a source apportionment study of size-resolved aerosol particles

Dominik van Pinxteren¹, Gerald Spindler¹, Konrad Müller¹, Kanneh Wadinga Fomba¹, Yoshiteru Iinuma¹, Fabian Rasch¹, Kay Weinhold¹, Wolfram Birmili¹, Alfred Wiedensohler¹, Gunter Löschau², Andrea Hausmann², Hartmut Herrmann¹

¹ Leibniz Institute for Tropospheric Research (TROPOS), Leipzig, Germany

² Saxon State Agency for Environment, Agriculture and Geology (LfULG), Dresden, Germany

In den Jahren 2013 – 2015 wurden umfangreiche Untersuchungen zu den Quellen partikulären Materials (PM) im Raum Leipzig durchgeführt. Durch partikelgrößenaufgelöste Bestimmung chemischer Hauptbestandteile sowie charakteristischer Markerverbindungen konnten eine Reihe wichtiger Quellen identifiziert und quantifiziert werden. Ultrafine Partikelmasse stammte im Sommer überwiegend aus Verkehr und photochemischen Sekundärquellen, während im Winter regionale bzw. antransportierte Emissionen aus der Verbrennung von Festbrennstoffen dominierten. PM im Gößenbereich des Akkumulationsmodes stammte überwiegend aus sekundären Quellen sowie aus Biomasse- und Kohleverbrennung im Winter. Die Hauptquellen grober Partikel waren unterschiedlich je nach betrachteter Standort/Jahreszeit/Anströmungskategorie und beinhalteten Seesalz, Stadtstaub, Verkehrsemissionen, Pilzsporen und Biomasseverbrennung. Die höchsten lokalen Reduktionspotentiale zeigten sich für Verkehrsemissionen, während für sekundäres Material und Festbrennstoffemissionen großflächigere Reduktionsmaßnahmen notwendig sind.

Introduction

Many cities in Europe and Germany, including Leipzig, are still challenged to comply with legal limit values, especially for pollutants such as NO_x and particulate matter (PM). As a major prerequisite for further efficient mitigation strategies, detailed knowledge of PM sources and their quantitative impacts at different sites is needed. To this end, the TROPOS has been cooperating since many years with the Saxon State Agency for Environment, Agriculture and Geology to study air quality and PM sources in Leipzig and surrounding areas. In 2013-2015, a PM source apportionment study took place at 4 sampling sites in the Leipzig area with continuous and non-continuous measurements of aerosol particles and their chemical composition. The comprehensive dataset served as the basis for detailed source apportionment using approaches of different complexity.

Methods

Particle sampling was performed at 4 sites in parallel: Leipzig-Mitte (LMI, traffic site), Eisenbahnstrasse (EIB, traffic and residential site), TROPOS (TRO, urban background site) and Melpitz (MEL, regional background site). Size-resolved sampling of aerosol particles was performed on 42 days in winter and summer for 24 hours using a 5-stage Berner-type impactor. In addition, continuous measurements of particle number size distributions and black carbon concentrations took place.

Particle samples were analysed for inorganic ions, organic and elemental carbon, water-soluble organic carbon, oxalate, monosaccharides, alkanes, polycyclic aromatic hydrocarbons, hopanes, and trace metals applying established methods at the atmospheric chemistry department of TROPOS.

Source apportionment was performed by positive matrix factorisation (PMF) applying the EPA PMF 5.0 software. PMF was performed separately for each of the 5 particles, leading to the quantification of PM

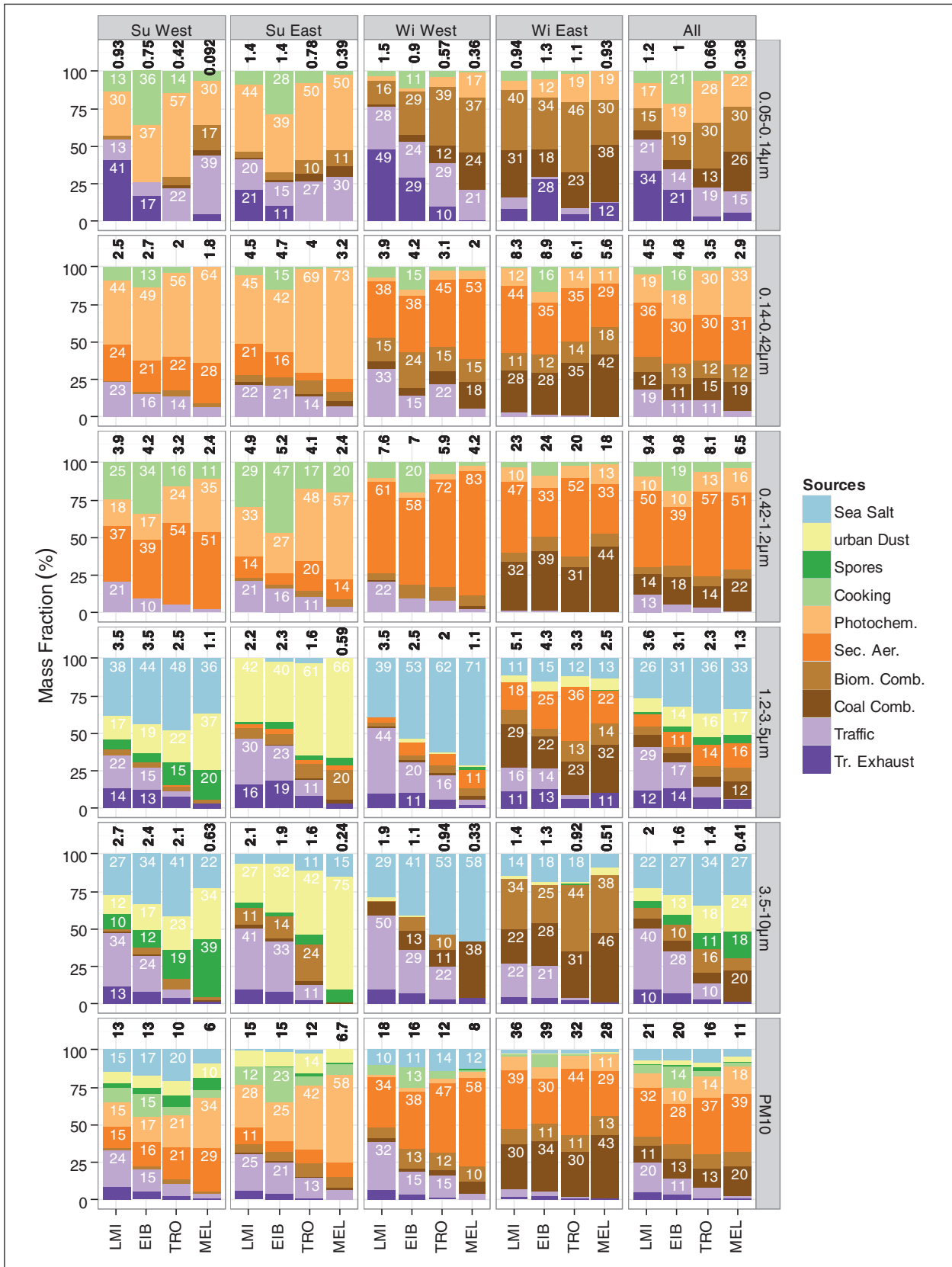


Fig. 1: Mean relative source contributions in different particle size ranges (including PM_{10}) at the 4 sites. Mean particle mass concentrations ($\mu g m^{-3}$) are printed in black on top of stacked bars. Numbers in white indicate the respective mass fractions (not shown if <10%). Data are given for two seasons (summer, "Su" winter, "Wi"), two main air mass inflow regimes (western inflow, "West"; eastern inflow, "East"), and as total campaign average ("All").

sources in quasi-ultrafine particles (aerodynamic diameter of 50-140 nm), accumulation mode particles (0.14-0.42 µm and 0.42-1.2 µm), and coarse particles (1.2-3.5 µm and 3.5-10 µm). Assignment of sources to the PMF factors was based on their chemical profiles (main constituents and characteristic tracers in factor) and their temporal concentration patterns at the different sites.

Results

In Fig. 1 the relative mean contributions of PMF-resolved sources are given for all 4 sites in different categories.

Ultrafine particles in summer originated mainly from traffic-related sources and photochemistry with ultrafine mass fractions of about 20-50% and 30-50%, respectively. At EIB a tentatively identified cooking source contributed about 1/3 to ultrafine particle mass. Particles from solid fuel combustion (mainly biomass combustion) strongly increased in winter explaining typically 50-70% of ultrafine particle mass.

Main sources of **accumulation mode particles** in summer were of secondary nature. The sum of two identified secondary PMF sources ("photochemistry" and more general "secondary aerosol") typically contributed about 60-90% to particle mass. Traffic contributed another 10-20% at the urban sites and cooking aerosol showed mean contributions up to about 50% at the residential EIB site. During winter, increased contributions from the general secondary aerosol (about 30-80%) and the solid fuel combustion sources (about 10-60%) were observed. Solid fuel combustion particle mass was dominated by biomass combustion during western inflow with generally much lower concentrations and coal combustion during eastern inflow with significantly increased source contributions.

For **coarse mode particles** the main sources were more diverse. In summer they included sea salt, urban dust, exhaust and general traffic emissions, fungal spores, and biomass burning. In winter, contributions from urban dust and fungal spores diminished, while the importance of biomass combustion for coarse particle mass increased, especially for eastern air mass origin. Coal combustion appeared as an additional important source in "Winter East".

In summary for **PM₁₀ mass concentrations**, traffic, secondary, and solid fuel combustion particles were identified as the most important sources in Leipzig. At the most polluted site, traffic typically contributed 30-40%, indicating a high potential for PM reductions. About half of traffic particle mass was in the coarse and 15% in the ultrafine size range. Technologies to reduce traffic emissions across the full particle size range would thus be favourable for improvements of PM at kerbside sites. Secondary material was another major source of PM at the urban sites (approx. 45% of PM₁₀ on average). However, 80% of it originated from regional sources, indicating that larger-scale reductions of precursors would be required to substantially reduce urban concentration values. Biomass combustion contributed about 10% to urban PM₁₀ concentrations in winter with up to 60% of it originating from local emissions in a residential area. Measures to minimise its impact on urban air quality thus seem reasonable. Finally, coal combustion was another major PM source when air masses in winter arrived from eastern European regions to the study area, explaining 30-40% of PM₁₀. PM₁₀ concentrations were generally highest in this scenario, including most of the EU limit exceeding days in this study. Therefore, continued efforts to reduce emissions on an EU wide level will help to improve air quality not only locally in the emission regions, but also on a larger scale by reducing trans-boundary pollution transport.

Funding

Funding of the project by the Saxon State Agency for Environment, Agriculture and Geology (LfULG) is acknowledged.

Spatial and temporal distribution of black carbon in the metropolitan area of Manila, Philippines

Simonas Kecorius¹, Thomas Müller¹, Wolfram Birmili¹, Kay Weinhold¹, Konrad Müller¹, Everlyn Tamayo², Mylene Cayetano², Honey Dawn Alas³, James Simpas³, Edgar Valla⁴, Hartmut Herrmann¹, Alfred Wiedensohler¹

¹ Leibniz Institute for Tropospheric Research (TROPOS), Leipzig, Germany

² University of Philippines Diliman, Manila, Philippines

³ Ateneo University, Manila Observatory, Manila, Philippines

⁴ De La Salle University; Manila, Philippines

Metro Manila, die Hauptstadt der Philippinen, hat mehr als 11,8 Millionen Einwohner und unterliegt einer rasch zunehmenden Luftverschmutzung. Mit der Entwicklung der Wirtschaft und wachsenden Wohlstand hat sich die Zahl der registrierten Kraftfahrzeuge von 1990 bis 2013 verfünfacht und erreichte Ende 2013 die Anzahl von 7,7 Millionen. Dieser rasche Anstieg der Fahrzeugflotte führte zu signifikant erhöhten Aerosolpartikel-Emissionen. Verkehrsbedingte Quellen sind für mehr als 60% der Feinstaubemission der Philippinen verantwortlich. Um die zukünftige Forschung voranzubringen und Informationen für politische Entscheidungsträger und Interessengruppen bereitzustellen, wurde die Intensiv-Aerosolmesskampagne MACE 2015 „Manila Aerosolcharakterisierung Experiment“ (März bis Juni 2015, Metro Manila) durch das Leibniz-Institut für Troposphärenforschung (TROPOS) und das philippinischen Forscherkonsortium „Researchers for Clean Air (RESCueAir)“ ins Leben gerufen. Der Hauptschwerpunkt der Messkampagne war die Untersuchung der räumlichen Variabilität und der Belastung von schwarzem Kohlenstoff (Ruß) in Metro Manila.

Introduction

Metro Manila, the capital of the Philippines, accounts for more than 11.8 million inhabitants and being the densest populated region in Philippines faces the rapidly increasing threat of air pollution. With the developing economy and growing wealth, the number of registered motor vehicles has quintupled from 1990 to 2013 and reached 7.7 million [LTO, 2013]. This rapid increase of vehicle fleet results in higher combustion generated aerosol emissions, which in turn becomes a dominant aerosol source in the urban atmosphere. Emission inventories report that traffic-related sources are responsible for more than 60% of the total country's particulate matter emission in Philippines [Vergel and Tiglao, 2013].

Aerosol particles, which are predominantly soot from diesel-fueled vehicles, contain heavy metals and Polycyclic Aromatic Hydrocarbons (PAHs). These particles are as small as 100 nm that can deeply penetrate into the respiratory system. It poses increased risks of childhood asthma, cancer, heart malformations and even premature deaths [Lee,



Fig. 1: Air pollution over Manila, Philippines.

2010]. Moreover, model projections indicate that by 2050 the contribution of ambient air pollution to premature mortality will double, and yet, Manila stakeholders and policy makers for the protection of public health rely on outdated clean air acts and regulations [Krupnick et al., 2003; Lelieveld et al., 2015].

Manila Aerosol Characterization Experiment 2015 (MACE 2015)

To guide future research and to provide information for policymakers and stakeholders, an

intensive aerosol research experiment called the "Manila Aerosol Characterization Experiment 2015" (MACE 2015), was carried out and jointly organized by the Leibniz Institute for Tropospheric Research (TROPOS) and the Consortium "Researcher for Clean Air" (RESCueAir) from March to June, 2015. RESCueAir is a consortium of researchers and academics from the University of the Philippines (UP) Diliman, the Manila Observatory (MO) of the Ateneo de Manila University (ADMU), De La Salle University (DLSU) and the Philippine Nuclear Research Institute (PNRI).

One stationary aerosol observational site was set-up at Manila Observatory (N 14.6359, E 121.0781) to investigate the properties of urban background aerosol. In parallel, the TROPOS aerosol measurement container was positioned at two distinct road-sites: Katipunan Ave. (N 14.6352, E 121.0745; March to May) and Taft Ave. (N 14.5656; E 120.9937, May to June) to understand the contribution of different vehicular fleet particulate emissions to traffic-related pollution. To recover the spatial distribution of urban aerosols at street level, additionally, a mobile measurement platform was designed and used daily to map aerosol particle properties on pre-defined routes.

Ambient Particle Number Size Distribution (PNSD) in a size range from 10 nm to 10 μm was measured using the combination of Mobility and Aerodynamic Particle Size Spectrometers. Particle light absorption and scattering coefficients were measured with a Multiple Angle Absorption Photometers (MAAP) and an integrating nephelometer, respectively. The particle light absorption coefficient was used to derive black carbon (BC) mass concentrations. Additionally, a Volatility Tandem Differential Mobility Analyzer (VTDMA), Condensation Particle Counters (CPC) and seven wavelength aethalometer were deployed to provide insights about mixing state, number concentration variability and the organic component of aerosol particles with a focus on soot particles. The mobile platform included CPC, portable aethalometer and Optical Particle Size Spectrometer. For off line analysis, a 5-stage Berner Impactor was used at Manila Observatory and at the Katipunan Ave. road site to measure particulate PAH mass size distribution. All instruments warrant a high degree of inter-comparability [Müller et al., 2011; Wiedensohler et al., 2012].

Results

Road and urban background sites. Diurnal variations of the black carbon (BC) mass concentration and the PNSD are shown in Fig. 2 for the whole measurement campaign. In the same figure, the BC

dependence on wind direction is presented in a polar plot. It can be seen that in all sites the physical properties of aerosol particles are highly variable. First, two contour plots show typical urban PNSDs at road sites, where ultrafine particles dominate the particle number size distribution. The lowest BC mass concentration measured at road sites were somehow similar, 12 and 14 $\mu\text{g m}^{-3}$ at Katipunan Ave. and Taft Ave., respectively. The same stands for the maximum values reaching 33 and 47 $\mu\text{g m}^{-3}$ of BC mass concentration at the mentioned sites. In comparison, these maximum BC mass concentrations are about factor of 10 higher than at a typical street site in Europe (e.g. Leipzig, Germany). However, the time of the day, when the maximum and minimum values were observed was different. At the Katipunan Ave., the minimum values were registered late afternoon and the maximum - around midnight. The lowest and highest BC mass concentrations at Taft Ave. were measured around 3 a.m. and from 6 to 9 a.m., respectively. It can also be seen that the increases in ultrafine particle number and BC mass concentrations at road sites are closely related. Traffic count data from Taft Ave. show an increase in vehicle number by a factor of 6 from 3 to 8 a.m. supporting the evidence that the variation of aerosol particle properties is directly linked to anthropogenic activities. Polar plot also reveal the dependency between wind direction and BC mass concentration (Fig. 2, right). At Katipunan Ave., the highest BC mass concentrations appear when the westerly winds prevail. It also shows the highest BC values are measured at nighttime. In Taft Ave., the north-east air transport results in the highest BC mass concentration. In both road site cases this means a direct transport of pollutants from the street to the measurement site.

At the urban background site, established at the Manila Observatory, the BC mass concentration and PNSD patterns were different compared to those at road sites. The highest and lowest BC concentrations were measured at 6 a.m. with a value of 18 $\mu\text{g m}^{-3}$ and noon with a value of 3 $\mu\text{g m}^{-3}$, respectively. The polar plot suggests that the highest BC values are related with the presence of north-west winds (Katipunan Ave. direction). Particle number size distribution differs from those observed at the road sites, not only by the absence of dominant ultrafine particle mode, but also showing the presence of more diverse aerosol particles. The morning (6 a.m.) increase in both, BC and particle number concentrations, shows the contribution of morning rush hour to urban background aerosol. This increase can also be found at Katipunan Ave. (see Fig. 2). A rapid increase of the number concentration of 10 nm particles with a constantly low BC mass concentration at Manila Observatory

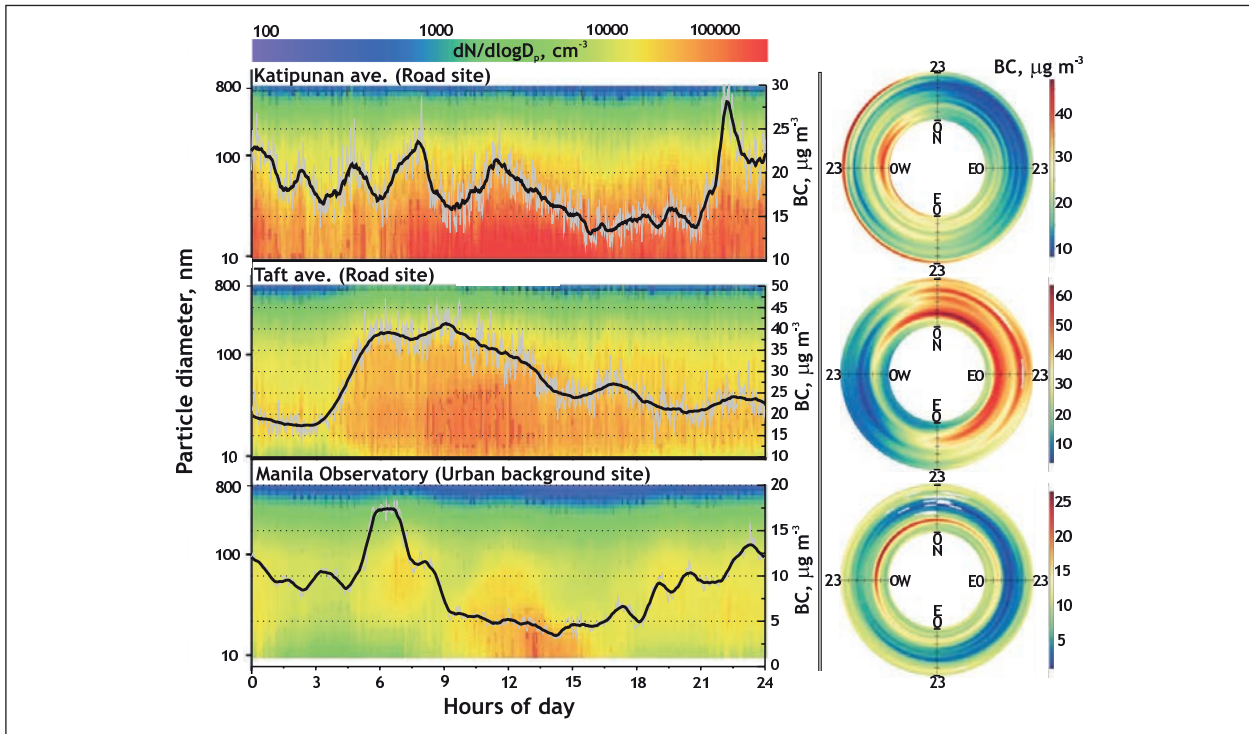


Fig. 2: Diurnal variation of the particle number size distribution (contour plot), BC mass concentration (black solid line) and the BC dependence on wind direction in the road and urban background sites.

suggests that new particle formation occurs in the urban environment.

Mobile Measurements. In parallel to stationary measurements, spatial distribution of aerosol particle properties were measured in two pre-defined routes along Katipunan (Fig. 3) and Taft (not shown here) avenues. The routes were selected to cover various possible exposures to pollutants in residential areas (left stretch in Fig. 3), busy intersections and relatively clean parks (right section in Fig. 3).

As can be seen from the Fig. 3, the highest concentration of BC was measured at the busy intersection (middle bottom in the Fig. 3) where two main streets, Katipunan Ave. and Aurora Boulevard meet. Moreover, a public transport terminal with constantly idling vehicles was located beside the intersection. As a result – a maximum BC mass concentration of $91 \mu\text{g m}^{-3}$ was registered. In the residential area (121.070 longitude and 14.637 latitude) the BC mass concentrations were half as large compared to the hotspot areas. However, despite considerably lower traffic intensity, the values still reached more than $40 \mu\text{g m}^{-3}$ and were as high as the ones measured along Katipunan Ave. This can be explained by easterly prevailing winds, which pick the pollutants from the avenue and disperse it over residential areas. In contrast, the BC mass concentration rarely exceeded $10 \mu\text{g m}^{-3}$ in the ADMU Campus, which is to the east

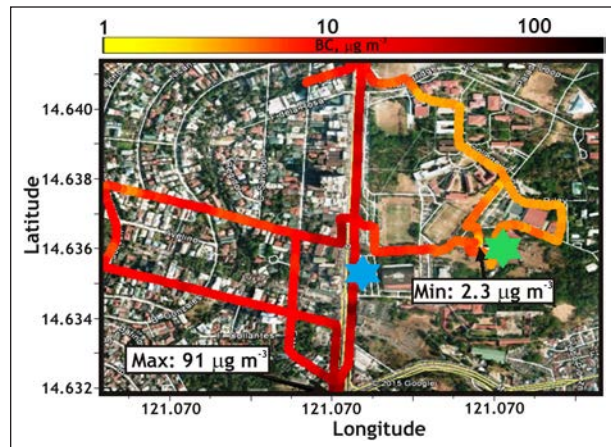


Fig. 3: Spatial distribution of black carbon mass concentration measured with portable aethalometer. The blue and green stars mark Katipunan road and Manila Observatory urban background sites, respectively.

from the avenue. These results show the importance of mobile measurements to fully understand the spatial distribution of pollutants and possible exposure in different urban environments.

PAHs. Results from an eight-day, 24-hour continuous sampling are shown in Fig. 4. Daily total particulate PAH (TPAH) mass concentration was ranging from 54 to 153 ng m^{-3} .

At the roadside site, the highest level of TPAHs was observed in ultrafine particles (stage 1) and

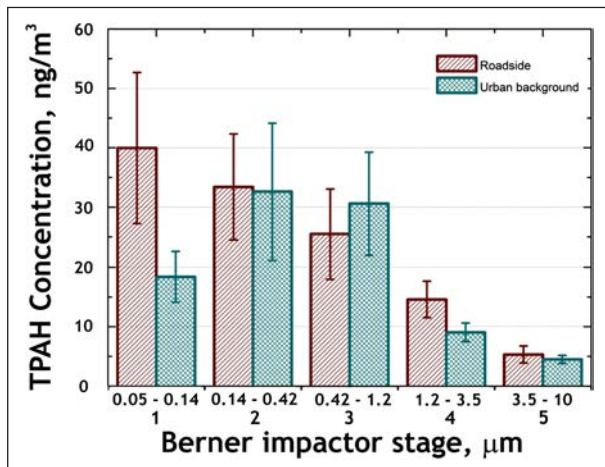


Fig. 4: Total PAH mass concentration in 5 Berner impactor stages at road and urban background sites. Error bars represent standard deviation.

reached the value of 40 ng m^{-3} . As the particle size increases, the TPAH concentration decreases. This is a characteristic of PAH size distribution that can be attributed to direct tailpipe emissions. For the urban background site, the highest TPAH level of 33 ng m^{-3} was detected in the accumulation mode (stage 2). It was also observed that in the particulate matter from stage 3, urban background TPAH mass concentration was about 20% higher than the values observed at the road site. This shows that regional TPAH transport to an urban environment is of similar importance as direct emissions.

Conclusions

An intensive aerosol research experiment, MACE2015, was conducted in Manila, Philippines, in 2015. Results show that road-side mass concentrations of BC are extraordinarily high and are mostly dominated by combustion particles. The highest diurnal BC mass concentration at Katipunan Ave. and Taft Ave. reached 33 and $47 \mu\text{g m}^{-3}$, respectively. These values were consistent with the winds prevailing from the street. Particle number size distributions at road sites were mostly influenced by ultrafine particles. Mobile measurements revealed the spatial distribution of BC. Hotspots with BC mass concentration over $90 \mu\text{g m}^{-3}$ and urban background zones were identified. Offline analysis of the 5 stage Berner impactor foils showed that daily total PAH mass concentration reaches 153 ng m^{-3} , with 30% of it found in ultrafine particles (impactor stage 1; 50-140 nm), which represents direct tailpipe emissions from vehicles. Future research will be focused on understanding how meteorological conditions influence the urban aerosol pollution, evaluating spatial patterns of particle exposure and dispersion at the roadside and determining the emission factors for different vehicular fleets.

Acknowledgements

Thanks to MO, UP and LA SALLE for supporting the campaign and hosting the people from TROPOS.

References

- Krupnick, A., R. Morgenstern, C. Fischer, et al. (2003), Air Pollution Control Policy Options for Metro Manila, Resources for the Future Discussion Paper, Washington, D.C.
- Lee, B.-K (2010), Sources, Distribution and Toxicity of Polyaromatic Hydrocarbons (PAHs) in Particulate Matter, Air Pollution. (V. Villanyi, Ed.) InTech. doi:10.5772/10045
- Lelieveld, J., J.S. Evans, M. Fnais, D. Giannadaki, A. Pozzer (2015), The contribution of outdoor air pollution sources to premature mortality on a global scale, *Nature*, 525, 367-371.
- LTO, Land Transportation Office, Republic of the Philippines, Philippine Statistics Authority (2013), Philippine Transportation Statistics, available online: <https://psa.gov.ph/content/transportation> and http://www.kokudokeikaku.go.jp/wat2/22_philippines.pdf Viewed on 2015-12-04.
- Müller, T., J.S. Henzing, G. de Leeuw (2011), Characterization and intercomparison of aerosol absorption photometers: result of two intercomparison workshops, *Atmos. Meas. Tech.*, 4, 245–268.
- Vergel, K., and M. Tiglao (2013), Estimation of Emissions and Fuel Consumption of Sustainable Transport Measures in Metro Manila, *Philippine Engineering Journal*, 34(1), 31-46.
- Wiedensohler, A., W. Birmili, A. Nowak, et al. (2012), Mobility particle size spectrometers: harmonization of technical standards and data structure to facilitate high quality long-term observations of atmospheric particle number size distributions, *Atmos. Meas. Tech.*, 5, 657–685.

Chemical characterization and sources of inorganic gaseous and PM₁₀ pollutants at the Melpitz site in Central Europe

Bastian Stieger¹, Gerald Spindler¹, Achim Grüner¹, Konrad Müller¹, Laurent Poulain¹, Markus Wallasch², Hartmut Herrmann¹

¹ Leibniz Institute for Tropospheric Research (TROPOS), Leipzig, Germany

² Federal Environment Agency (UBA), Dessau/Roßlau, Germany

An der TROPOS Forschungsstation Melpitz werden seit 2010 kontinuierlich die Partikel- und Gasphasenkonzentrationen anorganischer Bestandteile mit der MARGA (Monitor for AeRosols and Gases in ambient Air) quantifiziert. Die Kombination aus nass-chemischem rotierenden Denuder und Aerosolkammer sowie zweier ionenchromatographischer Systeme ermöglicht die stündliche Bestimmung der anionischen und kationischen Konzentrationen beider Phasen. Mit dieser hohen Zeitauflösung sowie der Nutzung von Rückwärtstrajektorien lassen sich mögliche Quellregionen für anorganische Partikel ausfindig machen.

Introduction

The standard method for the quantification of inorganic particulate ions is filter sampling followed by off-line ion chromatographic analysis. A disadvantage is the long sample duration of several hours up to several days. In the recent years, new analytical on-line instruments were developed with higher time resolution like the Aerodyne Aerosol Mass Spectrometer (AMS) [Sun *et al.*, 2010] and the wet chemical MARGA system [*ten Brink et al.*, 2007]. Besides information concerning the particle phase, the latter provides also the detection of corresponding trace gases due to the combination of rotating denuder and steam-jet aerosol collector.

Here, the source identification of the main particulate ions are presented by using the MARGA data at the TROPOS site Melpitz [Spindler *et al.*, 2013] from a 5-year measurement period (2010-2014).

MARGA instrument

The used MARGA system (Applikon, The Netherlands) measures the inorganic compounds in PM₁₀ (Cl⁻, NO₃⁻, SO₄²⁻, Na⁺, NH₄⁺, K⁺, Mg²⁺, Ca²⁺) and their corresponding trace gases (HCl, HONO, HNO₃, SO₂,

NH₃) at the TROPOS research station Melpitz since 2010. An air pump transports the ambient air firstly through a Teflon-coated PM₁₀-inlet. Afterwards, the water-soluble gases are separated within a Wet Rotating Denuder (WRD) in which the gas molecules diffuses rapidly into the aqueous solution [Keuken *et al.*, 1988]. Particles are more inert and follow the flow to the Steam-Jet Aerosol Collector (SJAC) that is a chamber with a supersaturation of water vapour [Khlystov *et al.*, 1995]. Herein, the particles grow to droplets and are collected. The aqueous solutions from the WRD and SJAC are pumped continuously by syringe pumps to the detector box where two ion chromatography systems analyses the anionic and cationic compounds in the sampled solutions. The ion chromatography systems work with an internal standard of lithium bromide (LiBr) for calibration.

Results

Longtime measurements. Gaseous ammonia in Fig. 1 reaches highest concentrations in spring when huge amounts are released due to agriculture activities or evaporation of semivolatile particles (ammonium nitrate or ammonium chloride) with increasing temperatures. The particulate ions show

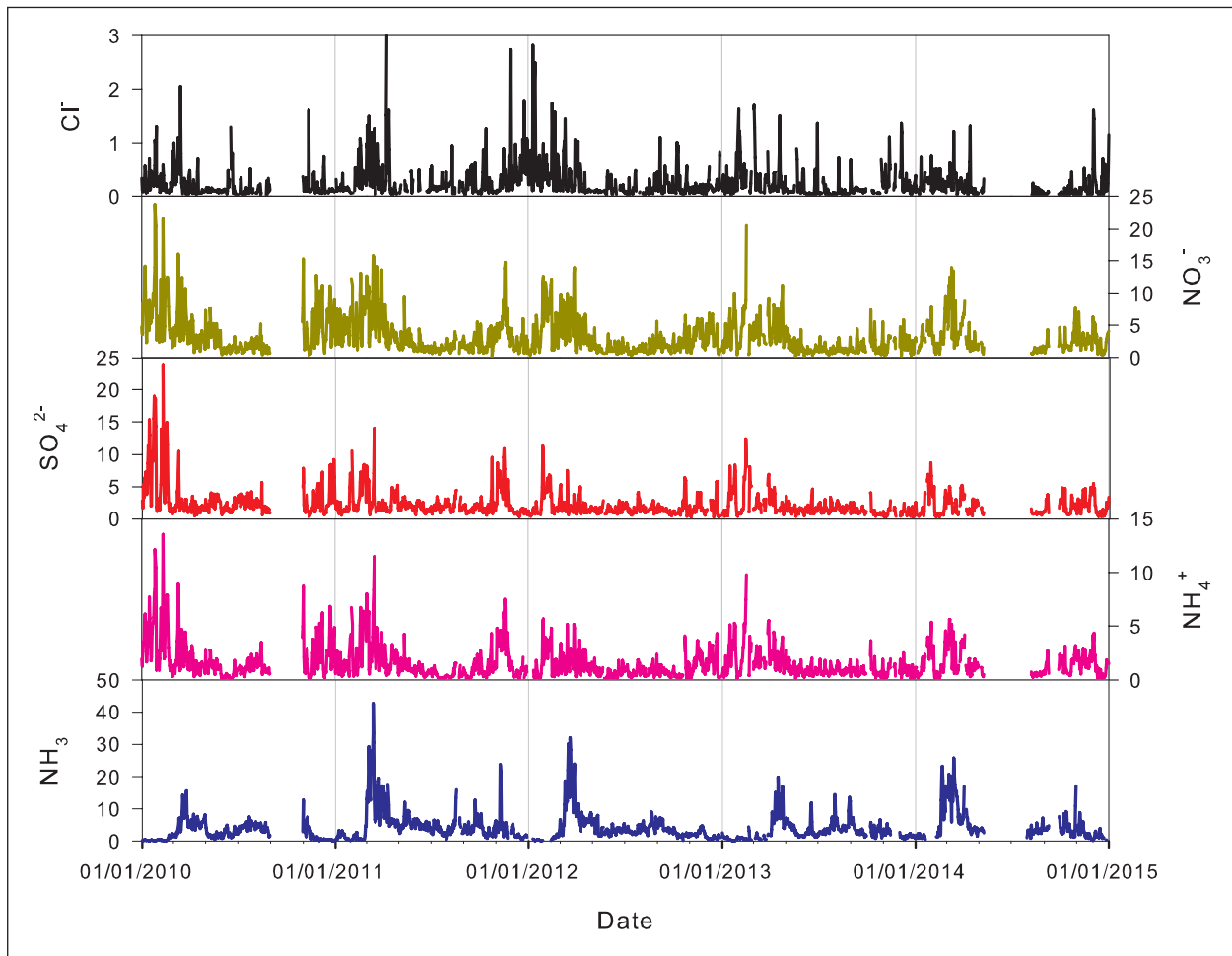


Fig. 1: Measured MARGA concentrations in $\mu\text{g m}^{-3}$ of the main particulate ions chloride (black), nitrate (olive), sulphate (red) and ammonium (pink) as well as the gaseous ammonia (blue) in Melpitz from 2010 until 2014.

highest concentrations during winter, which is due to the direct emission from anthropogenic combustion processes as well as from the formation of ammonium salts at lower temperatures. Another reason is the enrichment of particles within inversion layers that are more stable in winter.

Source identification of particulate ions. To study the most probable emission areas of the single pollutants, the Potential Source Contribution Function (PSCF) [Malm et al., 1985] is used. For this estimation the hourly 96h-HYSPLIT (HYbrid Single-Particle Lagrangian Integrated Trajectory) backward trajectories and the hourly MARGA data are combined. High PSCF values stand for probable emission area. The PSCF calculation for the measured gases is not prosperous because of their short tropospheric lifetimes.

In Fig. 2, the PSCF calculations for the main particulate ions are summarized. Chloride shows two significant source regions. An important contributor for high chloride concentrations in Melpitz is sea salt coming from the North Sea and the Northern Atlantic

Ocean with westerly winds. Furthermore, air masses from the east can contain high chloride concentrations that are emitted by anthropogenic coal combustion processes.

The dominant emission area for nitrate, sulphate and ammonium are located over South Poland, the Czech Republic and Slovakia. Higher probabilities for nitrate in West Europe can be explained by anthropogenic emission and by processed sea salt particles. It is known that chloride containing sea salt releases hydrochloric acid in presence of nitric acid [Twigg et al., 2015]. The chloride-nitrate exchange lead to aged sea salt particles and higher nitrate concentration in Melpitz with westerly winds.

The similar main emission area of the four particulate ions (Fig. 2) indicates that the ions are transported to Melpitz in form of the salts ammonium chloride, ammonium nitrate and ammonium sulphate. The highest concentrations were observed in winter (Fig. 1) when temperatures are low and the semi-volatile salts ammonium nitrate and chloride exist in the particle phase.

Conclusion

Since 2010, a MARGA system is used in Melpitz for the simultaneous measurement of trace gases and inorganic compounds in PM₁₀. The high time resolution of one hour is a significant advantage compared to the standard filter measurements. Combination of

the data with measured meteorology and calculated backward trajectories, makes it possible to estimate the probable source areas. Highest concentrations of the main particulate ions are connected with easterly winds, which transports anthropogenic polluted air from Eastern Europe to Melpitz.

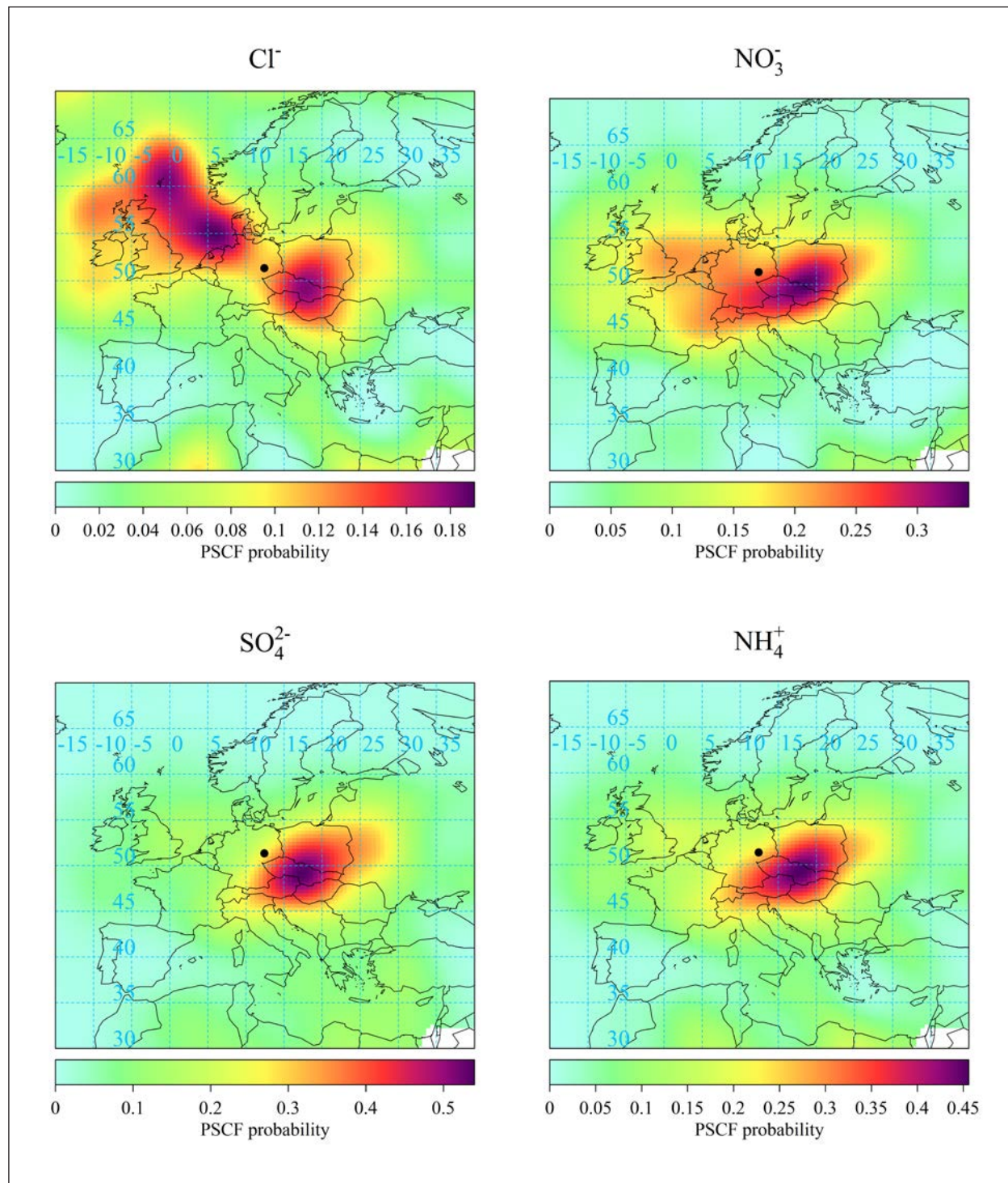


Fig. 2: PSCF plots of chloride (upper left), nitrate (upper right), sulphate (bottom left) and ammonium (bottom right) for the measurement period from 2010 until 2014.

References

- Keuken, M. P., C. A. M. Schoonebeek, A. Vanwensveenlouter, and J. Slanina (1988), Simultaneous Sampling of NH₃, HNO₃, HCl, SO₂ and H₂O₂ in Ambient Air by a Wet Annular Denuder System, *Atmos. Environ.*, 22(11), 2541-2548, doi:10.1016/0004-6981(88)90486-6.
- Khlystov, A., G. P. Wyers, and J. Slanina (1995), The Steam-Jet Aerosol Collector, *Atmos. Environ.*, 29(17), 2229-2234, doi:10.1016/1352-2310(95)00180-7.
- Malm, W. C., C. E. Johnson, and J. F. Bresch (1985), Application of Principal Component Analysis for Purposes of Identifying Source-Receptor Relationships, in *Receptor Methods for Source Apportionment - Real World Issues and Applications*, edited by T. G. Pace, Willimasburg, Virginia.
- Spindler, G., A. Grüner, K. Müller, S. Schlimper, and H. Herrmann (2013), Long-term size-segregated particle (PM₁₀, PM_{2.5}, PM₁) characterization study at Melpitz - influence of air mass inflow, weather conditions and season, *J. Atmos. Chem.*, 70(2), 165-195, doi:10.1007/s10874-013-9263-8.
- Sun, J. Y., Q. Zhang, M. R. Canagaratna, Y. M. Zhang, N. L. Ng, Y. L. Sun, J. T. Jayne, X. C. Zhang, X. Y. Zhang, and D. R. Worsnop (2010), Highly time- and size-resolved characterization of submicron aerosol particles in Beijing using an Aerodyne Aerosol Mass Spectrometer, *Atmos. Environ.*, 44(1), 131-140, doi:10.1016/j.atmosenv.2009.03.020.
- ten Brink, H., R. Otjes, P. Jongejan, and S. Slanina (2007), An instrument for semi-continuous monitoring of the size-distribution of nitrate, ammonium, sulphate and chloride in aerosol, *Atmos. Environ.*, 41, 2768-2779.
- Twigg, M. M., C. F. Di Marco, S. Leeson, N. van Dijk, M. R. Jones, I. D. Leith, E. Morrison, M. Coyle, R. Proost, A. N. M. Peeters, E. Lemon, T. Frelink, C. F. Braban, E. Nemitz, and J. N. Cape (2015), Water soluble aerosols and gases at a UK background site - Part 1: Controls of PM_{2.5} and PM₁₀ aerosol composition, *Atmos. Chem. Phys.*, 15(14), 8131-8145, doi:10.5194/acp-15-8131-2015.

Funding

The project is financially supported by the German Federal Environment Agency (UBA) with contracts No 351 01 093 and 351 01 070.

What influences CCN properties in central Europe?

Silvia Henning, Wolfram Birmili, Alexander Beyer, Laurent Poulain, Achim Grüner, Alfred Wiedensohler, Hartmut Hermann, Frank Stratmann

Basierend auf einem kontinuierlichen 3-Jahres-Datensatz zur Anzahlkonzentration von Wolken kondensationskernen (CCN), gemessen an der TROPOS Forschungsstation in Melpitz, wurden erste statistische Auswertungen zum CCN-Vorkommen und zur CCN-Hygrokopizität durchgeführt. Die Zusammenhänge dieser Größen mit den vorherrschenden Luftmassen wurde mit Hilfe einer Clusteranalyse untersucht. Der Hygrokopizitätsparameter κ wies einen Jahresgang mit höchsten Werten in den Wintermonaten (0.38 ± 0.01 bei 0.3% Übersättigung) und den niedrigsten Werten in den Spätsommer/Herbstmonaten (0.22 ± 0.02 bei 0.3% Übersättigung) auf. Dieser Jahresgang kann mit der vorherrschenden Großwetterlage in Zusammenhang gebracht werden, mit hoher CCN Aktivität während stabiler kalter Winterlagen und niedriger CCN Aktivität bei nordwestlicher Anströmung im Herbst.

In August 2012 standardised cloud condensation nucleus (CCN) long-term observations were launched at the TROPOS field station Melpitz, Germany. The station is part of the European Aerosols, Clouds, and Trace gases Research InfraStructure Network (ACTRIS), which aims at integrating European ground-based stations equipped with advanced atmospheric probing instrumentation for aerosols, clouds, and short-lived gas-phase species. Aerosol and CCN properties measured at this site are regionally representative for central Europe. Our monodisperse CCN measurements follow the recommendations of the ACTRIS Standard Operation Procedure (SOP, [Gysel *et al.*, 2013]) for CCN measurements. In addition to the CCN data, particle (CN) number size distribution measurements, a wide variety of chemical gas and particle measurements as well as standard meteorological parameters are available on a continuous basis at the Melpitz station.

The now available 3-year dataset (August 2012 to July 2015) of continuous CCN size spectra, for particle sizes between 25 and 300 nm at 5 different supersaturation (SS) levels (0.1, 0.2, 0.3, 0.5, 0.7%) has been analysed. The CCN and CN spectra were corrected for multiple charges and the size-dependent activation fraction (AF) was calculated by dividing

CCN (N_{CCN}) by total particle number concentration (N_{tot}). This was done for all SS levels. By fitting the resulting AF at certain SS with the sigmoid error function, the 50% activation diameter could be derived (D_{P50}). For given SS and D_{P50} , the corresponding hygroscopicity κ was calculated as given by Petters and Kreidenweis [2007].

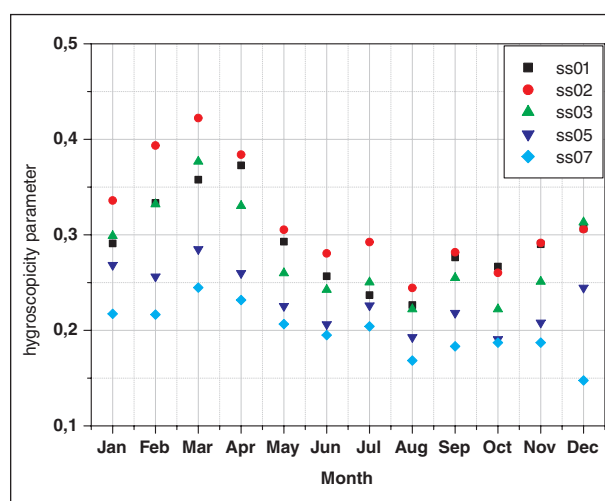


Fig. 1: Monthly mean over 3-year data set of the hygroscopicity parameter κ as derived from CCN measurements at five different supersaturations and from ACSM plus MAAP measurements.

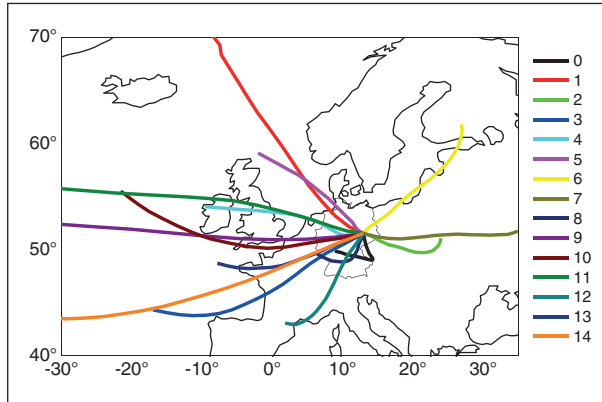


Fig. 2a: Mean back trajectories (96 h) for the 15 different clusters. Clusters were achieved not only from the backward trajectories but also considering of the vertical stratification of the atmosphere.

For the unclustered dataset the monthly mean values of κ vary between 0.2 and 0.4 for SS=0.3% (Fig.1) which compares well to the κ -value reported in literature for continental aerosol [Pringle et al., 2010; Wex et al., 2010]. The monthly mean values of N_{CCN} (@ SS=0.3%) vary between 1000 and 3000 [cm^{-3}], not following N_{tot} , but rather the number concentration of particles larger than 80 nm ($N_{>80\text{nm}}$). When relating the κ -value of the particles to their chemical composition (derived from bulk ACSM and MAAP data, not shown) an increase in the κ -value is connected to a decreasing organic and an increasing nitrate fraction. An annual cycle of the the κ -value was observed, with more hygroscopic particles during winter season, which is seen in the κ -value derived from the CCN data as well as in the κ -value derived from the chemical composition [Wu et al., 2013].

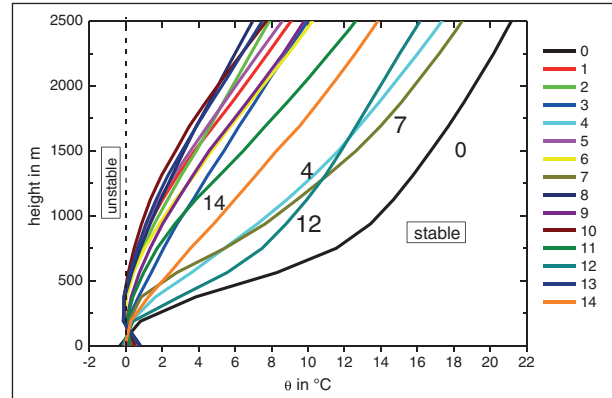


Fig. 2b: Mean vertical profiles of pseudo-potential temperature θ at Lindenberg. These profiles indicate the degree of atmospheric stratification. Five trajectory clusters with pronounced stable stratification are labelled. The profiles were normalised to $T=0^\circ\text{C}$ at a height of 100 m to avoid bias by excess heating of the surface.

The hygroscopicity parameter (κ -value) and the total CCN number concentration were examined as a function of the large scale weather situation using a k-means back trajectory cluster analysis. The current cluster results are still unpublished but the method is very similar to that employed in Ma et al. [2014]. Briefly, the cluster analysis makes use of 96 h backward trajectories (daily; start time 12:00 UTC), and the vertical profiles of pseudo-potential temperature θ based on radiosounding ascents (daily; 12:00 UTC). The cluster analysis was run multiple times in order to obtain a “best solution” that maximizes the differences in near-surface PM_{10} mass concentration among the 15 trajectory clusters. The mean trajectories for the 15 clusters and the mean vertical profiles of pseudo-potential temperature θ are given in Fig. 2a and 2b,

Tab. 1: Summary on the air mass properties for the 15 different clusters, which were determined for Melpitz, research site.

Cluster No.	Stability	Wind direction	Vorticity	Main season	PM10 level
0	very stable	stagnating	anticyclonic	winter	very high
1	unstable	North West	cyclonic	spring/autumn	low/very low
2	unstable	South East	anticyclonic	spring/summer	high
3	unstable	South West	cyclonic	spring/autumn	low
4	stable	West	anticyclonic	winter	high
5	unstable	North West	anticyclonic	summer	low
6	unstable	North East	anticyclonic	spring/autumn	low/medium
7	stable	East	anticyclonic	winter	very high
8	unstable	stagnant	anticyclonic	summer	medium
9	unstable	West	anticyclonic	spring/autumn	medium
10	very stable	South West	cyclonic	winter	high
11	unstable	West	cyclonic	summer	medium
12	stable	South West	cyclonic	winter	very low
13	unstable	West	cyclonic	winter	medium
14	unstable	West	cyclonic	summer	very low

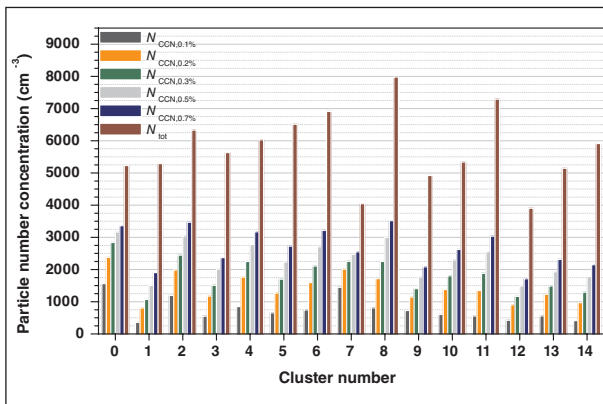


Fig. 3a: Averages over 3-year data set of the CCN particle number concentration at five different supersaturations. The data are sorted after the 15 different air mass clusters.

with a meteorological description of the different clusters being summarized in Tab. 1. The clustering analysis was performed for the whole 3-year CCN dataset.

A significant difference in CCN ability is found between very stable winter weather conditions with an enriched PM_{10} mass (cluster 0 & 7), and unstable spring / autumn weather situations (cluster 1, low / very low PM_{10} load). The ratio of N_{CCN} to N_{tot} at a supersaturation of 0.7% is 0.65 (cluster 0) vs. 0.35 (cluster 1) and N_{CCN} to N_{tot} for a supersaturation of 0.1% is 0.3 (cluster 0) vs. 0.05 (cluster 1) (Fig. 3a). For cluster 0 the air mass is stagnating for several days, the mass concentration is increasing and by the same time CCN ability increases as well, most probably due to the enrichment of soluble material on the pre-existing particles. In case of cluster 1 the boundary layer is well mixed and consequently a

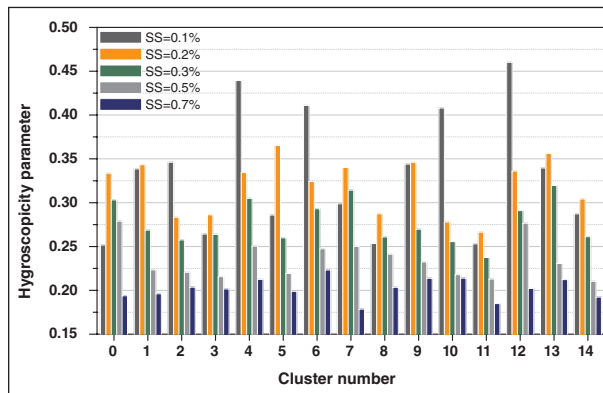


Fig. 3b: Averages over 3-year data set of the hygroscopicity parameter κ at five different supersaturations. The data are sorted after the 15 different air mass clusters as given in Tab. 1 and Fig. 1.

lower PM_{10} load is observed. However almost the same N_{tot} was found, most probably due to new particle formation and resulting particles that are yet too small to act as CCN. The hygroscopicity parameter κ exhibits a wide range of values comparing the different supersaturations for all clusters meaning that on average the aerosol particles are not homogeneously internally mixed (Fig. 3b). Over all for increasing supersaturation κ is decreasing, which implies decreasing hygroscopicity with decreasing particle diameter.

A cluster analysis considering data from continuous 3-year CCN measurements at the TROPOS measurement station Melpitz indicates that the observed CCN properties are predominantly influenced by the large scale weather situation, or in other words the origin and history of the air-mass.

References

- Gysel, M., and F. Stratmann (2013), WP3 -- NA3: In-situ chemical, physical and optical properties of aerosols, Deliverable D3.11: Standardized protocol for CCN measurements. <http://www.actris.net/Publications/ACTRISQualityStandards/tabid/11271/language/en-GB/Default.aspx>
- Ma, N., Birmili, W., Müller, T., Tuch, T., Cheng, Y. F., Xu, W. Y., Zhao, C. S., and Wiedensohler, A.: Tropospheric aerosol scattering and absorption over central Europe: a closure study for the dry particle state, *Atmos. Chem. Phys.*, **14**, 6241-6259, doi:10.5194/acp-14-6241-2014, 2014.
- Petters, M.D. and S.M. Kreidenweis (2007), A single parameter representation of hygroscopic growth and cloud condensation nucleus activity, *Atmos. Chem. Phys.*, **7**, 1961-1971.
- Pringle, K.J., H. Tost, A. Pozzer, U. Pöschl, and J. Lelieveld (2010), Global distribution of the effective aerosol hygroscopicity parameter for CCN activation, *Atmos. Chem. Phys.*, **10**, 5241–5255, doi:10.5194/acp-9-4131-2009.
- Wex, H., McFiggans, G., Henning, S., and F. Stratmann (2010): Influence of the external mixing state of atmospheric aerosol on derived CCN number concentrations, *Geophys. Res. Lett.*, **37**, L10805, doi:10.1029/2010GL043337.
- Wu, Z. J., et al. (2013), Relating particle hygroscopicity and CCN activity to chemical composition during the HCCT-2010 field campaign, *Atmos. Chem. Phys. Discuss.*, **13**, 7643-7680, doi:10.5194/acpd-13-7643-2013.

Regional aerosol modelling in the framework of HOPE

Christa Engler, Ina Tegen, Wolfram Birmili

Aerosolverteilungen wurden für die Feldkampagne HOPE (HD(CP)² Observational Prototype Experiment)I, die April bis Juni 2013 bei Jülich durchgeführt wurde, mit dem regionalskaligen Aerosoltransportmodell COSMO-MUSCAT berechnet. Aus den berechneten Aerosolmassenverteilungen von sieben Aerosolspezies wurden Anzahlgrößenverteilungen abgeleitet. Die Modellergebnisse wurden für den mit Aerosolmessungen am Standort Melpitz bei Leipzig verglichen. Aerosolanzahlkonzentrationen werden im submikronen Größenbereich vom Modell gut reproduziert. Im supramikronen Größenbereich unterschätzt das Modell die beobachteten Aerosolverteilungen, was auf eine fehlende Aerosolquelle im Modell hinweist.

Introduction

In association with the field experiment HOPE (HD(CP)² Observational Prototype Experiment) that was carried out from April to June 2013 near Jülich, regional-scale aerosol model simulations were performed. The aim of the HOPE experiment was to provide observational data on cloud properties and precipitation formation for model evaluation. While detailed aerosol measurements were not in the focus of the field experiment, information on aerosol concentration and size distribution are still required for estimates of cloud condensation nuclei (CCN) concentrations that can then be used for further investigations of aerosol-cloud interactions at the site. For ice nuclei distribution, an estimate based on model results of size-resolved Saharan dust particle size distributions that can be used for the campaign data has been provided by [Hande et al., 2015]. Here, estimates of aerosol number size distributions for seven aerosol species are provided by from results of the regional aerosol transport model COSMO-MUSCAT (COSMO: Consortium for Small-scale Modeling; MUSCAT: MultiScale Chemistry Aerosol Transport model) for the field campaign period. The results provide a basis for estimating CCN concentrations within the model domain.

Method

The regional-scale aerosol transport model COSMO-MUSCAT [Wolke et al., 2012] was used to simulate the bulk concentrations of anthropogenic and natural aerosol species (ammonium sulfate, ammonium nitrate, EC, OC, dust, sulfuric acid, sea salt). In addition, size-resolved atmospheric particle number concentrations were simulated for Saharan dust aerosol. While the number distributions of secondary aerosol species are particularly important to determine cloud condensation nuclei concentrations, dust particles are efficient ice nuclei.

For the estimation of the aerosol number size distributions, the mode mean diameter, density and standard deviation of the log-normal mode have been predefined for each aerosol species. The simulated mass concentrations were converted to total number concentrations by assuming spherical particles of a certain size and density individually for each component. Assuming a log-normal size distribution with a certain mean diameter and standard deviation, the total number concentration can then be used to estimate the number size distribution for each component. The sum of all individual size distributions results in the total particle size distribution, which can be compared to the observations.

Model simulations were performed for the period 2013-03-26 to 2013-06-20, which covers the period of the HOPE field campaign in Jülich. Furthermore the model was evaluated for the site Melpitz near Leipzig, since no specific aerosol measurements were carried out during the campaign at the Jülich site.

Results and Discussion

An example for model results of bulk aerosol concentrations of ammonium sulfate aerosol is shown in Fig. 1 for the day 2013-06-18, 12 UTC. The simulated concentrations are shown for the lowest model layer. The near-surface concentrations of ammonium sulfate vary by a factor of 3 between southern and northern parts of Germany. On this day the

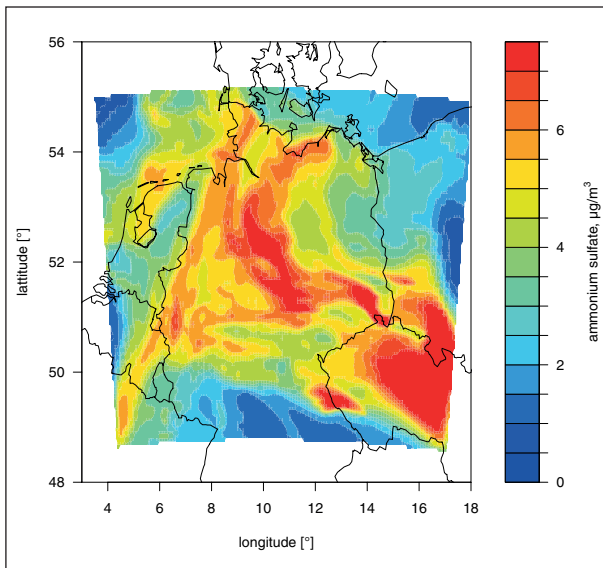


Fig. 1: Simulated ammonium sulfate concentrations in the lowest model layer for 18.6.2013. The simulations were performed with COSMO-MUSCAT.

concentrations at the Jülich site were approximately $5 \mu\text{g}/\text{m}^3$. The aerosol size distribution on this day resulting from conversion of the simulated bulk aerosol concentration into size resolved aerosol concentration at the Jülich site is shown in Fig. 2a. Here, ammonium sulfate contributes the main part to the modeled aerosol number concentrations. These results could not be verified at the Jülich site due to lack of observations. Therefore, comparisons of modeled and observed size distributions were performed at the Melpitz site near Leipzig (Fig. 2b) [Birmili et al., 2015]. While in the size range between 50 nm and 0.15 μm the model estimated number size distribution matches the observations well, the model underestimates the observations at smaller and larger particle sizes. This is also the case when comparing model results and observations for a full month (Fig. 2c). The underestimation at smaller sizes is due to the fact that the nucleation mode, which is present in the measurements, is not taken into account in the model. However, at this size range such an underestimate is less important for diagnosing CCN concentrations. The underestimate of the model results at larger particle sizes (also reflected in underestimates of PM2.5 and PM10 concentrations, not shown) may be more critical, however the number concentrations of the large particles are low. The model deficit may point to an aerosol type that is not included in the model, for example fugitive dust. Natural sea salt and desert dust aerosol are unlikely to be responsible for this deficit at the larger particle sizes, since the sea salt large mode was adjusted to observations, while independent comparisons of dust aerosol size distributions with observations during measurements at independent field campaigns have shown that simulated dust size distributions in the supermicron size range match well to ground and airborne dust size observations (e.g., [Heinold et al., 2011]).

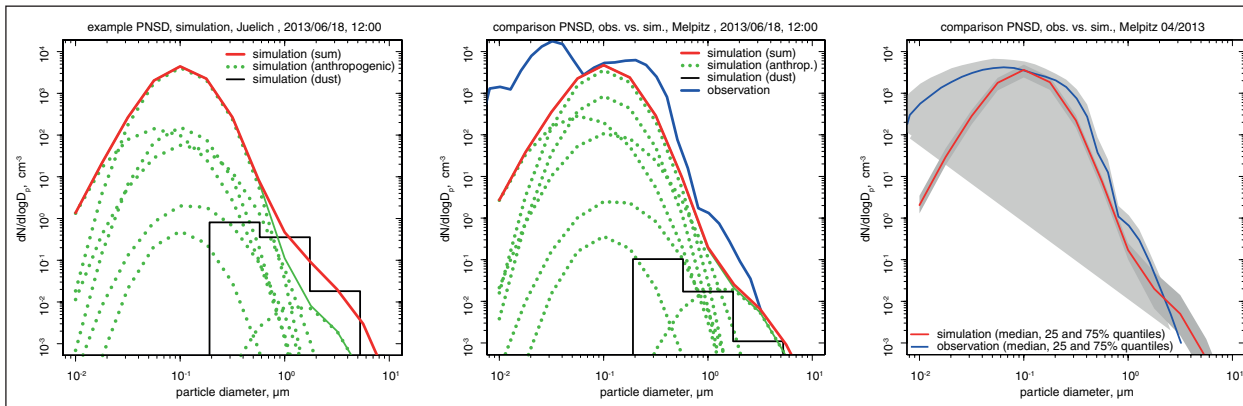


Fig. 2: Aerosol particle number size distribution for the example day 18.6.2013 at the sites Jülich (a) and Melpitz (b), and for the month April 2013 at Melpitz (c). The red lined mark the resulting simulated aerosol size distributions for the sum of the individual species (dotted green lines). Black lines represent modeled number size distribution of dust transported from the Sahara desert to the sites Jülich and Melpitz, respectively.

Further comparisons with observations will be carried out including utilizing information for aerosol profiles to ensure that the results are valid. Model simulations are also planned to simulate aerosol size

distributions with the aerosol microphysics module M7 to provide more information about the processes that control the aerosol size distribution for the campaign period.

References

- Birmili, W., K. Weinhold, M. Merkel, F. Rasch, A. Sonntag, A. Wiedensohler, S. Bastian, A. Schladitz, G. Löschau, J. Cyrys, M. Pitz, J. Gu, T. Kusch, H. Flentje, U. Quass, H. Kaminski, T. A. J. Kuhlbusch, F. Meinhardt, A. Schwerin, O. Bath, L. Ries, K. Wirtz, and M. Fiebig (2015), Long-term observations of tropospheric particle number size distributions and equivalent black carbon mass concentrations in the German Ultrafine Aerosol Network (GUAN), *Earth Syst. Sci. Data Discuss.*, 8(2), 935-993, doi:10.5194/essdd-8-935-2015.
- Hande, L. B., C. Engler, C. Hoose, and I. Tegen (2015), Seasonal variability of Saharan desert dust and ice nucleating particles over Europe, *Atmos. Chem. Phys.*, 15, 4389-4397, doi:10.5194/acp-15-4389-2015.
- Heinold, B., I. Tegen, K. Schepanski, M. Tesche, M. Esselborn, V. Freudenthaler, S. Gross, K. Kandler, P. Knippertz, D. Müller, A. Schladitz, C. Toledano, B. Weinzierl, A. Ansmann, D. Althausen, T. Müller, A. Petzold, and A. Wiedensohler (2011), Regional modelling of Saharan dust and biomass-burning smoke Part 1: Model description and evaluation, *Tellus B*, 63(4 (Special Issue)), 781-799, doi:10.1111/j.1600-0889.2011.00570.x.
- Wolke, R., W. Schröder, R. Schrödner, and E. Renner (2012), Influence of grid resolution and meteorological forcing on simulated European air quality: A sensitivity study with the modeling system COSMO-MUSCAT, *Atmos. Environ.*, 53(SI), 110-130, doi:10.1016/j.atmosenv.2012.02.085.

Funding

German Federal Ministry of Education and Research (BMBF), Bonn, Germany

Cooperation

Karlsruhe Institute of Technology (KIT)

Satellite-based characterization of the growth phase of deep convective cells over Central Europe

Fabian Senf¹, Felix Dietzsch², Anja Hünerbein¹, Hartwig Deneke¹

¹ Leibniz Institute for Tropospheric Research (TROPOS), Leipzig, Germany

² Deutscher Wetterdienst (DWD), Offenbach (Main), Germany

Hochreichende konvektive Wolken, die sich speziell an heißen Sommertagen zu Gewittern ausbilden, sind beeindruckende, aber auch gefahrbringende Phänomene des kontinentalen Wetters. Ein vertieftes wissenschaftliches Verständnis des Wachstumsprozesses dieser Wolken ist die notwendige Grundlage für die Vorhersage und Warnung vor diesen Unwetterereignissen mit großer gesellschaftlicher Relevanz. Des Weiteren ist der Einfluss des Menschen auf die Charakteristika hochreichender konvektiver Wolken weitgehend unverstanden. Aus diesen Gründen wurde die Wachstumsphase konvektiver Wolken über Mitteleuropa für die Jahre 2012 bis 2014 untersucht. Mit Hilfe von Meteosat-Daten wurden dynamische und mikrophysikalische Eigenschaften wachsender Gewitter auf Fallbasis zusammengestellt und analysiert. Betrachtet wurden unter anderem die Wolkenoberkantentemperatur, deren Abkühlrate, der effektive Wolkenpartikelradius sowie die Größe und Expansionsgeschwindigkeit des entstehenden Eisschirms. Es konnte unter anderem gezeigt werden, dass die Gesamtwachstumszeit im Mittel ca. 70 min beträgt und, dass schneller abkühlende Wolkenoberkanten mit schneller expandierenden Eisschirmen mit im Mittel kleineren Partikeln in Verbindung stehen.

Introduction

Deep convective clouds and their accompanying hazards are very fascinating, but also very dangerous phenomena of continental summer weather with large impact on society. Their forecast on various time scales is challenging and complicated by the inherent complexity of associated dynamical and microphysical processes. Geostationary satellites can play an important role to enhance our understanding of their growth properties, and can thus improve forecasting capabilities. Besides their safety and economic impacts, deep convection also plays an important role in the climate system. Convective updrafts transport a significant amount of water and air constituents into the upper troposphere / lower stratosphere. Furthermore, it has become increasingly important to quantify the impact of anthropogenic pollution on deep convective clouds and its effect on the global energy budget. However, impacts of aerosol-mediated cloud changes on our current and future climate are highly uncertain [Boucher *et al.*, 2013]. We therefore focus on convective development in Central Europe, with the objective to enhance our scientific understanding

of the convective initiation, convective life cycle, and development of severe storms.

Data and Methods

We use data from the optical imaging radiometer SEVIRI aboard the geostationary Meteosat Second Generation (MSG) satellites operated by EUMETSAT [Schmetz *et al.*, 2002]. The so-called rapid-scan service covering Europe with a typical pixel size of $3 \times 6 \text{ km}^2$ in Central Europe and a 5-min repeat cycle enables us to resolve details in the convective development.

For the years 2012 to 2014, more than one-hundred tracks of growing isolated deep convective cells have been manually assigned using subsequent satellite images [see Senf *et al.*, 2015]. For characterization, the infrared channels at 6.2 and 10.8 μm and the high-resolution visible (HRV) channel have been used. The 10.8- μm brightness temperature (BT10.8) is a window channel nearly unaffected by atmospheric gases and represents the cloud-top temperature for thick clouds. As a measure of convective growth, the cloud-top cooling (CTC) rate was determined from

the 5-min time trend of the along-track BT10.8. The anvil size and expansion speed was calculated from connected BT10.8 areas below 240 K and their time trends. Additionally, the KNMI cloud physical properties algorithm [Roebeling et al., 2006] has been applied to retrieve the cloud-top effective radius.

Results and Discussion

The majority of studied storms shows a distinct maximum in CTC rate, and its corresponding time was used for synchronization of the storm tracks. Figure 1 gives a schematic overview of the time-scales involved in the growth process of deep convective clouds. Characteristic stages are the time of maximum CTC and the time of maturity. The latter marks the transition between growth and mature phase and is defined based on the time trend of the brightness temperature difference between the 6.2- and 10.8- μm SEVIRI channels. The first part of the growth period, the early updraft intensification, lasts on average 34 min and ranges from the subjectively determined cloud detection time to the time of maximum CTC. The continued growth period thereafter lasts until the time of maturity with a similar temporal length. Typical CTC rates are in the order of

18 °C per 15 minutes corresponding to ascent rates of around 2.6 m/s. The typical anvil expansion speed is around 4.5 m/s at the time of maturity.

The connection between dynamical and microphysical cloud properties is shown in Fig. 2. Over all considered cases, the correlation has been calculated between the magnitude of the maximum CTC rate as a measure of updraft strength and the anvil edge velocities (Fig. 2, upper row) as well as the effective particle radius (Fig. 2, lower row) at different times relative to the time of maximum CTC. The correlation typically increases throughout the growth phase and reaches a maximum around 15 to 30 min after the time of maximum CTC. The anvil edge velocity is around twice as large as the maximum vertical ascent rate. Smaller cloud-top particles are found for larger vertical ascent rates which is physically plausible because ice crystals less time to growth in stronger updrafts.

In the future, we will combine satellite-based dynamical and microphysical cloud properties with lightning activity, radar-detected precipitation strength and additional environmental properties to further increase understanding of parameters that impact convective growth as well as to enhance future satellite-based detection capabilities with Meteosat.

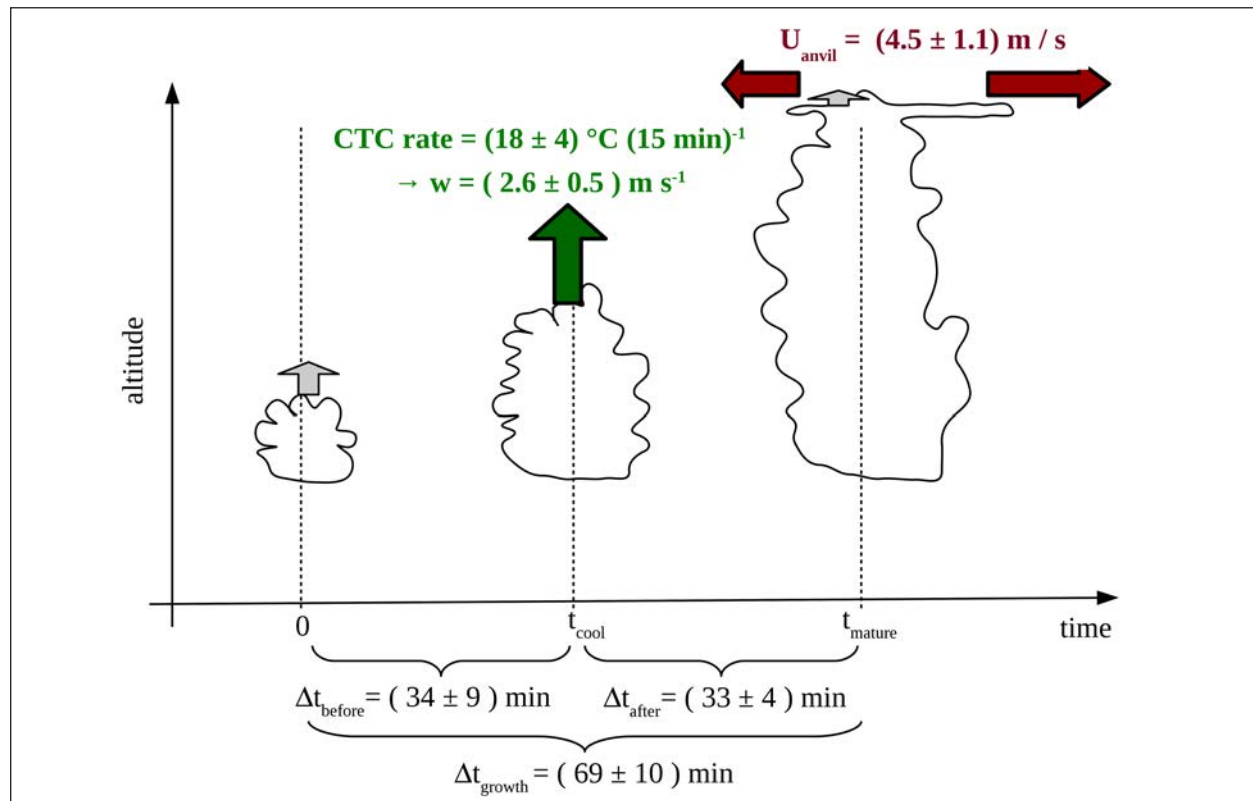


Fig. 1: Sketch of simplified cloud development. Green arrows mark cloud-top vertical motion and red arrows show the anvil expansion. The times of maximum CTC and of maturity as well as several growth periods are indicated. Given values represent the respective medians over all cases and the uncertainty intervals are obtained from the cross-case interquartile range.

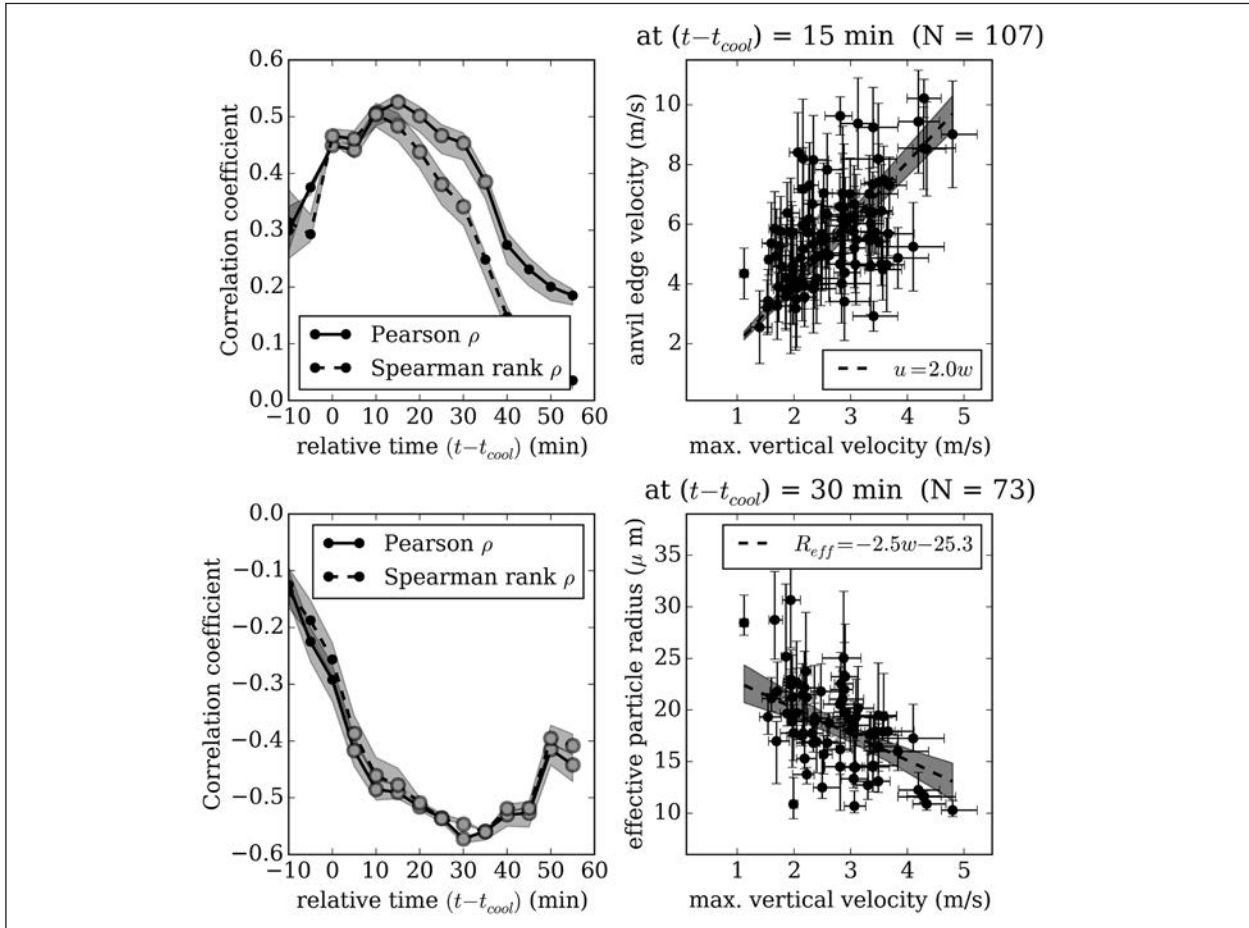


Fig. 2: Connection between maximum CTC rate and anvil edge velocity (upper row) and effective particle radius (lower row) taken at different times relative to the time of maximum CTC. Left panels: two cross-case correlation measures have been considered: Pearson (solid lines) and Spearman rank correlation coefficient (dashed lines). Open circles mark significant correlation at a one-percent level. Grey shades give uncertainty estimates based on tracking uncertainty. Right panels: Median properties (filled circles) and interquartile range (error bars) based on tracking uncertainty estimates are given for one specific relative time at which the maximum in correlation was detected. A linear least-squares fit is indicated by a dashed line and fit uncertainty is given by grey shades.

References

- Boucher, O., Randall, D., Artaxo, P., Bretherton, C., Feingold, G., et al. (2013). Clouds and aerosols. In Climate change 2013: the physical science basis. Contribution of Working Group I to the Fifth Assessment Report of the Intergovernmental Panel on Climate Change (pp. 571-657). Cambridge University Press.
- Roebeling, R. A., A. J. Feijt, and P. Stammes (2006), Cloud property retrievals for climate monitoring: Implications of differences between Spinning Enhanced Visible and Infrared Imager (SEVIRI) on Meteosat-8 and Advanced Very High Resolution Radiometer (AVHRR) on NOAA-17. *J. Geophys. Res.*, 111, D20120.
- Schmetz, J., P. Pili, S. Tjemkes, D. Just, J. Kerkmann, S. Rota, and A. Ratier (2002). An introduction to Meteosat second generation (MSG). *Bull. Amer. Meteor. Soc.*, 83(7), 977-992.
- Senf, F., F. Dietzsch, A. Hünerbein, and H. Deneke (2015), Characterization of initiation and growth of selected severe convective storms over Central Europe with MSG-SEVIRI, *J. Appl. Meteorol. Clim.*, 54(1), 207-224.

Funding

The study was partially funded by the OASE (Object-based Analysis and Seamless Prediction) project within the Hans Ertel Center for Weather Research of the German Weather Service.

Cooperation

Deutscher Wetterdienst (DWD), Offenbach (Main), Germany.

Combined Vertical-Velocity Observations with Doppler Lidar, Cloud Radar and Wind Profiler

Johannes Bühl¹, Martin Radenz¹, Albert Ansmann¹, Ronny Leinweber², Ulrich Görsdorf², Volker Lehmann²

¹ Leibniz Institute for Tropospheric Research (TROPOS), Leipzig, Germany

² Deutscher Wetterdienst (DWD), Lindenberg, Germany

Die Interaktion von Aerosol- und Wolkenpartikeln wird hauptsächlich von der vertikalen Luftbewegung angetrieben. Das macht die vertikale Luftbewegung zu einer äußerst wichtigen Messgröße. Doppler-Lidare und Wolkenradare können vertikale Bewegungen nur dort messen, wo Tracer in Form von Aerosolpartikeln, Wolkentropfen oder Eiskristallen vorliegen. Beide messen daher auch immer vertikale Luftbewegungen die von den Fallgeschwindigkeiten der Teilchen überlagert sind. Nur Wind-Profiler können die Luftbewegung auch in klarer Luft messen. Solche Geräte sind jedoch sehr groß, teuer und können daher nur von gut ausgerüsteten Institutionen betrieben werden. In Deutschland betreibt der Deutsche Wetterdienst (DWD) einen Wind-Profiler am Meteorologischen Observatorium in Lindenberg (MOL). Dort hat in 2013 die gemeinsame TROPOS/MOL Messkampagne COLRAWI (Combined Observations with Lidar, Radar and Wind Profiler) stattgefunden. Dabei wurden zum ersten Mal ein Doppler-Lidar, ein Wolkenradar und Wind-Profiler gemeinsam zur gleichzeitigen Beobachtung vertikaler Luftbewegungen genutzt [Bühl et al., 2015].

The interaction between aerosols, cloud droplets and ice crystals is driven mainly by vertical air motion. This makes vertical air velocity a highly desired measurement value. Observations of vertical air motion is possible with Doppler lidars and cloud radars. Observations are, however, restricted to regions of the atmosphere where enough aerosol or cloud particles prevail. In the clear air around clouds, only radar wind profilers can provide measurements of vertical air motion. Wind profilers are relatively large and expensive instruments and can only be operated by a very limited number of well-funded institutions. In Germany the German Meteorological Service (DWD) operates an Ultra-High-Frequency Wind Profiler at the Meteorological Observatory Lindenberg (MOL). In 2013, the common DWD/TROPOS measurement campaign COLRAWI (Combined Observations with Lidar, Radar and Wind Profiler) has been performed at MOL combining vertical observations from Doppler lidar, cloud radar and wind profiler [Bühl et al., 2015].

Methods

At MOL a large set of remote sensing instruments is being run by the DWD, including a Raman

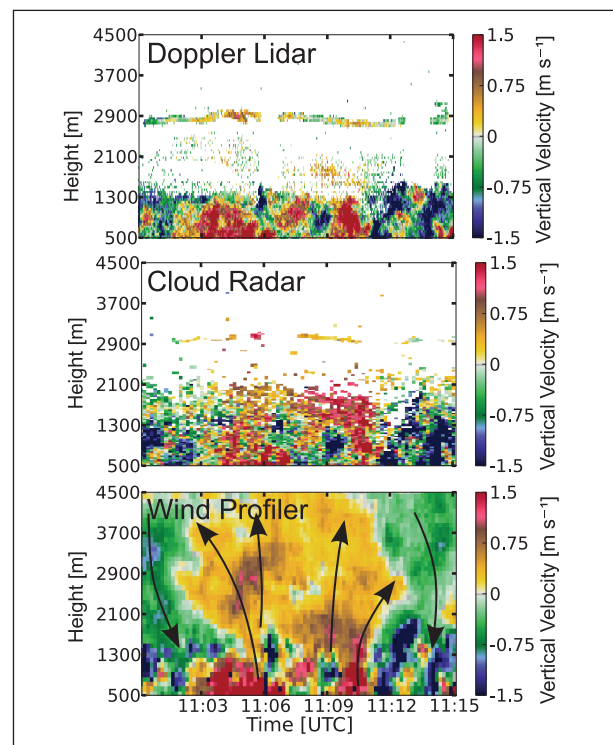


Fig. 1: Measurement example of a combined remote sensing measurements with (from top to bottom) Doppler lidar, cloud radar and wind profiler during the COLRAWI campaign.

lidar, ceilometers, microwave radiometers, a MIRA-35 cloud radar and the above-mentioned radar wind profiler. The wind profiler is normally used to derive 30min-profiles of horizontal wind speed up to the tropopause. During the COLRAWI campaign, the wind profiler was run in a special vertical-stare mode with 10s temporal and 100m vertical resolution. For the first time this wind profiler was used in this mode together with a Doppler lidar and a cloud radar in order to generate a combined dataset of cloud micro-physics with the Cloudnet framework [Illingworth *et al.*, 2007] together with vertical air velocity in and around cloud layers.

Examples of combined measurements

In Fig. 1, it is shown how cloud droplets and air motion can be obtained simultaneously. It is visible from that figure that vertical velocity measurements are provided by Doppler lidar and cloud radar in the

boundary layer (below 1300m height) and at cloud level (2900m height). The wind profiler, however, delivers a coherent picture of the vertical motions in the complete column up to 4500m height. In Fig. 2 an example is shown where combined measurements are used to derive the pure fall velocity of ice particles relative to the surrounding air. For this purpose, the vertical air motions measured by the wind profiler are subtracted from the vertical velocity of particles measured with the cloud radar and Doppler lidar.

Summary and Outlook

Measurements like those shown in Fig. 1 can be of great practical use, e.g. for initiating cloud models [e.g., Simmel *et al.*, 2015], process studies and long-term statistics of vertical motions. On the other hand, the pure fall velocity of particles relative to the surrounding air may be used to derive first-hand information about ice particle size and shape.

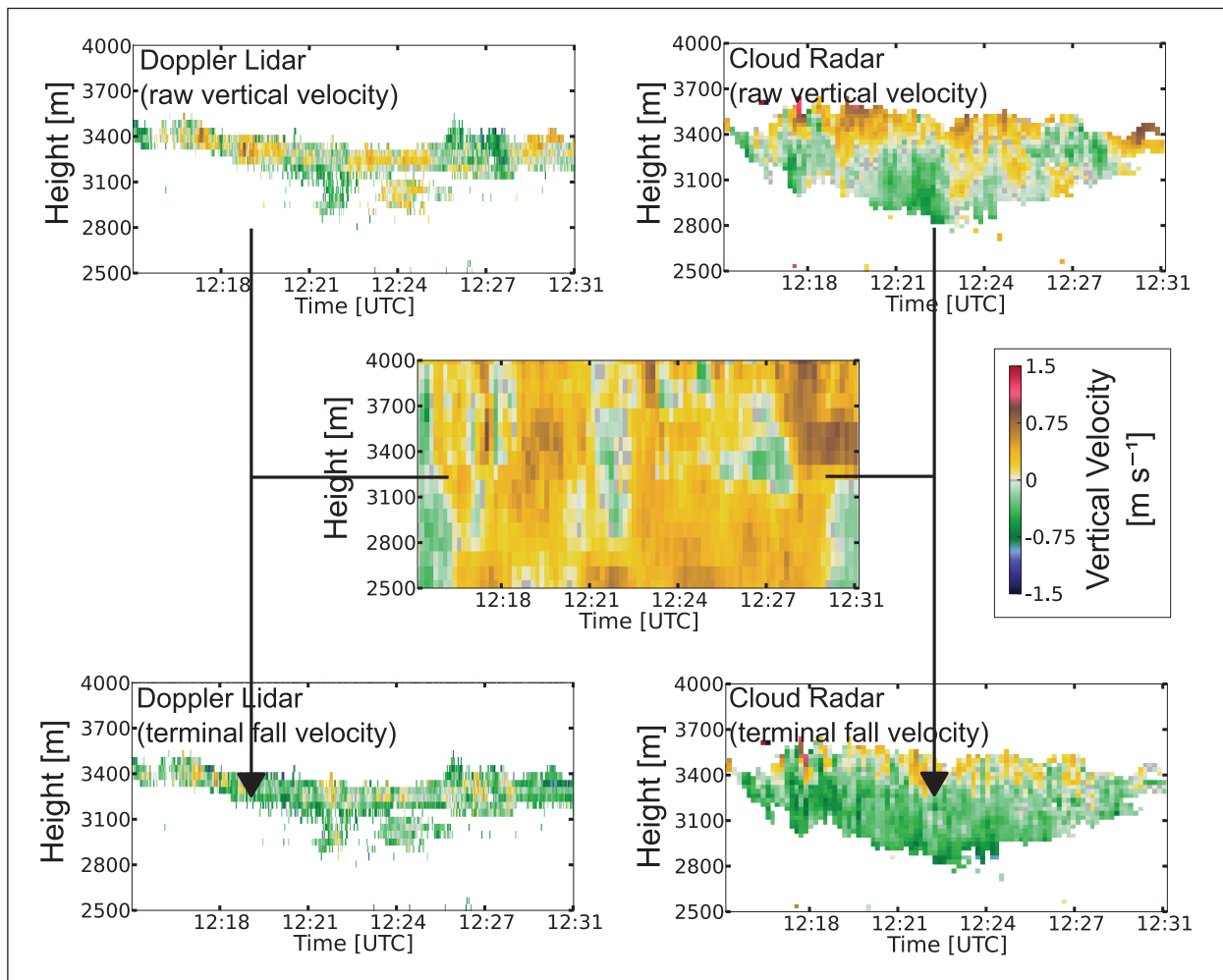


Fig. 2: The vertical velocity measurements of the wind profiler (center) are subtracted from those of the Doppler lidar (left column) and the cloud radar (right column). With the correction applied the measurements yield the fall speed of the particles relative to the surrounding air (bottom).

COLRAWI has shown that a combination of Doppler lidar, cloud radar and wind profiler makes it possible to derive the highly-desired vertical velocity of clear air in order to characterize different kinds of vertical motions in the atmosphere. It has been shown that the use of a wind profiler can fill the white spaces left

on the vertical-velocity picture drawn by Doppler lidars and cloud radars. Large-scale atmospheric motion becomes visible together with clouds, and the extent and strength of vertical-velocity fields can be studied independent of the presence of tracers, like aerosol particles or cloud droplets.

References

- Bühl, J., R. Leinweber, U. Görsdorf, M. Radenz, A. Ansmann, and V. Lehmann (2015), Combined vertical-velocity observations with Doppler lidar, cloud radar and wind profiler, *Atmos. Meas. Tech. (AMT)*, 8(8), 3527-3536, doi:10.5194/amt-8-3527-2015.
- Illingworth, A. J., R. J. Hogan, E. J. O'Connor, D. Bouniol, J. Delanoë, J. Pelon, A. Protat, M. E. Brooks, N. Gaussiat, D. R. Wilson, D. P. Donovan, H. K. Baltink, G. J. van Zadelhoff, J. D. Eastment, J. W. F. Goddard, C. L. Wrench, M. Haeffelin, O. A. Krasnov, H. W. J. Russchenberg, J. M. Piriou, F. Vinit, A. Seifert, A. M. Tompkins, and U. Willén (2007), Cloudnet, *Bull. Amer. Meteor. Soc.*, 88(6), 883-898, doi:10.1175/BAMS-88-6-883.
- Simmel, M., J. Bühl, A. Ansmann, and I. Tegen (2015), Ice phase in altocumulus clouds over Leipzig: Remote sensing observations and detailed modelling, *Atmos. Chem. Phys.*, 15, 10453-10470, doi:10.5194/acp-15-10453-2015.

Cooperation

Deutscher Wetterdienst (DWD), Germany

Spatio-temporal variability of surface solar irradiance with pyranometer network

Madhavan Bomidi, Hartwig Deneke, Andreas Macke

Die Zeitreihen der globalen solaren Transmission eines Pyranometer Messnetzes mit 99 Stationen wurde mit einer Wavelet-basierten Multiskalenanalyse untersucht, um das frequenzabhängige Leistungsspektrum und die Auswirkungen von zeitlichen und räumliche Skalen auf die Varianz und Korrelation zwischen Stationen zu untersuchen. Diese Analyse wurde für variable Bewölkungsbedingungen durchgeführt. Es wurde dabei festgestellt, dass an Tagen mit durchbrochener Bewölkung das Leistungsspektrum der Zeitreihe deutlich höhere Variabilität auf allen Skalen aufweist. Charakteristische Unterschiede des Leistungsspektrums wurden in unterschiedlichen Bewölkungssituationen beobachtet. Sowohl die räumliche Korrelation als auch die zeitliche Varianz hängen stark von der Länge des Mittelungsperiode ab. Diese Arbeit ermöglicht es uns, das Niveau der Übereinstimmung zu bestimmen, dass bei einem Vergleich von Punktmessungen mit einem Flächenmittel zu erwarten ist, wie es oft bei der Validierung von Satellitenprodukten und Atmosphärenmodellen gemacht wird.

Introduction

As part of the High Definition Clouds and Precipitation for advancing Climate Prediction (HD(CP)²) Observational Prototype Experiment (HOPE), a high density network of 99 pyranometer stations was set up around Juelich, Germany to capture the small-scale variability of cloud-induced surface radiation fields at an unprecedented spatial resolution. Each pyranometer station measures the downward short-wave global irradiance at 10 Hz resolution. The global transmittance (T) was derived from the observed global horizontal irradiance (G) by normalizing with a fixed value of extraterrestrial irradiance at the top of atmosphere (TOA), corrected for the sun distance. Detailed information about the data processing and uncertainty assessment are presented in *Madhavan et al. [2015]*. The time series variability of the flux transmittance fields from the pyranometer network were subject to a wavelet-based analysis to understand the spatial and temporal scaling properties under different sky conditions. The maximum overlap discrete wavelet transform and Haar wavelet were chosen for analyzing the time series flux transmittance measurements from the pyranometer network. A Haar wavelet corresponds to the rectangular

scaling and wavelet functions, which act as lowpass and bandpass filters respectively, with maximum time localization by reducing the support of filters and thus the range of edge effects. The time series of flux transmittance measurements from each station were decomposed into smooths (S_j) and details (D_j) for scales from 3 hours to 10 seconds.

Results and Discussion

The power spectrum of transmittance variability under broken clouds is always higher than that during clear, cirrus and overcast skies at all averaging time periods (Fig. 1). On a broken cloudy day, the variance of transmittance details are always higher and distinct at all averaging time periods. When the clouds are scattered, multiple reflections and scattering near the sides of the clouds produce a complex radiance distribution. For most scattered low level clouds of some vertical extent, this leads to higher global transmittances at the surface than that would result for clear skies. The same effect occurs when patches of cirrus or alto-cumulus clouds appear but do not steadily obscure the sun. Overall, a significantly large spatial and temporal variation under broken cloudy situations result in higher variances. During days with cirrus

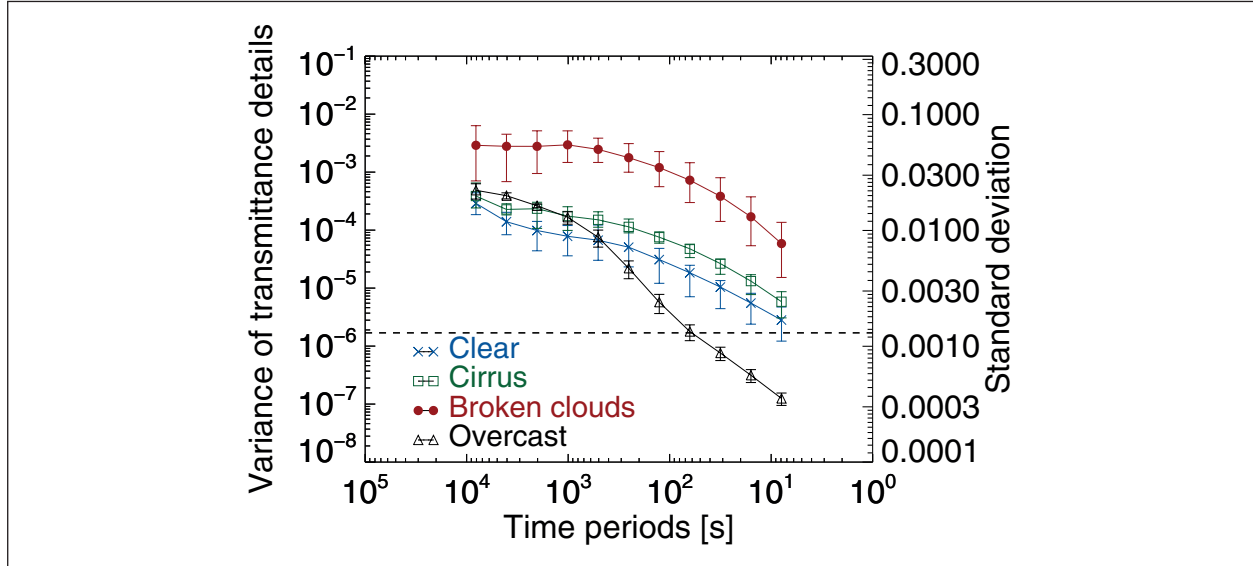


Fig. 1: Wavelet power spectrum of the variability in global transmittance fields on different prevailing sky conditions. The horizontal dashed line correspond to the combined instrumental uncertainty resulting from all components of a pyranometer system. The vertical bars around the mean values correspond to the limits of minimum and maximum variance or standard deviation.

clouds, the variance of transmittance details was lower at all scales compared to broken cloudy conditions, but higher than those resulting on a clear sky. Under a homogeneous thick overcast sky, the global irradiance is completely diffuse and the radiance of the cloud base observed from the ground will be uniform, resulting in lower variability of transmittance fields. However, under partly overcast skies, global transmittance of clouds can also be perturbed by multiple reflections of the solar radiation between the

underlying surface and the cloud base, leading to an increased variability.

It is essential to know how representative the time series of one station is for that observed at close-by stations under specific conditions. The auto-correlation between the transmittance details (or smooths) was observed to be decaying exponentially as the spatial separation between stations increased (Fig. 2). Also, the correlation between stations varied

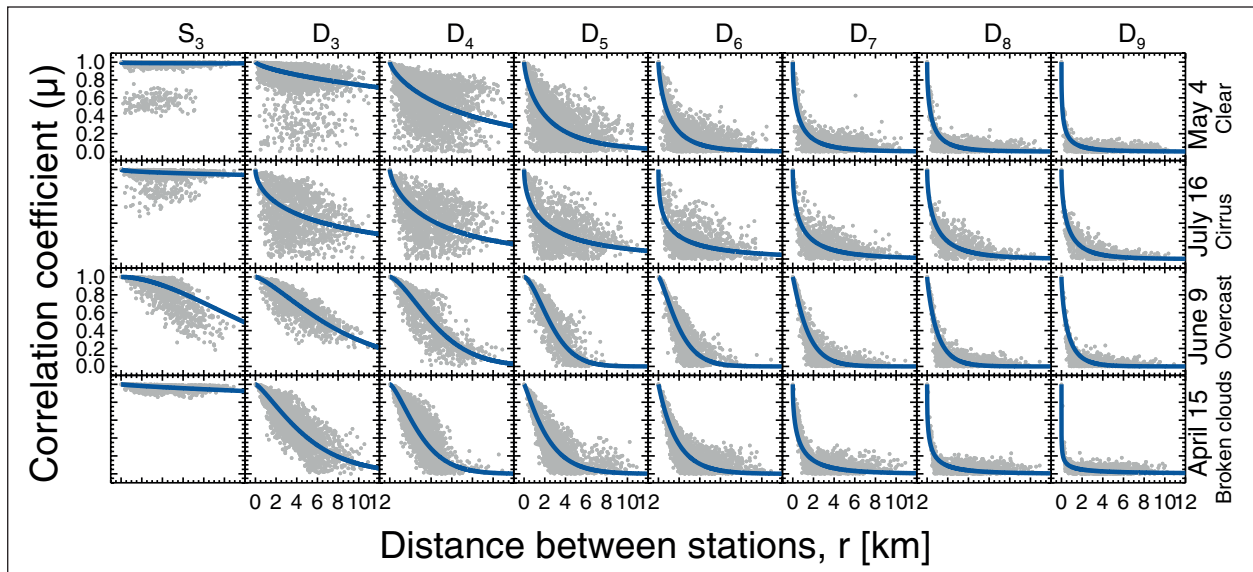


Fig. 2: Wavelet correlation as a function of distance between stations on different days: (a) clear – 4 May 2013 (top row), (b) cirrus – 16 July 2013 (second row), (c) overcast – 9 June 2013 (third row), and (d) broken clouds – 25 April 2013 (last row). Here S_3 corresponds transmittance smooths at a time scale of 3 h, while the transmittance details are represented for time periods 3-1.5 h (D_3), 1.5h-45 min (D_4), 45-22.5 min (D_5), 22.5-11.25 min (D_6), 11.25-5.6 min (D_7), 5.6-2.8 min (D_8), and 2.8-1.4 min (D_9).

widely depending on the type of cloud cover prevailing over the region on that day and the representative averaging time period of transmittance details. Under different sky conditions, remarkable differences were observed in the behavior of auto-correlation especially

for averaging time periods larger than 1.4–2.8 min. Finally, the temporal and spatial scaling properties obtained above for different sky conditions can be used to quantify the representative errors between point measurements and spatial means.

References

- Madhavan, B. L., J. Kalisch, and A. Macke (2015), Shortwave surface radiation network for observing small-scale cloud inhomogeneity fields, *Atmos. Meas. Tech. Discuss.*, 8, 2555–2589.

Cooperation

HD(CP)² project funded by the Federal Ministry of Education and Research (BMBF), Germany

Highly oxidized multifunctional organic compounds observed in tropospheric particles – a field and laboratory study

Anke Mutzel, Janine Schindelka, Laurent Poulain, Torsten Berndt, Yoshiteru Iinuma, Maria Rodigast, Olaf Böge, Stefanie Richters, Gerald Spindler, Hartmut Herrmann

Kürzlich wurden hochoxidierte multifunktionale organische Verbindungen (HOMs) mit einem O/C Verhältnis größer 0.7 entdeckt. Aufgrund ihres niedrigen Dampfdruckes werden sie als extreme niederflüchtige organische Verbindungen (ELVOCs) bezeichnet und können daher signifikant zur organischen Masse im troposphärischen Partikel beitragen. Auch wenn HOMs sehr erfolgreich in der Gasphase nachgewiesen wurden, so ist ihr Verbleib nach erfolgter Partitionierung in die Partikelphase weitgehend unverstanden.

Daher wurde im Rahmen dieser Studie versucht, HOMs bzw. verwandte Oxidationsprodukte in der Partikelphase nachzuweisen. Hierfür wurden zum einen Experimente zur α -Pinen Ozonolyse in der Aerosolkammer LEAK als auch eine umfangreiche Feldmesskampagne im Sommer 2013 an der Forschungsstation Melpitz durchgeführt. Die Analysen der erhaltenen Filterproben zeigten drei Hauptverbindungsklassen in der Partikelphase: 1) intakte HOMs mit einer oder mehreren Carbonylfunktion(en), 2) kurzkettige Carbonylverbindungen und 3) hochoxidierte Organosulfate (HOOS), wobei letztere eine bisher unbekannte Substanzklasse darstellen. In weiteren Versuchen zur Oxidation von Isopren mit OH-Radikalen konnte ebenfalls die Bildung von HOMs nachgewiesen werden, welche bis zu zwei Dritteln von organischen Peroxiden in der Partikelphase erklären können. Anhand der durchgeföhrten Feldstudie konnte gezeigt werden, dass die Partitionierung von HOMs aus der Gasphase zu einem Anstieg des Oxidationsgrads der Partikelphase führt. Damit konnte eindeutig die zentrale Rolle von HOMs für die Partikelphasenchemie von Aerosolen demonstriert werden.

Introduction

The existence of highly oxidized multifunctional organic compounds (HOMs) in the gas phase has been successfully demonstrated during lab and field studies [Ehn et al., 2012, 2014, Jokinen et al., 2014]. They are also often referred as extremely low-volatile organic compounds - ELVOCs. Recent studies revealed that the oxidation of biogenic volatile organic compounds (BVOCs) leads to the formation of HOMs with a molar yield of up to 7 % (α -pinene ozonolysis). At low aerosol loadings, the condensation of HOMs might be able to explain the entire SOA mass [Ehn et al., 2014]. Thus, HOMs significantly contribute to the formation of organic mass during monoterpene oxidation. Despite these observations, HOMs formed in the gas phase via autoxidation processes have not been detected in the particle phase beyond their contribution to organics and thus their fate after phase transfer and their possible chemical consequences remain unclear. In our study, we addressed this gap

by examining both the phase transfer of HOMs into particles and their further reactions within the particle phase. To this end, a series of experiments was conducted in the aerosol chamber LEAK (Leipziger Aerosol Kammer) investigating the ozonolysis of α -pinene and OH induced oxidation of isoprene. The obtained laboratory observations were also compared to field measurements conducted at the Melpitz research station during summer 2013.

Experiments

The aerosol chamber LEAK was used to examine HOM formation from α -pinene ozonolysis (2.4 ppb α -pinene). The chamber was operated as a continuous flow reactor (CFR). This approach enabled us to conduct chamber experiments extending over several days. Four experiments using different type of seed particles (sulfuric acid (H_2SO_4), sodium sulfate (Na_2SO_4), ammonium bisulfate (NH_4HSO_4) and a mixture of phthalic acid dipotassium salt

$(C_6H_4\text{-}1,2\text{-(CO}_2\text{K)}_2)$ and potassium hydrogen phthalate $(C_8H_5KO_4)$) were conducted in the chamber. Each experiment was allowed to react for 48 hours. A proton transfer reaction mass spectrometer (PTR-MS) was operated to monitor the α -pinene mixing ratio. The particle number concentration was monitored with a scanning mobility particle sizer (SMPS). Sample analysis of chamber-generated and ambient aerosol particles collected on filters was conducted by high-performance liquid chromatography electrospray ionization coupled to time-of-flight mass spectrometry (HPLC/(-)ESI-TOFMS) and ultra-performance liquid chromatography electrospray ionization coupled to time-of-flight mass spectrometry (UPLC/(-)IMS-QTOFMS). Filters were directly analysed and after derivatization with 2,4-dinitrophenylhydrazine (DNPH).

Gas phase HOMs were detected and quantified in LEAK and at the Melpitz research station by a NO_3^- -CI-API-TOF (chemical ionization atmospheric pressure interface time-of-flight) mass spectrometer (Airmodus Ltd., Tofwerk A.G) as NO_3^- ($M+NO_3^-$) adducts [Ehn et al., 2012; Jokinen et al., 2012].

Field measurements were performed at the TROPOS research station at Melpitz ($51.54^\circ N$, $12.93^\circ E$, 86 m a.s.l.), approximately 50 km east of Leipzig, Germany.

Further, experiments on the OH induced oxidation of isoprene (5/100 ppb) were performed. OH radicals were produced by photolytic cleavage of hydrogen peroxide (H_2O_2), which was injected either before turning on UV-lamps ($\lambda = 254$ nm) or continuously over the hole experiment time. For investigation

of SOA formation, experiments were performed either without or with seed particles (Na_2SO_4). Organic peroxides in SOA particles have been analysed with an iodometric-spectrophotometric method [Mutzel et al., 2013].

Results and Discussion

Based on our study we propose three reaction pathways of condensed HOMs from α -pinene ozonolysis: i) condensation into the particle phase without a structural change, ii) fragmentation reactions leading to short chain carbonyl compounds and iii) formation of highly oxidized organosulfates (HOOS). Several hints were found for all suggested pathways indicating that these processes occur simultaneously. It should be noted that none of the detected HOOS have been reported in the literature. Therefore, it can be stated that the condensation of HOMs leads to the formation of an up to now unknown class of compounds.

In terms of the HOM structures, the analysis demonstrated that the vast majority of the HOMs contains one or more carbonyl groups. Thus, this study provides the first evidence for the presence of HOMs in laboratory-generated and ambient SOA as well as the first experimentally obtained structural information of particle-phase HOMs (Fig. 1). Especially for the most abundant HOMs [Zhao et al., 2013] at m/z 308, 340, 342 and 310 [$M+NO_3^-$] important structural information were obtained by DNPH derivatization. The compounds detected at m/z 340, 342 and 372 [$M+NO_3^-$] have been described to be involved

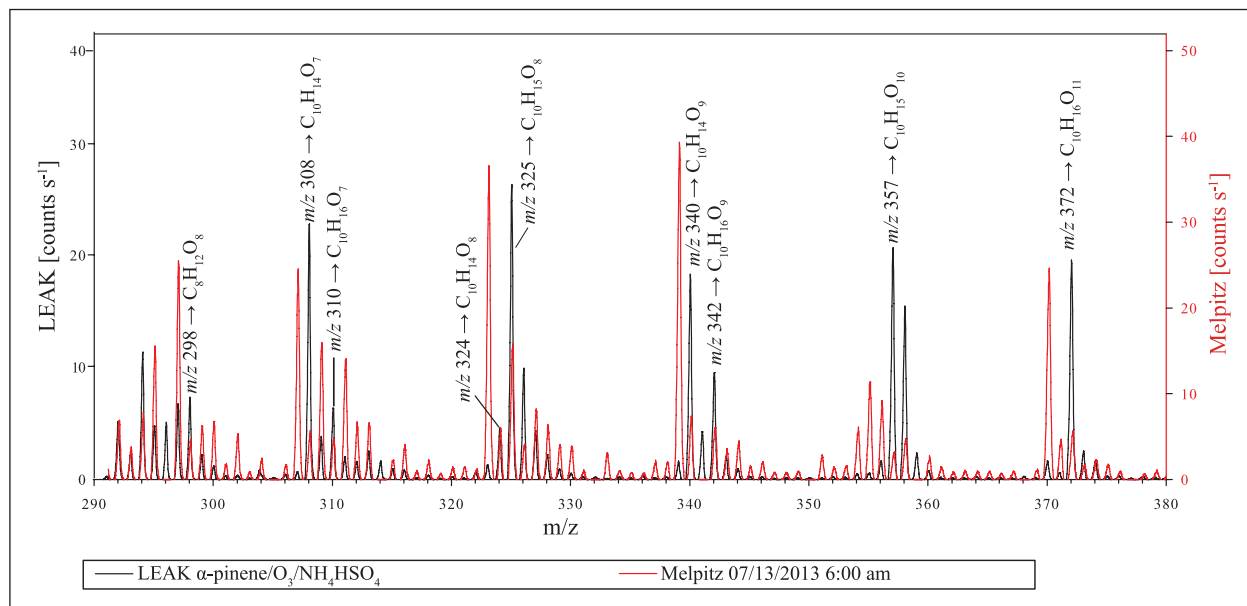


Fig. 1: Mass spectra obtained from CI-API-TOF measurements at the Melpitz research station (red) and during the ozonolysis of α -pinene in the aerosol chamber LEAK (black). Compounds were detected as NO_3^- adducts. Please note, that no OH radical scavenger was used. Thus, some signals also originate from OH radical reactions as it is discussed in the literature [Jokinen et al., 2014].

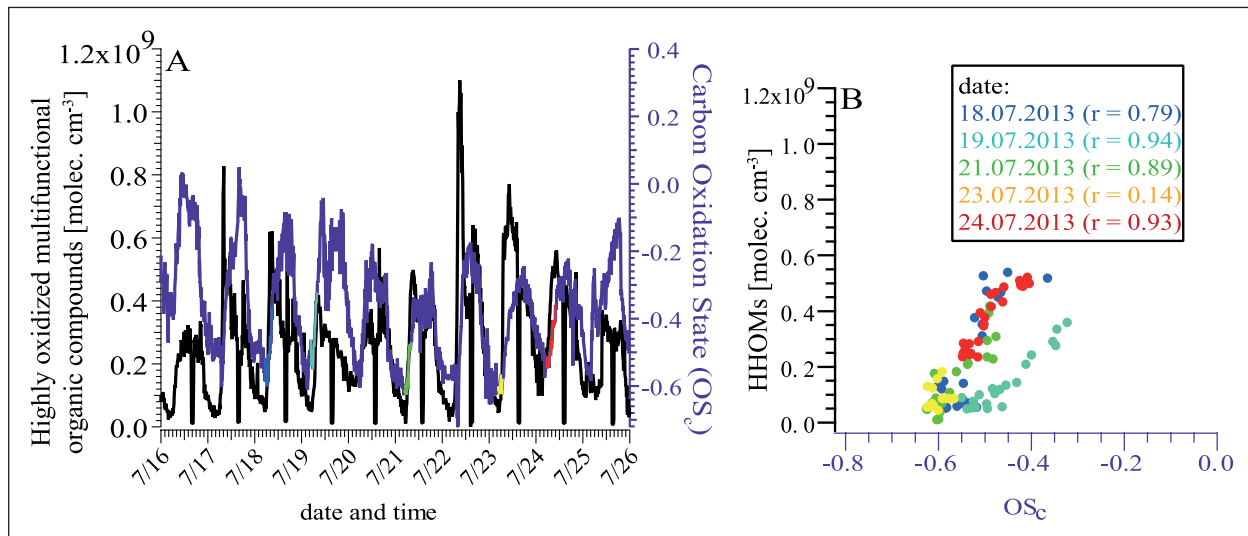


Fig. 2: Total concentration of HOMs (black) and particulate carbon oxidation state (OS_c , purple) during selected days of the measurement campaign in Melpitz (A). Scatter plot highlights the linear relationship that can be observed between gas-phase HOM concentration and particulate OS_c (B).

in particle formation whereas m/z 308 is suggested to be correlated with particle growth [Zhao et al., 2013]. For the first three compounds corresponding mono-DNPH derivatives were detected indicating a monocarbonyl compound. Contrary, for the m/z 308 [$M_w + NO_3^-$] compound a corresponding di-hydrazone signal was found indicating a dicarbonyl compound.

Especially HOMs detected at m/z 298, 308, 340, 342 and 372 [$M+NO_3^-$] were also reported in the literature and were assigned to $C_8H_{12}O_8$, $C_{10}H_{14}O_7$, $C_{10}H_{14}O_9$, $C_{10}H_{16}O_9$ and $C_{10}H_{14}O_{11}$ based on the high resolution mass spectrometric data [Ehn et al., 2012, 2014; Zhao et al., 2013]. Besides these compounds three additional signals were found at m/z 294, 310 and 324 [$M+NO_3^-$] corresponding to $C_{10}H_{16}O_6$, $C_{10}H_{16}O_7$ and $C_{10}H_{14}O_8$.

Up to now, the existence of carbonyl groups in HOMs was only subject to speculation, and the present study provides the first experimental evidence for the presence of carbonyl groups in the HOM skeleton.

Based on the obtained Melpitz field data set compared to the LEAK data set, it can be stated that the formation of a number of identical HOMs was observed. The conducted field study shows that the phase transfer of HOMs leads to a significantly higher oxidation state of ambient organic aerosol.

As it can be seen in Fig. 2, a good agreement between particulate OS_c and the total concentration of gas phase HOMs was found, suggesting that these compounds might directly contribute to the change in particle-phase OS_c (Fig. 2A). This is particularly clearly seen for the first hours of the morning when the formation of HOMs is the strongest. During this

period, a linear relationship between total HOM concentration in the gas phase and particulate OS_c was observed (Fig. 2B). Based on this it is expected that HOMs condense into the particle phase and thus, make up a large fraction of the organic mass.

A generation of HOMs was also observed for the oxidation of isoprene with OH radicals. This formation differs from monoterpene oxidation as HOMs are formed only from a second oxidation step. The precursor compound is hydroperoxy-methylbutenol (ISPOOH) which itself is the main primary oxidation product of isoprene in a low NO_x regime.

Observed HOMs products are C_5 compounds with up to 9 oxygen atoms. These high oxygen contents can structurally only be explained with a high amount of hydroperoxy groups in addition to alcohol and carbonyl functional groups. Further, the high oxygen content results in O/C ratios and oxidation states OS_c of up to 1.8 and 1.6, allowing them to be assigned to the group of ELVOCs. Support for this classification is given by a strong reduction of the HOMs gas phase concentrations simultaneously to a growth of particles observed in experiments with seed particles.

Further quantitative analysis of particle mass compounds showed that organic peroxides contribute a significant proportion of 17 % to the organic mass. Given that all HOMs partition to the particle phase and remain stable until analysis of the organic mass, isoprene HOMs can add 10 % to particle mass and thereby two third of the peroxide content can be explained.

References

- Ehn, M., E. Kleist, H. Junninen, T. Petäjä, G. Lonn, S. Schobesberger, M. Dal Maso, A. Trimborn, M. Kulmala, D. R. Worsnop, A. Wahner, J. Wildt, and T. F. Mentel (2012), Gas phase formation of extremely oxidized pinene reaction products in chamber and ambient air, *Atmos. Chem. Phys.*, 12(11), 5113-5127, doi:10.5194/acp-12-5113-2012.
- Ehn, M., J. A. Thornton, E. Kleist, M. Sipilä, H. Junninen, I. Pullinen, M. Springer, F. Rubach, R. Tillmann, B. Lee, F. Lopez-Hilfiker, S. Andres, I.-H. Acrí, M. Rissanen, T. Jokinen, S. Schobesberger, J. Kangasluoma, J. Kontkanen, T. Nieminen, T. Kurtén, L. B. Nielsen, S. Jørgensen, H. G. Kjaergaard, M. Canagaratna, M. Dal Maso, T. Berndt, T. Petäjä, A. Wahner, V.-M. Kerminen, M. Kulmala, D. R. Worsnop, J. Wildt, and T. F. Mentel (2014), A large source of low-volatility secondary organic aerosol, *Nature*, 506(7489), 476-479, doi:10.1038/nature13032.
- Jokinen, T., M. Sipilä, S. Richters, V.-M. Kerminen, P. Paasonen, F. Stratmann, D. Worsnop, M. Kulmala, M. Ehn, H. Herrmann, and T. Berndt (2014), Rapid Autoxidation Forms Highly Oxidized RO₂ Radicals in the Atmosphere, *Angewandte Chemie-International Edition*, 53(52), 14596-14600, doi:10.1002/anie.201408566.
- Mutzel, A., M. Rodigast, Y. Iinuma, O. Böge, and H. Herrmann (2013), An improved method for the quantification of SOA bound peroxides, *Atmos. Environ.*, 67, 365-369, doi:10.1016/j.atmosenv.2012.11.012.
- Zhao, J., J. Ortega, M. Chen, P. H. McMurry, and J. N. Smith (2013), Dependence of particle nucleation and growth on high-molecular-weight gas-phase products during ozonolysis of alpha-pinene, *Atmos. Chem. Phys.*, 13(15), 7631-7644, doi:10.5194/acp-13-7631-2013.

Highly oxidized multifunctional organic compounds (HOMs) from the ozonolysis of sesquiterpenes

Stefanie Richters, Hartmut Herrmann, Torsten Berndt

Sesquiterpene ($C_{15}H_{24}$) stellen neben Isopren (C_5H_8) und den Monoterpenen ($C_{10}H_{16}$) wichtige biogene organische Verbindungen dar, deren Oxidationsprodukte zur Bildung von sekundärem organischen Aerosol (SOA) in der Atmosphäre beitragen können. Bei Untersuchungen zur Oxidation von Monoterpenen wurden kürzlich hochoxidierte Reaktionsprodukte (HOMs) nachgewiesen, welche auf Grund ihrer Eigenschaften relevant für die SOA-Bildung sind.

In dieser Arbeit wurde die HOM-Bildung aus der Ozonolyse von drei Sesquiterpenen, α -Cedren, β -Caryophyllen und α -Humulen, in einer Freistrahlapparatur untersucht.

Für alle drei Sesquiterpene konnte HOM-Bildung beobachtet werden, welche dem bekannten Reaktionsmechanismus der Autoxidation entspricht. Außerdem wurden bei der Ozonolyse von β -Caryophyllen und α -Humulen weitere Signale detektiert, welche auf zusätzliche Reaktionspfade hinweisen. Die molaren HOM-Ausbeuten der drei Sesquiterpene liegen zwischen 0.5 und 1.8%. Dies deutet darauf hin, dass Sesquiterpen-HOMs nur in geringem Maßstab zur globalen SOA-Bildung beitragen können.

Introduction

The oxidation products of biogenic emissions, such as isoprene (C_5H_8), monoterpenes ($C_{10}H_{16}$) and sesquiterpenes ($C_{15}H_{24}$), are known to have an important impact on the global secondary organic aerosol (SOA) burden. It is currently a hot topic in atmospheric chemistry to ascertain how these low-volatile organic oxidation products are formed in the atmosphere.

Recently, *Ehn et al.* [2014] conclusively demonstrated the formation of highly oxidized multifunctional organic compounds (HOMs) from the ozonolysis of α -pinene, and their importance for SOA formation. The HOM detection became feasible by the latest developments of on-line mass spectrometric techniques [*Junninen et al.*, 2010]. Other terpene ozonolysis studies, using the same detection technique, have confirmed the findings by *Ehn et al.* [2014] and discovered that HOM formation with up to 12 O-atoms in the molecules proceeds on a time scale of seconds at atmospheric reactant concentrations [*Jokinen et al.*, 2014; *Mentel et al.*, 2015].

The HOM formation can be explained via an autoxidation mechanism, meaning RO_2 isomerization ($ROO \rightarrow QOOH$) and subsequently O_2 addition ($QOOH + O_2 \rightarrow R'OO$). This reaction sequence is

repeated several times. The first-generation closed-shell products of these highly oxidized RO_2 radicals are formed in the atmosphere from the reaction with NO, NO_2 , HO_2 or other RO_2 radicals.

The scope of this work are basic investigations on HOM formation from the ozonolysis of three sesquiterpenes (SQTs), namely α -cedrene, β -caryophyllene and α -humulene. The corresponding molecule structures are given in Fig. 1. SQTs are emitted to the atmosphere with about 18 million metric tons carbon per year corresponding to approximately 2.4% of the total annual biogenic emission of about 720 million metric tons carbon [*Sindelarova et al.*, 2014]. Locally, SQTs can be responsible for up to 70% of the biogenic emissions, e.g. in orange orchards [*Ciccioli et al.*, 1999].

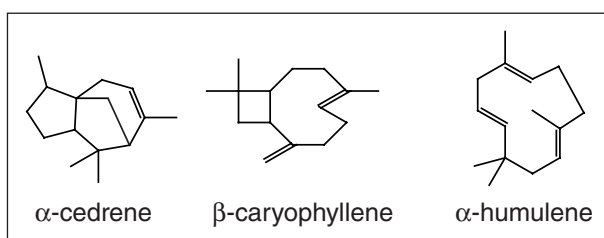


Fig. 1: Structures of the three sesquiterpenes investigated in this study.

Experimental

The experiments were carried out in a free-jet flow system at a temperature of 297 ± 1 K and a pressure of 1 bar purified air [Berndt et al., 2015]. This approach allows investigations with negligible wall losses and a reaction time of 3.0 - 7.9 s. The reaction products were detected and quantified by means of chemical ionization - atmospheric pressure interface - time-of-flight (CI-APi-TOF) mass spectrometry (Airmodus, Tofwerk) sampling the centre flow at the tube outlet with a rate of 10 L min^{-1} (STP, standard temperature and pressure). Nitrate or acetate were used as the reagent ions in the ionization process. Gas chromatography with a flame ionization detector (GC-FID; Agilent 6890) as well as Proton Transfer Reaction – Mass Spectrometry (PTR-MS; HS PTR-QMS 500, Ionicon) served as the analytical techniques for SQT quantification.

Results

Figure 2 shows an example of a product mass spectrum from the ozonolysis of α -cedrene in the mass to charge range 350 - 505 Th using nitrate ionization. The position of the dominant signals in the spectrum differs by 32 nominal mass units each (361, 393, 425, 457 and 489 Th) and were assigned to highly oxidized RO_2 radicals according to the general formula $\text{O}_2\text{O-C}_{15}\text{H}_{23-x}(\text{OOH})_x\text{O}_2$ with $x = 1 - 5$. Here, “ x ” represents the number of hydroperoxide moieties in the molecule. The two oxygen atoms “O,O”- arise from the initial ozone attack and the final O_2 characterizes the RO_2 radical. The number “ x ” was determined in experiments with heavy water (D_2O) in the reaction

gas allowing to exchange the H-atoms in the OOH groups by D-atoms. The resulting signal shift in the mass spectrum indicates “ x ”. The origin of the O-atoms in the highly oxidized products was investigated using either “normal” ozone ($^{16}\text{O}_3$) or “heavy” ozone ($^{18}\text{O}_3$) in the ozonolysis. From the comparison of the product spectra it was followed that two O-atoms in the HOMs arose from ozone, indicated as “O,O”, and the others from O_2 from the air. This finding is in line with earlier results from monoterpene ozonolysis [Jokinen et al., 2014]. The formation of the detected highly oxidized RO_2 radicals (Fig. 2) as well as the corresponding closed-shell products can be explained by an autoxidation mechanism [Jokinen et al., 2014].

Similar ozonolysis experiments have been conducted for β -caryophyllene and α -humulene as well. It is to be noted, that the product spectra were more complex in the case of these SQTs. Obviously, other reaction pathways are also important for HOM generation beside the autoxidation steps. More experimental work is needed for a better understanding of HOM formation from the ozonolysis of β -caryophyllene and α -humulene.

The total, molar HOM yield was measured as a function of reacted SQT applying nitrate and acetate ionization, see Fig. 3. The HOM yields slightly decreased for all SQTs for higher SQT conversions. This could tentatively be explained by consecutive product formation of the highly oxidized RO_2 radicals which are not detectable with the used technique. For α -cedrene, the total HOM concentrations yielded $0.6_{-0.3}^{+0.6}\%$ of the reacted α -cedrene for both ionization techniques. In the case of β -caryophyllene, the observed molar HOM yield was $0.5_{-0.3}^{+0.5}\%$ using nitrate ionization and $1.8_{-0.9}^{+1.8}\%$ using acetate ionization. This

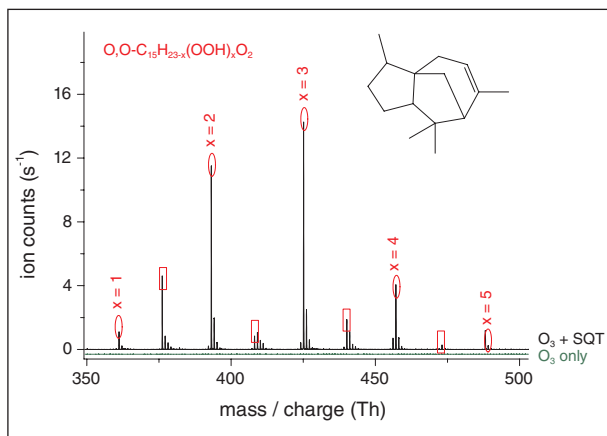


Fig. 2: Ozonolysis of α -cedrene: Highly oxidized RO_2 radicals ($\text{O}_2\text{O-C}_{15}\text{H}_{23-x}(\text{OOH})_x\text{O}_2$, $x = 1 - 5$, red oval lines) and corresponding C_{15} -closed-shell products ($\text{C}_{15}\text{H}_{22}\text{O}_{7-13}$, red rectangular lines), nitrate ionization. The green spectrum line (O_3 only) shows the background experiment in which only ozone (no SQT) was present.

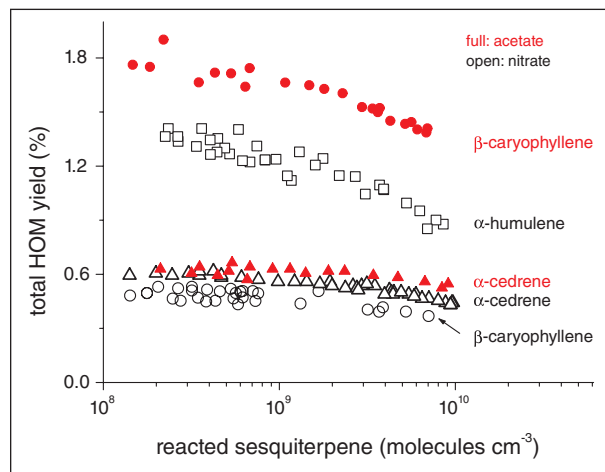


Fig. 3: Total, molar HOM yield from the ozonolysis of the three SQTs as a function of reacted SQT using either acetate (full red symbols) or nitrate (open black symbols) for ionization.

large difference by a factor of 3.6 reflects the higher detection sensitivity of acetate compared with nitrate for special classes of HOMs. The molar HOM concentrations from the ozonolysis of α -humulene resulted in a total HOM yield of $1.4^{+1.4}_{-0.7}\%$ using nitrate ionization. A comparison with results from acetate ionization was impossible caused by experimental restrictions in this reaction system.

In conclusion, the SQT ozonolysis reactions investigated here showed relatively low molar HOM yields between 0.5 and 1.8% being slightly lower than those from α -pinene ozonolysis which lay between 3 - 7% [Ehn et al., 2014; Jokinen et al., 2014]. Thus, only a limited contribution of SQT-derived HOMs to the global SOA formation can be expected.

References

- Berndt, T., S. Richters, R. Kaethner, J. Voigtlander, F. Stratmann, M. Sipilä, M. Kulmala, and H. Herrmann (2015), Gas-phase ozonolysis of cycloalkenes: formation of highly oxidized RO₂ radicals and their reactions with NO, NO₂, SO₂, and other RO₂ radicals, *J. Phys. Chem. A*, 119(41), 10336-10348, doi:10.1021/acs.jpca.5b07295.
- Ciccioli, P., E. Brancaleoni, M. Frattoni, V. Di Palo, R. Valentini, G. Tirone, G. Seufert, N. Bertin, U. Hansen, O. Csiky, R. Lenz, and M. Sharma (1999), Emission of reactive terpene compounds from orange orchards and their removal by within-canopy processes, *J. Geophys. Res.*, 104(D7), 8077-8094, doi:10.1029/1998jd100026.
- Ehn, M., J. A. Thornton, E. Kleist, M. Sipilä, H. Junninen, I. Pullinen, M. Springer, F. Rubach, R. Tillmann, B. Lee, F. Lopez-Hilfiker, S. Andres, I. H. Acir, M. Rissanen, T. Jokinen, S. Schobesberger, J. Kangasluoma, J. Kontkanen, T. Nieminen, T. Kurtén, L. B. Nielsen, S. Jørgensen, H. G. Kjaergaard, M. Canagaratna, M. D. Maso, T. Berndt, T. Petäjä, A. Wahner, V. M. Kerminen, M. Kulmala, D. R. Worsnop, J. Wildt, and T. F. Mentel (2014), A large source of low-volatility secondary organic aerosol, *Nature*, 506(7489), 476-479, doi:10.1038/nature13032.
- Jokinen, T., M. Sipilä, S. Richters, V. M. Kerminen, P. Paasonen, F. Stratmann, D. Worsnop, M. Kulmala, M. Ehn, H. Herrmann, and T. Berndt (2014), Rapid autoxidation forms highly oxidized RO₂ radicals in the atmosphere, *Angew. Chem., Int. Ed.*, 53(52), 14596-14600, doi:10.1002/anie.201408566.
- Junninen, H., M. Ehn, T. Petäjä, L. Luosujärvi, T. Kotiaho, R. Kostainen, U. Rohner, M. Gonin, K. Fuhrer, M. Kulmala, and D. R. Worsnop (2010), A high-resolution mass spectrometer to measure atmospheric ion composition, *Atmos. Meas. Tech.*, 3(4), 1039-1053, doi:10.5194/amt-3-1039-2010.
- Mentel, T. F., M. Springer, M. Ehn, E. Kleist, I. Pullinen, T. Kurtén, M. Rissanen, A. Wahner, and J. Wildt (2015), Formation of highly oxidized multifunctional compounds: autoxidation of peroxy radicals formed in the ozonolysis of alkenes – deduced from structure–product relationships, *Atmos. Chem. Phys.*, 15(12), 6745-6765, doi:10.5194/acp-15-6745-2015.
- Sindelarova, K., C. Granier, I. Bouarar, A. Guenther, S. Tilmes, T. Stavrakou, J. F. Müller, U. Kuhn, P. Stefani, and W. Knorr (2014), Global data set of biogenic VOC emissions calculated by the MEGAN model over the last 30 years, *Atmos. Chem. Phys.*, 14(17), 9317-9341, doi:10.5194/acp-14-9317-2014.

Funding

National Academic Scholarship Foundation (Studienstiftung des deutschen Volkes)

Cooperation

University of Helsinki, Helsinki, Finland

Can we define an asymptotic value for the ice active surface site density for heterogeneous ice nucleation?

Dennis Niedermeier^{1,2}, Stefanie Augustin-Bauditz¹, Susan Hartmann¹, Heike Wex¹, Karolina Ignatius¹, Frank Stratmann¹

¹ Leibniz Institute for Tropospheric Research (TROPOS), Leipzig, Germany

² Department of Physics, Michigan Technological University, Houghton, Michigan, USA

Die Eiskeimfähigkeit monodisperser Feldspat-Partikel verschiedener Größen wurde mit Hilfe des Leipzig Aerosol Cloud Interaction Simulators im Immersionsgefriermode untersucht. Dabei zeigte sich, dass nicht alle unterkühlten Tropfen heterogen einfroren und der Anteil gefrorener Tropfen direkt proportional zur Partikeloberfläche ist. Das beobachtete Gefrierverhalten konnte mit Hilfe des kombinierten „stoCHastic modEl of similar and poiSSon distributed ice nuclei“ und „Soccer Ball Models“ (CHESS-SBM) beschrieben werden. Basierend auf unseren Ergebnissen und unter Einbeziehung von Beobachtungen anderer Forschergruppen konnte ein Grenzwert der „ice active surface site density“ n_s für Mineralstaub abgeleitet werden. Dieser Grenzwert stellt eine Obergrenze der Eisaktivität dar und ist somit ein wichtiger Eingangsparameter für atmosphärische Modellierungen.

Introduction

Atkinson *et al.* [2013] reported that “feldspar minerals dominate ice nucleation by mineral dusts under mixed-phase cloud conditions, despite feldspar being a minor component of dust emitted from arid regions”. Studies of Wex *et al.* [2014] and Augustin-Bauditz *et al.* [2014] further illustrate the relevance of feldspar for ice nucleation. Augustin-Bauditz *et al.* [2014] investigated the freezing behaviour of droplets each containing a single feldspar particle with a diameter of 300 nm. They observed a levelling off of the frozen droplet fraction at about 0.8 for temperatures above the homogeneous ice nucleation limit ($T > -38^\circ\text{C}$).

In this study [Niedermeier *et al.*, 2015], we deepen the investigations concerning the ice nucleating ability of the same feldspar by focusing on size-segregated, monodisperse particles and verifying whether the levelling off in the frozen fraction scales with particle surface area. This would give indications concerning the number and distribution of ice nucleating sites in the particle population. For the experiments the Leipzig Aerosol Cloud Interaction Simulator (LACIS) [Hartmann *et al.*, 2011] is applied. The Soccer

ball model (SBM) [Niedermeier *et al.*, 2011, 2014] is combined with the stoCHastic modEl of similar and poiSSon distributed ice nuclei (CHESS model) [Hartmann *et al.*, 2013] to represent the determined ice nucleation behaviour and to derive the ice active surface site density, n_s .

Experimental Results and CHESS-SBM

In Fig. 1, experimentally determined frozen fractions are presented for droplets each containing one feldspar particle of a certain size. In different experiments the particle size was varied. In all cases, the measured frozen fractions increase with decreasing temperature and level off at values lower than 1 at temperatures well above the homogeneous freezing temperature. The value of the frozen fraction in the leveling off range depends on particle size. This observed behavior indicates that not all particles feature an ice nucleating site with the (average) number of sites per particle scaling linearly with particle surface area.

In order to theoretically describe the observed ice nucleating behavior we assume that the ice nucleating sites are Poisson distributed over the droplet

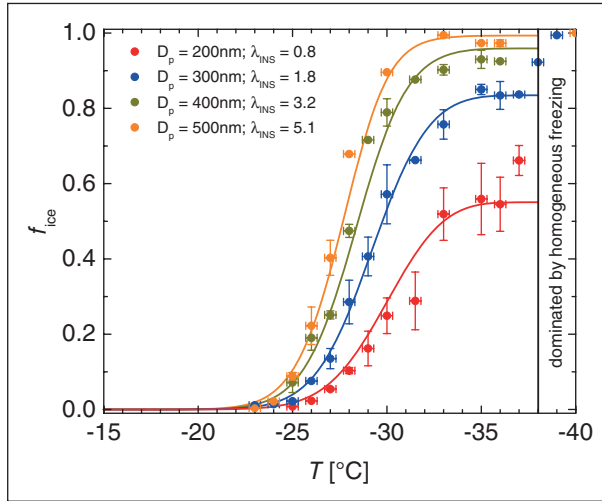


Fig. 1: LACIS frozen fraction f_{ice} as a function of temperature as water droplets containing differently sized feldspar particles (λ_{INS} values are given as well). The solid lines represented SBM fits to the frozen fractions.

population with λ_{INS} being the average number of ice nucleating sites per droplet. λ_{INS} is a key parameter of the CHESS model. Furthermore each ice nucleating site is assigned a specific contact angle (equivalent to ice nucleation rate), based on a Gaussian probability density function (PDF) – a key feature of the SBM. Consequently, the resulting CHESS-SBM includes the probability of a droplet to contain an ice nucleating site connected with probability of the site to induce ice nucleation at a certain temperature.

As it is possible to directly derive λ_{INS} for the feldspar sample, only two unknown CHESS-SBM parameters, the mean μ_{θ} and the standard deviation σ_{θ} of the PDF, are left which can be determined through fitting the CHESS-SBM to the experimental data. The calculated CHESS-SBM curves (with $\mu_{\theta} = 1.29$ rad and $\sigma_{\theta} = 0.10$ rad) are shown in Fig. 1 fitting the experimental LACIS data with reasonable accuracy.

Asymptotic value of the ice active site density

As an instrument-independent quantity, the temperature-dependent ice active surface site density, n_s , [e.g., Connolly et al., 2009] has been established in the past in order to describe and compare the ice nucleating behavior of various particle types. Consequently, n_s is used here for comparing our experimental results with those of other studies.

Several laboratory studies quantifying the ice nucleating ability of various desert dust samples, which are summarized in Hoose and Möhler [2012] suggest the existence of an asymptotic value for n_s because a leveling off can be observed for $T > -38^\circ\text{C}$. Based on these results and our findings for feldspar,

we can derive an asymptotic value for n_s which we call $n_s^* = \lambda_{\text{INS}} / S_p$ with S_p being the particle surface area.

In Fig. 2, in addition to experimentally determined n_s values of different natural mineral dusts, a CHESS-SBM curve (grey area) is shown which is based on the parameters determined for our feldspar sample (i.e., $\mu_{\theta} = 1.29$ rad and $\sigma_{\theta} = 0.10$ rad). This parameterization further includes a range of nucleation times commonly used in laboratory studies (in some of the original studies the time scales were not reported). Additionally to determine the values for n_s^* to be used for the CHESS-SBM parameterization, we assume the feldspar content in these desert dusts to range between 1% and 25% based on findings for various desert soils [Atkinson et al., 2013 and reference therein]. The different desert dusts can be very well represented by the CHESS-SBM.

Implications

The ice nucleating ability of natural mineral dusts is dominated by the contained feldspar amount in the temperature range where feldspar is an efficient ice nucleator. Based on our knowledge about feldspar, an asymptotic value for the ice active surfaces site density, n_s^* , can be determined as a measure for the ice nucleation potential of natural dusts. Care has to be taken when extrapolating n_s curves for mineral

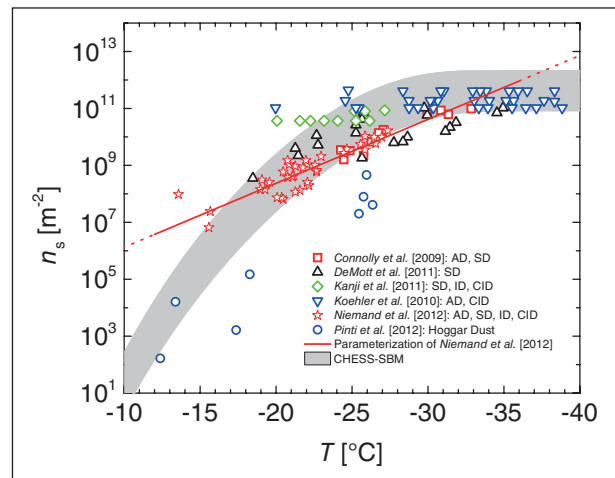


Fig. 2: The differently colored symbols represent n_s values determined in various studies for various desert dusts: Asian Dust (AD), Canary Island Dust (CID), Israeli Dust (ID), and Saharan Dust (SD). Note that these data points have already been presented in Fig. 11b of Hoose and Möhler [2012]. The red line represents the parameterization of Niemand et al. [2012] for desert dusts valid in the temperature range $[-36^\circ\text{C}, -12^\circ\text{C}]$. Dotted lines represent the extrapolation of the parameterization. The gray shaded curve depicts the CHESS-SBM-based n_s parameterization for the feldspar sample for the nucleation times/cooling rate range $dT/dt = 0.1\text{--}10.0 \text{ K min}^{-1}$ and the n_s^* spread of 8.40×10^{10} to $2.13 \times 10^{12} \text{ m}^{-2}$ assuming the feldspar amount in the desert dusts to range between 1% and 25%.

dusts to lower or higher temperature. It might lead to orders of magnitude overestimations of n_s (compare Niemand et al. [2012] parameterization, which is valid in the temperature range of -12°C to -36°C , to the CHESS-SBM curve in Fig. 2). If it is possible to determine a n_s^* value for a given particulate material, it is possible to determine the (average) number of ice nucleating sites per particle surface area. This finding could be used in atmospheric modeling applications

in order to define size-class specific number of ice nucleating sites for various materials and hence a realistic maximum of particles' ice nucleation activity. In order to parameterize the ice nucleation behavior of mineral dusts in cloud resolving models, we recommend the usage of the CHESS-SBM together with the here given parameters of the contact angle distribution.

References

- Atkinson, J. D., B. J. Murray, M. T. Woodhouse, T. F. Whale, K. J. Baustian, K. S. Carslaw, S. Dobbie, D. O'Sullivan, and T. L. Malkin (2013), The importance of feldspar for ice nucleation by mineral dust in mixed-phase clouds, *Nature*, **498**, 355–358, doi:10.1038/nature12278.
- Augustin-Bauditz, S., H. Wex, S. Kanter, M. Ebert, D. Niedermeier, F. Stoltz, A. Prager, and F. Stratmann (2014), The immersion mode ice nucleation behavior of mineral dusts: A comparison of different pure and surface modified dusts, *Geophys. Res. Lett.*, **41**, 7375–7382, doi:10.1002/2014GL061317.
- Connolly, P. J., O. Möhler, P. R. Field, H. Saathoff, R. Burgess, T. Choularton, and M. Gallagher (2009), Studies of heterogeneous freezing by three different desert dust samples, *Atmos. Chem. Phys.*, **9**, 2805–2824, doi:10.5194/acp-9-2805-2009.
- DeMott, P. J., et al. (2011), Resurgence in ice nuclei measurement research, *Bull. Am. Meteorol. Soc.*, **92**, 1623–1635, doi:10.1175/2011BAMS3119.1.
- Hartmann, S., D. Niedermeier, J. Voigtlander, T. Clauss, R. A. Shaw, H. Wex, A. Kiselev, and F. Stratmann (2011), Homogeneous and heterogeneous ice nucleation at LACIS: Operating principle and theoretical studies, *Atmos. Chem. Phys.*, **11**, 1753–1767, doi:10.5194/acp-11-1753-2011.
- Hartmann, S., S. Augustin, T. Clauss, H. Wex, T. Šantl-Temkiv, J. Voigtlander, D. Niedermeier, and F. Stratmann (2013), Immersion freezing of ice nucleation active protein complexes, *Atmos. Chem. Phys.*, **13**, 5751–5766, doi:10.5194/acp-13-5751-2013.
- Hoose, C., and O. Möhler (2012), Heterogeneous ice nucleation on atmospheric aerosols: A review of results from laboratory experiments, *Atmos. Chem. Phys.*, **12**, 9817–9854, doi:10.5194/acp-12-9817-2012.
- Kanji, Z. A., P. J. DeMott, O. Möhler, and J. P. D. Abbott (2011), Results from the University of Toronto continuous flow diffusion chamber at ICIS2007: Instrument intercomparison and ice onsets for different aerosol types, *Atmos. Chem. Phys.*, **11**, 31–41, doi:10.5194/acp-11-31-2011.
- Koehler, K. A., S. M. Kreidenweis, P. J. DeMott, M. D. Petters, A. J. Prenni, and O. Möhler (2010), Laboratory investigations of the impact of mineral dust aerosol on cold cloud formation, *Atmos. Chem. Phys.*, **10**, 11,955–11,968, doi:10.5194/acp-10-11955-2010.
- Niedermeier, D., R. Shaw, S. Hartmann, H. Wex, T. Clauss, J. Voigtlander, and F. Stratmann (2011), Heterogeneous ice nucleation: Exploring the transition from stochastic to singular freezing behavior, *Atmos. Chem. Phys.*, **11**, 8767–8775, doi:10.5194/acp-11-8767-2011.
- Niedermeier, D., B. Ervens, T. Clauss, J. Voigtlander, H. Wex, S. Hartmann, and F. Stratmann (2014), A computationally efficient description of heterogeneous freezing: A simplified version of the Soccer ball model, *Geophys. Res. Lett.*, **41**, 736–741, doi:10.1002/2013GL058684.
- Niedermeier, D., S. Augustin-Bauditz, S. Hartmann, H. Wex, K. Ignatius, and F. Stratmann (2015), Can we define an asymptotic value for the ice active surface site density for heterogeneous ice nucleation?, *J. Geophys. Res. - Atmos.*, **120**, 5036–5046, doi:10.1002/2014JD022814.
- Niemand, M., et al. (2012), A particle-surface-area-based parameterization of immersion freezing on desert dust particles, *J. Atmos. Sci.*, **69**, 3077–3092, doi:10.1175/JAS-D-11-0249.1.
- Pinti, V., C. Marcolla, B. Zobrist, C. R. Hoyle, and T. Peter (2012), Ice nucleation efficiency of clay minerals in the immersion mode, *Atmos. Chem. Phys.*, **12**, 5859–5878, doi:10.5194/acp-12-5859-2012.
- Wex, H., P. J. DeMott, Y. Tobo, S. Hartmann, M. Rösch, T. Clauss, L. Tomsche, D. Niedermeier, and F. Stratmann (2014), Kaolinite particles as ice nuclei: Learning from the use of different kaolinite samples and different coatings, *Atmos. Chem. Phys.*, **14**, 5529–5546, doi:10.5194/acp-14-5529-2014.

Funding

Federal Ministry of Education and Research (BMBF), Bonn, Germany
 German Research Foundation (DFG), Bonn, Germany
 Alexander von Humboldt-Foundation, Bonn, Germany

Modelling of the marine multiphase DMS chemistry with the new CAPRAM DMS-Module 1.0

Erik Hans Hoffmann¹, Andreas Tilgner¹, Roland Schrödner^{1,2}, Ralf Wolke¹, Hartmut Herrmann¹

¹ Leibniz Institute for Tropospheric Research (TROPOS), Leipzig, Germany

² now at: Lund University, Centre for Environmental and Climate Research, Sölvegatan 37, 22362 Lund, Sweden

Die Oxidation von DMS in der marinen troposphärischen Grenzschicht ist von großer Bedeutung für die Chemie der Atmosphäre und das Erdklimasystem, da DMS essentiell für die Prozessierung und Neubildung von marinen Aerosolpartikeln ist. Jedoch bestehen noch große Unsicherheiten bezüglich der Bedeutung von Multiphasenprozessen an der DMS-Oxidation. Daher war das Ziel der hier beschrieben Studien, die Entwicklung eines komplexen Multiphasenchemiemechanismus zur Beschreibung der marinen DMS-Halogen-Chemie sowie dessen Anwendung im Chemieprozessmodell SPACCIM (Spectral Aerosol Cloud Chemistry Interaction Model). Mittels des entwickelten DMS Moduls (DM1.0; 162 Multiphasenprozesse) wurden intensive Studien für marine Hintergrundbedingungen durchgeführt. Die Studien zeigten, dass die Multiphaseninteraktion von DMS und dessen Oxidationsprodukten mit reaktiven Halogenverbindungen sowie die Chemie der wässrigen Aerosolphase einen bedeutenden Anteil am DMS-Abbau und der Umwandlung in SO₂ und MSA haben.

Introduction

Oceans cover approximately 70% of Earth's surface and are the general emitter of dimethyl sulphide (DMS), the major natural sulphur source [Andreae, 1990]. The main DMS oxidation products are methyl sulfonic acid (MSA) and sulphuric acid/SO₂. Hence, DMS is of high importance for the formation of non-sea salt sulphate (nss-SO₄²⁻) aerosol and secondary particulate matter and thus for global climate [Quinn and Bates, 2011]. Despite many previous model studies on the DMS oxidation, there are still important knowledge gaps, particularly in aqueous-phase DMS chemistry, of its atmospheric fate [Barnes *et al.*, 2006]. Therefore, the present study aimed at the investigation of the multiphase DMS chemistry in the marine boundary layer (MBL). For this purpose, the new CAPRAM DMS module 1.0 (DM1.0) was developed and applied in the parcel model SPACCIM [Wolke *et al.*, 2005] for pristine-ocean simulations.

Mechanism development and modelling

Despite intensive efforts on the process modelling in the past, a detailed representation of multiphase DMS processes in state-of-the-art mechanisms was still lacking causing thus very inadequate predictions. To close this gap, a comprehensive multiphase DMS chemistry mechanism, the DM1.0, was developed. The newly developed reaction module includes 103 gas-phase reactions, 5 phase transfers and 54 aqueous-phase reactions. The DM1.0 has been coupled with the multiphase chemistry mechanism MCMv3.2/CAPRAM4.0α+HM2.1 [Rickard *et al.*, 2015; Bräuer *et al.* 2013, 2016] to investigate the multiphase DMS oxidation in the MBL. SPACCIM studies were carried out for a pristine ocean scenario. The scenario includes non-permanent cloud conditions with 8 cloud passages. The cloud passages allow the investigation of the influence of deliquesced particles and clouds on multiphase DMS chemistry during both day- and night-time conditions. To test

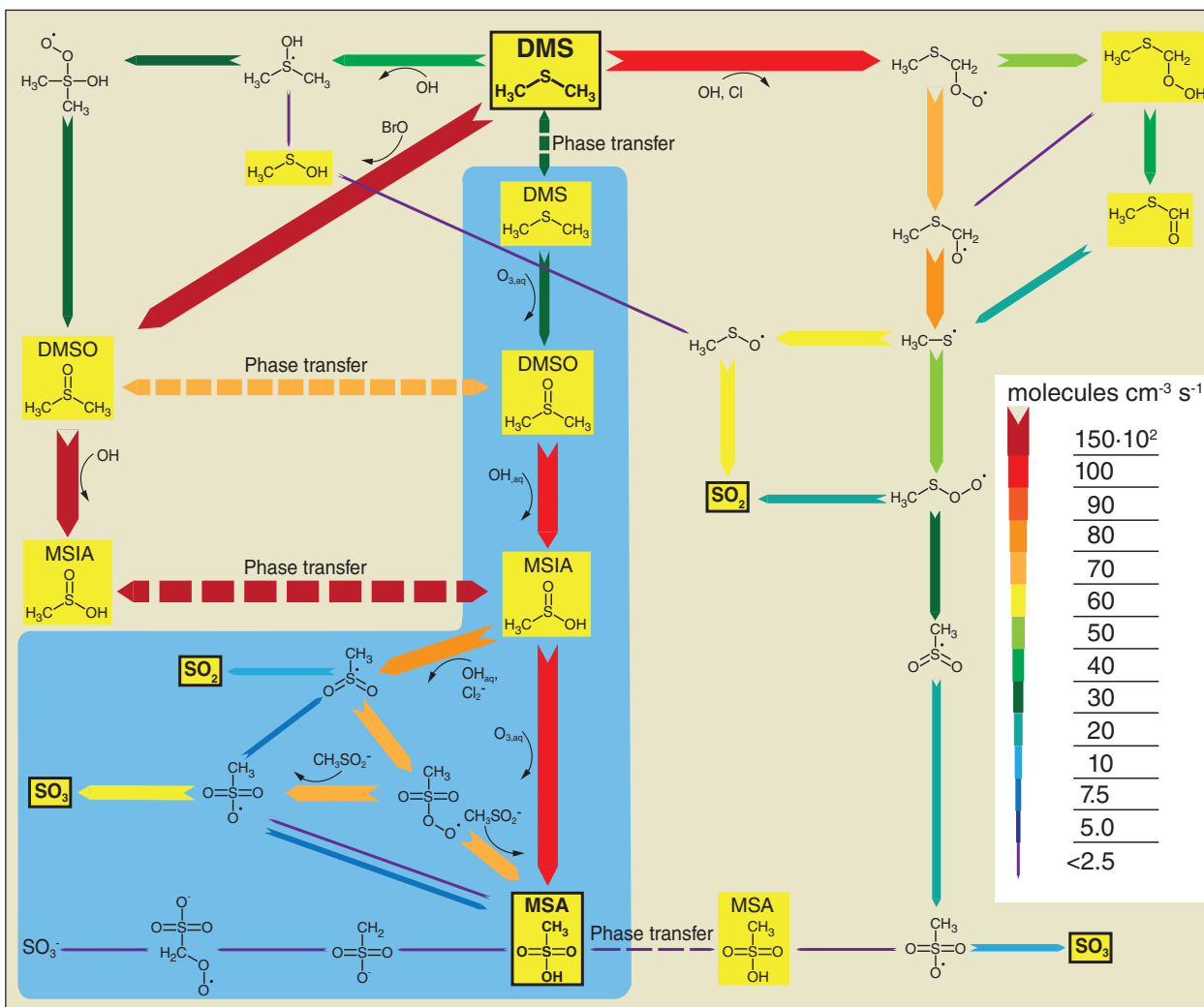


Fig. 1: Schematic depiction of key averaged source and sink fluxes (share on oxidation of > 5%) of the full scenario throughout the whole model period in 10^2 molecules $\text{cm}^{-3} \text{s}^{-1}$. The blue area highlights aqueous-phase reactions and the ochre area depicts gas-phase reactions. Produced stable compounds are shaded yellow, dashed lines represent phase transfer processes and the main products are bold.

the influence of various chemical subsystems on multiphase DMS chemistry different sensitivity runs were performed. Investigations of multiphase chemistry of DMS and its important oxidation products are done using concentration-time profiles and detailed time-resolved reaction flux analyses. Such detailed flux analyses determine the most important chemical cycles (see Fig. 1) and help to understand the time evolution of the concentration profiles. The model results were also compared to previous model studies and atmospheric measurements.

Model results

The model studies discovered the significance of aqueous-phase processes for the fate of DMS and its oxidation products (see Fig. 1). Overall, about 7% of DMS is effectively oxidised by O_3 in the cloud phase. Moreover, the simulations implied the importance of

reactive halogens for the chemistry of DMS and its oxidation products. Halogen radicals contribute overall with about 71% to DMS oxidation and gaseous Cl and BrO are identified as main oxidants (Cl: 23.6%, BrO: 46.1%). Under the simulated conditions, the aqueous-phase chemistry considerably reduces the SO_2 yield. The conversion efficiency of DMS to SO_2 in the gas phase was found to be between 0.2 and 0.6 for the pristine ocean scenario run with the full DM1.0 and a simulation without treating aqueous-phase chemistry in DM1.0, respectively. The investigations imply that the thermal decomposition of $\text{CH}_3\text{SO}_3^\cdot$ into SO_3 is the main contributor to gas-phase production of H_2SO_4 from DMS, with a total yield of 7.2% to sulphate production. Moreover, clouds and background concentrations of NO_x and O_3 showed strong effects on the yield of SO_2 . In contrast to former studies, the DM1.0 is able to carry the aqueous-phase production of MSA from reactions of methyl sulfinic acid (MSIA)

with O₃ (see Fig.1). These reactions contribute with about 57.7% to MSA production. Therewith, for the first time the simulations were able to capture measured MSA aerosol concentration levels of about 0.2 µg m⁻³ [Phinney et al., 2006] without using assumptions as done in former studies [e.g., Lucas and Prinn, 2002]. This finding indicates the key role of the aqueous-phase DMS chemistry. Moreover, DMS oxidation yields were observed between 0.01 and 0.47 MSA in different sensitivity runs, which are much higher compared to current implementations in higher-scale chemistry transport models (CTMs).

Conclusions and outlook

Overall, the simulation implies that multiphase DMS oxidation produces equal amounts of MSA and sulphate impacting both new particle formation and

cloud albedo. This finding is in contradiction to present CTMs where only gas-phase DMS chemistry is treated and only minor amounts of MSA are formed. Thus, the present studies imply that a state-of-the-art treatment of multiphase DMS chemistry in higher-scale CTMs is required to advanced current model predictions and their implications, e.g., for the climate. Thus, future work will focus on the development of reduced marine multiphase chemistry mechanisms and compact parameterisations for applications in sophisticated CTMs.

References

- Andreae, M. O. (1990), Ocean-atmosphere interactions in the global biogeochemical sulfur cycle, *Mar. Chem.*, 30(1-3), 1-29, doi:10.1016/0304-4203(90)90059-L.
- Barnes, I., J. Hjorth, and N. Mihalopoulos (2006), Dimethyl sulfide and dimethyl sulfoxide and their oxidation in the atmosphere, *Chem. Rev.*, 106(3), 940-975, doi:10.1021/Cr020529+.
- Bräuer, P., A. Tilgner, R. Wolke, and H. Herrmann (2013), Mechanism development and modelling of tropospheric multiphase halogen chemistry: The CAPRAM Halogen Module 2.0 (HM2), *J. Atmos. Chem.*, 70(1), 19-52, doi:10.1007/s10874-013-9249-6.
- Bräuer, P., C. Mouchel-Vallon, A. Tilgner, A. Mutzel, O. Böge, M. Rodigast, L. Poulain, D. van Pinxteren, B. Aumont, and H. Herrmann (2016), Development of a protocol designed for the self-generation of explicit aqueous phase oxidation schemes of organic compounds, *Atmos. Chem. Phys. Discuss., in preparation*.
- Lucas, D. D., and R. G. Prinn (2002), Mechanistic studies of dimethylsulfide oxidation products using an observationally constrained model, *J. Geophys. Res. - Atmos.*, 107(D14), doi:10.1029/2001jd000843.
- Phinney, L., W. R. Leaitch, U. Lohmann, H. Boudries, D. R. Worsnop, J. T. Jayne, D. Toom-Sauntry, M. Wadleigh, S. Sharma, and N. Shantz (2006), Characterization of the aerosol over the sub-arctic north east Pacific Ocean, *Deep-Sea Res. Pt. II*, 53(20-22), 2410-2433, doi:10.1016/J.Dsr2.2006.05.044.
- Quinn, P. K., and T. S. Bates (2011), The case against climate regulation via oceanic phytoplankton sulphur emissions, *Nature*, 480(7375), 51-56, doi:10.1038/nature10580.
- Rickard, A., et al. (2015), The Master Chemical Mechanism Version MCM v3.2, available at: <http://mcm.leeds.ac.uk/MCMv3.2/> (last access: 05-05-2015).
- Wolke, R., A. M. Sehili, M. Simmel, O. Knoth, A. Tilgner, and H. Herrmann (2005), SPACCIM: A parcel model with detailed microphysics and complex multiphase chemistry, *Atmos. Environ.*, 39(23-24), 4375-4388, doi:10.1016/J.Atmosenv.2005.02.038.

Cooperation

Dr. P. Bräuer, University of East Anglia, School of Environmental Sciences, Centre for Ocean and Atmospheric Sciences, Norwich, NR4 7TJ, UK

3-D multiphase chemistry modelling in the context of HCCT-2010

Roland Schrödner^{1,2}, Ralf Wolke¹, Andreas Tilgner¹, Dominik van Pinxteren¹, Hartmut Herrmann¹

¹ Leibniz Institute for Tropospheric Research (TROPOS), Leipzig, Germany

² now at: Lund University, Centre for Environmental and Climate Research, Sövegatan 37, 22362 Lund, Sweden

Simulationen mit dreidimensionalen atmosphärischen Modellen können einen wichtigen Beitrag zum Verständnis dieser Prozesse und zur Interpretation von Feldmessungen leisten. Deshalb wurde eine detaillierte und realitätsnahe Beschreibung komplexer wolkenchemischer Prozesse sowie ihrer Interaktionen im Chemietransportmodell COSMO-MUSCAT realisiert. Das weiterentwickelte Modellsystem wurde für umfangreiche 2-D-Prozessstudien und zur Modellierung von zwei ausgewählten Episoden des Feldexperiments HCCT-2010 (Hill Cap Cloud Thuringia 2010) genutzt. Dadurch konnten räumliche und dynamische Einflüsse der Multiphasenchemie in Wolken z. B. auf troposphärische Oxidantien und die sekundäre Aerosolmasse untersucht werden. Erstmals wurde hierbei ein chemischer Mechanismus mit der Komplexität von C3.0RED für 3-D-Simulationen realer Episoden verwendet. Ferner wurden die Modellergebnisse mit HCCT-2010 Messungen verglichen. Dieser Vergleich zeigte generelle Übereinstimmungen vieler Konzentrationsverläufe. Für einige partikuläre organische Verbindungen wurden aber auch interessante Unterschiede gefunden.

The tropospheric multiphase system consists of several highly connected processes, in which clouds play a key role. To treat detailed cloud chemistry in the chemistry transport model (CTM) COSMO-MUSCAT [Wolke *et al.*, 2012], the model was enhanced by a description of aqueous-phase chemical processes. To assess the chemical effects observed in 2-D process studies [Schrödner *et al.*, 2014] on a larger scale and to investigate the 3-D cloud processing as well as to demonstrate the general 3-D applicability of the detailed aqueous-phase chemistry of C3.0RED [Deguillaume *et al.*, 2009], the enhanced model was applied for real 3-D case studies simulating two selected time periods connected to the HCCT-2010 field campaign [van Pinxteren *et al.*, 2012]. The setup of HCCT-2010 is shown in Fig. 1. For the prevailing south-westerly wind directions, the airflow roughly passes the three measurement sites. Measurements of the aerosol-cloud processing were only performed under suitable flow conditions [Tilgner *et al.*, 2014].

Methods

Due to the close proximity of the measurement sites to each other, a very high horizontal model resolution was chosen. To reduce the computational costs, the model is nested 2 times, whereas the horizontal resolution is doubled with every nesting step and the

aqueous-phase chemistry is only treated for the innermost nest (0.7km horizontal resolution; thickness of lowest model layer ~20m). The initial and boundary data for the chemical composition of the atmosphere for the outer nest (N3) were obtained from a Europe-wide simulation, whereas reanalysis data of COSMO-DE runs (covering Germany) are used for the meteorological initial and boundary conditions.

Firstly, the model performance with respect to the meteorological fields and selected gas-phase concentrations was evaluated on the outer nests by a comprehensive comparison with available observations. Overall, the main characteristics of the compared species and the airflow at Mt. Schmücke are simulated quite well. Therefore, we conclude that the initial and boundary conditions for the innermost domain are reasonable for the chosen periods. For the investigations of cloud chemical processes, simulations with C3.0RED, with INORG (simple inorganic aqueous-phase chemistry) [Sehili *et al.*, 2005], and without aqueous-phase chemistry are compared with each other and with measured data.

Results

The formation of the sulphate mass as well as the relative difference of between C3.0RED and INORG of gas phase OH and NO₃ during the cloud

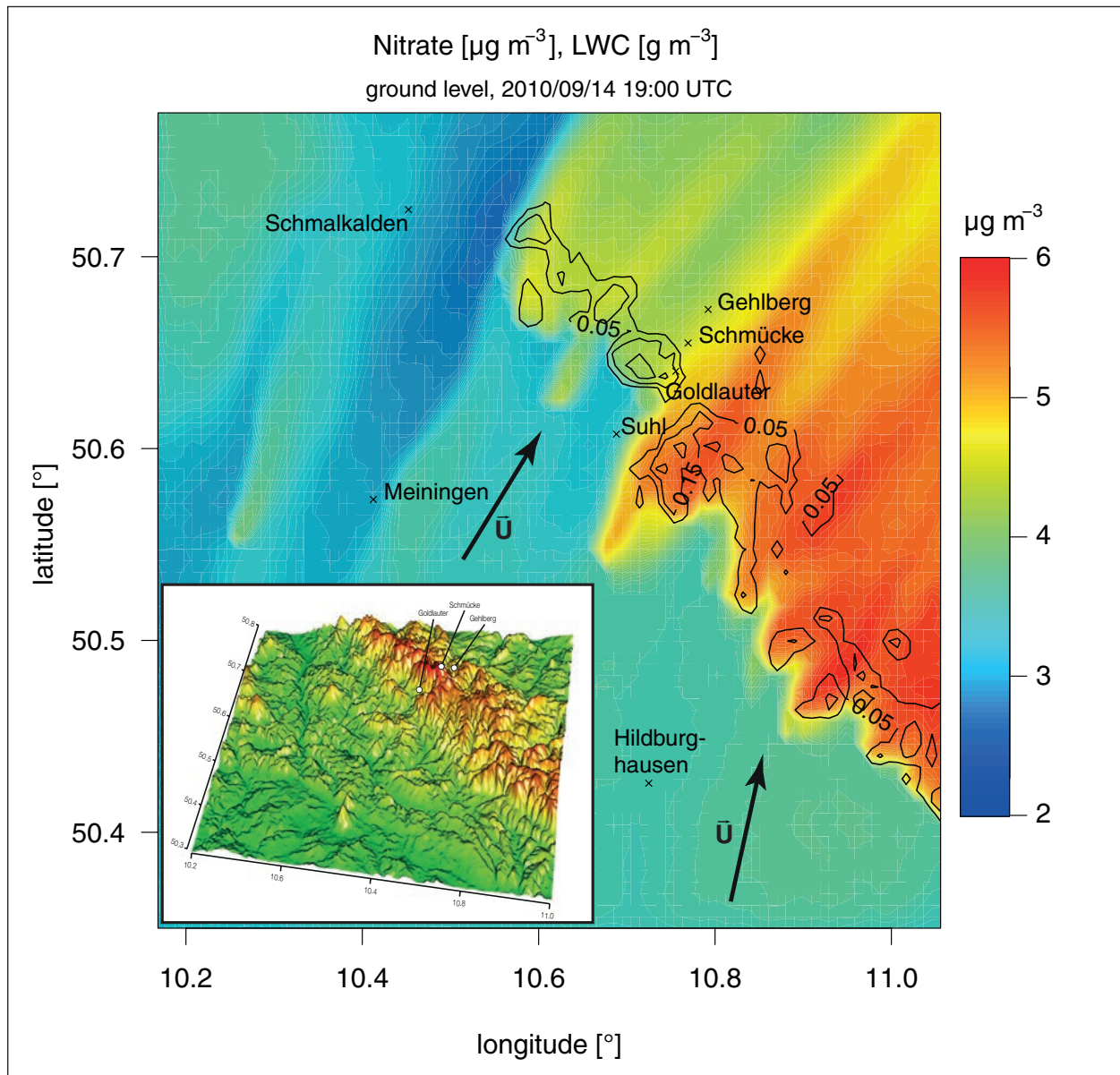


Fig. 1: Modelled nitrate mass (coloured) and modelled cloud liquid water content (contour lines) for HCCT scenario FCE1.1 at 14/09/2010, 19:00 UTC. In the lower left corner, the topography of the model domain is shown.

event FCE1.1 is presented in Figs. 1 and 2. In general, the effects observed in the earlier 2-D studies [Schrödner et al., 2014] could be confirmed. However, the decrease of the gas phase concentrations of the major oxidants OH and NO_3 was more pronounced with a net decrease ~20 km after the cloud of up to 20% and 99%, respectively. Hence, the slowed down oxidation of gas phase VOCs lead to larger deviations between C3.0RED and INORG for the concentrations of e.g., isoprene, α -pinene, and limonene after the cloud passage.

As observed in the 2-D cases, the pH decreases during the cloud passage due to the formation of sulphate and nitrate. Because of the low nighttime pH in C3.0RED (caused by uptake of N_2O_5 and

subsequent nitrate formation), the sulphate formation via O_3 becomes unimportant. This leads to ~20% lower nighttime sulphate mass concentrations compared to INORG. However during the day, the additional sulphate formation via HNO_4 , which is not present in INORG, results in locally up to ~10% higher sulphate mass concentrations in C3.0RED. During FCE1.1, the cloud processing at the mountain ridge can be clearly seen in the simulations. Furthermore, the cloud processing (e.g., sulphate formation) is horizontally rather inhomogeneous and not necessarily correlated with the LWC.

The simulation results were compared to selected measurements conducted at the Mt. Schmücke measurement site (in-cloud). In general, the model

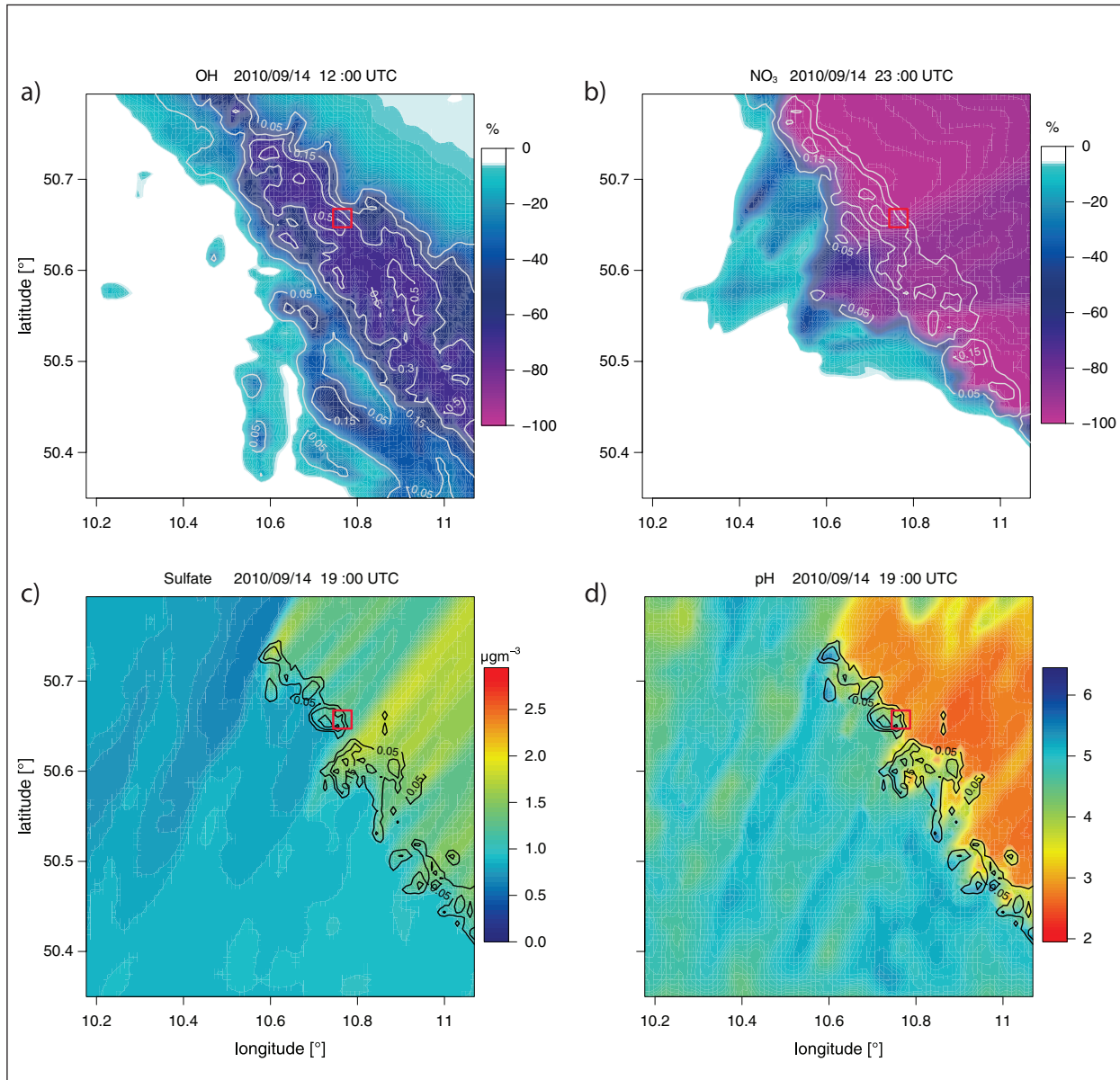


Fig. 2: Relative differences INORG of the gas phase concentrations of OH (a) and NO_3 (b) within the lowermost $\sim 1000\text{m}$. Modelled mass concentrations of sulphate (c) and the pH (d) in the lowest model layer. The square depicts Mt. Schmücke.

is able to follow the observed variability of the LWC. However, sometimes deviations of more than 0.1 gm^{-3} are observed. In Fig. 3, selected modelled and measured time series during FCE1.1 are compared. Overall, considerable differences between a simple or no aqueous-phase chemistry representation and the application of the detailed aqueous-phase mechanism C3.0RED are found. The results show that the sulphate formation during the considered cases depends on both the available SO_2 and the modelled LWC. Therefore, the largest deviations between the simulation with and without aqueous-phase chemistry occur for high LWCs (e.g., FCE1.1 around noon). Similar results can be seen for nitrate during the night. However, also during the day, the modelled

nitrate mass differs slightly between the runs with and without aqueous-phase chemistry due to the uptake of HNO_3 . Around noon during FCE1.1, the pH values and the sulphate/nitrate masses agree well with the measurements.

Overall, the conducted studies showed the 3-D CTM applicability of the complex multiphase chemical mechanisms C3.0RED. Significant spatial cloud effects were revealed. Further simulations should be conducted to provide a more comprehensive picture of agreements and disagreements between measurement and model results, and to improve the understanding of multiphase chemical processes.

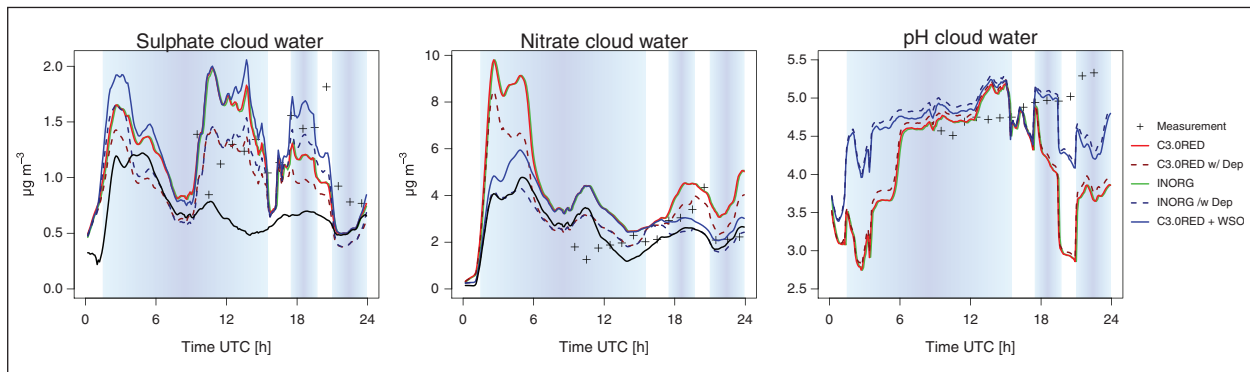


Fig. 3: Modelled and measured concentration time series of sulphate and nitrate in cloud water as well as the pH of the cloud water during FCE1.1 at the summit station. The blue shaded area indicates times when a cloud was simulated.

References

- Deguillaume, L., A. Tilgner, R. Schrödner, R. Wolke, N. Chaumerliac, and H. Herrmann (2009), Towards an operational aqueous phase chemistry mechanism for regional chemistry-transport models: CAPRAM-RED and its application to the COSMO-MUSCAT model, *J. Atmos. Chem.*, 64, 1-35, doi:10.1007/s10874-010-9168-8.
- Tilgner, A., L. Schöne, P. Bräuer, D. van Pinxteren, E. Hoffmann, G. Spindler, S. A. Styler, S. Mertes, W. Birmili, R. Otto, M. Merkel, K. Weinhold, A. Wiedensohler, H. Deneke, R. Schrödner, R. Wolke, J. Schneider, W. Haunold, A. Engel, A. Wéber, and H. Herrmann (2014), Comprehensive assessment of meteorological conditions and airflow connectivity during HCCT-2010, *Atmos. Chem. Phys.*, 14 (Special Issue: HCCT-2010: A complex ground-based experiment on aerosol-cloud interaction), 9105-9128, doi:10.5194/acp-14-9105-2014.
- Schrödner, R., A. Tilgner, R. Wolke, and H. Herrmann (2014), Modeling the multiphase processing of an urban and a rural air mass with COSMO-MUSCAT, *Urban Climate*, 10, 720-731, doi:10.1016/j.ulclim.2014.02.001.
- Sehili, A. M., R. Wolke, O. Knoth, M. Simmel, A. Tilgner, and H. Herrmann (2005), Comparison of different model approaches for the simulation of multiphase processes, *Atmos. Environ.*, 39(23-24), 4403-4417.
- van Pinxteren, D., et al. (2012), Hill Cap Cloud Thuringia 2010 (HCCT-2010): A ground based integrated study on aerosol cloud interaction, in Biennial Report 2010/2011, edited by A. Macke, H. Herrmann and I. Tegen, pp. 30-39, Leibniz Institute for Tropospheric Research, Leipzig.
- Wolke, R., W. Schröder, R. Schrödner, and E. Renner (2012), Influence of grid resolution and meteorological forcing on simulated European air quality: A sensitivity study with the modeling system COSMO-MUSCAT, *Atmos. Environ.*, 53 (SI), 110-130, doi:10.1016/j.atmosenv.2012.02.085.

Funding

The German Federal Environmental Foundation (DBU), Germany
Jülich Supercomputing Centre (JSC), Germany

Cooperation

Deutscher Wetterdienst (DWD), Offenbach, Germany

Large Eddy Simulations of Island Effects in the Caribbean Trade Wind Region

Michael Jähn, Oswald Knoth, Ina Tegen, Moritz Haarig, Albert Ansmann

Large-Eddy-Simulationen (LES) werden für das Gebiet der Karibikinsel Barbados zur Untersuchung von Inseleffekten bezüglich Grenzschichtmodifikation, Wolkenbildung und vertikaler Durchmischung von Aerosolen durchgeführt. Beobachtungen aus der SALTRACE-Messkampagne werden als Eingabe für die Modellläufe genutzt. Es werden u.a. die Sensitivität bezüglich Modellgitterweite, mariner Grenzschichtentwicklung und Inselorographie untersucht. Vergleiche zwischen LES-Modellergebnissen und Daten aus Lidarmessungen zeigen gute Übereinstimmungen in der Formierung der konvektiven Strukturen am Tag.

Introduction

The understanding of the interaction between a topographically structured island, trade winds, the trade inversion layer and daytime dependent heating is a very challenging topic in boundary layer (BL) meteorology. One example of these island effects is a leeward updraft zone, which is commonly visualized by satellite imagery in the shape of cloud streets or atmospheric wakes. The impacts of islands on meteorological parameters like atmospheric stability, dynamics, cloud properties or turbulence are often difficult to detect with measurements. For that reason, numerical models are essential tools to improve the understanding of these effects. Island-induced clouds, even originating from small and flat islands, result in an enhancement of vertical heat and moisture exchange and can cause severe rainfall events in extreme cases. Island effects may influence measurements that are conducted on islands, both long-term observations and field campaigns. For this study, data from the SALTRACE (Saharan Aerosol Long-range Transport and Aerosol-Cloud-Interaction Experiment) field campaign in June/July 2013 is taken to initialize model runs and for comparisons. All simulations are performed with ASAM [All Scale Atmospheric Model; *Jähn et al.*, 2015]. Detailed results are presented and discussed in *Jähn et al.* [2016].

LES model setup

Since Barbados is a 24 km wide (west-east) and 34 km long (south-north) island, a model domain with a spatial extent of $102.4 \times 102.4 \text{ km}^2$ is chosen. The island is located at the domain centre. The model top is set to 5 km altitude. Due to the presence of the island area, non-cyclic lateral boundary conditions have to be used. The island topography has a resolution of 200 m in the model. Measured night time radiosonde profiles of temperature and humidity at 22 June 2013 are directly used for model initialization, which reduces the complexity of the simulations due to the absence of horizontal inhomogeneities and a time-varying background state.

Simulation results

Figure 1 shows the surface wind fields and liquid water path for three simulation cases at 14:00 local time (LT). Due to the daytime island heating, the moderate trade wind flow and undisturbed background conditions, the conceptual model of island effects is affirmed and visible in the model data (REF case in Fig. 1). Island convection leads to downwind flow distortion, which results in a near-surface flow convergence together with a well-defined updraft band of at least 40 km length that is aligned along the mean wind direction in the downwind region of

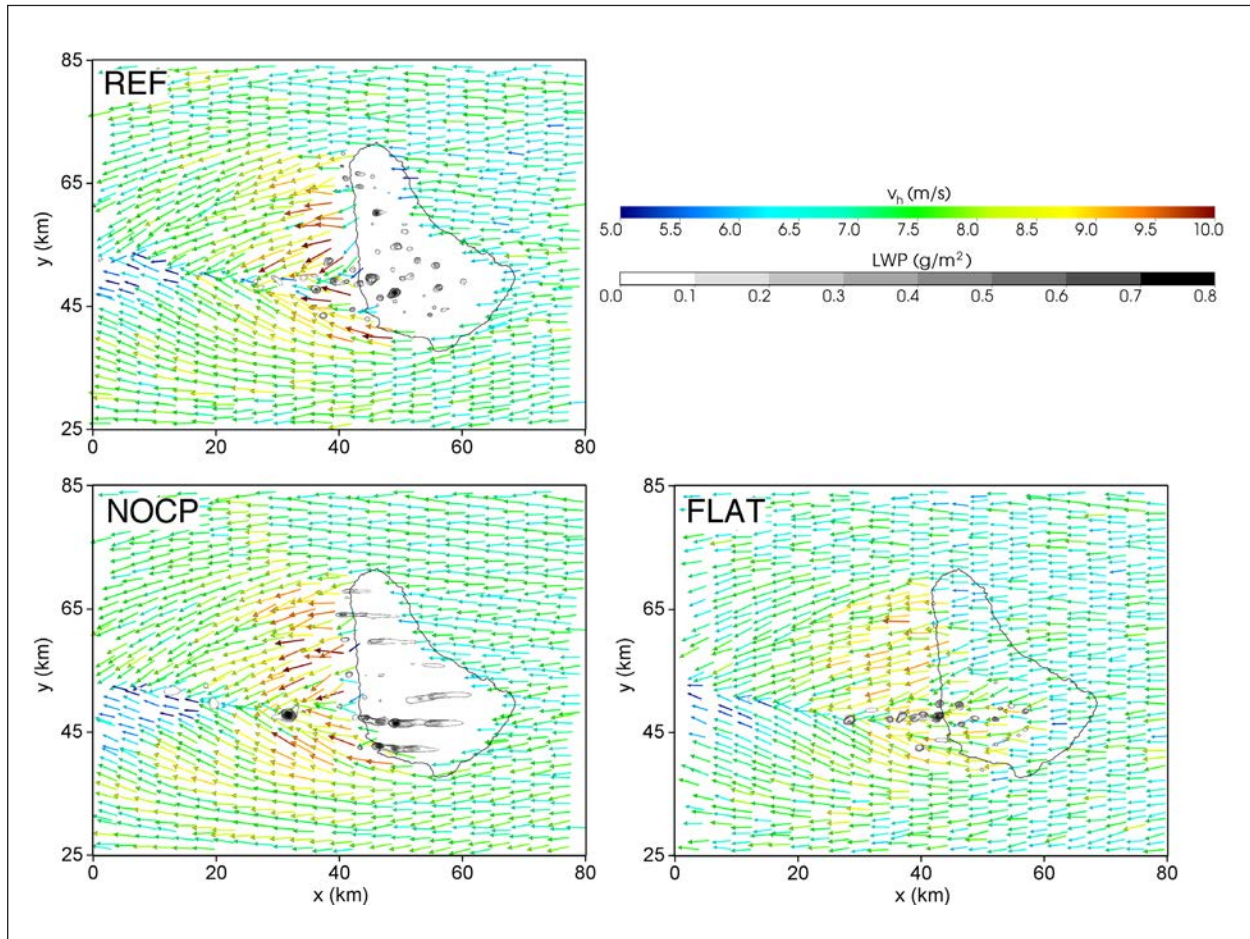


Fig. 1: Horizontal cut planes of surface wind vectors and contours of liquid water path for three simulation cases on 22 June 2013. Results of the reference case (REF), without a well-mixed marine boundary layer (NOCP) and without island topography (FLAT) are shown, respectively.

Barbados. If the turbulent inflow generation is turned off, i.e., no marine boundary layer develops (NOCP case in Fig. 1), cloud properties are drastically changed over and in the lee of the island. There, cloud cover, liquid water path and cloud base height have significantly higher values compared to the reference case. Also, the cloud morphology is different, having horizontally aligned cloud bands instead of scattered cumulus clouds. If island orography is not taken into account (FLAT case in Fig. 1), the downwind flow convergence pattern is still present. However, there is a weaker flow acceleration and the flow field is less turbulent due to a flat island surface and the absence of orographic turbulence. This has also subsequent effects on the spatial distribution of island-induced shallow cumulus clouds, which are more concentrated in the southern part of Barbados.

Vertical mixing of aerosols and layer transport has been analysed by including passive tracers in the LES model, which represent the incoming Saharan dust layers over Barbados. Layers of turbulent downward mixing have been detected between 1200 m and 1700 m altitude. It can be concluded that if the dust

layer reaches this height range, turbulent downward mixing of aerosol takes place, which is separated from large-scale subsidence effects.

Comparison with Raman lidar data

From the stationary Raman Lidar BERTHA, which was deployed near the west coast of Barbados at the CIMH (Caribbean Institute for Meteorology and Hydrology) campus, cloud base heights and thickness are estimated and compared with the LES data. Combining these two techniques, a consistent picture of the diurnal convective activity and cloud generation over the island was gained for the most part. Figure 2 shows the diurnal variation of cloud base heights during 22 June 2013 derived from LES and lidar, respectively. The spread gives an indication about the cloud thickness due to the fact that if a cloud overpasses the lidar beam, it is very likely that cloud water near the cloud top is detected at first and/or at the end of the overpass. However, in some cases, the observations indicate individual clouds that start at an altitude of 1600 m. At noon, the cloud base

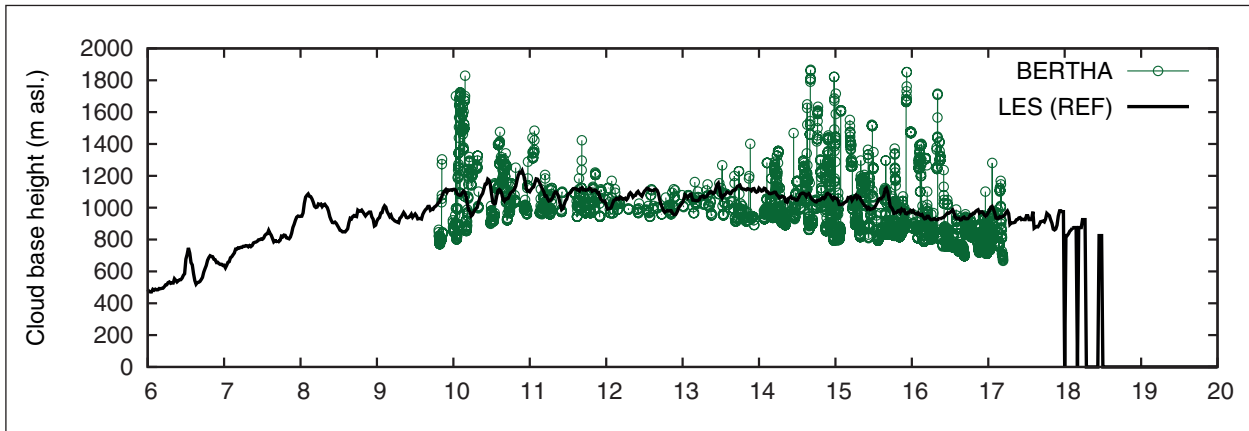


Fig. 2: Temporal evolution of the spatially averaged cloud base height from the LES REF case (black line) and cloud base height derived from BERTHA lidar measurements (green circles) during the 22 June 2013 at the west coast near the CIMH.

rises to higher altitudes and the clouds are generally thinner, which is reflected by the low variation in the lidar signal at this time period.

Conclusions and outlook

The performed simulations provided a detailed image of boundary layer structure downwind of the island, cloud and vertical mixing processes, which agree well with lidar measurements. The model data can also help to better interpret the ground-based

observations gained during the SALTRACE campaign at the Barbados west coast (CIMH field site). ASAM continues to be utilized for large eddy simulations of different boundary layer types (urban, marine, convective, canopy or arctic BL etc.). It is possible to use ASAM as an application-oriented tool for several kinds of problems, e.g., urban heat islands on a building-resolved scale, effects of land-use and terrain heterogeneity or as a concurrent LES model during field campaigns.

References

- Jähn, M., D. Muñoz-Esparza, F. Chouza, O. Reitebuch, O. Knoth, M. Haarig, and A. Ansmann (2016), Investigations of boundary layer structure, cloud characteristics and vertical mixing of aerosols at Barbados with large eddy simulations, *Atmos. Chem. Phys.*, 16, 651-674.

- Jähn, M., O. Knoth, M. König, and U. Vogelsberg (2015), Asam v2.7: a compressible atmospheric model with a cartesian cut cell approach, *Geosci. Model Dev.*, 8(2), 317-340.

Cooperation

German Aeronautics and Space Research Centre (DLR), Germany

Parcel model studies on iron mobilization in mineral aerosol

Ulrike Vogelsberg, Ralf Wolke, Andreas Tilgner, Khanneh Wadinga Fomba, Hartmut Herrmann, Ina Tegen

Eisen ist das am häufigsten vorkommende Übergangsmetall in der Erdkruste und in atmosphärischen Aerosolen mineralischen Ursprungs. Wasserlösliche Aerosolbestandteile können die biologische Produktivität im Ozean erhöhen oder als Katalysator in wolkenchemischen Prozessen wirken. Zur Untersuchung der Lösungsprozesse mineralischer Aerosolbestandteile wurden verschiedene Ansätze in das chemische Luftpaketmodell SPACCIM implementiert. Diese Lösungsansätze basieren u.a. auf Parametrisierungen von Labormessungen. Mit dem weiterentwickelten SPACCIM sowie dem erweiterten Multiphasenmechanismus RACM/CAPRAM wurden Modellsimulationen zur Eisenprozessierung für zwei markante Staubsturmepisoden über West-Afrika im Winter 2012 durchgeführt. Die Modellergebnisse wurden ferner mit Messungen am Cape Verde Atmospheric Observatory (CVAO) verglichen.

Introduction

Every year huge quantities of mineral dust particles are being emitted into the atmosphere causing physical and chemical interaction processes and are subsequently deposited in other environments. Yet, the environmental influence of mineral dust is not fully understood. This study specifically focuses on (i) the dissolution of mineral iron, (ii) the further chemical atmospheric processing of soluble iron and its later deposition. Water-soluble iron is known to potentially increase biological productivity in remote ocean regions after deposition or to affect atmospheric chemistry, e.g. by acting as catalyst in cloud chemical cycles. Results from laboratory studies suggest that highly acidic aerosol water and high tropospheric aerosol concentrations of oxalate can be driving forces for the iron dissolution in airborne dust particles (e.g., *Ito and Shi* [2015]). Parameterisations based on these experimental measurements consider such effects describing the dissolution process of mineral dust in atmospheric chemistry models.

Model setup

To study the chemical processing of airborne mineral dust particles the chemical air parcel model SPACCIM (Spectral Aerosol Cloud Chemistry Interaction Model [*Wolke et al.*, 2005]) is used and

extended by several approaches describing both the dissolution and precipitation of mineral particles. The dissolution of salts (e.g. NaCl) and mineral oxides (such as kaolinite) is treated by different approaches. The iron dissolution approaches implemented in SPACCIM are based on parameterisations from laboratory studies [*Shi et al.*, 2011; *Ito and Shi*, 2015]. The gas- and aqueous-phase chemistry is driven by the RACM/CAPRAM (Regional Atmospheric Chemistry Mechanism [*Stockwell et al.*, 1997]/Chemical Aqueous Phase Radical Mechanism [*Ervens et al.*, 2003]) mechanism, which was extended for dissolution processes [*Meskhidze et al.*, 2005 and references therein].

Cases

In winter 2012, two distinct dust storms occurred over West Africa advecting huge amounts of dust towards the Atlantic Ocean and the Cape Verde Islands. Satellite data and 5 days backward trajectories at 500 m height (Fig. 1a) imply a continental origin of the air masses from North Africa between January 19th to 25th with dust sources originating from East Algeria and North Mauritania. In February, 5-days backward trajectories moved over Europe (Fig. 1b), resulting from a low-pressure system over North Africa and the Mediterranean. Laboratory results of the soluble content from dust samples

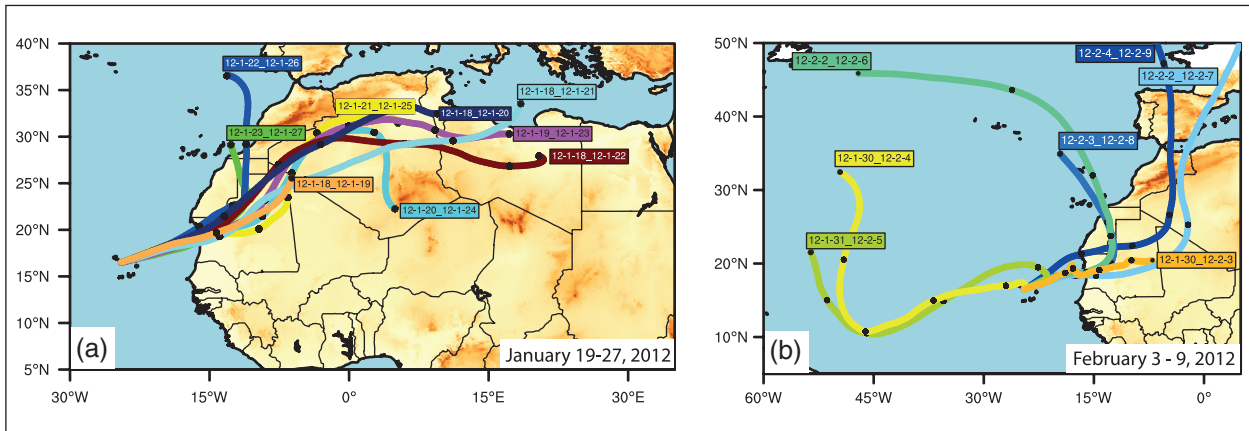


Fig. 1: The origin of air masses in winter 2012 is represented by 5-day backward trajectories at 500m height from calculations of the HYSPLIT model for the dust period in January (a) and February (b).

collected at CVAO allowed for comparison with model results.

The meteorological input parameters for SPACCIM were derived from HYSPLIT (Hybrid Single Particle Lagrangian Integrated Trajectory Model) backward trajectories at 200 m height. The chemical background concentrations were calculated as spatial mean from MACC (Monitoring Atmospheric Composition and Climate) data. Simulation time for each trajectory was about two days. The mineralogical composition of the dust was taken from *Journet et al. [2014]*.

Results and Discussion

Comparisons of the measured soluble iron content from the CVAO dust samples and results of the modelling studies are shown in Fig. 2. However, modelling and laboratory results have to be interpreted carefully due to large uncertainties in the origin and composition of dust particles and air masses. Since reference dust material from the source region is not available, the processing of dust is quite uncertain and dust samples might contain already soluble material due to e.g. weathering processes in the source region or combustion products from anthropogenic emissions.

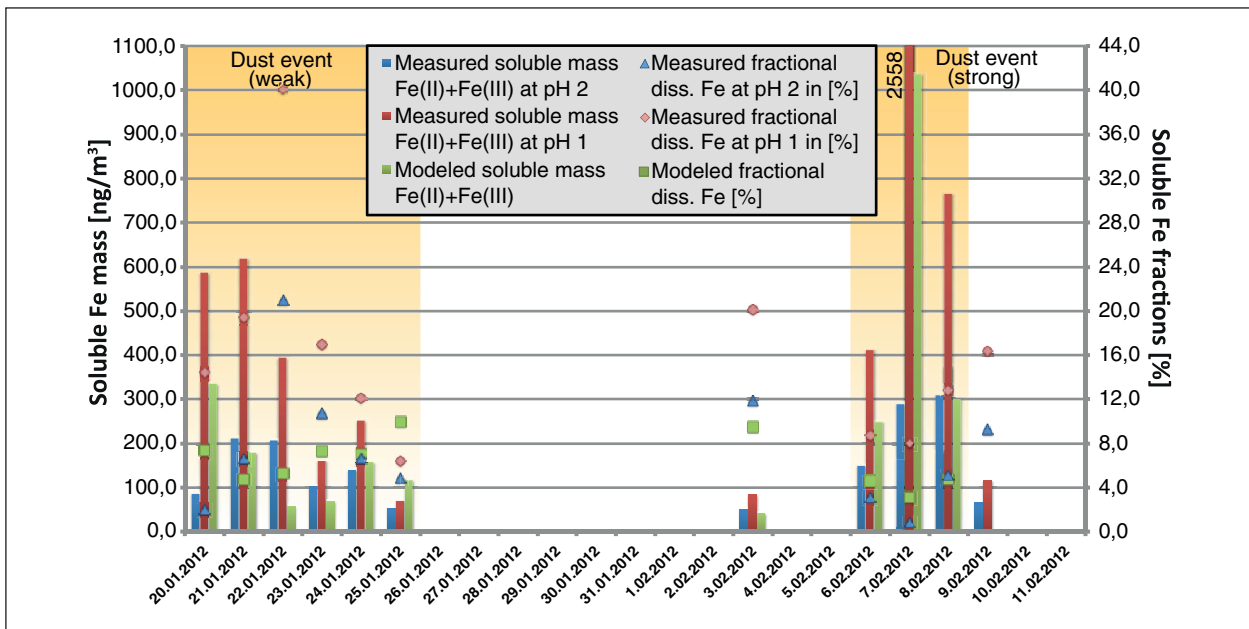


Fig. 2: Total mass (left axis) and mass fraction (right axis) of the soluble iron content from laboratory measurements (red and blue) and from model calculations (green).

January 2012. The dust episode was characterized by dust loads of 40 to 180 µg/m³ for PM10 over the Cape Verde Islands. The total iron content of the dust samples reached approximately 1% to 2.7% of PM10 mass. The amount of measured soluble iron showed a large difference ranging from 2% to 21% and 6% to 40% for dissolution experiments at pH 2 and pH 1, respectively. Similar behaviour was observed in the model results showing diverging amounts of dissolved iron apparently unrelated to the amount of total iron. This is caused by the strong pH dependence of the dissolution mechanism in the model framework, which is influenced by varying pH values throughout the advection. Thereby, different dust masses and varying meteorological patterns affect the acidity of solubilised particles. Low liquid-water content increased the acidity at the particle surface in the model, with overall pH values varying between 0.5 and 2 in all trajectory calculations.

February 2012. Highest dust concentrations of up to 800 µg/m³ for PM10 were measured on February 7th. The total iron content reached 2% to 4.2% of the total PM10 mass. Laboratory results show an inverse relationship between dust mass and soluble iron content for 6-9th February. High dust loads are linked with lower soluble iron fractions. Model results are comparable to the measurements with lowest dissolved iron fraction calculated for highest dust concentrations resulting from higher calculated pH values.

References

- Ervens, B., C. George, J. E. Williams, G. V. Buxton, G. A. Salmon, M. Bydner, F. Wilkinson, F. Dentener, P. Mirabel, R. Wolke, and H. Herrmann (2003), CAPRAM2.4 (MODAC mechanism): an extended and condensed tropospheric aqueous phase mechanism and its application, *J. Geophys. Res.*, 108(D14), 4426, doi:10.1029/2002JD002202.
- Ito, A., and Z. Shi (2016), Delivery of anthropogenic bioavailable iron from mineral dust and combustion aerosols to the ocean, *Atmos. Chem. Phys.*, 16, 85-99, doi:10.5194/acp-16-85-2016.
- Journet, E., Y. Balkanski, and S. P. Harrison (2014), A new data set of soil mineralogy for dust-cycle modeling, *Atmos. Chem. Phys.*, 14(8), 3801–3816, doi:10.5194/acp-14-3801-2014.
- Meskhidze, N., W. L. Chameides, and A. Nenes (2005), Dust and pollution: A recipe for enhanced ocean fertilization?, *J. Geophys. Res.*, 110(D3), D03301, doi:10.1029/2004JD005082.

Funding

This work was funded by the German Federal Ministry of Education and Research (BMBF) as part of the SOPRAN III project (FKZ 03F0662AJ).

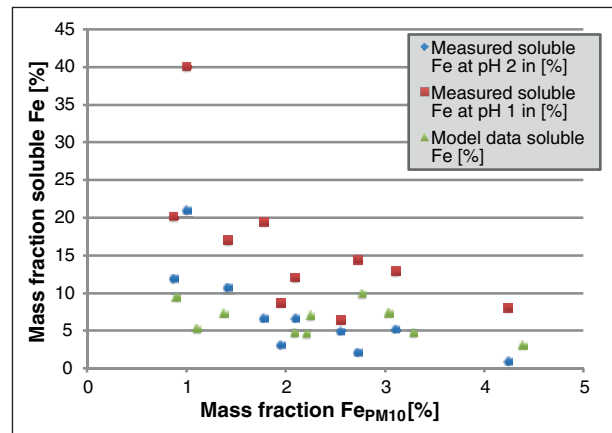


Fig. 3: Scatter plot showing the relation between soluble iron content and total iron content (PM10) of the dust samples (blue and red) and of the model results (green).

Discussion. The modelled soluble iron content is exclusively formed by the dissolution of mineral particles, while the sources of measured soluble iron from CVAO dust samples are not clear. However, the laboratory measurements of strongly acidified dust samples show in general lower fractional solubility with higher iron content (Fig. 3). Simulation results do not fully reflect this behaviour but are within a reasonable range to the field measurements. The model results are mostly closer to the results at pH 2 than to the results at pH 1.

- Shi, Z., S. Bonneville, M. D. Krom, K. S. Carslaw, T. D. Jickells, A. R. Baker, and L. G. Benning (2011), Iron dissolution kinetics of mineral dust at low pH during simulated atmospheric processing, *Atmos. Chem. Phys.*, 11(3), 995-1007, doi:10.5194/acp-11-995-2011.
- Stockwell, W. R., F. Kirchner, and M. Kuhn (1997), A new mechanism for regional atmospheric chemistry modeling, *J. Geophys. Res.*, 102(D22), 25847-25879, doi:10.1029/97JD00849.
- Wolke, R., A. M. Sehili, M. Simmel, O. Knoth, A. Tilgner, and H. Herrmann (2005), SPACCIM: A parcel model with detailed microphysics and complex multiphase chemistry, *Atmos. Environ.*, 39, 4375-4388, doi:10.1016/j.atmosenv.2005.02.038.

Towards understanding the interannual variability in Saharan dust emissions

Robert Wagner, Kerstin Schepanski, Bernd Heinold, Ina Tegen

Nordafrikanische Staubquellen wurden über einen Zeitraum von vier Jahren (2006-2010) mithilfe der Staubprodukte des geostationären Satelliten MSG-SEVIRI kontinuierlich beobachtet sowie deren raum-zeitliche Verteilung ausgewertet. Dabei zeigte sich, dass die Aktivierung von Staubquellen und damit die Mineralstaubemissionen in die Atmosphäre neben einem charakteristischen Tages- und Jahresgang auch eine starke interannuale Variabilität aufweisen. Anhand der beiden Jahre 2007 und 2008 – gekennzeichnet durch einen signifikanten Anstieg in der Anzahl der beobachteten Staubausbrüche – wurden unter Nutzung verschiedener Beobachtungs- und Modelldaten mögliche Ursachen hierfür herausgearbeitet. Dies führte zum Ergebnis, dass 2008 zahlreiche einzelne Faktoren zur häufigeren Aktivierung von Staubquellen beitrugen, welche teilweise in komplexer Wechselwirkung zueinander stehen und sich gegenseitig verstärkten. Dazu gehören u. a. Veränderungen in der Ausprägung und Position typischer nordafrikanischer Zirkulationsmuster sowie Variationen in der Niederschlagsverteilung in der Sahel-Zone, welche letztendlich die Staubemissionen durch Auswirkungen auf die oberflächennahen Windgeschwindigkeiten oder durch Modifikationen der Bodentextur kontrollierten. Die Ergebnisse dieser Studie legen nahe, dass diese atmosphärischen Veränderungen durch Anomalien der Meeresoberflächentemperaturen in den angrenzenden Ozeanen gesteuert wurden.

Introduction

North Africa, including the Saharan desert, is the largest source of mineral dust worldwide and is characterized by a multiplicity of different source regions. Local and large-scale meteorological processes like the morning breakdown of nocturnal low-level jets, convective systems, or cyclonic activity can cause the activation of potential dust sources, mainly due to impacts on the strength of surface-near winds. These dust source activations (DSA) show a strong variability on diurnal, seasonal, and interannual time scales. Whereas the diurnal and seasonal variations can be linked to the dominant local atmospheric circulation pattern [Schepanski *et al.*, 2009], causes for the interannual variability of DSA are largely unclear [Tegen *et al.*, 2013].

Methodology

The continuous observation of the North African dust sources requires geostationary satellites with a high temporal resolution. Therefore we inferred DSA events from 15-minute infrared dust index images calculated from Meteosat Second Generation

(MSG) Spinning Enhanced Visible and Infrared Imager (SEVIRI) and classified the observed DSA into a $1^\circ \times 1^\circ$ gridded map [Schepanski *et al.*, 2007, 2012]. The analysis was conducted for four years covering March 2006 to February 2010 and allows the identification of changes in time and space, both of the number of DSAs and their spatial distribution. Satellite observations and results from numerical model simulations on regional scale, using the atmosphere-dust model system COSMO-MUSCAT (COSMO: Consortium for Small-scale Modeling; MUSCAT: MultiScale Chemistry Aerosol Transport), and continental scale, using atmospheric fields from the reanalysis dataset from NCEP (National Center for Environmental Prediction), were used complementarily to identify atmospheric and oceanic features that may control the DSA over North Africa.

Differences in the DSA pattern

The time series of the monthly totals of the observed number of DSA as shown in Fig. 1 reveals a clear interannual variability in the dust source activity over North Africa. This variability is particularly significant for the two years 2007 and 2008, as

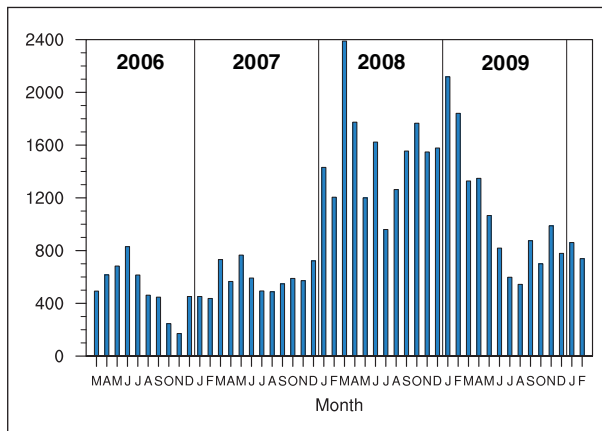


Fig. 1: Time series of the number of DSA per $1^\circ \times 1^\circ$ grid cell for North Africa for March 2006 to February 2010.

a sudden and strong increase in the number of DSA occurred between the end of 2007 and early 2008. The number of dust events in 2008 was increased by a factor of three compared to 2007. The spatial analysis of frequent dust source activations, expressed as the DSA frequency (DSA_F) for each grid cell and presented in Fig. 2, shows that an increased DSA_F is evident for almost all parts of the Saharan desert. This increase was particularly obvious in the Bodélé Depression and the Western Sahara (Fig. 2c). Monthly maps of DSA_F for 2007 and 2008 illustrate a spread of increased DSA numbers rather than a general increased level over all places at the same time. Regions of increased DSA_Fs were observed first in December 2007 over the mountainous regions south of the Tibesti Massif (including the Bodélé Depression), and occurred first in the Western Sahara and in the vicinity of the Atlas Mountains in March 2008. In almost all regions the observed DSA_Fs stayed at this - compared to the both previous years - unusual high level until mid-2009.

Discussion of potential reasons for differences in DSA 2007 and 2008

The analyses of wind and pressure fields using NCEP reanalysis data for the large scale and COSMO-MUSCAT simulations for the North-African scale suggest that the variability of several individual forcing mechanisms contributed to the enhanced number of DSA in 2008. It includes the classical North African circulation features like the West African heat low and the formation of Mediterranean cold surges, which predominantly result in changes in the Sahel rainfall distribution and the mid-tropospheric wind pattern. Ultimately, changes in the near-surface wind speed distribution and finally variability in DSAs occur. All these different atmospheric forcing mechanism

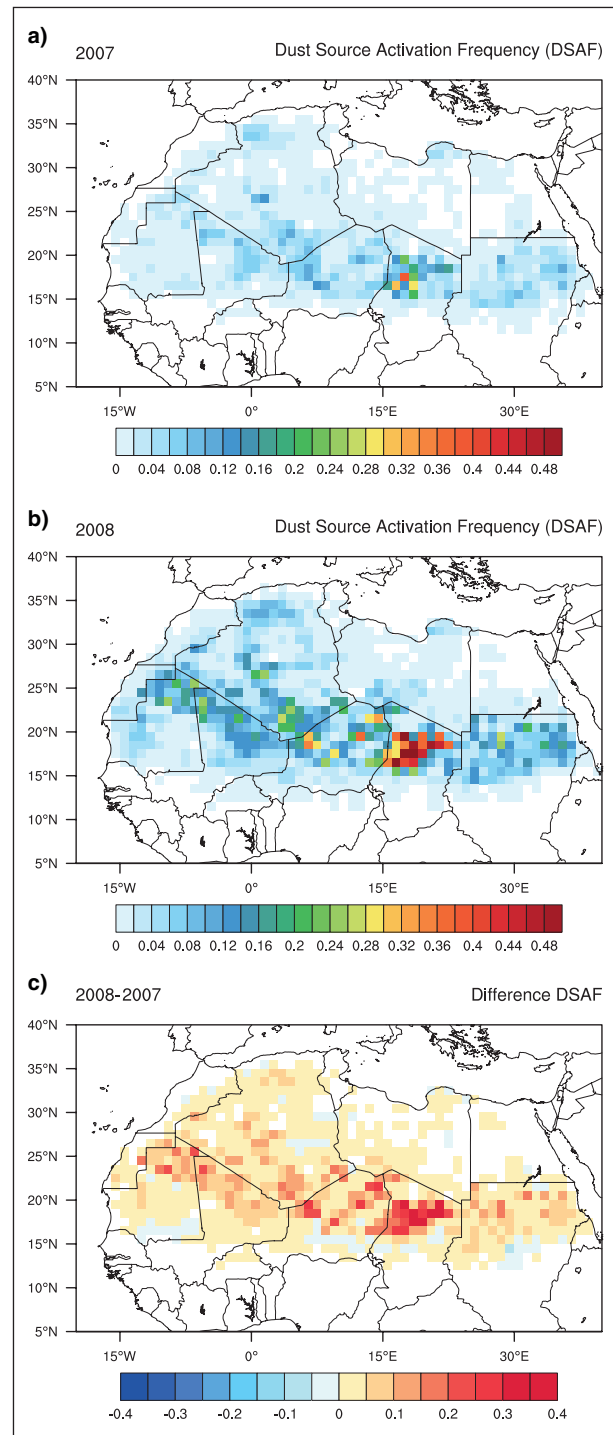


Fig. 2: DSA_F maps for 2007 (a) and 2008 (b). Shown is the fraction of DSA per day for all grid boxes with at least one DSA per year. Regions with very active dust sources are usually located at the foothills of the mountains areas in the Sahel-Zone. (c) shows the difference in DSA_F for 2008 minus 2007.

and the area of their predominant relevance for the DSA variability are summarized in Fig. 3. The results further show that these modifications were appreciably caused by Sea Surface Temperature (SST) changes in surrounding ocean basins in the two

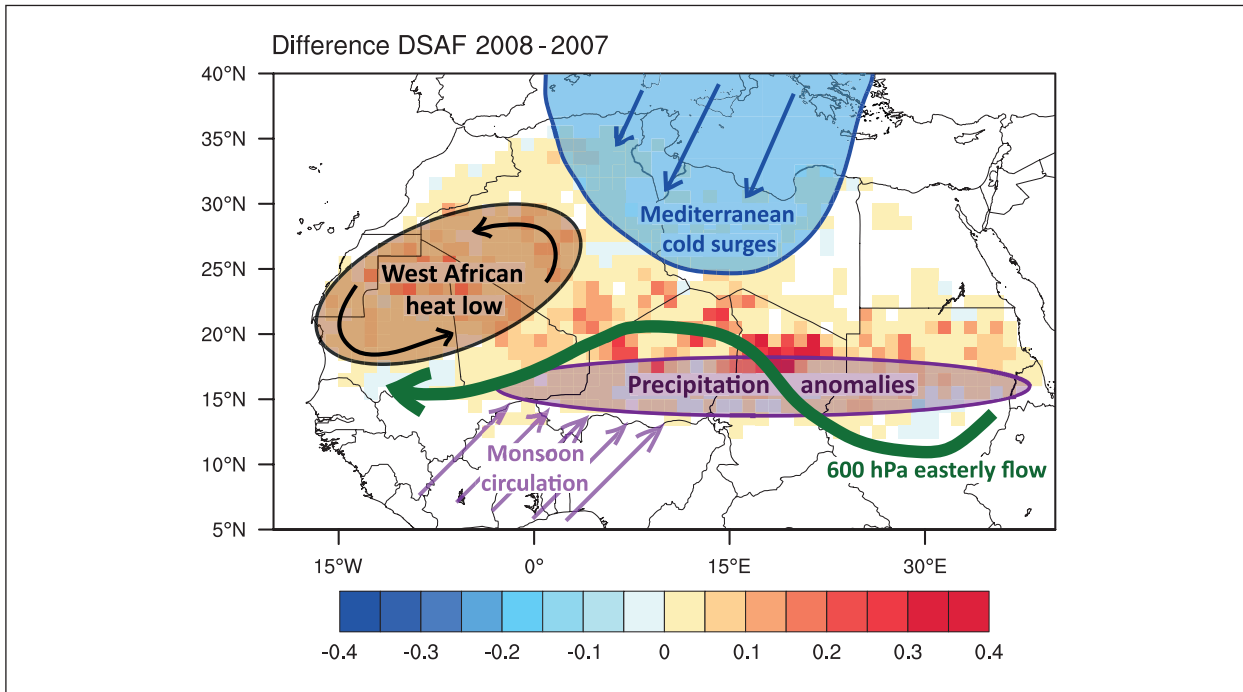


Fig. 3: Overview of the main atmospheric mechanism, which have contributed to the differences in DSA for 2007 and 2008.

years. These SST changes act as a controlling factor, which governs the development and strength of most of the regional circulation patterns and finally forces the DSA. Despite the differences in the strength and frequency of occurrence of atmospheric circulation patterns, it appears that wind erosion from alluvial sediments in desert valleys of the Saharan mountains contributes significantly to the enhanced level of DSA

in 2008. In 2007, the monsoonal precipitation in some regions was higher than in 2008, which may have altered the susceptibility of these sediments for dust emission. Amongst others this topic will be further investigated at TROPOS in context of the project “InterDust” to achieve a better understanding of the interannual variability in DSA as part of the North African dust cycle.

References

- Schepanski, K., I. Tegen, B. Laurent, B. Heinold, and A. Macke (2007), A new Saharan dust source activation frequency map derived from MSG-SEVIRI IR-channels, *Geophys. Res. Lett.*, 34(18), doi:10.1029/2007gl030168.
- Schepanski, K., I. Tegen, M. C. Todd, B. Heinold, G. Bönnisch, B. Laurent, and A. Macke (2009), Meteorological processes forcing Saharan dust emission inferred from MSG-SEVIRI observations of subdaily dust source activation and numerical models, *Journal of Geophysical Research*, 114(D10), doi:10.1029/2008jd010325.
- Schepanski, K., I. Tegen, and A. Macke (2012), Comparison of satellite based observations of Saharan dust source areas, *Remote Sens. Environ.*, 123, 90-97, doi:10.1016/j.rse.2012.03.019.
- Tegen, I., K. Schepanski, and B. Heinold (2013), Comparing two years of Saharan dust source activation obtained by regional modelling and satellite observations, *Atmos. Chem. Phys.*, 13(5), 2381-2390, doi:10.5194/acp-13-2381-2013.

Funding

Leibniz-SAW-Project “Dust at the interface – modelling and remote sensing”

Cooperation

Deutscher Wetterdienst (DWD), Offenbach, Germany

First year activities within the Central Asian Dust Experiment (CADEX): lidar observations, chemical aerosol analysis, and dust transport modeling

Julian Hofer¹, Dietrich Althausen¹, K. Wadinga Fomba¹, Konrad Müller¹, Bernd Heinold¹, Sabur F. Abdullaev², Abduvosit Makhmudov², Georg Schettler³, Holger Baars¹, Ronny Engelmann¹, Albert Ansmann¹

¹ Leibniz Institute for Tropospheric Research (TROPOS), Leipzig, Germany

² S.U. Umarov Physical-Technical Institute, Academy of Sciences of the Republic of Tajikistan, Dushanbe, Tajikistan

³ Helmholtz Centre Potsdam, GFZ German Research Centre for Geosciences, Potsdam, Germany

Anfang Oktober 2014 startete das vom Bundesministerium für Bildung und Forschung geförderte deutsch-tadschikische Gemeinschaftsprojekt CADEX (Central Asian Dust Experiment). Das Projekt ist eine Kooperation zwischen dem Leibniz-Institut für Troposphärenforschung und dem Physikalisch-Technischen Institut der tadschikischen Akademie der Wissenschaften. Im Rahmen des Projekts werden zum ersten Mal in Tadschikistan Lidarmessungen durchgeführt. Das Ziel des Projektes ist die Charakterisierung des Aerosols über Zentralasien. Insbesondere der Transport von Wüstenstaub und dessen Einfluss auf Wetter und Klima sollen damit besser verstanden werden. In diesem Beitrag wird ein Messbeispiel eines Staubfalles vom April 2015 in Tadschikistan präsentiert.

Introduction

Tajikistan lies in the global dust belt in close proximity of some major dust sources like the Taklimakan desert. Central Asia and especially Tajikistan are highly affected by climate change. For example, dramatic glacier shrinking took place in the last decades, which has also an effect on the water resources of Tajikistan and the whole Central Asian area.

Aerosol observations in Tajikistan are therefore highly important to understand regional and global transport of mineral dust and its effects on radiation budget, cloud formation etc.

Up to now, only few experiments were performed to characterize the aerosol over Central Asia. The knowledge of the vertical aerosol distribution over Tajikistan and especially the transport of mineral dust over Central Asia is insufficient. Therefore CADEX aims to provide long-term data on vertical profiles of the backscatter coefficient, the extinction coefficient, and the particle depolarization ratio.

Instruments and Methods

The measurement instruments are operated at a measurement site ($38^{\circ}33'34''$ N, $68^{\circ}51'22''$ E, 864 m a.s.l.) of the Academy of Sciences of the Republic of Tajikistan in the capital of Tajikistan Dushanbe.

Lidar measurements. The automated multiwavelength polarization Raman lidar Polly^{XT} is used for the lidar measurements [Althausen *et al.*, 2009]. The system has been updated and improved by installing an additional depolarization channel and by replacing most of the electronic components with the current Polly^{XT} systems standard parts [Engelmann *et al.*, 2015]. The lidar measurements are performed continuously (24/7). The data are used to determine the vertical profiles of the backscatter and extinction coefficients, the depolarization and the lidar ratios as well as the Ångström exponents.

Collocated with the lidar measurements the Tajik colleagues operate a CIMEL sun photometer that is part of the AERONET (Aerosol Robotic Network).

Ground-based in-situ measurements. At the measurement site a Digitel high volume sampler (HVS DHA-80) collects aerosol samples on quartz filters for chemical analysis. Additionally GFZ German Research Centre for Geosciences Potsdam contributes a Grimm optical particle counter (EDM 180). The quartz filters are analyzed on organic carbon and elemental carbon as well as the ionic composition is measured with ion chromatography. Furthermore, trace metals are determined with Total Reflection X-Ray Fluorescence.

Modeling. The regional-scale dust model COSMO-MUSCAT (COSMO: Consortium for Small-scale Modeling; MUSCAT: MultiScale Chemistry Aerosol Transport) [Heinold et al., 2007; Heinold et al., 2011] will be used to simulate the dust transport across Tajikistan. The simulations are run with 28 km grid spacing on a model domain covering Arabia, Central Asia, and the Taklimakan. Operational forecasts from the European Centre for Medium-Range Weather Forecasts (ECMWF) are used to initialize and force boundaries and Monitoring Atmospheric Composition and Climate (MACC) aerosol forecasts provide the input for dust aerosol boundary conditions.

First results

Up to now a vast number of dust cases have been observed in Dushanbe during the first 10

months of measurements. As an example case, measurements from April 13th to 15th 2015 are presented here.

Figure 1 shows the temporal development of the range corrected signal of the 1064 nm channel from 2015-04-12 18:00 UTC to 2015-04-15 05:59 UTC. The dust layer arrives on 2015-04-12 after 18:00 UTC at above 5 km height. The slowly descending dust layer finally extends between 2.5 and 5 km height, while clouds (grey) are detected sporadically embedded in it. The vertical profiles of the dust optical properties are presented in Fig. 2. They are averaged from 2015-04-13 15:10 - 16:10 UTC (indicated with the light blue box in Fig. 1 a)) and calculated with the Raman method [Ansmann et al., 1992]. The particle depolarization ratios (Fig. 2 c)) reach about 0.3 for 532 nm and 0.2 for 355 nm, the lidar ratios are about 40 sr (Fig. 2 d)) and the Ångström exponent is relatively low with about 0.3 (Fig. 2 e)). These values are characteristic for West Asian dust [Mamouri et al., 2013; Nisantzi et al., 2015].

After 2015-04-13 18:00 UTC (Fig. 1 a)) down mixing of this dust layer can be observed accompanied with some rain during the next days (Fig. 1 b)). This is also consistent with the chemical measurements of the aerosol which show a very large dust fraction on April 14th and 15th 2015 (Fig. 3.). The connection of ground-based chemical measurements with the lidar optical profiles is a promising first result which shows the useful combination of the two experimental approaches. The next step will be to use the

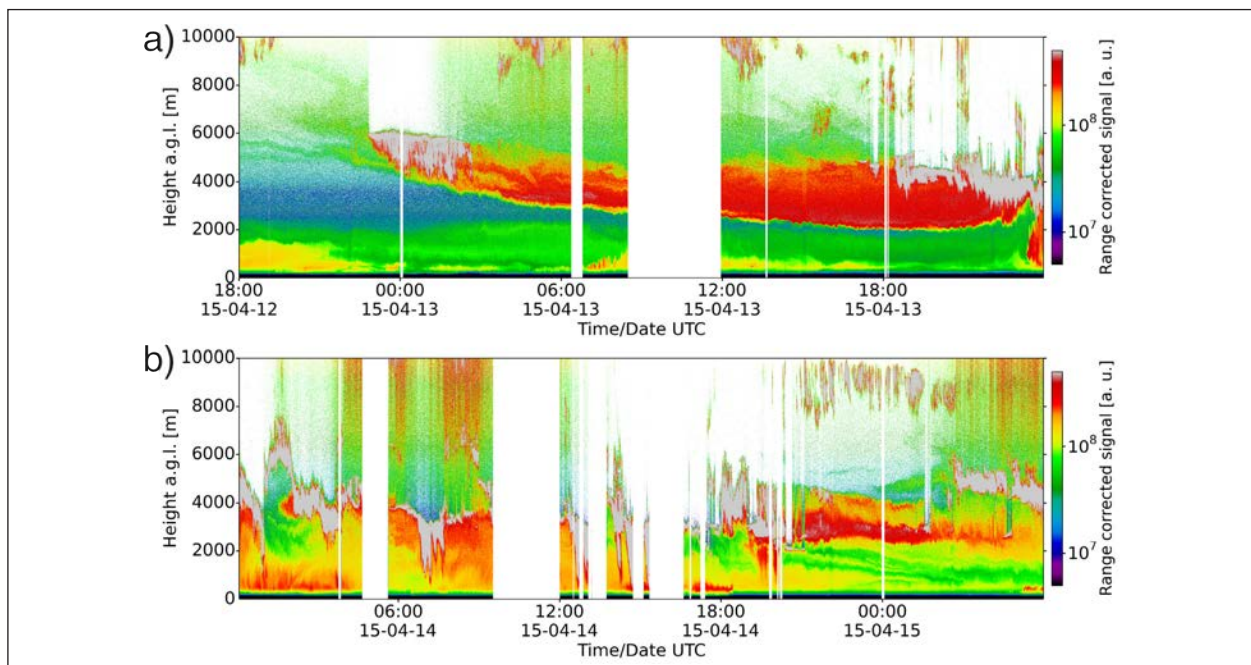


Fig. 1: Temporal development of the range corrected signal of the 1064 nm wavelength lidar channel from 2015-04-12 18:00 UTC to 2015-04-13 25:58 UTC (a), from 2015-04-14 00:04 UTC to 2015-04-15 05:59 UTC (b).

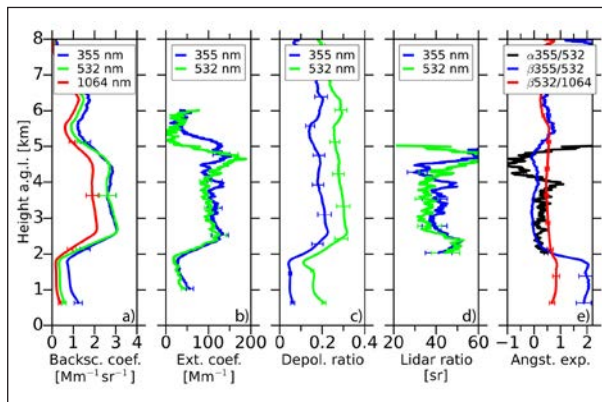


Fig. 2: Profiles of the optical aerosol data determined between 2015-04-13 15:10 - 16:10 UTC. The lidar signals are smoothed with 743 m before calculating the optical properties. Mean particle backscatter coefficient at 355 nm, 532 nm and 1064 nm wavelength (a). Extinction coefficient at 355 nm and 532 nm wavelength (b). Particle depolarization ratio at 355 nm and 532 nm wavelength (c). Lidar ratio at 355 nm and 532 nm wavelength (d). Ångström exponents (e).

COSMO-MUSCAT model to simulate the transport of dust over Tajikistan. After thorough model evaluation using the measurements, the simulations will be used to study mixing processes and dust radiative effects.

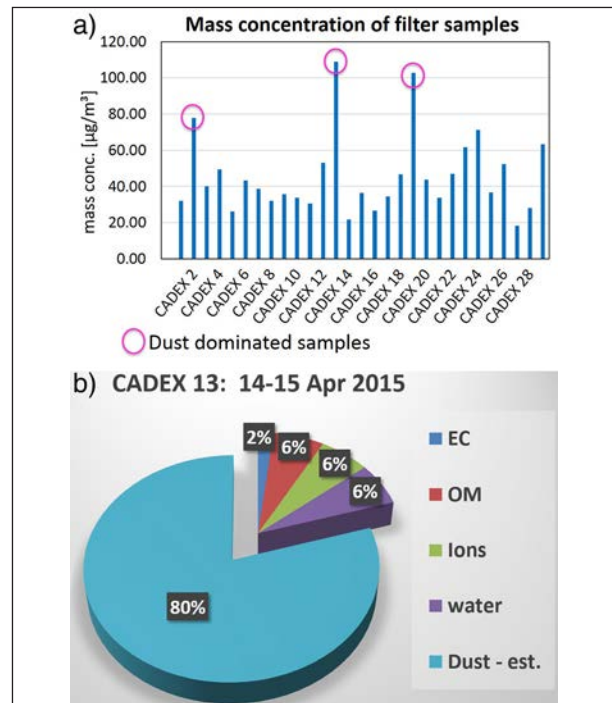


Fig. 3: Time series of the mass concentration from the first filters measured with the Digitel high volume sampler during the CADEX campaign. Pink circles indicate dust dominated samples (a). Measured content of CADEX filter number 13 probed between 2015-04-14 00:00 UTC and 2015-04-15 24:00 UTC (b).

References

- Althausen, D., R. Engelmann, H. Baars, B. Heese, A. Ansmann, D. Müller, and M. Komppula (2009), Portable Raman Lidar PollyXT for Automated Profiling of Aerosol Backscatter, Extinction, and Depolarization, *J. Atmos. Oceanic Technol.*, 26(11), 2366-2378, doi:10.1175/2009JTECHA1304.1.
- Ansmann, A., U. Wandinger, M. Riebesell, C. Weitkamp, and W. Michaelis (1992), Independent measurement of extinction and backscatter profiles in cirrus clouds by using a combined Raman elastic-backscatter lidar, *Appl. Opt.*, 31(33), 7113-7131, doi:10.1364/AO.31.007113.
- Engelmann, R., T. Kanitz, H. Baars, B. Heese, D. Althausen, A. Skupin, U. Wandinger, M. Komppula, I. S. Stachlewska, V. Amiridis, E. Marinou, I. Mattis, H. Linné, and A. Ansmann (2015), EARLINET Raman Lidar PollyXT: the neXT generation, *Atmos. Meas. Tech. Discuss.*, 8(7), 7737-7780, doi:10.5194/amtd-8-7737-2015.
- Heinold, B., J. Helmert, O. Hellmuth, R. Wolke, A. Ansmann, B. Marticorena, B. Laurent, and I. Tegen (2007), Regional modeling of Saharan dust events using LM-MUSCAT: Model description and case studies, *J. Geophys. Res. Atmos.*, 112(D11), doi:10.1029/2006JD007443.
- Heinold, B., I. Tegen, K. Schepanski, M. Tesche, M. Esselborn, V. Freudenthaler, S. Gross, K. Kandler, P. Knippertz, D. Müller, A. Schladitz, C. Toledano, B. Weinzierl, A. Ansmann, D. Althausen, T. Müller, A. Petzold, and A. Wiedensohler (2011), Regional modelling of Saharan dust and biomass-burning smoke. Part 1: Model description and evaluation, *Tellus B*, 63(4), 781-799, doi:10.1111/j.1600-0889.2011.00570.x.
- Mamouri, R. E., A. Ansmann, A. Nisantzi, P. Kokkalis, A. Schwarz, and D. Hadjimitsis (2013), Low Arabian dust extinction-to-backscatter ratio, *Geophys. Res. Lett.*, 40(17), 4762-4766, doi: 10.1002/grl.50898.
- Nisantzi, A., R. E. Mamouri, A. Ansmann, G. L. Schuster, and D. G. Hadjimitsis (2015), Middle East versus Saharan dust extinction-to-backscatter ratios, *Atmos. Chem. Phys.*, 15(12), 7071-7084, doi:10.5194/acp-15-7071-2015.

Funding

German Federal Ministry of Education and Research (BMBF), Bonn, Germany

Cooperation

S.U. Umarov Physical-Technical Institute, Academy of Sciences of the Republic of Tajikistan, Dushanbe, Tajikistan
 Helmholtz Centre Potsdam, GFZ German Research Centre for Geosciences, Potsdam, Germany

Characterization of ice particle and cloud drop residuals sampled during the HALO cloud missions ML-CIRRUS and ACRIDICON-CHUVA

Stephan Mertes, Udo Kästner, Stephan Günzel

Im Rahmen des Schwerpunktprogramm 1294 der Deutschen Forschungsgemeinschaft DFG hat TROPOS einen Gegenstrom-Impaktor (engl.: Counterflow Virtual Impactor, CVI) Einlass für das deutsche Forschungsflugzeug HALO entwickelt (HALO-CVI). Der HALO-CVI sammelt Eispartikel und/oder Tropfen bei Wolkendurchflügen mit HALO und stellt deren Residuen zur physiko-chemischen Analyse bereit. Während des Mid-Latitude Cirrus (ML-CIRRUS) Projekts (Missionsflüge März/April 2014 über Westeuropa) und des ACRIDICON-CHUVA Projekts (Missionsflüge September 2014 über dem brasilianischen Regenwald) wurde der HALO-CVI erfolgreich betrieben. Bei ML-CIRRUS gibt es aufgrund der HALO-CVI Messungen starke Anzeichen für Unterschiede in den Bildungsvorgängen von natürlichen und Kondensstreifen induzierten Zirren aber auch innerhalb natürlicher Zirren (*in-situ* und warm conveyor belt Zirren). In der Untersuchung hochreichend konvektiver Wolkensysteme während ACRIDICON-CHUVA tragen die HALO-CVI Messungen dazu bei, Unterschiede in der vertikalen Entwicklung dieser Wolken als auch in der Prozessierung und im Vertikaltransport von Grenzschichtaerosolen durch diese Wolken in sauberer und durch Biomasseverbrennung verschmutzten Luftmassen zu erfassen.

Introduction

Within the priority program SPP-1294 of the German Research Foundation DFG "Atmospheric and Earth System Research with the Research Aircraft HALO (High Altitude and Long Range Research Aircraft)", TROPOS developed a dedicated Counterflow Virtual Impactor (HALO-CVI). This kind of inlet [e.g., *Mertes et al.*, 2005] samples only cloud

particles and releases dry ice particle or cloud drop residues (IPR, CDR), which are then available for a physico-chemical characterization, by driving the condensed ice or water phase into the gas phase. Since IPR and CDR are closely related to the original ice nucleating particle (INP) and cloud condensation nuclei (CCN), the HALO-CVI is a powerful tool for airborne *in-situ* investigations of aerosol-cloud-interactions with the research aircraft HALO.



Fig. 1: Inlets and wing probes installed at the German research aircraft HALO for the ML-CIRRUS mission. The position of the HALO-CVI inlet developed by TROPOS (shown in the enlarged detail) is indicated.

Experimental Setup of the HALO-CVI system

The controlled counterflow coming out of a CVI inlet tip allows only hydrometeors above a certain size to enter the sampling system and simultaneously pre-segregates smaller interstitial particles and gases. The hydrometeors are impacted into a particle-free and dry sample flow inside the inlet which leads to a complete evaporation of the condensed water phase, whereby their residual particles are released for analysis. The HALO-CVI is installed on the upper fuselage of the HALO aircraft (Fig. 1) and its sample line is connected to the control and measurement rack installed in the pressurized cabin. Here the residual number concentration, sub-micrometer size distribution and absorption coefficient are measured. From the latter a residual black carbon (BC) mass concentration can be determined. Moreover, the electrical current of the residual particles is measured from which the number of charges per hydrometeor can be derived.

Since the HALO missions are coordinated measurements of different collaborating partners further residual aerosol properties are measured by other groups. This includes the chemical composition, number concentration of BC particles, super-micrometer size distribution and CCN and INP capability.

HALO cloud missions

ML-CIRRUS. The Mid-Latitude Cirrus project (mission flights in March/April 2014) investigates the formation, microphysical properties, life cycle, and climate impact of natural and aviation influenced cirrus clouds over Western Europe [Voigt et al., 2016]. The HALO-CVI measurements should mainly provide insight into the formation mechanisms (in-situ or liquid phase origin) of natural cirrus and aged contrails or contrail cirrus. This implies homogeneous and heterogeneous ice nucleation, where the latter includes

deposition nucleation and immersion freezing. Immersion freezing is expected for liquid clouds lifted up by warm conveyor belts to higher altitudes.

Figure 2 shows two residual particle number size distributions measured when HALO flew through aviation induced cirrus clouds (contrail cirrus) during the mission flight on 07.04.2014 over Germany. Both size distributions have a pronounced accumulation mode at particle diameters between 100 and 200 nm, and there seems to be a distinct Aitken mode below 100 nm as well. This might be an indication for a different IPR origin and composition and consequently for different ice nucleation processes forming the probed cirrus clouds. This will be further investigated, naturally under consideration of further ML-CIRRUS mission flights.

ACRIDICON-CHUVA. The objective in this project is the investigation of the vertical evolution of tropical deep convective clouds including their aerosol cloud processing, aerosol vertical transport and precipitation behavior in clean and biomass burning polluted air masses [Wendisch et al., 2015]. In this context HALO-CVI measurements were carried out during the in-situ vertical profiling in the lower warm region as well as in the anvil outflow region of these cloud systems above the Amazonian rainforest south (polluted) and north (clean) of Manaus, Brazil in October 2014.

Vertical profiles of air temperature, drop charges, residual number concentration and black carbon mass concentration from two ascents and one descent of HALO during the cloud profiling mission flight AC18 (28.09.2014) are shown in Fig. 3. These profiles are measured within 3 hours in a rather clean air mass. Temperature as well as cloud microphysics did not significantly change with height. Residual particle number and black carbon mass concentration reach values of about 2000 cm^{-3} and $0.1 \mu\text{g m}^{-3}$, respectively. This means that soot particles originating from the boundary layer are at least transported up to 6000m when they are incorporated into drops. Drop charges are found to be negative close to cloud base between 40 to 100 elementary charges and positive above, where the convective clouds are still liquid at temperatures above -10°C , not exceeding 20 elementary charges. The polarity of the drop charges change at an altitude of about 3000 m. This vertical pattern of the cloud electrification might have influence on the thunderstorm development and formation of precipitation by increasing the drop coalescence efficiencies and ice formation [Beard et al., 2004]. The measured parameters shown in Fig.3 will be analyzed for other ACRIDICON-CHUVA mission flights to arrive at more general results.

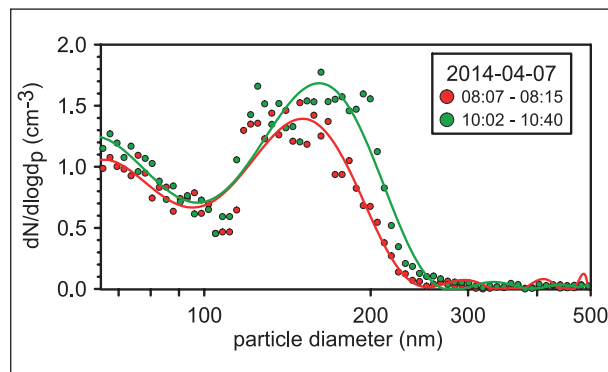


Fig. 2: Residual particle number size distributions measured by means of the HALO-CVI inlet inside aviation influenced cirrus clouds over Germany on 07.04.2014 during ML-CIRRUS.

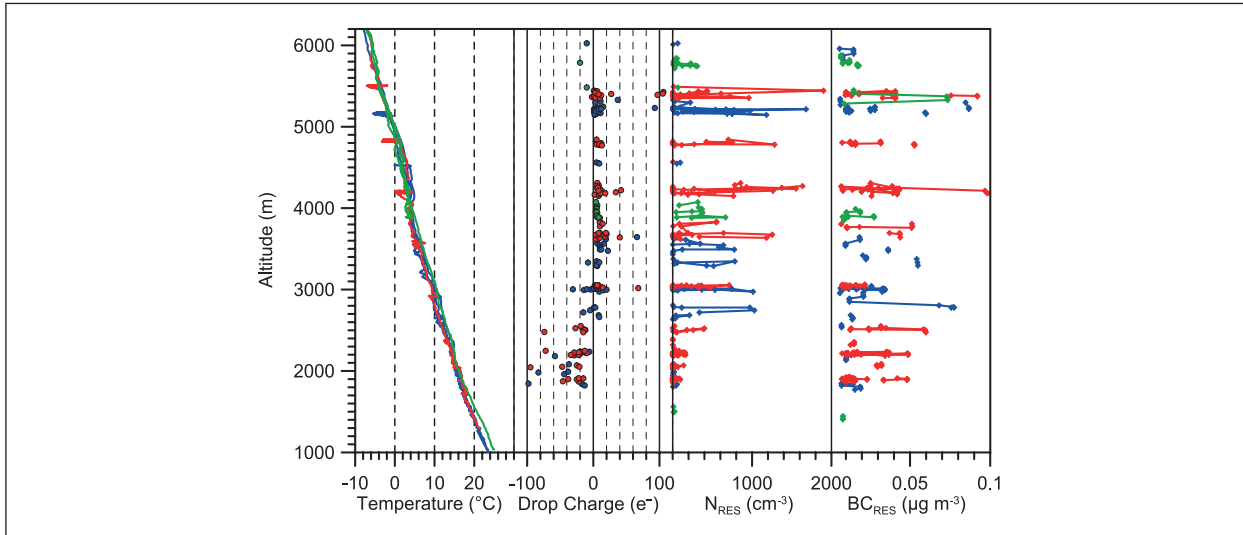


Fig. 3: Vertical profiles of air temperature, drop charge, residual particle number concentration (N_{RES}) and black carbon mass concentration (BC_{RES}) measured in tropical deep convective clouds over the Amazonian rainforest on 28.09.2014 during ACRIDICON-CHUVA. Drop charge, N_{RES} and BC_{RES} are obtained from in-situ drop collection with the HALO-CVI.

References

- Beard, K. V., H. T. Ochs, and C. H. Twohy (2004), Aircraft measurements of high average charges on cloud drops in layer clouds, *Geophys. Res. Lett.*, 31(14), doi:10.1029/2004GL020465.
- Mertes, S., K. Lehmann, A. Nowak, A. Massling, and A. Wiedensohler (2005), Link between aerosol hygroscopic growth and droplet activation observed for hill-capped clouds at connected flow conditions during FEBUKO, *Atmos. Environ.*, 39(23-24), 4247-4256, doi:10.1016/j.atmosenv.2005.02.010.
- Voigt, C., U. Schumann, A. Minikin, A. Abdelmonem, A. Afchine, S. Borrmann, M. Böttcher, B. Buchholz, L. Bugliaro, A. Costa, J. Curtius, M. Dollner, A. Dörnbrack, V. Dreiling, V. Ebert, A. Ehrlich, A. Fix, L. Forster, F. Frank, D. Fütterer, K. Graf, J.-U. Groß, S. Groß, B. Heinold, T. Hüneke, E. Järvinen, T. Jurkat, S. Kaufmann, M. Kenntner, M. Klingebiel, T. Klimach, R. Kohl, M. Krämer, B. Mayer, S. Mertes, S. Molleker, A. Petzold, K. Pfeilsticker, M. Rapp, M. Rautenhaus, P. Reuter, C. Rolf, D. Rose, D. Sauer, A. Schäfler, R. Schlage, H. Schlager, M. Schnaiter, J. Schneider, P. Spichtinger, S. P., R. Weigel, B. Weinzierl, M. Wendisch, F. Werner, H. Wernli, M. Wirth, A. Zahn, H. Ziereis, and M. Zöger (2016), ML-CIRRUS - The airborne experiment on natural cirrus and contrail cirrus with the new high altitude long range research aircraft HALO, *Bull. Amer. Meteor. Soc.*, submitted.
- Wendisch, M., U. Pöschl, M. O. Andreae, L. A. T. Machado, R. Albrecht, H. Schlager, D. Rosenfeld, S. T. Martin, A. Abdelmonem, A. Afchine, A. Araújo, P. Artaxo, H. Aufmhoff, H. M. J. Barbosa, S. Borrmann, R. Braga, B. Buchholz, M. A. Cecchini, A. Costa, J. Curtius, M. Dollner, M. Dorf, V. Dreiling, V. Ebert, A. Ehrlich, F. Ewald, G. Fisch, A. Fix, F. Frank, D. Fütterer, C. Heckl, F. Heidelberg, T. Hüneke, E. Jäkel, E. Järvinen, T. Jurkat, S. Kanter, U. Kästner, M. Kenntner, J. Kesselmeier, T. Klimach, M. Knecht, R. Kohl, T. Kölling, M. Krämer, M. Krüger, T. C. Krisna, J. V. Lavric, K. Longo, C. Mahnke, A. O. Manzi, B. Mayer, S. Mertes, A. Minikin, S. Molleker, S. Münch, B. Nilius, K. Pfeilsticker, C. Pöhler, A. Roiger, D. Rose, D. Rosenow, D. Sauer, M. Schnaiter, J. Schneider, C. Schulz, R. A. F. de Souza, A. Spanu, P. Stock, D. Vila, C. Voigt, A. Walser, D. Walter, R. Weigel, B. Weinzierl, F. Werner, M. A. Yamasoe, H. Ziereis, T. Zinner, and M. Zöger (2016), Introduction of the ACRIDICON-CHUVA campaign studying tropical deep convective clouds and precipitation over Amazonia using the new German research aircraft HALO, *Bull. Amer. Meteor. Soc.*, accepted.

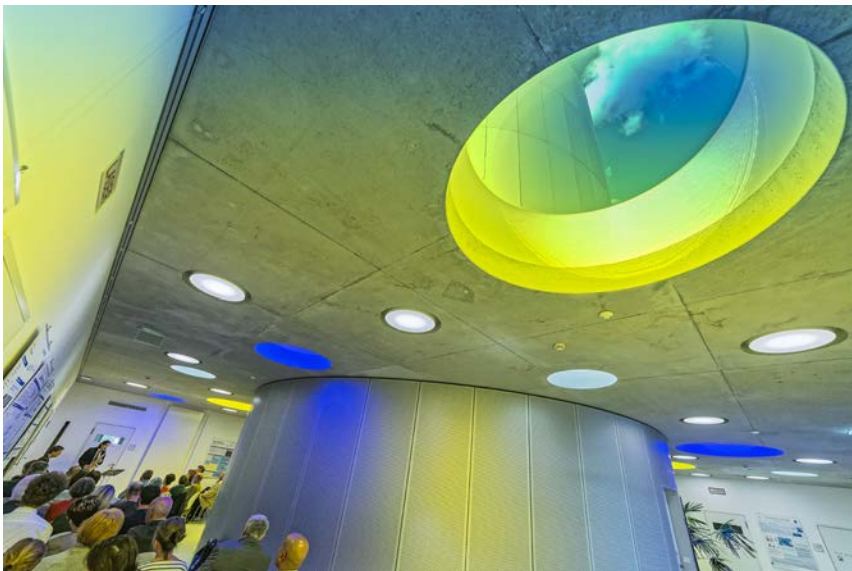
Funding

Priority program SPP-1294 of the German Research Foundation DFG “Atmospheric and Earth System Research with the Research Aircraft HALO (High Altitude and Long Range Research Aircraft)”, grants HE 939/25-1 and ME 3534/1-2.

Cooperation

Max Planck Institute for Chemistry, Mainz, Germany
 Johannes Gutenberg University Mainz, Germany
 Goethe University Frankfurt, Germany
 German Aerospace Center (DLR), Oberpfaffenhofen, Germany
 Research Center Jülich, Germany
 Karlsruhe Institute of Technology (KIT), Germany

Appendices



Publications

Publication statistics

	2014	2015
Total number of publications	287	322
Books (author, editor)	0	0
Book sections	7	1
Conference proceedings	0	0
Publications, peer-reviewed	91	106
Publications, other	5	34
Lectures, invited	17	11
Conference contributions / Lectures, other	167	170

Publications

2014

- Augustin-Bauditz, S., Wex, H., Kanter, S., Ebert, M., Niedermeier, D., Stoltz, F., Prager, A. and Stratmann, F.** 2014. The immersion mode ice nucleation behavior of mineral dusts: A comparison of different pure and surface modified dusts. *Geophys. Res. Lett.*, **41**, 1-8. doi:10.1002/2014GL061317.
- Beddows, D. C. S., Dall’Osto, M., Harrison, R. M., Kulmala, M., Asmi, A., Wiedensohler, A., Laj, P., Fjaeraa, A. M., Sellegrí, K., Birmili, W., Bukowiecki, N., Weingartner, E., Baltensperger, U., Zdimal, V., Zikova, N., Putaud, J.-P., Marinoni, A., Tunved, P., Hansson, H.-C., Fiebig, M., Kivekäs, N., Swietlicki, E., Lihavainen, H., Asmi, E., Ulevicius, V., Aalto, P. P., Mihalopoulos, N., Kalivitis, N., Kalapov, I., Kiss, G., de Leeuw, G., Henzing, B., O’Dowd, C., Jennings, S. G., Flentje, H., Meinhardt, F., Ries, L., van der Gon, H. A. C. D. and Visschedijk, A. J. H.** 2014. Variations in tropospheric submicron particle size distributions across the European Continent 2008-2009. *Atmos. Chem. Phys.*, **14**, 4327–4348. doi:10.5194/acp-14-4327-2014.
- Berndt, T., Jokinen, T., Sipilä, M., Mauldin III, R. L., Herrmann, H., Stratmann, F., Junninen, H. and Kulmala, M.** 2014. H_2SO_4 formation from the gas-phase reaction of stabilized Criegee Intermediates with SO_2 : Influence of water vapour content and temperature. *Atmos. Environ.*, **89**, 603-612. doi:10.1016/j.atmosenv.2014.02.062.
- Berndt, T., Sipilä, M., Stratmann, F., Petäjä, T., Vanhanen, J., Mikkilä, J., Patokoski, J., Taipale, R., Mauldin III, R. L. and Kulmala, M.** 2014. Enhancement of atmospheric $\text{H}_2\text{SO}_4 / \text{H}_2\text{O}$ nucleation: Organic oxidation products versus amines. *Atmos. Chem. Phys.*, **14**, 751-764. doi:10.5194/acp-14-751-2014.
- Berndt, T., Voigtlander, J., Stratmann, F., Junninen, H., Mauldin III, R. L., Sipilä, M., Kulmala, M. and Herrmann, H.** 2014. Competing atmospheric reactions of CH_2OO with SO_2 and water vapour. *Phys. Chem. Chem. Phys.*, **16**, 19130-19136. doi:10.1039/c4cp02345e.
- Bian, Y. X., Zhao, C. S., Ma, N., Chen, J. and Xu, W. Y.** 2014. A study of aerosol liquid water content based on hygroscopicity measurements at high relative humidity in the North China Plain. *Atmos. Chem. Phys.*, **14**, 6417–6426. doi:10.5194/acp-14-6417-2014.
- Birmili, W., Rückerl, R., Hoffmann, B., Weinmayr, G., Schins, R., Kuhlbusch, T. A. J., Vogel, A., Weber, K., Franck, U., Cyrys, J. and Peters, A.** 2014. Ultrafeine Aerosolpartikel in der Außenluft: Perspektiven zur Aufklärung ihrer Gesundheitseffekte (Ultrafine aerosol particles in ambient air: Perspectives to elucidate their health effects). *Gefahrst. Reinhalt. L.*, **74**, 492-500.
- Brückner, M., Pospichal, B., Macke, A. and Wendisch, M.** 2014. A new multispectral cloud retrieval method for ship-based solar transmissivity measurements. *J. Geophys. Res. - Atmos.*, **119**, Online first 6 October 2014. doi:10.1002/2014JD021775.

Appendices: Publications

- Brunner, D., Savage, N., Jorba, O., Eder, B., Giordano, L., Badia, A., Balzarini, A., Baró, R., Bianconi, R., Chemel, C., Curci, G., Forkel, R., Jiménez-Guerrero, P., Hirtl, M., Hodzic, A., Honzak, L., Im, U., Knoté, C., Makar, P., Manders-Groot, A., van Meijgaard, E., Neal, L., Pérez, J. L., Pirovano, G., San José, R., **Schröder, W.**, Sokhi, R. S., Syrakov, D., Torian, A., Tuccella, P., Werhahn, J., **Wolke, R.**, Yahya, K., Zabkar, R., Zhang, Y., Hogrefe, C. and Galmarini, S. 2014. Comparative analysis of meteorological performance of coupled chemistry-meteorology models in the context of AQMEII phase 2. *Atmos. Environ.*, Available online. doi:10.1016/j.atmosenv.2014.12.032.
- Bumke, K., Schlundt, M., **Kalisch, J.**, **Macke, A.** and Kleta, H. 2014. Measured and parameterized energy fluxes for Atlantic transects of Polarstern. *J. Phys. Oceanogr.*, **44**, 482-491.
- Chen, Z., Liu, W., **Heese, B.**, **Althausen, D.**, **Baars, H.**, Cheng, T., Shu, X. and Zhang, T. 2014. Aerosol optical properties observed by combined Raman-elastic backscatter lidar in winter 2009 in Pearl River Delta, south China. *J. Geophys. Res. - Atmos.*, **119**, 2496-2510. doi:10.1002/2013JD020200.
- Cimini, D., Rizi, V., Di Girolamo, P., Marzano, F. S., **Macke, A.**, Pappalardo, G. and Richter, A. 2014. Overview: Tropospheric profiling: State of the art and future challenges – introduction to the AMT special issue. *Atmos. Meas. Tech. (AMT)*, **7**, 2981-2986. doi:10.5194/amt-7-2981-2014.
- Crippa, M., Canonaco, F., Lanz, V. A., Äijälä, M., Allan, J. D., Carbone, S., Capes, G., Ceburnis, D., Dall’Osto, M., Day, D. A., DeCarlo, P. F., Ehn, M., Eriksson, A., Freney, E., Hildebrandt Ruiz, L., Hillamo, R., Jimenez, J.-L., Junninen, H., Kiendler-Scharr, A., Kortelainen, A.-M., Kulmala, M., Laaksonen, A., Mensah, A. A., Mohr, C., Nemitz, E., O’Dowd, C., Ovadnevaite, J., Pandis, S. N., Petäjä, T., **Poulain, L.**, Saarikoski, S., Sellegri, K., Swietlicki, E., Tiitta, P., Worsnop, D. R., Baltensperger, U. and Prévôt, A. S. H. 2014. Organic aerosol components derived from 25 AMS data sets across Europe using a consistent ME-2 based source apportionment approach. *Atmos. Chem. Phys.*, **14**, 6159-6176. doi:10.5194/acp-14-6159-2014.
- Curci, G., Hogrefe, C., Bianconi, R., Im, U., Balzarini, A., Baró, R., Brunner, D., Forkel, R., Giordano, L., Hirtl, M., Honzak, L., Jiménez-Guerrero, P., Knoté, C., Langer, M., Makar, P., Pirovano, G., Pérez, J. L., San José, R., Syrakov, D., Tuccella, P., Werhahn, J., **Wolke, R.**, Žabkar, R., Zhang, J. and Galmarini, S. 2014. Uncertainties of simulated aerosol optical properties induced by assumptions on aerosol physical and chemical properties: An AQMEII-2 perspective. *Atmos. Environ.*, Available online. doi:10.1016/j.atmosenv.2014.09.009.
- Dahlkötter, F., Gysel, M., Sauer, D., Minikin, A., Baumann, R., **Seifert, P.**, **Ansmann, A.**, Fromm, M., Voigt, C. and Weinzierl, B. 2014. The Pagami Creek smoke plume after long-range transport to the upper troposphere over Europe – Aerosol properties and black carbon mixing state. *Atmos. Chem. Phys.*, **14**, 6111-6137. doi:10.5194/acp-14-6111-2014.
- Di Biagio, C., Formenti, P., **Styler, S. A.**, Pangui, E. and Doussin, J.-F. 2014. Laboratory chamber measurements of the longwave extinction spectra and complex refractive indices of African and Asian mineral dust. *Geophys. Res. Lett.*, **41**, 6289-6297. doi:10.1002/2014GL060213.
- Ehn, M., Thornton, J. A., Kleist, E., Sipilä, M., Junninen, H., Pullinen, I., Springer, M., Rubach, F., Tillmann, R., Lee, B., Lopez-Hilfiker, F., Andres, S., Acir, I.-H., Rissanen, M., **Jokinen, T.**, Schobesberger, S., Kangasluoma, J., Kontkanen, J., Nieminen, T., Kurtén, T., Nielsen, L. B., Jørgensen, S., Kjaergaard, H. G., Canagaratna, M., Dal Maso, M., **Berndt, T.**, Petäjä, T., Wahner, A., Kerminen, V.-M., Kulmala, M., Worsnop, D., Wildt, J. and Mentel, T. F. 2014. A large source of low-volatility secondary organic aerosol. *Nature*, **506**, 476-479. doi:10.1038/nature13032.
- Fiedler, S., **Schepanski, K.**, Knippertz, P., **Heinold, B.** and **Tegen, I.** 2014. How important are atmospheric depressions and mobile cyclones for emitting mineral dust aerosol in North Africa? *Atmos. Chem. Phys.*, **14**, 8983-9000. doi:10.5194/acp-14-8983-2014.
- Fomba, K. W.**, **Müller, K.**, **van Pinxteren, D.**, **Poulain, L.**, **van Pinxteren, M.** and **Herrmann, H.** 2014. Long-term chemical characterization of tropical and marine aerosols at the Cape Verde Atmospheric Observatory (CVAO) from 2007 to 2011. *Atmos. Chem. Phys.*, **14**, 8883-8904. doi:10.5194/acp-14-8883-2014.
- Fountoukis, C., Megaritis, A. G., Skyllakou, K., Charalampidis, P. E., Pilinis, C., Denier van der Gon, H. A. C., Crippa, M., Canonaco, F., Mohr, C., Prévôt, A. S. H., Allan, J. D., **Poulain, L.**, Petäjä, T., Tiitta, P., Carbone, S., Kiendler-Scharr, A., Nemitz, E., O’Dowd, C., Swietlicki, E. and Pandis, S. N. 2014. Organic aerosol concentration and composition over Europe: Insights from comparison of regional model predictions with aerosol mass spectrometer factor analysis. *Atmos. Chem. Phys.*, **14**, 9061-9076. doi:10.5194/acp-14-9061-2014.
- Friberg, J., Martinsson, B. G., Andersson, S. M., Brenninkmeijer, C. A. M., **Herrmann, M.**, van Velthoven, P. F. J. and Zahn, A. 2014. Sources of increase in lowermost stratospheric sulphurous and carbonaceous aerosol background concentrations during 1999 – 2008 derived from CARIBIC flights. *Tellus B*, **66**, 23428. doi:10.3402/tellusb.v66.23428.

Appendices: Publications

- George, C., D'Anna, B., **Herrmann, H.**, **Weller, C.**, Vaida, V., Donaldson, D. J., Bartels-Rausch, T. and Ammann, M. 2014. *Emerging areas in atmospheric photochemistry*. V. F. McNeill and P. A. Ariya (Ed.), In: *Atmospheric and aerosol chemistry*. Springer, Berlin, Heidelberg, p. 1-54. (Topics in current chemistry ; 339).
- Gonser, S. G., Klein, F., **Birmili, W.**, **Größ, J.**, Kulmala, M., Manninen, H. E., **Wiedensohler, A.** and Held, A. 2014. Ion – particle interactions during particle formation and growth at a coniferous forest site in central Europe. *Atmos. Chem. Phys.*, **14**, 10547-10563. doi:10.5194/acp-14-10547-2014.
- Granados-Muñoz, M. J., Guerrero-Rascado, J. L., Bravo-Aranda, J. A., Navas-Guzmán, F., Valenzuela, A., Lyamani, H., Chaikovsky, A., **Wandinger, U.**, **Ansmann, A.**, Dubovik, O., Grudo, J. O. and Alados-Arboledas, L. 2014. Retrieving aerosol microphysical properties by Lidar-Radiometer Inversion Code (LIRIC) for different aerosol types. *J. Geophys. Res. - Atmos.*, **119**, 4836–4858. doi:10.1002/2013JD021116.
- Guo, J., **Tilgner, A.**, Yeung, C. P., Wang, Z., Louie, P. K. K., Luk, C. W. Y., Xu, Z., Yuan, C., Gao, Y., Poon, S., **Herrmann, H.**, Lee, S., Lam, K. S. and Wang, T. 2014. Atmospheric peroxides in a polluted subtropical environment: Seasonal variation, sources and sinks, and importance of heterogeneous processes. *Environ. Sci. Technol.*, **48**, 1443-1450. doi:10.1021/es403229x.
- Harris, E., Sinha, B., **van Pinxteren, D.**, Schneider, J., **Poulain, L.**, Collett, J., D'Anna, B., Fahlbusch, B., Foley, S., **Fomba, K. W.**, George, C., **Gnauk, T.**, **Henning, S.**, Lee, T., **Mertes, S.**, Roth, A., **Stratmann, F.**, Borrmann, S., Hoppe, P. and **Herrmann, H.** 2014. In-cloud sulfate addition to single particles resolved with sulfur isotope analysis during HCCT-2010. *Atmos. Chem. Phys.*, **14**, 4219-4235. doi:10.5194/acp-14-4219-2014.
- Healy, R. M., Evans, G. J., Murphy, M., Jurányi, Z., Tritscher, T., Laborde, M., Weingartner, E., Gysel, M., **Poulain, L.**, **Kamilli, K. A.**, **Wiedensohler, A.**, O'Connor, I. P., McGillicuddy, E., Sodeau, J. R. and Wenger, J. C. 2014. Predicting hygroscopic growth using single particle chemical composition estimates. *J. Geophys. Res. - Atmos.*, **119**, 9567-9577. doi:10.1002/2014JD021888.
- Healy, R. M., Riemer, N., Wenger, J. C., Murphy, M., West, M., **Poulain, L.**, **Wiedensohler, A.**, O'Connor, I. P., McGillicuddy, E., Sodeau, J. R. and Evans, G. J. 2014. Single particle diversity and mixing state measurements. *Atmos. Chem. Phys.*, **14**, 6289-6299. doi:10.5194/acp-14-6289-2014.
- Henning, S.**, **Dieckmann, K.**, **Ignatius, K.**, **Schäfer, M.**, **Zedler, P.**, Harris, E., Sinha, B., **van Pinxteren, D.**, **Mertes, S.**, **Birmili, W.**, **Merkel, M.**, **Wu, Z.**, **Wiedensohler, A.**, **Wex, H.**, **Herrmann, H.** and **Stratmann, F.** 2014. Influence of cloud processing on CCN activation behavior in the Thuringian Forest, Germany during HCCT-2010. *Atmos. Chem. Phys.*, **14**, 7859-7868. doi:10.5194/acp-14-7859-2014.
- Hillemann, L., Zschoppe, A., Caldow, R., Sem, G. J. and **Wiedensohler, A.** 2014. An ultrafine particle monitor for size-resolved number concentration measurements in atmospheric aerosols. *J. Aerosol Sci.*, **68**, 14-24. doi:10.1016/j.jaerosci.2013.10.007.
- Hoffmann, F., **Siebert, H.**, Schumacher, J., Riechelmann, T., **Katzwinkel, J.**, Kumar, B., Götzfried, P. and Raasch, S. 2014. Entrainment and mixing at the interface of shallow cumulus clouds: Results from a combination of observations and simulations. *Meteorol. Z.*, Online first. doi:10.1127/0941-2948/2014/0597.
- Högström, R., Quincey, P., Sarantidis, D., Lüönd, F., Nowak, A., Riccobono, F., **Tuch, T.**, Sakurai, H., Owen, M., Heinonen, M., Keskinen, J. and Yli-Ojanperä, J. 2014. First comprehensive inter-comparison of aerosol electrometers for particle sizes up to 200 nm and concentration range 1000 cm⁻³ to 17000 cm⁻³. *Metrologia*, **51**, 293-303. doi:10.1088/0026-1394/51/3/293.
- Horváth, Á.**, Seethala, C. and **Deneke, H.** 2014. View angle dependence of AMSR-E and MODIS liquid water path retrievals in warm oceanic clouds. *J. Geophys. Res. - Atmos.*, **119**, 8304-8328. doi:10.1002/2013JD021355.
- Hünerbein, A.**, **Deneke, H.**, **Macke, A.**, Eboll, K. and Görsdorf, U. 2014. Combining satellite- and ground-based observations to analyze cloud frontal systems. *J. Appl. Meteorol. Clim.*, **53**, 2538-2552. doi:10.1175/JAMC-D-13-0274.1.
- Im, U., Bianconi, R., Solazzo, E., Kioutsioukis, I., Badia, A., Balzarini, A., Baró, R., Bellasio, R., Brunner, D., Chemel, C., Curci, G., Flemming, J., Forkel, R., Giordano, L., Jiménez-Guerrero, P., Hirtl, M., Hodzic, A., Honzak, L., Jorba, O., Knote, C., Kuenen, J. P., Makar, P. A., Manders-Groot, A., Neal, L., Pérez, J. L., Pirovano, G., Pouliot, G., San Jose, R., Savage, N., **Schröder, W.**, Sokhi, R. S., Syrakov, D., Torian, A., Tuccella, P., Werhahn, J., **Wolke, R.**, Yahya, K., Zabkar, R., Zhang, Y., Zhang, J., Hogrefe, C. and Galmarini, S. 2014. Evaluation of operational online-coupled regional air quality models over Europe and North America in the context of AQMEII phase 2. Part I: Ozone. *Atmos. Environ.*, Available online. doi:10.1016/j.atmosenv.2014.09.042.

Appendices: Publications

- Im, U., Bianconi, R., Solazzo, E., Kioutsioukis, I., Badia, A., Balzarini, A., Baró, R., Bellasio, R., Brunner, D., Chemel, C., Curci, G., van der Gon, H. D., Flemming, J., Forkel, R., Giordano, L., Jiménez-Guerrero, P., Hirtl, M., Hodzic, A., Honzak, L., Jorba, O., Knoté, C., Makar, P. A., Manders-Groot, A., Neal, L., Pérez, J. L., Pirovano, G., Pouliot, G., San Jose, R., Savage, N., **Schroder, W.**, Sokhi, R. S., Syrakov, D., Torian, A., Tuccella, P., Wang, K., Werhahn, J., **Wolke, R.**, Zabkar, R., Zhang, Y., Zhang, J., Hogrefe, C. and Galmarini, S. 2014. Evaluation of operational online-coupled regional air quality models over Europe and North America in the context of AQMEII phase 2. Part II: Particulate Matter. *Atmos. Environ.*, Available online. doi:10.1016/j.atmosenv.2014.08.072.
- Jokinen, T.**, Sipilä, M., **Richters, S.**, Kerminen, V.-M., Paasonen, P., **Stratmann, F.**, Worsnop, D., Kulmala, M., Ehni, M., **Herrmann, H.** and **Berndt, T.** 2014. Rapid autoxidation forms highly oxidized RO₂ radicals in the atmosphere. *Angew. Chem. Int. Edit.*, **53**, 14596-14600. doi:10.1002/anie.201408566.
- Jokinen, T.**, Sipilä, M., **Richters, S.**, Kerminen, V.-M., Paasonen, P., **Stratmann, F.**, Worsnop, D., Kulmala, M., Ehni, M., **Herrmann, H.** and **Berndt, T.** 2014. Schnelle Autoxidation bildet hochoxidierte RO₂-Radikale in der Atmosphäre. *Angew. Chem.*, **126**, 14825-14829. doi:10.1002/ange.201408566.
- Kahnt, A., **Iinuma, Y.**, Blockhuys, F., **Mutzel, A.**, Vermeylen, R., Kleindienst, T. E., Jaoui, M., Offenberg, J. H., Lewandowski, M., **Böge, O.**, **Herrmann, H.**, Maenhaut, W. and Claeys, M. 2014. 2-Hydroxyterpenylic acid: An oxygenated marker compound for α-Pinene Secondary Organic Aerosol in ambient fine aerosol. *Environ. Sci. Technol.*, **48**, 4901-4908. doi:10.1021/es500377d.
- Kahnt, A.**, **Iinuma, Y.**, **Mutzel, A.**, **Böge, O.**, Claeys, M. and **Herrmann, H.** 2014. Campholenic aldehyde ozonolysis: A mechanism leading to specific biogenic secondary organic aerosol constituents. *Atmos. Chem. Phys.*, **14**, 719-736. doi:10.5194/acp-14-719-2014.
- Kamilli, K. A.**, **Poulain, L.**, **Held, A.**, **Nowak, A.**, **Birmili, W.** and **Wiedensohler, A.** 2014. Hygroscopic properties of the Paris urban aerosol in relation to its chemical composition. *Atmos. Chem. Phys.*, **14**, 737-749. doi:10.5194/acp-14-737-2014.
- Kanitz, T.**, **Ansmann, A.**, **Foth, A.**, **Seifert, P.**, **Wandinger, U.**, **Engelmann, R.**, **Baars, H.**, **Althausen, D.**, Casiccia, C. and Zamorano, F. 2014. Surface matters: Limitations of CALIPSO V3 aerosol typing in coastal regions. *Atmos. Meas. Tech. (AMT)*, **7**, 2061-2072. doi:10.5194/amt-7-2061-2014.
- Kanitz, T.**, **Engelmann, R.**, **Heinold, B.**, **Baars, H.**, **Skupin, A.** and **Ansmann, A.** 2014. Tracking the Saharan air layer with shipborne lidar across the tropical Atlantic. *Geophys. Res. Lett.*, **41**, 1044-1050. doi:10.1002/2013GL058780.
- Katzwinkel, J.**, **Siebert, H.**, Heus, T. and Shaw, R. A. 2014. Measurements of turbulent mixing and subsiding shells in trade wind cumuli. *J. Atmos. Sci.*, **71**, 2810–2822. doi:10.1175/JAS-D-13-0222.1.
- Knoth, O.** and Wensch, J. 2014. Generalized split-explicit Runge-Kutta methods for the compressible Euler equations. *Mon. Wea. Rev.*, **142**, 2067-2081. doi:10.1175/MWR-D-13-00068.1.
- Korhonen, K., Giannakaki, E., Mielonen, T., Pfüller, A., Laakso, L., Vakkari, V., **Baars, H.**, **Engelmann, R.**, Beukes, J. P., Van Zyl, P. G., Ramandh, A., Ntsangwane, L., Josipovic, M., Tiitta, P., Fourie, G., Ngwana, I., Chiloane, K. and Komppula, M. 2014. Atmospheric boundary layer top height in South Africa: Measurements with lidar and radiosonde compared to three atmospheric models. *Atmos. Chem. Phys.*, **14**, 4263-4278. doi:10.5194/acp-14-4263-2014.
- Kristensen, T. B.**, Prisle, N. L. and Bilde, M. 2014. Cloud droplet activation of mixed model HULIS and NaCl particles: Experimental results and kappa-Köhler theory. *Atmos. Res.*, **137**, 167–175. doi:10.1016/j.atmosres.2013.09.017.
- Krüger, M. L., **Mertes, S.**, Klimach, T., Cheng, Y. F., Su, H., Schneider, J., Andreae, M. O., Pöschl, U. and Rose, D. 2014. Assessment of cloud supersaturation by size-resolved aerosol particle and cloud condensation nuclei (CCN) measurements. *Atmos. Meas. Tech. (AMT)*, **7**, 2615-2629. doi:10.5194/amt-7-2615-2014.
- Kumar, P., Morawska, L., **Birmili, W.**, Paasonen, P., Hu, M., Kulmala, M., Harrison, R. M., Norford, L. and Britter, R. 2014. Ultrafine particles in cities. *Environ. Internat.*, **66**, 1-10. doi:10.1016/j.envint.2014.01.013.
- Liu, H. J., Zhao, C. S., **Nekat, B.**, Ma, N., **Wiedensohler, A.**, **van Pinxteren, D.**, **Spindler, G.**, **Müller, K.** and **Herrmann, H.** 2014. Aerosol hygroscopicity derived from size-segregated chemical composition and its parameterization in the North China Plain. *Atmos. Chem. Phys.*, **14**, 2525-2539. doi:10.5194/acp-14-2525-2014.
- Ma, N.**, **Birmili, W.**, **Müller, T.**, **Tuch, T.**, Cheng, Y. F., Xu, W. Y., Zhao, C. S. and **Wiedensohler, A.** 2014. Tropospheric aerosol scattering and absorption over Central Europe: A closure study for the dry particle state. *Atmos. Chem. Phys.*, **14**, 6241-6259. doi:10.5194/acp-14-6241-2014.

Appendices: Publications

- Ma, N.**, Zhao, C. S., Chen, J., Xu, W. Y., Yan, P. and Zhou, X. J. 2014. A novel method for distinguishing fog and haze based on PM2.5, visibility, and relative humidity. *Sci. China Ser. D - Earth Sci.*, **57**, 1-9. doi:10.1007/s11430-014-4885-5.
- Madhavan, B. L.** and Wu, Y. 2014. *Spectroscopic techniques for atmospheric sensing*. Y. Dwivedi, S. B. Rai, and J. P. Singh (Ed.), In: *Spectroscopic techniques for security, forensic and environmental applications*. Nova Science Pub Inc, New York, p. 221-252. (Chemistry research and applications).
- Mamouri, R. E. and **Ansmann, A.** 2014. Fine and coarse dust separation with polarization lidar. *Atmos. Meas. Tech. (AMT)*, **7**, 3717-3735. doi:10.5194/amt-7-3717-2014.
- Mann, G. W., Carslaw, K. S., Reddington, C. L., Pringle, K. J., Schulz, M., Asmi, A., Spracklen, D. V., Ridley, D. A., Woodhouse, M. T., Lee, L. A., Zhang, K., Ghan, S. J., Easter, R. C., Liu, X., Stier, P., Lee, Y. H., Adams, P. J., Tost, H., Lelieveld, J., Bauer, S. E., Tsigaridis, K., van Noije, T. P. C., Strunk, A., Vignati, E., Bellouin, N., Dalvi, M., Johnson, C. E., Bergman, T., Kokkola, H., von Salzen, K., Yu, F., Luo, G., Petzold, A., **Heintzenberg, J.**, Clarke, A., Ogren, J. A., Gras, J., Baltensperger, U., Kaminski, U., Jennings, S. G., O'Dowd, C. D., Harrison, R. M., Beddows, D. C. S., Kulmala, M., Viisanen, Y., Ulevicius, V., Mihalopoulos, N., Zdimal, V., Fiebig, M., Hansson, H.-C., Swietlicki, E. and Henzing, J. S. 2014. Intercomparison and evaluation of global aerosol microphysical properties among AeroCom models of a range of complexity. *Atmos. Chem. Phys.*, **14**, 4679-4713. doi:10.5194/acp-14-4679-2014.
- Martinsson, B. G., Friberg, J., Andersson, S. M., **Weigelt, A.**, **Hermann, M.**, **Assmann, D.**, **Voigtlander, J.**, Brenninkmeijer, C. A. M., van Velthoven, P. J. F. and Zahn, A. 2014. Comparison between CARIBIC aerosol samples analysed by accelerator-based methods and optical particle counter measurements. *Atmos. Meas. Tech. (AMT)*, **7**, 2581-2596. doi:10.5194/amt-7-2581-2014.
- Miller, R., Knippertz, P., Pérez, C., Perlitz, J. and **Tegen, I.** 2014. *Impact of dust radiative forcing upon climate*. P. Knippertz and J.-B. Stuut (Ed.), In: *Mineral dust: A key player in the earth system*. Springer, Dordrecht, p. 327-358.
- Müller, T.**, Virkkula, A. and Ogren, J. A. 2014. Constrained two-stream algorithm for calculating aerosol light absorption coefficient from the Particle Soot Absorption Photometer. *Atmos. Meas. Tech. (AMT)*, **7**, 4049-4070. doi:10.5194/amt-7-4049-2014.
- Nguyen, Q. T., **Kristensen, T. B.**, Hansen, A. M. K., Skov, H., Bossi, R., Massling, A., Sørensen, L. L., Bilde, M., Glasius, M. and Nørgaard, J. K. 2014. Characterization of humic-like substances in Arctic aerosols. *J. Geophys. Res. - Atmos.*, **119**, 5011-5027. doi:10.1002/2013JD020144.
- Niedermeier, D.**, Ervens, B., **Clauss, T.**, **Voigtlander, J.**, **Wex, H.**, **Hartmann, S.** and **Stratmann, F.** 2014. A computationally efficient description of heterogeneous freezing: A simplified version of the Soccer ball model. *Geophys. Res. Lett.*, **41**, 736-741. doi:10.1002/grl.51242.
- Niedermeier, N.**, Held, A., **Müller, T.**, **Heinold, B.**, Schepanski, K., **Tegen, I.**, Kandler, K., Ebert, M., Weinbruch, S., Read, K., Lee, J., **Fomba, K. W.**, **Müller, K.**, **Herrmann, H.** and **Wiedensohler, A.** 2014. Mass deposition fluxes of Saharan mineral dust to the tropical northeast Atlantic Ocean: An intercomparison of methods. *Atmos. Chem. Phys.*, **14**, 2245-2266. doi:10.5194/acp-14-2245-2014.
- Nisantzi, A., Mamouri, R. E., **Ansmann, A.** and Hadjimitsis, D. 2014. Injection of mineral dust into the free troposphere during fire events observed with polarization lidar at Limassol, Cyprus. *Atmos. Chem. Phys.*, **14**, 12155-12165. doi:10.5194/acp-14-12155-2014.
- Nordmann, S.**, Cheng, Y. F., Carmichael, G. R., Yu, M., Denier van der Gon, H. A. C., Zhang, Q., Saide, P. E., Pöschl, U., Su, H., **Birmili, W.** and **Wiedensohler, A.** 2014. Atmospheric black carbon and warming effects influenced by the source and absorption enhancement in central Europe. *Atmos. Chem. Phys.*, **14**, 12683-12699. doi:10.5194/acp-14-12683-2014.
- Pappalardo, G., Amodeo, A., Apituley, A., Comeron, A., Freudenthaler, V., Linné, H., **Ansmann, A.**, Bösenberg, J., D'Amico, G., Mattis, I., Mona, L., **Wandinger, U.**, Amiridis, V., Alados-Arboledas, L., Nicolae, D. and Wiegner, M. 2014. EARLINET: Towards an advanced sustainable European aerosol lidar network. *Atmos. Meas. Tech. (AMT)*, **7**, 2389-2409. doi:10.5194/amt-7-2389-2014.
- Pfeifer, S.**, **Birmili, W.**, **Schladitz, A.**, **Müller, T.**, **Nowak, A.** and **Wiedensohler, A.** 2014. A fast and easy-to-implement inversion algorithm for mobility particle size spectrometers considering particle size spectrometers considering particle number size distribution information outside of the detection range. *Atmos. Meas. Tech. (AMT)*, **7**, 95-105. doi:10.5194/amt-7-95-2014.
- Pietikäinen, J.-P., Mikkonen, S., Hamed, A., Hienola, A. I., **Birmili, W.**, Kulmala, M. and Laaksonen, A. 2014. Analysis of nucleation events in the European boundary layer using the regional aerosol-climate model REMO-HAM with a solar radiation-driven OH-proxy. *Atmos. Chem. Phys.*, **14**, 11711-11729. doi:10.5194/acp-14-11711-2014.

Appendices: Publications

- Poulain, L., Birmili, W., Canonaco, F., Crippa, M., Wu, Z. J., Nordmann, S., Spindler, G.,** Prévôt, A. S. H., Wiedensohler, A. and Herrmann, H. 2014. Chemical mass balance of 300 °C non-volatile particles at the tropospheric research site Melpitz, Germany. *Atmos. Chem. Phys.*, **14**, 10145–10162. doi:10.5194/acp-14-10145-2014.
- Richters, S. and Berndt, T.** 2014. Gas-phase reaction of monomethylhydrazine with ozone: Kinetics and OH radical formation. *Int. J. Chem. Kinet.*, **46**, 1-9. doi:10.1002/kin.20816.
- Scheinhardt, S., van Pinxteren, D., Müller, K., Spindler, G. and Herrmann, H.** 2014. Hydroxymethanesulfonic acid in size-segregated aerosol particles at nine sites in Germany *Atmos. Chem. Phys.*, **14**, 4531-4538. doi:10.5194/acp-14-4532-2014.
- Schladitz, A., Merkel, M., Bastian, S., Birmili, W., Weinhold, K., Löschau, G. and Wiedensohler, A.** 2014. A concept of an automated function control for ambient aerosol measurements using mobility particle size spectrometers. *Atmos. Meas. Tech. (AMT)*, **7**, 1065–1073. doi:10.5194/amt-7-1065-2014.
- Schmidt, J., Ansmann, A., Bühl, J., Baars, H., Wandinger, U., Müller, D. and Malinka, A. V.** 2014. Dual-FOV Raman and Doppler lidar studies of aerosol-cloud interactions: Simultaneous profiling of aerosols, warm-cloud properties, and vertical wind. *J. Geophys. Res. - Atmos.*, **119**, 5512-5527. doi:10.1002/2013JD020424.
- Schöne, L. and Herrmann, H.** 2014. Kinetic measurements of the reactivity of hydrogen peroxide and ozone towards small atmospherically relevant aldehydes, ketones and organic acids in aqueous solutions. *Atmos. Chem. Phys.*, **14**, 4503-4514. doi:10.5194/acp-14-4503-2014.
- Schöne, L., Schindelka, J., Szeremeta, E., Schaefer, T., Hoffmann, D., Rudzinski, J., Szmigielski, R. and Herrmann, H.** 2014. Atmospheric aqueous phase radical chemistry of the isoprene oxidation products methacrolein, methyl vinyl ketone, methacrylic acid and acrylic acid - kinetics and product studies. *Phys. Chem. Chem. Phys.*, online 4 Feb 2014. doi:10.1039/C3CP54859G.
- Schrödner, R., Tilgner, A., Wolke, R. and Herrmann, H.** 2014. Modeling the multiphase processing of an urban and a rural air mass with COSMO–MUSCAT. *Urban Climate*, **10**, 720-731. doi:10.1016/j.uclim.2014.02.001.
- Schroedner, R., Wolke, R., Tilgner, A. and Herrmann, H.** 2014. *The influence of cloud chemical processes on the formation of secondary particulate matter*. D. Steyn and R. Mathur (Ed.), In: *Air pollution modeling and its application XXIII : Proceedings of the 33rd NATO/SPS International Technical Meeting on Air Pollution Modeling and Its Application (Miami, Florida, USA, 26-30 August 2013)*. Springer, Cham, p. 97-102. (Springer Proceedings in Complexity).
- Setyan, A., Song, C., **Merkel, M.**, Knighton, W. B., Onasch, T. B., Canagaratna, M. R., Worsnop, D. R., **Wiedensohler, A.**, Shilling, J. E. and Zhang, Q. 2014. Chemistry of new particle growth in mixed urban and biogenic emissions – insights from CARES. *Atmos. Chem. Phys.*, **14**, 6477–6494. doi:10.5194/acp-14-6477-2014.
- Sipilä, M., **Jokinen, T., Berndt, T., Richters, S.**, Makkonen, R., Donahue, N. M., Mauldin III, R. L., Kurtén, T., Paasonen, P., Sarnela, N., Ehn, M., Junninen, H., Rissanen, M. P., Thornton, J., **Stratmann, F., Herrmann, H.**, Worsnop, D. R., Kulmala, M., Kerminen, V.-M. and Petäjä, T. 2014. Reactivity of stabilized Criegee intermediates (sCIs) from isoprene and monoterpene ozonolysis toward SO₂ and organic acids. *Atmos. Chem. Phys.*, **14**, 12143-12153. doi:10.5194/acp-14-12143-2014.
- Skupin, A., Ansmann, A., Engelmann, R., Baars, H. and Müller, T.** 2014. The Spectral Aerosol Extinction Monitoring System (SÆMS): Setup, observational products, and comparisons. *Atmos. Meas. Tech. (AMT)*, **7**, 701-712. doi:10.5194/amt-7-701-2014.
- Slemr, F., Weigelt, A., Ebinghaus, R., Brenninkmeijer, C., Baker, A., Schuck, T., Rauthe-Schöch, A., Riede, H., Leedham, E., **Hermann, M.**, van Velthoven, P., Oram, D., O'Sullivan, D., Dyroff, C., Zahn, A. and Ziereis, H. 2014. Mercury plumes in the global upper troposphere observed during flights with the CARIBIC observatory from May 2005 until June 2013. *Atmosphere*, **5**, 342-369. doi:10.3390/atmos5020342.
- Spiegel, J. K., Buchmann, N., Mayol-Bracero, O. L., Cuadra Rodríguez, L. A., Valle Diaz, C. J., Prather, K. A., **Mertes, S.** and Eugster, W. 2014. Do cloud properties in a Puerto Rican tropical montane cloud forest depend on occurrence of long-range transported African dust? *Pure Appl. Geophys.*, online first. doi:10.1007/s00024-014-0830-y.
- Stanelle, T., Bey, I., Raddatz, T., Reick, C. and **Tegen, I.** 2014. Anthropogenically induced changes in twentieth century mineral dust burden and the associated impact on radiative forcing. *J. Geophys. Res. - Atmos.*, **119**, 13526-13546. doi:10.1002/2014JD022062.
- Taipale, R., Sarnela, N., Rissanen, M., Junninen, H., Rantala, P., Korhonen, F., Siivola, E., **Berndt, T.**, Kulmala, M., Mauldin III, R. L., Petäjä, T. and Sipilä, M. 2014. New instrument for measuring atmospheric concentrations of non-OH oxidants of SO₂. *Boreal Environ. Res.*, **19**, 55-70.

Appendices: Publications

- Tao, J. C., Zhao, C. S., **Ma, N.** and Liu, P. F. 2014. The impact of aerosol hygroscopic growth on the single-scattering albedo and its application on the NO₂ photolysis rate coefficient. *Atmos. Chem. Phys.*, **14**, 12055-12067. doi:10.5194/acp-14-12055-2014.
- Tegen, I.** and Schulz, M. 2014. *Numerical dust models*. P. Knippertz and J.-B. Stuut (Ed.), In: *Mineral dust: A key player in the earth system*. Springer, Dordrecht, p. 201-222.
- Teich, M., van Pinxteren, D.** and **Herrmann, H.** 2014. Determination of nitrophenolic compounds from atmospheric particles using hollow-fiber liquid-phase microextraction and capillary electrophoresis/mass spectrometry analysis. *Electrophoresis*, **35**, 1353-1361. doi:10.1002/elps.201300448.
- Tilgner, A., Schöne, L., Bräuer, P., van Pinxteren, D., Hoffmann, E., Spindler, G., Styler, S. A., Mertes, S., Birmili, W., Otto, R., Merkel, M., Weinhold, K., Wiedensohler, A., Deneke, H., Schrödner, R., Wolke, R., Schneider, J., Haunold, W., Engel, A., Wéber, A. and Herrmann, H.** 2014. Comprehensive assessment of meteorological conditions and airflow connectivity during HCCT-2010. *Atmos. Chem. Phys.*, **14**, 9105-9128. doi:10.5194/acp-14-9105-2014.
- Titos, G., Lyamani, H., Cazorla, A., Sorribas, M., Foyo-Moreno, I., **Wiedensohler, A.** and Alados-Arboledas, L. 2014. Study of the relative humidity dependence of aerosol light-scattering in southern Spain. *Tellus B*, **66**, 24536-24550. doi:10.3402/tellusb.v66.24536.
- Tjernström, M., Leck, C., Birch, C. E., Bottenheim, J. W., Brooks, B. J., Brooks, I. M., Bäcklin, L., Chang, R. Y.-W., de Leeuw, G., Di Liberto, L., de la Rosa, S., Granath, E., Graus, M., Hansel, A., Heintzenberg, J., Held, A., Hind, A., Johnston, P., Knulst, J., Martin, M., Matrai, P. A., Mauritzen, T., Müller, M., Norris, S. J., Orellana, M. V., **Orsini, D. A.**, Paatero, J., Persson, P. O. G., Gao, Q., Rauschenberg, C., Ristovski, Z., Sedlar, J., Shupe, M. D., Sierau, B., Sirevaag, A., Sjogren, S., Stetzer, O., Swietlicki, E., Szczodrak, M., Vaattovaara, P., Wahlberg, N., Westberg, M. and Wheeler, C. R. 2014. The Arctic Summer Cloud-Ocean Study (ASCOS): Overview and experimental design. *Atmos. Chem. Phys.*, **14**, 2823-2869. doi:10.5194/acp-14-2823-2014.
- van Pinxteren, D., Neusüß, C. and Herrmann, H.** 2014. On the abundance and source contributions of dicarboxylic acids in size-resolved aerosol particles at continental sites in Central Europe. *Atmos. Chem. Phys.*, **14**, 3913-3928. doi:10.5194/acp-14-3913-2014.
- Vladutescu, D. V., **Madhavan, B. L.**, Gross, B. M., Aguirre, A., Moshary, F., Ahmed, S. A., Razani, M. and Blake, R. A. 2014. Assessment of Langley and NASA-GISS calibration techniques for MFRSR aerosol retrieval. *IEEE T. Geosci. Remote*, **52**, 5880-5894. doi:10.1109/TGRS.2013.2293633
- Weissmann, M., Göber, M., Hohenegger, C., Janjic, T., Keller, J., Ohlwein, C., Seifert, A., Trömel, S., Ulbrich, T., Wapler, K., Bollmeyer, C. and **Deneke, H.** 2014. Initial phase of the Hans-Ertel Centre for Weather Research – A virtual centre at the interface of basic and applied weather and climate research. *Meteorol. Z.*, **23**, 193-208. doi:10.1127/0941-2948/2014/0558.
- Weller, C., Tilgner, A., Bräuer, P. and Herrmann, H.** 2014. Modeling the impact of iron-carboxylate photochemistry on radical budget and carboxylate degradation in cloud droplets and particles. *Environ. Sci. Technol.*, **48**, 5652-5659. doi:10.1021/es4056643.
- Werner, F., **Ditas, F., Siebert, H., Simmel, M., Wehner, B.**, Pilewski, P., **Schmeissner, T.**, Shaw, R. A., **Hartmann, S., Wex, H.**, Roberts, G. C. and Wendisch, M. 2014. Twomey effect observed from collocated microphysical and remote sensing measurements over shallow cumulus. *J. Geophys. Res. - Atmos.*, **119**, 1534-1545. doi:10.1002/2013JD020131.
- Wex, H., DeMott, P. J., Tobo, Y., Hartmann, S., Rösch, M., Clauss, T., Tomsche, L., Niedermeier, D. and Stratmann, F.** 2014. Kaolinite particles as ice nuclei: Learning from the use of different types of kaolinite and different coatings. *Atmos. Chem. Phys.*, **14**, 5529-5546. doi:10.5194/acp-14-5529-2014.
- Wiedensohler, A., Birmili, W., Putaud, J.-P. and Ogren, J.** 2014. *Recommendations for aerosol sampling*. I. Colbeck and M. Lazaridis (Ed.), In: *Aerosol science : Technology and applications*. John Wiley & Sons, Chichester, p. 45-60.
- Wolke, R., Schroeder, W., Schroedner, R. and Renner, E.** 2014. *Influence of grid resolution and biomass burning emissions on air quality simulations: A sensitivity study with the modelling system COSMO-MUSCAT*. D. G. Steyn, P. J. H. Builtjes, and R. M. A. Timmermans (Ed.), In: *Air pollution modeling and its application XXII : Proceedings of the 32nd NATO/SPS International Technical Meeting on Air Pollution Modeling and Its Application (Utrecht, The Netherlands, 7 - 11 May 2012)*. Springer, Dordrecht, p. 559-563. (NATO Science for Peace and Security Series - C : Environmental Security).
- Zhang, N., Bashir, S., Qin, J., **Schindelka, J.**, Fischer, A., Nijenhuis, I., **Herrmann, H.**, Wick, L. Y. and Richnow, H. H. 2014. Compound Specific Stable Isotope Analysis (CSIA) to characterize transformation mechanisms of α-hexachlorocyclohexane. *J. Hazard. Mater.*, **280**, 750-757. doi:10.1016/j.jhazmat.2014.08.046.

Appendices: Publications

Zieger, P., Fierz-Schmidhauser, R., **Poulain, L.**, Müller, T., Birmili, W., Spindler, G., Wiedensohler, A., Baltensperger, U. and Weingartner, E. 2014. Influence of water uptake on the aerosol particle light scattering coefficients of the Central European aerosol. Tellus B, **66**, 22716-22729. doi:10.3402/tellusb.v66.22716.

2015

Ait-Helal, W., Beeldens, A., Boonen, E., Borbon, A., Boréave, A., Cazaunau, M., Chen, H., Daële, V., Dupart, Y., Gaimoz, C., Gallus, M., George, C., Grand, N., Grosselin, B., **Herrmann, H.**, Ifang, S., Kurtenbach, R., Maille, M., Marjanovic, I., Mellouki, A., Miet, K., **Mothes, F.**, **Poulain, L.**, **Rabe, R.**, Zapf, P., Kleffmann, J. and Doussin, J.-F. 2015. On-road measurements of NMVOCs and NO_x: Determination of light-duty vehicles emission factors from tunnel studies in Brussels city center. Atmos. Environ., **122**, 799-807. doi:10.1016/j.atmosenv.2015.09.066.

Althauser, D., Emeis, S., Behrendt, A., Jäckel, S., Münkel, C. and Wiegner, M. 2015. Lidar-Techniken zur entfernungsaufgelösten Fernmessung atmosphärischer Größen und erste technische Regeln zu diesen neuen Messverfahren. Gefahrst. Reinhalt. L., **75**, 235-240.

Altstädtter, B., Platis, A., **Wehner, B.**, Scholtz, A., Wildmann, N., **Herrmann, M.**, Kähner, R., **Baars, H.**, Bange, J. and Lampert, A. 2015. ALADINA – an unmanned research aircraft for observing vertical and horizontal distributions of ultrafine particles within the atmospheric boundary layer. Atmos. Meas. Tech. (AMT), **8**, 1627-1639. doi:10.5194/amt-8-1627-2015.

Andersson, S. M., Martinsson, B. G., Vernier, J.-P., Friberg, J., Brenninkmeijer, C. A. M., **Herrmann, M.**, van Velthoven, P. F. J. and Zahn, A. 2015. Significant radiative impact of volcanic aerosol in the lowermost stratosphere. Nat. Commun., **6**:7692. doi: 10.1038/ncomms8692.

Andrade, M., Zaratti, F., Forno, R., Gutiérrez, R., Moreno, I., Velarde, F., Ávila, F., Roca, M., Sánchez, M. F., Laj, P., Jaffrezo, J. L., Ginot, P., Sellegri, K., Ramonet, M., Laurent, O., **Weinhold, K.**, **Wiedensohler, A.**, Krejci, R., Bonasoni, P., Cristofanelli, P., Whiteman, D., Vimeux, F., Dommergue, A. and Magand, O. 2015. Set to work of a new climate monitoring station in the Central Andes of Bolivia: The GAW/Chacaltaya station (Puesta en marcha de una nueva estación de monitoreo en los andes centrales de Bolivia: La estación GAW/Chacaltaya station. Revista Boliviana de Física, **26**, 6-15.

Baergen, A. M., **Styler, S. A.**, **van Pinxteren, D.**, Müller, K., **Herrmann, H.** and Donaldson, D. J. 2015. Chemistry of urban grime: Inorganic ion composition of grime vs particles in Leipzig, Germany. Environ. Sci. Technol., **49**, 12688-12696. doi:10.1021/acs.est.5b03054.

Barta, A., Horvath, G., **Horváth, Á.**, Egri, Á., Blahó, M., Barta, P., Bumke, K. and **Macke, A.** 2015. Testing a polarimetric cloud imager aboard research vessel Polarstern: Comparison of color-based and polarimetric cloud detection algorithms. Appl. Optics, **54**, 1065-1077. doi:10.1364/AO.54.001065.

Beekmann, M., Prévôt, A. S. H., Drewnick, F., Sciare, J., Pandis, S. N., Denier van der Gon, H. A. C., Crippa, M., Freutel, F., **Poulain, L.**, Ghersi, V., Rodriguez, E., Beirle, S., Zotter, P., von der Weiden-Reinmüller, S.-L., Bressi, M., Fountoukis, C., Petetin, H., Szidat, S., Schneider, J., Rosso, A., El Haddad, I., Megaritis, A., Zhang, Q. J., Michoud, V., Slowik, J. G., Moukhtar, S., Kolmonen, P., Stohl, A., Eckhardt, S., Borbon, A., Gros, V., Marchand, N., Jaffrezo, J. L., Schwarzenboeck, A., Colomb, A., **Wiedensohler, A.**, Borrman, S., Lawrence, M., Baklanov, A. and Baltensperger, U. 2015. In situ, satellite measurement and model evidence on the dominant regional contribution to fine particulate matter levels in the Paris megacity. Atmos. Chem. Phys., **15**, 9577-9591. doi:10.5194/acp-15-9577-2015.

Berndt, T., Kaethner, R., **Voigtländer, J.**, **Stratmann, F.**, Pfeifle, M., Reichle, P., Sipilä, M., Kulmala, M. and Olzmann, M. 2015. Kinetics of the unimolecular reaction of CH₂OO and the bimolecular reactions with the water monomer, acetaldehyde and acetone under atmospheric conditions. Phys. Chem. Chem. Phys., **17**, 19862-19873. doi:10.1039/c5cp02224j.

Berndt, T., **Richters, S.**, Kaethner, R., **Voigtländer, J.**, **Stratmann, F.**, Sipilä, M., Kulmala, M. and **Herrmann, H.** 2015. Gas-phase ozonolysis of cycloalkenes: Formation of highly oxidized RO₂ radicals and their reactions with NO, NO₂, SO₂, and other RO₂ radicals. J. Phys. Chem. A, **119**, 10336-10348. doi:10.1021/acs.jpca.5b07295.

Binietoglou, I., Basart, S., Alados-Arboledas, L., Amiridis, V., Argyrouli, A., **Baars, H.**, Baldasano, J. M., Balis, D., Belegante, L., Bravo-Aranda, J. A., Burlizzi, P., Carrasco, V., Chaikovsky, A., Comerón, A., D'Amico, G., Filioglou, M., Granados-Muñoz, M. J., Guerrero-Rascado, J. L., Ilic, L., Kokkalis, P., Maurizi, A., Mona,

Appendices: Publications

- L., Monti, F., Muñoz-Porcar, C., Nicolae, D., Papayannis, A., Pappalardo, G., Pejanovic, G., Pereira, S. N., Perrone, M. R., Pietruczuk, A., Posyniak, M., Rocadenbosch, F., Rodríguez-Gómez, A., Sicard, M., Siomos, N., Szkop, A., Terradellas, E., Tsekeli, A., Vukovic, A., **Wandinger, U.** and **Wagner, J.** 2015. A methodology for investigating dust model performance using synergistic EARLINET/AERONET dust concentration retrievals. *Atmos. Meas. Tech. (AMT)*, **8**, 3577-3600. doi:10.5194/amt-8-3577-2015.
- Birmili, W., Sun, J., Weinhold, K., Merkel, M., Rasch, F., Spindler, G., Wiedensohler, A.,** Bastian, S., Löschnau, G., Schladitz, A., Quass, U., Kuhlbusch, T. A. J., Kaminski, H., Cyrys, J., Pitz, M., Gu, J., Kusch, T., Flentje, H., Meinhardt, F., Schwerin, A., Bath, O., Ries, L., Gerwig, H., Wirtz, K. and Weber, S. 2015. Atmospheric aerosol measurements in the German Ultrafine Aerosol Network (GUAN) - Part III: Black Carbon mass and particle number concentrations 2009-2014. *Gefahrst. Reinhalt. L.*, **75**, 479-488.
- Boonen, E., Akylas, V., Barmpas, F., Boréave, A., Bottalico, L., Cazaunau, M., Chen, H., Daële, V., De Marco, T., Doussin, J. F., Gaimoz, C., Gallus, M., George, C., Grand, N., Grosselin, B., Guerrini, G. L., **Herrmann, H.**, Ifang, S., Kleffmann, J., Kurtenbach, R., Maille, M., Manganelli, G., Mellouki, A., Miet, K., **Mothes, F.**, Moussiopoulos, N., **Poulain, L.**, **Rabe, R.**, Zapf, P. and Beeldens, A. 2015. Construction of a photocatalytic de-polluting field site in the Leopold II tunnel in Brussels. *J. Environ. Manage.*, **155**, 136-144. doi:10.1016/j.jenvman.2015.03.001.
- Bühl, J., Leinweber, R., Görsdorf, U., Radenz, M., Ansmann, A.** and Lehmann, V. 2015. Combined vertical-velocity observations with Doppler lidar, cloud radar and wind profiler. *Atmos. Meas. Tech. (AMT)*, **8**, 3527-3536. doi:10.5194/amt-8-3527-2015.
- Chen, Q., Heald, C. L., Jimenez, J. L., Canagaratna, M. R., Zhang, Q., He, L.-Y., Huang, X.-F., Campuzano-Jost, P., Palm, B. B., **Poulain, L.**, Kuwata, M., Martin, S. T., Abbatt, J. P. D., Lee, A. K. and Liggio, J. 2015. Elemental composition of organic aerosol: The gap between ambient and laboratory measurements. *Geophys. Res. Lett.*, **42**, 4182-4189. doi:10.1002/2015GL063693.
- Ciuraru, R., Fine, L., **van Pinxteren, M.**, D'Anna, B., **Herrmann, H.** and George, C. 2015. Photosensitized production of functionalized and unsaturated organic compounds at the air-sea interface. *Sci. Rep.*, **5:12741**, 10. doi:10.1038/srep12741.
- Ciuraru, R., Fine, L., **van Pinxteren, M.**, D'Anna, B., **Herrmann, H.** and George, C. 2015. Unravelling new processes at interfaces: Photochemical isoprene production at the sea surface. *Environ. Sci. Technol.*, **49**, 13199-13205. doi:10.1021/acs.est.5b02388.
- Crenn, V., Sciare, J., Croteau, P. L., Verlhac, S., Fröhlich, R., Belis, C. A., Aas, W., Äijälä, M., Alastuey, A., Artiñano, B., Baisnée, D., Bonnaire, N., Bressi, M., Canagaratna, M., Canonaco, F., Carbone, C., Cavalli, F., Coz, E., Cubison, M. J., Esser-Gietl, J. K., Green, D. C., Gros, V., Heikkinen, L., **Herrmann, H.**, Lunder, C., Minguijón, M. C., Močnik, G., O'Dowd, C. D., Ovadnevaite, J., Petit, J.-E., Petralia, E., **Poulain, L.**, Priestman, M., Riffault, V., Ripoll, A., Sarda-Esteve, R., Slowik, J. G., Setyan, A., **Wiedensohler, A.**, Baltensperger, U., Prévôt, A. S. H., Jayne, J. T. and Favez, O. 2015. ACTRIS ACSM intercomparison - Part 1: Reproducibility of concentration and fragment results from 13 individual Quadrupole Aerosol Chemical Speciation Monitors (Q-ACSM) and consistency with co-located instruments. *Atmos. Meas. Tech. (AMT)*, **8**, 5063-5087. doi:10.5194/amt-8-5063-2015.
- D'Amico, G., Amodeo, A., **Baars, H.**, Binietoglou, I., Freudenthaler, V., **Mattis, I.**, **Wandinger, U.** and Pappalardo, G. 2015. EARLINET Single Calculus Chain – overview on methodology and strategy. *Atmos. Meas. Tech. (AMT)*, **8**, 4891-4916. doi:10.5194/amt-8-4891-2015.
- Denjean, C.**, Formenti, P., Picquet-Varrault, B., Camredon, M., Pangui, E., Zapf, P., Katrib, Y., Giorio, C., Tapparo, A., Temime-Roussel, B., Monod, A., Aumont, B. and Doussin, J. F. 2015. Aging of secondary organic aerosol generated from the ozonolysis of α -pinene: Effects of ozone, light and temperature. *Atmos. Chem. Phys.*, **15**, 883-897. doi:10.5194/acp-15-883-2015.
- Denjean, C.**, Formenti, P., Picquet-Varrault, B., Pangui, E., Zapf, P., Katrib, Y., Giorio, C., Tapparo, A., Monod, A., Temime-Roussel, B., Decorse, P., Mangeney, C. and Doussin, J. F. 2015. Relating hygroscopicity and optical properties to chemical composition and structure of secondary organic aerosol particles generated from the ozonolysis of α -pinene. *Atmos. Chem. Phys.*, **15**, 3339-3358. doi:10.5194/acp-15-3359-2015.
- Drinovec, L., Močnik, G., Zotter, P., Prévôt, A. S. H., Ruckstuhl, C., Coz, E., Rupakheti, M., Sciare, J., **Müller, T.**, **Wiedensohler, A.** and Hansen, D. A. 2015. The “dual-spot” Aethalometer: An improved measurement of aerosol black carbon with real-time loading compensation. *Atmos. Meas. Tech. (AMT)*, **8**, 1965-1979. doi:10.5194/amt-8-1965-2015.

Appendices: Publications

- Emde, C., Barlakas, V., Cornet, C., Evans, F., Korkin, S., Ota, Y., Labonne, L. C., Lyapustin, A., **Macke, A.**, Mayer, B. and Wendisch, M. 2015. IPRT polarized radiative transfer model intercomparison project – Phase A. *J. Quant. Spectrosc. Radiat. Transfer*, **164**, 8-36. doi:10.1016/j.jqsrt.2015.05.007.
- Evan, A. T., Fiedler, S., Zhao, C., Menut, L., **Schepanski, K.**, Doherty, O. and Flamant, C. 2015. Derivation of an observation-based map of North African dust emission. *Aeolian Res.*, in press. doi:10.1016/j.aeolia.2015.01.001.
- Feistel, R., Lovell-Smith, J. W. and **Hellmuth, O.** 2015. Virial approximation of the TEOS-10 equation for the fugacity of water in humid air. *Int. J. Thermophys.*, **36**, 44-68. doi:10.1007/s10765-014-1784-0.
- Feistel, R., Lovell-Smith, J. W. and **Hellmuth, O.** 2015. Erratum to: Virial approximation of the TEOS-10 equation for the fugacity of water in humid air. *Int. J. Thermophys.*, **36**, 204. doi:10.1007/s10765-014-1827-6.
- Feistel, R., Wielgosz, R., Bell, S. A., Camões, M. F., Cooper, J. R., Dexter, P., Dickson, A. G., Fisicaro, P., Harvey, A. H., Heinonen, M., **Hellmuth, O.**, Kretzschmar, H.-J., Lovell-Smith, J. W., McDougall, T. J., Pawlowicz, R., Ridout, P., Seitz, S., Spitzer, P., Stoica, D. and Wolf, H. 2015. Metrological challenges for measurements of key climatological observables: Oceanic salinity and pH, and atmospheric humidity. Part 1: Overview. *Metrologia*, Online first. doi:10.1088/0026-1394/53/1/R1.
- Fiedler, S., Knippertz, P., Woodward, S., Martin, G., Bellouin, N., Ross, A. N., **Heinold, B.**, **Schepanski, K.**, Birch, C. E. and **Tegen, I.** 2015. A process-based evaluation of dust-emitting winds in the CMIP5 simulation of HadGEM2-ES. *Clim. Dyn.*, First online: 16 May 2015 (1-24). doi:10.1007/s00382-015-2635-9.
- Fomba, K. W., van Pinxteren, D., Müller, K., Iinuma, Y., Lee, T., Collett Jr., J. L. and Herrmann, H.** 2015. Trace metal characterization of aerosol particles and cloud water during HCCT 2010. *Atmos. Chem. Phys.*, **15**, 8751-8765. doi:10.5194/acp-15-8751-2015.
- Foth, A., **Baars, H.**, Di Girolamo, P. and Pospichal, B. 2015. Water vapour profiles from Raman lidar automatically calibrated by microwave radiometer data during HOPE. *Atmos. Chem. Phys.*, **15**, 7753-7763. doi:10.5194/acp-15-7753-2015.
- Friberg, J., Martinsson, B. G., Sporre, M. K., Andersson, S. M., Brenninkmeijer, C. A. M., **Herrmann, M.**, van Velthoven, P. F. J. and Zahn, A. 2015. Influence of volcanic eruptions on midlatitude upper tropospheric aerosol and consequences for cirrus clouds. *Earth and Space Science*, **2**, 285-300. doi:10.1002/2015EA000110.
- Fröhlich, R., Crenn, V., Setyan, A., Belis, C. A., Canonaco, F., Favez, O., Riffault, V., Slowik, J. G., Aas, W., Ajälä, M., Alastuey, A., Artiñano, B., Bonnaire, N., Bozzetti, C., Bressi, M., Carbone, C., Coz, E., Croteau, P. L., Cubison, M. J., Esser-Gietl, J. K., Green, D. C., Gros, V., Heikkilä, L., **Herrmann, H.**, Jayne, J. T., Lunder, C. R., Minguillón, M. C., Močnik, G., O'Dowd, C. D., Ovadnevaite, J., Petralia, E., **Poulain, L.**, Priestman, M., Ripoll, A., Sarda-Estève, R., **Wiedensohler, A.**, Baltensperger, U., Sciare, J. and Prévôt, S. H. 2015. ACTRIS ACSM intercomparison – Part 2: Intercomparison of ME-2 organic source apportionment results from 15 individual, co-located aerosol mass spectrometers. *Atmos. Meas. Tech. (AMT)*, **8**, 2555–2576. doi:10.5194/amt-8-2555-2015.
- Gallus, M., Akylas, V., Barmpas, F., Beeldens, A., Boonen, E., Boréave, A., Cazaunau, M., Chen, H., Daële, V., Doussin, J. F., Dupart, Y., Gaimoz, C., George, C., Grosselin, B., **Herrmann, H.**, Ifang, S., Kurtenbach, R., Maille, M., Mellouki, A., Miet, K., **Mothes, F.**, Moussiopoulos, N., **Poulain, L.**, **Rabe, R.**, Zapf, P. and Kleffmann, J. 2015. Photocatalytic de-pollution in the Leopold II tunnel in Brussels: NO_x abatement results. *Build. Environ.*, **84**, 125-133. doi:10.1016/j.buildenv.2014.10.032.
- Gallus, M., Ciuraru, R., **Mothes, F.**, Akylas, V., Barmpas, F., Beeldens, A., Bernard, F., Boonen, E., Boréave, A., Cazaunau, M., Charbonnel, N., Chen, H., Daële, V., Dupart, Y., Gaimoz, C., Grosselin, B., **Herrmann, H.**, Ifang, S., Kurtenbach, R., Maille, M., Marjanovic, I., Michoud, V., Mellouki, A., Miet, K., Moussiopoulos, N., **Poulain, L.**, Zapf, P., George, C., Doussin, J. F. and Kleffmann, J. 2015. Photocatalytic abatement results from a model street canyon. *Environ. Sci. Pollut. Res.*, 1-12. doi:10.1007/s11356-015-4926-4.
- Giannakaki, E., Pfüller, A., Korhonen, K., Mielonen, T., Laakso, L., Vakkari, V., **Baars, H.**, **Engelmann, R.**, Beukes, J. P., Van Zyl, P. G., Josipovic, M., Tiitta, P., Chiloane, K., Piketh, S., Lihavainen, H., Lehtinen, K. E. J. and Komppula, M. 2015. One year of Raman lidar observations of free-tropospheric aerosol layers over South Africa. *Atmos. Chem. Phys.*, **15**, 5429-5442. doi:10.5194/acp-15-5429-2015.
- Giordano, L., Brunner, D., Flemming, J., Im, U., Hogrefe, C., Bianconi, R., Badia, A., Balzarini, A., Baro, R., Chemel, C., Curci, G., Forkel, R., Jimenez-Guerrero, P., Hirtl, M., Hodzic, A., Honzak, L., Jorba, O., Knotek, C., Kuenen, J. J. P., Makar, P. A., Manders-Groot, A., Neal, L., Perez, J. L., Pirovano, G., Pouliot, G., San Jose, R., Savage, N., **Schröder, W.**, Sokhi, R. S., Syrakov, S., Torian, A., Tuccella, P., Werhahn, J., **Wolke, R.**, Yahya, K., Žabkar, R., Zhang, Y. and Galmarini, S. 2015. Assessment of the MACC reanalysis and its influence as chemical boundary conditions for regional air quality modeling in AQMEII-2. *Atmos. Environ.*, Online first. doi:10.1016/j.atmosenv.2015.02.034.

Appendices: Publications

- Groß, S., Freudenthaler, V., **Schepanski, K.**, Toledano, C., Schäfler, A., **Ansmann, A.** and Weinzierl, B. 2015. Optical properties of long-range transported Saharan dust over Barbados as measured by dual-wavelength depolarization Raman lidar measurements. *Atmos. Chem. Phys.*, **15**, 11067-11080. doi:10.5194/acp-15-11067-2015.
- Hande, L. B., **Engler, C.**, Hoose, C. and **Tegen, I.** 2015. Seasonal variability of Saharan desert dust and ice nucleating particles over Europe. *Atmos. Chem. Phys.*, **15**, 4389-4397. doi:10.5194/acp-15-4389-2015.
- Hartmann, S., Wex, H., Clauss, T., Augustin-Bauditz, S., Niedermeier, D., Rösch, M. and Stratmann, F.** 2015. Immersion freezing of kaolinite: Scaling with particle surface area. *J. Atmos. Sci.*, Online first. doi:10.1175/JAS-D-15-0057.1.
- Heinold, B.**, Knippertz, P. and Beare, R. J. 2015. Idealised large-eddy simulations of nocturnal low-level jets over subtropical desert regions and implications for dust-generating winds. *Q. J. Roy. Meteor. Soc.*, **141**, 1740-1752. doi:10.1002/qj.2475.
- Heintzenberg, J.**, Cereceda-Balic, F., Vidal, V. and Leck, C. 2015. Scavenging of black carbon in Chilean coastal fogs. *Sci. Total Environ.*, Online first. doi:10.1016/j.scitotenv.2015.09.057.
- Heintzenberg, J.**, Leck, C. and Tunved, P. 2015. Potential source regions and processes of aerosol in the summer Arctic. *Atmos. Chem. Phys.*, **15**, 6487-6502. doi:10.5194/acp-15-6487-2015.
- Hellmuth, O.** and Shchekin, A. K. 2015. Determination of interfacial parameters of a soluble particle in a nonideal solution from measured deliquescence and efflorescence humidities. *Atmos. Chem. Phys.*, **15**, 3851-3871. doi:10.5194/acp-15-3851-2015.
- Herrmann, H., Schaefer, T., Tilgner, A., Styler, S. A., Weller, C., Teich, M. and Otto, M.** 2015. Tropospheric aqueous-phase chemistry: Kinetics, mechanisms, and its coupling to a changing gas phase. *Chem. Rev.*, **115**, 4259-4334. doi:10.1021/cr500447k.
- Hiranuma, N., **Augustin-Bauditz, S.**, Bingemer, H., Budke, C., Curtius, J., Danielczok, A., Diehl, K., Dreischmeier, K., Ebert, M., Frank, F., Hoffmann, N., Kandler, K., Kiselev, A., Koop, T., Leisner, T., Möhler, O., Nillius, B., Peckhaus, A., Rose, D., Weinbruch, S., **Wex, H.**, Boose, Y., DeMott, P. J., Hader, J. D., Hill, T. C. J., Kanji, Z. A., Kulkarni, G., Levin, E. J. T., McCluskey, C. S., Murakami, M., Murray, B. J., **Niedermeier, D.**, Petters, M. D., O'Sullivan, D., Saito, A., Schill, G. P., Tajiri, T., Tolbert, M. A., Welti, A., Whale, T. F., Wright, T. P. and Yamashita, K. 2015. A comprehensive laboratory study on the immersion freezing behavior of illite NX particles: A comparison of seventeen ice nucleation measurement techniques. *Atmos. Chem. Phys.*, **15**, 2489-2518. doi:10.5194/acp-15-2489-2015.
- Iinuma, Y.**, Keywood, M. and **Herrmann, H.** 2015. Characterisation of primary and secondary organic aerosols in Melbourne airshed: The influence of biogenic emissions, wood smoke and bushfires. *Atmos. Environ.*, Online first. doi:10.1016/j.atmosenv.2015.12.014.
- Illingworth, A. J., Barker, H. W., Beljaars, A., Ceccaldi, M., Chepfer, H., Clerbaux, N., Cole, J., Delanoë, J., Domenech, C., Donovan, D. P., Fukuda, S., Hirakata, M., Hogan, R. J., **Huenerbein, A.**, Kollias, P., Kubota, T., Nakajima, T., Nakajima, T. Y., Nishizawa, T., Ohno, Y., Okamoto, H., Oki, R., Sato, K., Satoh, M., Shephard, M., Velázquez-Blázquez, A., **Wandinger, U.**, Wehr, T. and van Zadelhoff, G.-J. 2015. The EarthCARE Satellite: The next step forward in global measurements of clouds, aerosols, precipitation and radiation. *Bull. Amer. Meteor. Soc.*, **96**, 1311-1332. doi:10.1175/BAMS-D-12-00227.1.
- Jähn, M., Knoth, O., König, M. and Vogelsberg, U.** 2015. ASAM v2.7: A compressible atmospheric model with a Cartesian cut cell approach. *Geosci. Model Dev.*, **8**, 317-340. doi:10.5194/gmd-8-317-2015.
- Jäkel, E., Mey, B., Levy, R., Gu, X., Yu, T., Li, Z., **Althausen, D., Heese, B.** and Wendisch, M. 2015. Adaption of the MODIS aerosol retrieval algorithm using airborne spectral surface reflectance measurements over urban areas: A case study. *Atmos. Meas. Tech. (AMT)*, **8**, 5237-5249. doi:10.5194/amt-8-5237-2015.
- Jokinen, T., Berndt, T.**, Makkonen, R., Kerminen, V.-M., Junninen, H., Paasonen, P., **Stratmann, F., Herrmann, H.**, Guenther, A., Worsnop, D. R., Kulmala, M., Ehn, M. and Sipilä, M. 2015. Production of extremely low volatile organic compounds from biogenic emissions: Measured yields and atmospheric implications. *Proc. Nat. Acad. Sci. (PNAS)*, PNAS Early Edition (1-6). doi:10.1073/pnas.1423977112.
- Kecorius, S., Zhang, S., Wang, Z., Größ, J., Ma, N., Wu, Z., Ran, L., Hu, M., Wang, P., Ulevičius, V. and Wiedensohler, A.** 2015. Nocturnal aerosol particle formation in the North China plain. *Lith. J. Phys.*, **55**, 44-53.
- Keywood, M., Cope, M., Meyer, C. P. M., **Iinuma, Y.** and Emmerson, K. 2015. When smoke comes to town: The impact of biomass burning smoke on air quality. *Atmos. Environ.*, Online first. doi:10.1016/j.atmosenv.2015.03.050.

Appendices: Publications

- Kim, P. S., Jacob, D. J., Fisher, J. A., Travis, K., Yu, K., Zhu, L., Yantosca, R. M., Sulprizio, M. P., Jimenez, J. L., Campuzano-Jost, P., Froyd, K. D., Liao, J., Hair, J. W., Fenn, M. A., Butler, C. F., Wagner, N. L., Gordon, T. D., **Welti, A.**, Wennberg, P. O., Crounse, J. D., St. Clair, J. M., Teng, A. P., Millet, D. B., Schwarz, J. P., Markovic, M. Z. and Perring, A. E. 2015. Sources, seasonality, and trends of southeast US aerosol: An integrated analysis of surface, aircraft, and satellite observations with the GEOS-Chem chemical transport model. *Atmos. Chem. Phys.*, **15**, 10411-10433. doi:10.5194/acp-15-10411-2015.
- Knippertz, P., **Tegen, I.**, **Schepanski, K.**, Laurent, B., Osika, D., Orji, B., Abdou, K. and Hamza, I. 2015. *Dust*. D. J. Parker and M. Diop (Ed.), In: *The forecasters' handbook for West Africa*. Wiley-Blackwell, Hoboken, p. in press.
- Kristensen, T. B.**, Du, L., Nguyen, Q. T., Nojgaard, J. K., Bender Koch, C., Faurskov Nielsen, O., Hallar, A. G., Lowenthal, D. H., **Nekat, B.**, **van Pinxteren, D.**, **Herrmann, H.**, Glasius, M., Kjaergaard, H. G. and Bilde, M. 2015. Chemical properties of HULIS from three different environments. *J. Atmos. Chem.*, **72**, 65-80. doi:10.1007/s10874-015-9302-8.
- Kupiszewski, P., Weingartner, E., Vochezer, P., Schnaiter, M., Bigi, A., Gysel, M., Rosati, B., Toprak, E., **Mertes, S.** and Baltensperger, U. 2015. The Ice Selective Inlet: a novel technique for exclusive extraction of pristine ice crystals in mixed-phase clouds. *Atmos. Meas. Tech. (AMT)*, **8**, 3087-3106. doi:10.5194/amt-8-3087-2015.
- Lovell-Smith, J. W., Feistel, R., Harvey, A. H., **Hellmuth, O.**, Bell, S. A., Heinonen, M. and Cooper, J. R. 2015. Metrological challenges for measurements of key climatological observables: Oceanic salinity and pH, and atmospheric humidity. Part 4: Atmospheric relative humidity. *Metrologia*, Online first. doi:10.1088/0026-1394/53/1/R40.
- Ma, N.** and **Birmili, W.** 2015. Estimating the contribution of photochemical particle formation to ultrafine particle number averages in an urban atmosphere. *Sci. Total Environ.*, **512-513**, 154-166. doi:10.1016/j.scitotenv.2015.01.009.
- Mamouri, R. E. and **Ansmann, A.** 2015. Dust-related ice nuclei profiles from polarization lidar: Methodology and case studies. *Atmos. Chem. Phys.*, **15**, 3463-3477. doi:10.5194/acp-15-3463-2015.
- Mutzel, A.**, **Poulain, L.**, **Berndt, T.**, **Iinuma, Y.**, **Rodigast, M.**, **Böge, O.**, **Richters, S.**, **Spindler, G.**, Sipilä, M., Jokinen, T., Kulmala, M. and **Herrmann, H.** 2015. Highly oxidized multifunctional organic compounds observed in tropospheric particles: A field and laboratory study. *Environ. Sci. Technol.*, **49**, 7754-7761. doi:10.1021/acs.est.5b00885.
- Mutzel, A.**, **Rodigast, M.**, **Iinuma, Y.**, **Böge, O.** and **Herrmann, H.** 2015. Monoterpene SOA – Contribution of first-generation oxidation products to formation and chemical composition. *Atmos. Environ.*, Online available (1-9). doi:10.1016/j.atmosenv.2015.10.080.
- Niedermeier, D.**, **Augustin-Bauditz, S.**, **Hartmann, S.**, **Wex, H.**, **Ignatius, K.** and **Stratmann, F.** 2015. Can we define an asymptotic value for the ice active surface site density for heterogeneous ice nucleation? *J. Geophys. Res. - Atmos.*, **120**, 5036-5045. doi:10.1002/2014JD022814.
- Nozière, B., Kalberer, M., Claeys, M., Allan, J., D'Anna, B., Decesari, S., Finessi, E., Glasius, M., Grgić, I., Hamilton, J. F., Hoffmann, T., **Iinuma, Y.**, Jaoui, M., Kahnt, A., Kampf, C. J., Kourtchev, J. D., Maenhaut, W., Marsden, N., Saarikoski, S., Schnelle-Kreis, J., Surratt, J. D., Szidat, S., Szmigielski, R. and Wisthaler, A. 2015. The molecular identification of organic compounds in the atmosphere: State of the art and challenges. *Chem. Rev.*, **115**, 3919-3983. doi:10.1021/cr5003485.
- Paramonov, M., Kerminen, V.-M., Gysel, M., Aalto, P. P., Andreae, M. O., Asmi, E., Baltensperger, U., Bougiatioti, A., Brus, D., Frank, G. P., Good, N., Gunthe, S. S., Hao, L., Irwin, M., Jaatinen, A., Jurányi, Z., King, S. M., Kortelainen, A., Kristensson, A., Lihavainen, H., Kulmala, M., Lohmann, U., Martin, S. T., McFiggans, G., Mihalopoulos, N., Nenes, A., O'Dowd, C. D., Ovadnevaite, J., Petäjä, T., Pöschl, U., Roberts, G. C., Rose, D., Svenningsson, B., Swietlicki, E., Weingartner, E., Whitehead, J., **Wiedensohler, A.**, Wittbom, C. and Sierau, B. 2015. A synthesis of cloud condensation nuclei counter (CCNC) measurements within the EUCAARI network. *Atmos. Chem. Phys.*, **15**, 12211-12229. doi:10.5194/acp-15-12211-2015.
- Petetin, H., Beekmann, M., Colomb, A., Denier van der Gon, H. A. C., Dupont, J.-C., Honoré, C., Michoud, V., Morille, Y., Perrussel, O., Schwarzenböck, A., Sciare, J., **Wiedensohler, A.** and Zhang, Q. J. 2015. Evaluating BC and NO_x emission inventories for the Paris region from MEGAPOLI aircraft measurements. *Atmos. Chem. Phys.*, **15**, 9799-9818. doi:10.5194/acp-15-9799-2015.
- Pikridas, M., Sciare, J., Freutel, F., Crumeyrolle, S., von der Weiden-Reinmüller, S.-L., Borbon, A., Schwarzenboeck, A., **Merkel, M.**, Crippa, M., Kostenidou, E., Psichoudaki, M., Hildebrandt, L., Engelhart, G. J., Petäjä, T.,

Appendices: Publications

- Prévôt, A. S. H., Drewnick , F., Baltensperger, U., **Wiedensohler, A.**, Kulmala, M., Beekmann, M. and Pandis, S. N. 2015. In situ formation and spatial variability of particle number concentration in a European megacity. *Atmos. Chem. Phys.*, **15**, 10219-10237. doi:10.5194/acp-15-10219-2015.
- Platis, A., Altstädter, B., **Wehner, B.**, Wildmann, N., Lampert, A., **Hermann, M.**, **Birmili, W.** and Bange, J. 2015. An observational case study on the influence of atmospheric boundary-layer dynamics on new particle formation. *Bound.-Lay. Meteorol.*, Online first: 19 September 2015. doi:10.1007/s10546-015-0084-y.
- Pummer, B. G., Budke, C., **Augustin-Bauditz, S.**, **Niedermeier, D.**, Felgitsch, L., Kampf, C. J., Huber, R. G., Liedl, K. R., Loerting, T., Moschen, T., Schauperl, M., Tollinger, M., Morris, C. E., **Wex, H.**, Grothe, H., Pöschl, U., Koop, T. and Fröhlich-Nowoisky, J. 2015. Ice nucleation by water-soluble macromolecules. *Atmos. Chem. Phys.*, **15**, 4077-4091. doi:10.5194/acp-15-4077-2015.
- Richters, S.**, **Herrmann, H.** and **Berndt, T.** 2015. Gas-phase rate coefficients of the reaction of ozone with four sesquiterpenes at 295 ± 2 K. *Phys. Chem. Chem. Phys.*, **17**, 11658-11669. doi:10.1039/c4cp05542.
- Risius, S., Xu, H., Di Lorenzo, F., Xi, H., **Siebert, H.**, Shaw, R. A. and Bodenschatz, E. 2015. Schneefernerhaus as a mountain research station for clouds and turbulence. *Atmos. Meas. Tech. (AMT)*, **8**, 3209-3218. doi:10.5194/amt-8-3209-2015.
- Rodigast, M.**, **Mutzel, A.**, **Iinuma, Y.**, **Haferkorn, S.** and **Herrmann, H.** 2015. Characterisation and optimisation of a sample preparation method for the detection and quantification of atmospherically relevant carbonyl compounds in aqueous medium. *Atmos. Meas. Tech. (AMT)*, **8**, 2409-2416. doi:10.5194/amt-8-2409-2015.
- Rose, C., Sellegrí, K., Velarde, F., Moreno, I., Ramonet, M., **Weinhold, K.**, Krejci, R., Ginot, P., Andrade, M., **Wiedensohler, A.** and Laj, P. 2015. Frequent nucleation events at the high altitude station of Chacaltaya (5240 m a.s.l.), Bolivia. *Atmos. Environ.*, **102**, 18-29. doi:10.1016/j.atmosenv.2014.11.015.
- Ryder, C. L., McQuaid, J. B., Flamant, C., Washington, R., Brindley, H. E., Highwood, E. J., Marsham, J. H., Parker, D. J., Todd, M. C., Banks, J. R., Brooke, J. K., Engelstaedter, S., Estelles, V., Formenti, P., Garcia-Carreras, L., Kocha, C., Marenco, F., Rosenberg, P., Sodemann, H., Allen, C. J. T., Bourdon, A., Bart, M., Cavazos-Guerra, C., Chevaillier, S., Crosier, J., Darbyshire, E., Dean, A. R., Dorsey, J. R., Kent, J., O'Sullivan, D., **Schepanski, K.**, Szpek, K., Trembath, J. and Woolley, A. 2015. Advances in understanding mineral dust and boundary layer processes over the Sahara from Fennec aircraft observations. *Atmos. Chem. Phys.*, **15**, 8479-8520. doi:10.5194/acp-15-8479-2015.
- Šantl-Temkiv, T., Sahyoun, M., Finster, K., **Hartmann, S.**, **Augustin-Bauditz, S.**, **Stratmann, F.**, **Wex, H.**, **Clauss, T.**, Nielsen, N. W., Sørensen, J. H., Korsholm, U. S., Wick, L. Y. and Karlson, U. G. 2015. Characterization of airborne ice-nucleation-active bacteria and bacterial fragments. *Atmos. Environ.*, **109**, 105-117. doi:10.1016/j.atmosenv.2015.02.060.
- Schaefer, T.**, **van Pinxteren, D.** and **Herrmann, H.** 2015. Multiphase chemistry of glyoxal: Revised kinetics of the alkyl radical reaction with molecular oxygen and the reaction of glyoxal with OH, NO_3^- , and SO_4^{2-} in aqueous solution. *Environ. Sci. Technol.*, **49**, 343-350. doi:10.1021/es505860s.
- Schepanski, K.**, Klüser, L., **Heinold, B.** and **Tegen, I.** 2015. Spatial and temporal correlation length as a measure for the stationarity of atmospheric dust aerosol distribution. *Atmos. Environ.*, **122**, 10-21. doi:10.1016/j.atmosenv.2015.09.034.
- Schepanski, K.**, Knippertz, P., Fiedler, S., Timouk, F. and Demarty, J. 2015. The sensitivity of nocturnal low-level jets and near-surface winds over the Sahel to model resolution, initial conditions and boundary-layer setup. *Q. J. Roy. Meteor. Soc.*, **141**, 1442-1456. doi:10.1002/qj.2453.
- Schladitz, A.**, Leníček, J., Beneš, I., Kováč, M., Skorkovský, J., Soukup, A., Jandlová, J., **Poulain, L.**, Plachá, H., Löschnau, G. and **Wiedensohler, A.** 2015. Air quality in the German-Czech border region: A focus on harmful fractions of PM and ultrafine particles. *Atmos. Environ.*, **122**, 236-249. doi:10.1016/j.atmosenv.2015.09.044.
- Schmeissner, T.**, Shaw, R. A., **Ditas, J.**, **Stratmann, F.**, Wendisch, M. and **Siebert, H.** 2015. Turbulent mixing in shallow trade wind cumuli: Dependence on cloud life cycle. *J. Atmos. Sci.*, **72**, 1447-1465. doi:10.1175/JAS-D-14-0230.1.
- Schmidt, J.**, **Ansmann, A.**, **Bühl, J.** and **Wandinger, U.** 2015. Strong aerosol–cloud interaction in altocumulus during updraft periods: Lidar observations over central Europe. *Atmos. Chem. Phys.*, **15**, 10687-10700. doi:10.5194/acp-15-10687-2015.
- Senf, F.**, **Dietzsch, F.**, **Hünerbein, A.** and **Deneke, H.** 2015. Characterization of initiation and growth of selected severe convective storms over Central Europe with MSG-SEVIRI. *J. Appl. Meteorol. Clim.*, **54**, 207-224.

Appendices: Publications

- Sicard, M., D'Amico, G., Comerón, A., Mona, L., Alados-Arboledas, L., Amodeo, A., **Baars, H.**, Baldasano, J. M., Belegante, L., Binietoglou, I., Bravo-Aranda, J. A., Fernández, A. J., Fréville, P., Garcia-Vizcaino, D., Giunta, A., Granados-Muñoz, M. J., Guerrero-Rascado, J. L., Hadjimitsis, D., Haefele, A., Hervo, M., Iarlori, M., Kokkalis, P., Lange, D., Mamouri, R. E., Mattis, I., Molero, F., Montoux, N., Muñoz, A., Muñoz Porcar, C., Navas-Guzmán, F., Nicolae, D., Nisantzi, A., Papagiannopoulos, N., Papayannis, A., Pereira, S., Preißler, J., Pujadas, M., Rizi, V., Rocadenbosch, F., Sellegri, K., Simeonov, V., Tsaknakis, G., Wagner, F. and Pappalardo, G. 2015. EARLINET: Potential operationality of a research network. *Atmos. Meas. Tech. (AMT)*, **8**, 4587-4613. doi:10.5194/amt-8-4587-2015.
- Siebert, H.**, Shaw, R. A., Ditas, J., **Schmeissner, T.**, Malinowski, S. P., Bodenschatz, E. and Xu, H. 2015. High-resolution measurement of cloud microphysics and turbulence at a mountaintop station. *Atmos. Meas. Tech. (AMT)*, **8**, 3219-3228. doi:10.5194/amt-8-3219-2015.
- Simmel, M., Bühl, J., Ansmann, A. and Tegen, I.** 2015. Ice phase in altocumulus clouds over Leipzig: Remote sensing observations and detailed modelling. *Atmos. Chem. Phys.*, **15**, 10453-10470. doi:10.5194/acp-15-10453-2015.
- Slobodda, J., **Hünerbein, A.**, Lindsrot, R., Preusker, R., Ebelt, K. and Fischer, J. 2015. Multichannel analysis of correlation length of SEVIRI images around ground-based cloud observatories to determine their representativeness. *Atmos. Meas. Tech. (AMT)*, **8**, 567-578. doi:10.5194/amt-8-567-2015.
- Sundström, A.-M., Nikandrova, A., Atlaskina, K., Nieminen, T., Vakkari, V., Laakso, L., Beukes, J. P., Arola, A., van Zyl, P. G., Josipovic, M., Venter, A. D., Jaars, K., Pienaar, J. J., Piketh, S., **Wiedensohler, A.**, Chiloane, E. K., de Leeuw, G. and Kulmala, M. 2015. Characterization of satellite-based proxies for estimating nucleation mode particles over South Africa. *Atmos. Chem. Phys.*, **15**, 4983-4996. doi:10.5194/acp-15-4983-2015.
- Tigges, L., **Wiedensohler, A.**, **Weinhold, K.**, Gandhi, J. and Schmid, H.-J. 2015. Bipolar charge distribution of a soft X-ray diffusion charger. *J. Aerosol Sci.*, **90**, 77-86. doi:10.1016/j.jaerosci.2015.07.002.
- Toenges-Schuller, N., Schneider, C., Niederau, A., Vogt, R. and **Birmili, W.** 2015. Modelling particle number concentrations in a typical street canyon in Germany and analysis of future trends. *Atmos. Environ.*, **111**, 127-135. doi: 10.1016/j.atmosenv.2015.04.006.
- van Pinxteren, M.**, Fiedler, B., **van Pinxteren, D.**, Iinuma, Y., Kötzinger, A. and **Herrmann, H.** 2015. Chemical characterization of sub-micrometer aerosol particles in the tropical Atlantic Ocean: Marine and biomass burning influences. *J. Atmos. Chem.*, Online first May 2015. doi:10.1007/s10874-015-9307-3.
- von Bismarck-Osten, C., **Birmili, W.**, Ketzel, M. and Weber, S. 2015. Statistical modelling of aerosol particle number size distributions in urban and rural environments – A multi-site study. *Urban Climate*, **11**, 51-66. doi:10.1016/j.uclim.2014.11.004.
- Wang, Z., Su, H., Wang, X., **Ma, N.**, **Wiedensohler, A.**, Pöschl, U. and Cheng, Y. 2015. Scanning supersaturation condensation particle counter applied as a nano-CCN counter for size-resolved analysis of the hygroscopicity and chemical composition of nanoparticles. *Atmos. Meas. Tech. (AMT)*, **8**, 2161-2172. doi:10.5194/amt-8-2161-2015.
- Wang, Z. B.**, Hu, M., Pei, X. Y., Zhang, R. Y., Paasonen, P., Zheng, J., Yue, D. L., Wu, Z. J., Boy, M. and **Wiedensohler, A.** 2015. Connection of organics to atmospheric new particle formation and growth at an urban site of Beijing. *Atmos. Environ.*, **103**, 7-17. doi:10.1016/j.atmosenv.2014.11.069.
- Wapler, K., Harnisch, F., Pardowitz, T. and **Senf, F.** 2015. Characterisation and predictability of a strong and a weak forcing severe convective event - a multi-data approach. *Meteorol. Z.*, **24**, 393-410. doi:10.1127/metz/2015/0625.
- Wehner, B.**, Werner, F., **Ditas, F.**, Shaw, R. A., Kulmala, M. and **Siebert, H.** 2015. Observations of new particle formation in enhanced UV irradiance zones near cumulus clouds. *Atmos. Chem. Phys.*, **15**, 11701-11711. doi:10.5194/acp-15-11701-2015.
- Weller, C.** and **Herrmann, H.** 2015. Kinetics of nitrosamine and amine reactions with NO₃ radical and ozone related to aqueous particle and cloud droplet chemistry. *Atmos. Res.*, **151**, 64-71. doi:10.1016/j.atmosres.2014.02.023.
- Wex, H., Augustin-Bauditz, S.**, Boose, Y., Budke, C., Curtius, J., Diehl, K., Dreyer, A., Frank, F., **Hartmann, S.**, Hiranuma, N., Jantsch, E., Kanji, Z. A., Kiselev, A., Koop, T., Möhler, O., **Niedermeier, D.**, Nillius, B., **Rösch, M.**, Rose, D., Schmidt, C., Steinke, I. and **Stratmann, F.** 2015. Intercomparing different devices for the investigation of ice nucleating particles using Snomax as test substance. *Atmos. Chem. Phys.*, **14**, 1463-1485. doi:10.5194/acp-15-1463-2015.
- Whalley, L. K., Stone, D., George, I. J., **Mertes, S.**, **van Pinxteren, D.**, **Tilgner, A.**, **Herrmann, H.**, Evans, M. J. and Heard, D. E. 2015. The influence of clouds on radical concentrations: Observations and modelling

Appendices: Publications

- studies of HO_x during the Hill Cap Cloud Thuringia (HCCT) campaign in 2010. *Atmos. Chem. Phys.*, **15**, 3289-3301. doi:10.5194/acp-15-3289-2015.
- Wolf, R., El Haddad, I., Crippa, M., Decesari, S., Slowik, J. G., **Poulain, L.**, Gilardoni, S., Rinaldi, M., Carbone, S., Canonaco, F., Huang, R.-J., Baltensperger, U. and Prévot, A. S. H. 2015. Marine and urban influences on summertime PM_{2.5} aerosol in the Po basin using mobile measurements. *Atmos. Environ.*, **120**, 447-454. doi:10.1016/j.atmosenv.2015.09.007.
- Worringen, A., Kandler, K., Benker, N., Dirsich, T., **Mertes, S.**, **Schenk, L.**, Kästner, U., Frank, F., Nillius, B., Bundke, U., Rose, D., Curtius, J., Kupiszewski, P., Weingartner, E., Vochezer, P., Schneider, J., Schmidt, S., Weinbruch, S. and Ebert, M. 2015. Single-particle characterization of ice-nucleating particles and ice particle residuals sampled by three different techniques. *Atmos. Chem. Phys.*, **15**, 4161-4178. doi:10.5194/acp-15-4161-2015.
- Wu, Z. J., Poulain, L., Birmili, W., Größ, J., Niedermeier, N., Wang, Z. B., Herrmann, H. and Wiedensohler, A.** 2015. Some insights into the condensing vapors driving new particle growth to CCN sizes on the basis of hygroscopicity measurements. *Atmos. Chem. Phys.*, **15**, 13071-13083. doi:10.5194/acp-15-13071-2015.
- Yttri, K. E., Schnelle-Kreis, J., Maenhaut, W., Abbaszade, G., Alves, C., Bjerke, A., Bonnier, N., Bossi, R., Claeys, M., Dye, C., Evtyugina, M., Garcia-Gacio, D., Hillamo, R., Hoffer, A., Hyder, M., **Iinuma, Y.**, Jaffrezo, J. L., Kasper-Giebl, A., Kiss, G., Lopez-Mahia, P. L., Pio, C., Piot, C., Ramirez-Santa-Cruz, C., Sciare, J., Teinila, K., Vermeylen, R., Vicente, A. and Zimmermann, R. 2015. An intercomparison study of analytical methods used for quantification of levoglucosan in ambient aerosol filter samples. *Atmos. Meas. Tech. (AMT)*, **8**, 125-147. doi:10.5194/amt-8-125-2015.
- Zermeño-Díaz, D., Zhang, C., Kollias, P. and **Kalesse, H.** 2015. The role of shallow cloud moistening in MJO and Non-MJO convective events over the ARM Manus site. *J. Atmos. Sci.*, **72**, 4797-4820. doi:10.1175/JAS-D-14-0322.1.
- Zhang, N., Geronimo, I., Paneth, P., **Schindelka, J.**, **Schaefer, T.**, **Herrmann, H.**, Vogt, C. and Richnow, H. H. 2015. Analyzing sites of OH radical attack (ring vs. side chain) in oxidation of substituted benzenes via dual stable isotope analysis ($\delta^{13}\text{C}$ and $\delta^2\text{H}$). *Sci. Total Environ.*, Online first. doi:10.1016/j.scitotenv.2015.10.075.
- Zhang, N., **Schindelka, J.**, **Herrmann, H.**, George, C., Rosell, M., Herrero-Martín, S., Klán, P. and Richnow, H. H. 2015. Investigation of humic substance photosensitized reactions via carbon and hydrogen isotope fractionation. *Environ. Sci. Technol.*, **49**, 233-242. doi:10.1021/es502791f.
- Zhang, S. L., Ma, N., Kecorius, S., Wang, P. C., Hu, M., Wang, Z. B., Größ, J., Wu, Z. J. and Wiedensohler, A.** 2015. Mixing state of atmospheric particles over the North China Plain. *Atmos. Environ.*, Online first. doi:10.1016/j.atmosenv.2015.10.053.
- Zhang, Y., Mahowald, N., Scanza, R. A., Journet, E., Desboeufs, K., Albani, S., Kok, J. F., Zhuang, G., Chen, Y., Cohen, D. D., Paytan, A., Patey, M. D., Achterberg, E. P., Engelbrecht, J. P. and **Fomba, K. W.** 2015. Modeling the global emission, transport and deposition of trace elements associated with mineral dust. *Biogeosciences*, **12**, 5771-5792. doi:10.5194/bg-12-5771-2015.
- Zhang, Y., Wang, X., Wen, S., **Herrmann, H.**, Weiqiang, Y., Huang, X., Zhang, Z., Huang, Z., He, Q. and George, C. 2015. On-road vehicle emissions of glyoxal and methylglyoxal from tunnel tests in urban Guangzhou, China. *Atmos. Environ.*, Online first. doi:10.1016/j.atmosenv.2015.12.017.

Appendices: University courses

University courses

Lecturer	Course	WS 2013/ 2014	SS 2014	WS 2014/ 2015	SS 2015	WS 2015/ 2016
Ansmann, A. Althausen, D. Seifert, P. Engelmann, R.	Active Remote Measurement in Atmospheric Research (2 sh) Seminar Active Remote Sensing (2 sh)	x x		x x		x x
Deneke, H. Pospichal, B. (LIM*)	Advanced Training Module of the Leipzig Graduate School on Clouds, Aerosols and Radiation (LGS-CAR) “Indirekt Aerosol Effect”, TROPOS, July 01-02, 2014		x			
Hermann, M. Siebert, H. Wendisch, M.	Airborne Physical Measurements + Exercise (2 sh)	x		x		
Herrmann, H.	Atmospheric Chemistry I + Exercises (3 sh) Atmospheric Chemistry II + Exercises (3 sh) Atmospheric Chemistry Seminar (1 sh) Atmospheric Chemistry Lab course (1 sh)	x x x	x x x	x x	x	x x
	Guest lecture: Tropospheric Multiphase Chemistry, Shandong University (SDU), Jinan, October 22-24, 2013	x				
	The “Second Sino-European School on Atmospheric Chemistry” (SESAC), Shanghai, China, October 19-31, 2015					
	Advanced Training Module of the Leipzig Graduate School on Clouds, Aerosols and Radiation (LGS-CAR) “Heterogenous Chemistry”, TROPOS, November 25-26, 2014			x		
Macke, A.	Atmospheric Radiation (1 sh)		x		x	
Macke, A. Wendisch, M. (LIM)	Advanced Training Module of the Leipzig Graduate School on Clouds, Aerosols and Radiation (LGS-CAR) “Polarization”, TROPOS, February 11-12, 2014	x				
Macke, A. Quaas, J. (LIM)	Advanced Training Module of the Leipzig Graduate School on Clouds, Aerosols and Radiation (LGS-CAR) “Clouds in a Changing Climate System”, TROPOS, September 28-29, 2015				x	
Macke, A. Deneke, H.	Satellite Remote Sensing + Exercises (2 sh)		x		x	

Appendices: University courses

Lecturer	Course	WS 2013/ 2014	SS 2014	WS 2014/ 2015	SS 2015	WS 2015/ 2016
Macke, A. Stratmann, F.	Cloud Physics + Exercises (3 sh)		x		x	
Mutzel, A.	Advanced Study Analytics and Spektroscopy, Athmospheric Chemistry (2 x 2 sh)					x
Stratmann, F.	Advanced Training Module of the Leipzig Graduate School on Clouds, Aerosols and Radiation (LGS-CAR) "Heterogeneous Ice Nucleation", TROPOS, April 22-23, 2015				x	x
Tegen, I.	Modeling of Atmospheric Trace Substances (2 sh) Seminar Modeling of Atmospheric Trace Substances (1 sh)	x		x	x	x
	Modelling of the Atmosphere (2 sh)	x		x	x	
	Basics of Mesoscale Model Simulations + Exercises (3 sh)		x	x	x	
	Advanced Training Module of the Leipzig Graduate School on Clouds, Aerosols and Radiation (LGS-CAR) "Absorbing Aerosols", TROPOS, October 15-16, 2013	x				
Wandinger, U.	Scattering and Atmospheric Optics (2 sh) Seminar Applied Scattering Theory (1 sh)		x x		x x	x x
Wiedensohler, A. Stratmann, F. Birmili, W. Müller, T.	Atmospheric Aerosols (2 sh) Seminar Atmospheric Aerosols (1 sh) incl. Laboratory practise (until SS 2015), Seminar (from WS 2015/2016)	x x		x x		x x
Wiedensohler, A.	Winterschool on "Atmospheric Aerosol Physics, Measurements, and Sampling Techniques", Indian Institute of Technology Madras, India, January 13-16, 2014	x				
	"International School on Atmospheric Aerosol Physics, Measurement, and Sampling", Institute of Environmental Science and Meteorology University of the Philippines, Diliman, Q.C., March 31 to April 3, 2014		x			
	10th Summer School on Atmospheric Aerosol Physics, Measurement, and Sampling, Hyytiälä, Finland, May 4-10, 2014		x			

Appendices: University courses / Academical degrees

Lecturer	Course	WS 2013/ 2014	SS 2014	WS 2014/ 2015	SS 2015	WS 2015/ 2016
Wiedensohler, A.	GAWTEC School on Atmospheric Aerosol Physics, Measurement, and Sampling, Schneefernerhaus, Zugspitze, November, 2014			x		
	11th Summer School on Atmospheric Aerosol Physics, Measurement, and Sampling Hyytiälä, Finland, May 1-8, 2015			x		
	Latin American and Caribbean Aerosol Measurements School: From measurements technologies to applications, La Paz, Bolivia, June, 22-27, 2015			x		
van Pinxteren, M.	Guest lecture: Analysis and Spectroscopy: Gas Chromatography, Lecture in an one week course	x				

* Leipzig Institute for Meteorology (LIM), Leipzig University

Academical degrees

Completed academic qualifications 2014/2015

Academic degree*	Name	Title	Faculty	Year
Dr. rer. nat. habil.	Schepanski, K.	Controls on dust entrainment into the atmosphere	Leipzig University, Faculty of Physics and Earth Sciences	2015
Ph. D.	Bräuer, P.	Extension and application of a tropospheric aqueous phase chemical mechanism (CAPRAM) for aerosol and cloud models	Leipzig University, Faculty of Physics and Earth Sciences	2015
	Bühl, J.	Combined lidar and radar observations of vertical motions and heterogeneous ice formation in mixed-phase layered clouds - Field studies and long-term monitoring	Leipzig University, Faculty of Physics and Earth Sciences	2015
	Clauß, T.	Development and Application of Optical Methods for the Characterization of the Ice Phase in Mixed-Phase Aerosol	Leipzig University, Faculty of Physics and Earth Science	2015
	Ditas, F.	Microphysical properties of aerosol particles in the trade wind regime and their influence on the number concentration of activated particles in trade wind cumulus clouds	Leipzig University, Faculty of Physics and Earth Sciences	2014

Appendices: Academical degrees

Academic degree*	Name	Title	Faculty	Year
Ph. D.	Ditas, J.	On the small-scale dynamics of cloud edges	Leipzig University, Faculty of Physics and Earth Sciences	2014
	Engler, C.	Meteorologische Einflüsse auf die Konzentrationen feiner und grober atmosphärischer Aerosolpartikel in Deutschland	Leipzig University, Faculty of Physics and Earth Sciences	2014
	Hanschmann, T.	Unsicherheiten in der Erfassung des kurzwelligen Wolkenstrahlungseffektes	Leipzig University, Faculty of Physics and Earth Sciences	2014
	Hartmann, S.	An immersion freezing study of mineral dust and bacterial ice nucleating particles	Leipzig University, Faculty of Physics and Earth Sciences	2015
	Horn, S.	Simulations of complex atmospheric flows using GPUs - the model ASAMgpu	Leipzig University, Faculty of Physics and Earth Sciences	2015
	Huang, S.	Chemical composition of the submicrometer aerosol over the Atlantic Ocean	Leipzig University, Faculty of Physics and Earth Sciences	2015
	König, M.	Large-Eddy simulation modelling for urban scale	Leipzig University, Faculty of Physics and Earth Sciences	2014
	Mutzel, A.	Influence of the reaction conditions on the oxidation of atmospheric first-generation monoterpene oxidation products	Leipzig University, Faculty of Chemistry and Mineralogy	2014
	Nekat, B.	Chemical composition and source apportionment of submicron aerosol particles sampled in Wuqing (China)	Leipzig University, Faculty of Chemistry and Mineralogy	2014
	Niedermeier, N.	Experimental determination of the mass deposition flux of mineral dust at the Cape Verde Islands	Leipzig University, Faculty of Physics and Earth Sciences	2014
	Pfeifer, S.	Verknüpfung aerodynamischer und optischer Eigenschaften nichtkugelförmiger atmosphärischer Grobstaubpartikel	Leipzig University, Faculty of Physics and Earth Sciences	2014
	Rösch, M.	Untersuchungen zur Generierung und zum Immersionsgefrierverhalten supermikroner, quasimonodisperser Mineralstaubpartikel	Leipzig University, Faculty of Physics and Earth Sciences	2015
	Schmidt, J.	Dual-field-of-view Raman lidar measurements of cloud microphysical properties: Investigation of aerosol-cloud interaction	Leipzig University, Faculty of Physics and Earth Sciences	2014

Appendices: Academical degrees

Academic degree*	Name	Title	Faculty	Year
Ph. D.	Weigelt, A.	An optical particle counter for the regular application onboard a passenger aircraft: Instrument modification, characterization and results from the first year of operation	Leipzig University, Faculty of Physics and Earth Sciences	2015
M.Sc.	Badeke, R.	Untersuchung physikalischer Eigenschaften des atlantisch-marinen Grenzschichtaerosols	TU Bergakademie Freiberg	2015
	Bär, J.	Zur Parametrisierung trockener und nasser Partikeldeposition in der mesoskaligen Transportmodellierung am Beispiel von Seesalz und Wüstenstaub	Leipzig University, Faculty of Physics and Earth Sciences	2015
	Bechler, J.	An investigation of the hygroscopic growth and cloud condensation nucleus activity of mixed organic/inorganic aerosol particles	Leipzig University, Faculty of Physics and Earth Sciences	2015
	Bier, A.	Studies on the modelling of the behaviour of liquid particles/droplets below the melting point of water at the Leipzig Aerosol Cloud Interaction Simulator (LACIS) with FLUENT/FPM	Leipzig University, Faculty of Physics and Earth Sciences	2014
	Düsing, S.	Schließung Aerosoloptischer Eigenschaften zwischen luftgetragenen und in-situ- und bodengebundenen LIDAR-Messungen	Leipzig University, Faculty of Physics and Earth Sciences	2015
	Emmrich, S.	The effect of cities on aerosol and cloud properties concerning the planetary boundary layer observed with rural and urban lidar and sun photometer measurements in Melpitz and Leipzig	Leipzig University, Faculty of Physics and Earth Sciences	2015
	Grawe, S.	Investigations on the Immersion Freezing Behavior of Ash Particles at the Leipzig Aerosol Cloud Interaction Simulator (LACIS)	Leipzig University, Faculty of Physics and Earth Sciences	2015
	Hellner, L.	Untersuchungen des Immersionsgefrierverhaltens natürlicher Böden am Leipzig Aerosol Cloud Interaction Simulator (LACIS)	Leipzig University, Faculty of Physics and Earth Sciences	2015
	Herenz, P.	Investigations corresponding the influence of temporal change of the termodynamic state on the surface area structure of ice particles	Leipzig University, Faculty of Physics and Earth Sciences	2014
	Heun, J.	Numerische Lösung der linearen Wellengleichung in Gebieten mit kompliziertem Rand	Leipzig University of Applied Sciences	2015
	Hoffmann, E.	Modellierung der troposphärischen Multiphasenchemie mit MCM-CAPRAM unter marinen und kontinentalen Hintergrundbedingungen	Leipzig University, Faculty of Physics and Earth Sciences	2014

Appendices: Academical degrees

Academic degree*	Name	Title	Faculty	Year
M.Sc.	Kähner, R.	Design and theoretical description of a streaming tube for the investigation of atmospheric chemical processes	Leipzig University of Applied Sciences	2014
	Kanter, S.	Untersuchungen zum Immersionsgefrierverhalten von Illit und Feldspatpartikeln am Leipzig Aerosol Cloud Interaction Simulator (LACIS)	Leipzig University, Faculty of Physics and Earth Sciences	2014
	Kundisch, M.	Influence of air mass origin and seasons on aerosol particle size distribution and soot concentration at Chacaltaya (5,421 m ASL), Bolivia 2012	Leipzig University, Faculty of Physics and Earth Sciences	2014
	Markwitz, C.	Simulation of stratiform mixed-phase clouds in the Arctic boundary layer	Leipzig University, Faculty of Physics and Earth Sciences	2015
	Padelt, J.	Untersuchungen zum Einfluss des thermodynamischen Umgebungszustandes und des Eisnukleationspartikels (INP) auf das Gefrieren und die Oberflächenstruktur der entstehenden Eiskristalle	Leipzig University, Faculty of Physics and Earth Sciences	2015
	Rau, A.	Zeitaufgelöste Messungen kurzkettiger Dicarbonsäuren (DCAs) in atmosphärischen Partikeln	Leipzig University, Faculty of Physics and Earth Sciences	2015
	Rempel, M.	Objekt-basierte Bewertung der Güte von COSMO-DE Konvektionsvorhersagen mittels Meteosat	Leipzig University, Faculty of Physics and Earth Sciences	2015
	Rittmeister, F.	The African dust and smoke layer over the tropical Atlantic during the spring season 2013: Ship-based lidar observations from Guadeloupe to Cape Verde	Leipzig University, Faculty of Physics and Earth Sciences	2015
	Särchinger, M.	Untersuchung des Einflusses meteorologischer Faktoren und des regionalen Hintergrunds auf die Aerosolbelastung in der Stadt Leipzig	Leipzig University, Faculty of Physics and Earth Sciences	2015
	Schmidt, M.	Einfluss von meteorologischen Parametern und Anströmungen auf die PM-Massenkonzentration und Zusammensetzung in Melpitz - eine Langzeitstudie (1992-2012)	Leipzig University, Faculty of Physics and Earth Sciences	2014
	Stieger, B.	Aerosol- und Wolkenchemie: Kinetische und mechanistische Untersuchungen der Reaktionen von NO_3^- - und SO_4^{2-} -Radikalen mit sauerstoffhaltigen organischen Verbindungen in wässriger Lösung	Leipzig University, Faculty of Chemistry and Mineralogy	2014
	Szodry, K.-E.	Meteorologische Situationen, die die Entstehung von Staubfahnen in Island begünstigen	Leipzig University, Faculty of Physics and Earth Sciences	2015

Appendices: Academical degrees

Academic degree*	Name	Title	Faculty	Year
M.Sc.	Wagner, R.	American dust bowl - Das Zusammenspiel von Dürre, Gewittern und Haboobs	Leipzig University, Faculty of Physics and Earth Sciences	2015
	Walther, J.	Schattenbandradiometer GUVIS-3511 - Strahlungsmessung und Bestimmung optischer Eigenschaften von Aerosol zu Wasser und zu Land	Leipzig University, Faculty of Physics and Earth Sciences	2014
B.Sc.	Bohlmann, S.	Heterogene Eisbildung über Südostasien	Leipzig University, Faculty of Physics and Earth Sciences	2014
	Hellmuth, F.	Investigation of the regional variability of the ice water content produced by supercooled stratiform clouds	Leipzig University, Faculty of Physics and Earth Sciences	2015
	Kunz, C.	Heterogene Eisbildung im Amazonasgebiet	Leipzig University, Faculty of Physics and Earth Sciences	2014
	Lemme, A.	Über den Einfluss von Saharastaub auf die hochreichende Konvektion im tropischen Atlantik	Leipzig University, Faculty of Physics and Earth Sciences	2015
	Schimmel, W.	Numerische Simulation großer kinetischer Systeme der troposphärischen Luftchemie	Leipzig University of Applied Sciences	2015
	Tatzelt, Ch.	Fernerkundung der Wolkenklassen mit Hilfe der Kombination von aktiven und passiven Satellitendaten	Leipzig University, Faculty of Physics and Earth Sciences	2015
	Ulrich, M.	Characterization of Mediterranean dust outbreak events	Leipzig University, Faculty of Physics and Earth Sciences	2014

* Habil.: Habilitation, Ph. D.: Doctoral theses, Dipl.: Diploma, M.Sc.: Master of Science, B.Sc.: Bachelor of Science

Summary of completed academic qualifications

Academical degrees	Number		Total
	2014	2015	
Habilitation		1	1
Doctoral theses	10	8	18
Master of Science	9	16	25
Bachelor of science	3	4	7

Appendices: Awards / Guest scientists

Awards

Name	Prize	Awarding institution	Comments/Description
A. Wiedensohler	Highly Cited Researcher 2014	Thomson Reuters	Highly Cited Researchers 2014 represents some of world's leading scientific minds. Over three thousand researchers earned the distinction by writing the greatest numbers of reports officially designated by Essential Science Indicators SM as Highly Cited Papers.
A. Wiedensohler E. Brüggemann G. Spindler K. Müller	Haagen Smit Prize 2014	Journal Atmospheric Environment	The award is given annually to a maximum of two outstanding papers published in the journal "Atmospheric Environment".
S. Scheinhardt	Paul-Crutzen Prize 2015	German Chemical Society (GDCh) professional group for environmental chemistry and ecotoxicology	The prize is given annually for outstanding achievements in the area of environmental chemistry and ecotoxicology, in this case for a publication regarding effect of climate change on air quality in Dresden.
A. Wiedensohler	Highly Cited Researcher 2015	Thomson Reuters	Highly Cited Researchers 2015 represents some of world's leading scientific minds. Over three thousand researchers earned the distinction by writing the greatest numbers of reports officially designated by Essential Science Indicators SM as Highly Cited Papers.

Guest scientists

Name	Period of stay	Institution
Zhang, S.	01.01. - 30.06.14	Chinese Academy of Science, Beijing, China
Marinou, E.	25.03. - 25.05.14	National Observatory of Athens, Greece
Covert, D.	05.04. - 02.05.14	Joint Institute for the Study of the Atmosphere and Ocean (JISAO), Seattle, USA
Shen, X.	06.04. - 16.04.14	Chinese Academy of Meteorological Sciences, Beijing, China
Sun, J.	06.04. - 16.04.14	Chinese Academy of Meteorological Sciences, Beijing, China
Aswathy, E.	15.04. - 30.04.14	Indian Institute of Technology Madras, India
Pfitzenmaier, L.	22.04. - 28.05.14	Delft University of Technology, The Netherlands
Silva, A.	30.04. - 21.07.14	Universidad de Concepcion, Chile

Appendices: Guest scientists

Name	Period of stay	Institution
Zhou, P.	02.06. - 20.06.14	Unviersity of Helsinki, Finland
Morosov, I.	27.07. - 27.08.14	Institute for Chemical Physics, Moskau, Russia
Syromyatnikov, A.	27.07. - 27.08.14	Institute for Chemical Physics, Moskau, Russia
Weinzierl, B.	01.09. - 05.09.14	German Aerospace Center (DLR), Oberpfaffenhofen, Germany
Baergen, A.	01.09. - 10.10.14	University Toronto, Canada
Filep, A.	12.09. - 11.11.14	University of Szeged, Szeged, Hungary
Marinou, E.	21.09. - 21.10.14	National Observatory of Athens, Greece
Li, X.	01.10.14 - 31.09.15	Fudan University Shanghai, China
Alas, H.	09.11. - 31.12.14	Manila Observatory, Diliman, Philippines
Tamayo, E.	09.11. - 31.12.14	Manila Observatory, Diliman, Philippines
Avila, F.	29.11. - 15.12.14	Universidad Mayor de San Adres, La Paz, Bolivia
Binietoglou, I.	08.12. - 19.12.14	National Institute of R&D for Optoelectronics, Magurele, Ilfov, Romania
Wang, X.	07.01. - 14.11.15	Max Planck Institute for Chemistry, Mainz, Germany
Wu, Z.	20.01. - 27.02.15	Peking University, Beijing, China
Donaldson, J.	26.01. - 28.02.15	University of Toronto, Canada
Wiedemann, K.	02.02. - 23.02.15	University of Arizona, USA
Garimella, S.	23.02. - 06.03.15	Massachusetts Institute of Technology, USA
Leng, C.	07.04 - 31.12.15	Chinese Academy of Science, Beijing, China
Kandler, L.	20.04. - 30.04.15	TU Darmstadt, Germany
Kohl, R.	20.04. - 30.04.15	Goethe University Frankfurt am Main, Germany
Fabian, F.	20.04. - 30.04.15	Goethe University Frankfurt am Main, Germany
Rose, D.	20.04. - 30.04.15	Goethe University Frankfurt am Main, Germany
Shneider, J.	20.04. - 30.04.15	Max Planck Institute for Chemistry, Mainz, Germany
Garimella, S.	20.04. - 30.04.15	Massachusetts Institute of Technology, Massachusetts, USA
Grayson, J.	04.05. - 29.05.15	University of British Columbia, Canada

Appendices: Guest scientists

Name	Period of stay	Institution
Zhang, K.	10.05. - 15.11.15	Chinese Academy of Science, Beijing, China
Mamouri, R.	17.05. - 31.05.15	Cyprus University of Technology, Limassol, Cyprus
Wang, M.	18.05. - 07.08.15	McMaster University, Canada
Mattis, I.	19.05. - 28.05.15	Deutscher Wetterdienst, Meteorologisches Observatorium, Hohenpeissenberg, Germany
Müller, G.	19.05. - 28.05.15	Deutscher Wetterdienst, Meteorologisches Observatorium, Hohenpeissenberg, Germany
Shrivastava, A. K.	01.06. - 30.6.15	Indian Institute of Tropical Meteorology, Delhi, India
Donahue, N.	06.06. - 13.06.15	Steinbrenner Institute for Environmental Education and Research, Carnegie Mellon University, Pittsburgh, USA
Stammes, P.	17.06. - 29.06.15	Royal Netherlands Meteorological Institute, De Bilt, The Netherlands
Emde, C.	21.06. - 26.06.15	Ludwig Maximilian University, Munich, Germany
Makhmudov, A.	27.06. - 11.07.15	Academy of Sciences of the Republic of Tajikistan, Dushanbe, Tajikistan
Zhao, P.	10.07. - 20.08.15	Environmental Meteorological Center of Beijing, China
Sarkawt, H.	13.07. - 14.08.15	University of Leicester, Leicester, UK
Schechner, Y.	17.07. - 22.07.15	University of Haifa, Israel
Sun, X.	01.08.15 - 31.01.16	Chinese Academy of Science, Beijing, China
Zhang, Y.	01.08.15 - 31.01.16	Chinese Academy of Science, Beijing, China
Hu, M.	05.08. - 25.08.15	College of Environmental Science and Engineering, Peking University, China
Venables, D.	15.08.15 - 31.07.16	University College Cork, Ireland
Makhmudov, A.	22.08. - 29.08.15	Academy of Sciences of the Republic of Tajikistan, Dushanbe, Tajikistan
Minikulov, N.	22.08. - 29.08.15	Academy of Sciences of the Republic of Tajikistan, Dushanbe, Tajikistan
Abdullaev, S.	22.08. - 29.08.15	Academy of Sciences of the Republic of Tajikistan, Dushanbe, Tajikistan
Nazarov, B.	22.08. - 29.08.15	Academy of Sciences of the Republic of Tajikistan, Dushanbe, Tajikistan
Saliba, M.	25.08. - 31.08.15	University of Malta, Gozo, Malta
Kohn, M.	27.08. - 10.9.2015	Eidgenössische Technische Hochschule Zürich, Schweiz

Appendices: Guest scientists / Visits of TROPOS scientists

Name	Period of stay	Institution
Alas, H.	05.09. - 02.11.15	Manila Observatory, Diliman, Philippines
Stammes, P.	12.09. - 12.12.15	Royal Netherlands Meteorological Institute, De Bilt, The Netherlands
Tamayo, E.	27.09. - 29.10.15	University of the Philippines, Manila, Philippines
Khedidji, S.	01.10.15 - 31.03.17	Université colonel Akli Mouhand-oulhadj de Bouira, Algeria
Munao, D.	05.10. - 19.12.15	University of Malta, Gozo, Malta
Wang, Y.	05.10. - 16.11.15	Peking University, Beijing, China
Lei, T.	05.10. - 16.11.15	Max Planck Institute for Chemistry, Mainz, Germany
Wu, Z.	05.10. - 20.11.15	Peking University, Beijing, China
Levis, A.	13.10. - 18.10.15	University of Haifa, Israel
Aides, A.	13.10. - 22.10.15	University of Haifa, Israel
Makhmudov, A.	01.11. - 21.11.15	Academy of Sciences of the Republic of Tajikistan, Dushanbe, Tajikistan
Kroflic, A.	01.11.15 - 31.10.16	National Institute of Chemistry Ljubljana, Slovenia

Visits of TROPOS scientists

Name	Period of stay	Institution
Wiedensohler, A.	11.01. - 21.01.14	Indian Institute of Technology Madras, Chennai, India
	28.03. - 05.04.14	University of the Philippines Diliman, Quezon City, Philippines
Engelmann, R.	19.05. - 28.05.14	National Observatory, Athens, Greece
Herrmann, H.	08.07. - 18.07.14	Shanghai-University, China

Meetings

Meetings	Date	National/ international	Number of participants
Leipzig Graduate School “Polarization” Advanced Training Module (ATM), Leipzig	11. - 12.02.14	international	20
1. Leipziger Staubtag (i.e. “Dust Day”), Leipzig	06.03.14	national	60
Yearly SOPRAN Meeting, Leipzig	25. - 26.03.14	national	60
Cloudnet Workshop, Leipzig	16.04.14	international	20
Leipzig Graduate School “Indirect Aerosol Effect” Advanced Training Module (ATM), Leipzig	01. - 02.07.14	international	20
ACTRIS WP3 Workshop, Leipzig	04.10.14	international	20
SOPRAN Meeting: AEOLOTRON CAMPAIGN, Heidelberg	06.10.14	international	15
“Soot Aerosols” Measurement Methods and Perspectives, Leipzig	08.10.14	international	50
Leipzig Graduate School “Atmospheric Chemistry” Advanced Training Module (ATM), Leipzig	25. - 26.11.14	international	20
Melpitz Column Planning Meeting, Leipzig	17. - 18.3.15	international	30
Yearly SOPRAN Meeting, Mainz	17. - 18.03.15	national	60
Leipzig Graduate School “Heterogeneous Ice Nucleation” Advanced Training Module (ATM), Leipzig	22. - 23.04.15	international	20
15th ELS 2015 Electromagnetic and Light Scattering Conference 2015, Leipzig	21. - 26.06.15	international	140
2. Leipziger Staubtag (i.e. “Dust Day”), Leipzig	07.07.15	international	60
ICCE 2015 - 15th EuCheMS International Conference on Chemistry and the Environment, Leipzig Co-organisation by TROPOS, Leipzig	20. - 25.09.15	international	500
GUAN Workshop, Leipzig	21. - 23.09.15	international	20
Leipzig Graduate School “Clouds in a changing climate system” Advanced Training Module (ATM), Leipzig	28./29.09.15	international	20

Appendices: Meetings / International and national field campaigns

Meetings	Date	National/international	Number of participants
Melpitz Column First Data Workshop, Leipzig	16. - 17.11.15	international	30
ACTRIS-D Kick-off Meeting, Frankfurt am Main	20.11.15	national	25
ACTRIS WP 2 and Collocated Meetings, Leipzig	23. - 27.11.15	international	100

International and national field campaigns

Campaign	Project partner
ACCEPT experiment Analysis of the Composition of Clouds with Extended Polarization Techniques Experiment TROPOS: Remote Sensing Dept.	Ludwig Maximilian University, Munich; Metek GmbH, Elmshorn, Germany; University of Technology, Delft, The Netherlands; Royal Meteorological Institute of the Netherlands (KNMI), The Netherlands
ACRIDICON-CHUVA 18 scientific mission flights with HALO research aircraft TROPOS: EACMph. Dept.*	Germany (ACRIDICON Consortium), USA, Brazil
SOPRAN Aerosol measurements in the AEOLOTRON: SOPRAN laboratory campaign in Heidelberg TROPOS: Chemistry Dept.	University of Heidelberg; University of Oldenburg; Leibniz Institute for Baltic Sea Research Warnemünde (IOW); Max Planck Institute for Chemistry, Mainz; Helmholtz Centre for Ozean Research Kiel (GEOMAR), Germany; CNRS IRCELYON, Lyon, France; University of Manchester, UK
Aerosol Measurements on the research vessel Polarstern TROPOS: EACMph. Dept., Chemistry Dept.	no partners
BACCHUS TROPOS: Remote Sensing Dept.	Germany, Cyprus
CADEX Central Asian Dust EXperiment TROPOS: Remote Sensing Dept., Modelling Dept.	S.U. Umarov Physical-Technical Institute of Academy of Sciences of the Republic of Tajikistan; Helmholtz Centre Potsdam - GFZ German Research Centre for Geosciences, Germany
CAREBeijing-North China Plain Campaigns of Air Quality Research in Beijing TROPOS: Chemistry Dept., EACMph. Dept.	China, France, UK, USA, Germany
Chacaltaya permanent field experiment in Chacaltaya/Bolivia (visit in June 2014) TROPOS: EACMph. Dept.	Universidad Mayor de San Andrés, La Paz, Bolivia

Appendices: International and national field campaigns

Campaign	Project partner
CHARADMExp campaign (Characterization of Aerosol mixtures of Dust And Marine origin) TROPOS: Remote Sensing Dept.	ESA, National Observatory of Athens, Greece
CLOUD9 (Cosmics Leaving Outdoor Droplets) TROPOS: EACMph. Dept.	Switzerland, Austria, Finland, Germany, Portugal, Russia, UK, USA, Sweden
CLOUDNET (permanent experiment) Cloud Measurement Network Leipzig, Germany TROPOS: Remote Sensing Dept.	CLOUDNET Consortium
Colrawi TROPOS: Remote Sensing Dept.	Meteorological Observatory Lindenberg of DWD (Deutscher Wetterdienst), Germany
EARLINET (permanent experiment) European Aerosol Research Lidar Network Leipzig, Germany TROPOS: Remote Sensing Dept.	EARLINET Consortium
EMEP¹/ACTRIS Winter Campaign Melpitz TROPOS: Chemistry Dept., EACMph. Dept.	Switzerland, Czech Republic, Denmark, Spain, Ireland, Italy, The Netherlands, Norway, UK (EMEP-Consortium)
F-BEACH (Fichtelgebirge Biogenic Emissions and Aerosol Chemistry) TROPOS: Chemistry Dept.	University of Bayreuth; Johannes Gutenberg University Mainz, Germany
FIN02 Campaign at AIDA TROPOS: EACMph. Dept.	Germany, Italy, Switzerland, USA, UK, Israel
Freezing of Proteins TROPOS: EACMph. Dept.	Lund University, Lund, Sweden; Aarhus University, Aarhus, Denmark
GUAN German Ultrafine Aerosol Network TROPOS: EACMph. Dept., Chemistry Dept.	Federal Environment Agency (UBA), Langen; German Research Center for Environmental Health, Munich; Saxon State Ministry of the Environment and Agriculture, Dresden; Institute of Energy and Environmental Technology e.V. (IUTA), Duisburg; Deutscher Wetterdienst (DWD) Hohenpeissenberg, Germany; ISSEP, Liège, Belgium
IGOS-CARIBIC Monthly intercontinental measurement flights Civil Aircraft for Remote Sensing and In situ measurement in Tropospheric and Lower Stratosphere based on the Instrumentation Container Concept TROPOS: EACMph. Dept.	CARIBIC Consortium

Appendices: International and national field campaigns

Campaign	Project partner
INUIT-LACIS-Campaign Ice Nuclei Research Unit - LACIS TROPOS: EACMph. Dept.	Max Planck Institute for Chemistry, Mainz; Goethe University Frankfurt am Main; TU Darmstadt, Germany; Swiss Federal Institute of Technology Zurich, Switzerland
LfULG Aerosol TROPOS: Chemistry Dept., EACMph. Dept.	Saxon State Ministry of the Environment and Agriculture, Dresden, Germany
LINC Leipzig Ice Nucleation Counter Comparison Campaign TROPOS: EACMph. Dept.	Swiss Federal Institute of Technology Zurich, Switzerland
Melpitz Column 2015 Characterization of aerosol particles and their properties in the column above the research station Melpitz TROPOS: all departments	TU Braunschweig; University of Tübingen; Saxon State Ministry of the Environment and Agriculture, Dresden; University of Bayreuth; Hochschule Düsseldorf; TU Darmstadt; Deutscher Wetterdienst (DWD), Offenbach, Germany; Paul Scherrer Institute, Villigen, Switzerland
Meteor-M117 Analysis of aerosol particles and the sea surface microlayer in upwelling regions of the Baltic Sea TROPOS: Chemistry Dept.	University of Oldenburg; Leibniz Institute for Baltic Sea Research Warnemünde (IOW); University of Hamburg, Germany
ML-CIRRUS 12 scientific mission flights with HALO TROPOS: EACMph. Dept.	Germany (ML-CIRRUS Consortium)
Mobile Research Station on Polarstern Research Vessel Transect PS83 (ANT-XXIX/10) TROPOS: EACMph. Dept., Chemistry Dept.	Helmholtz Centre for Ozean Research Kiel (GEOMAR); Alfred Wegener Institute for Polar and Marine Research (AWI), Bremerhaven; Leipzig Institute for Meteorology (LIM), Leipzig University; Max Planck Institute for Meteorology, Hamburg; University of Hamburg, Germany
Mobile Research Station on Polarstern Research Vessel Transect PS95 TROPOS: Remote Sensing Dept., EACMph. Dept., Chemistry Dept.	Helmholtz Centre for Ozean Research Kiel (GEOMAR); Alfred Wegener Institute for Polar and Marine Research (AWI), Bremerhaven; Leipzig Institute for Meteorology (LIM), Leipzig University; Max Planck Institute for Meteorology, Hamburg; University of Hamburg, Germany
PollyNet (permanent experiment) Network of institutions with a PollyXT TROPOS: Remote Sensing Dept.	PollyNet Consortium
INUIT-LACIS-Campaign Ice Nuclei Research Unit - LACIS TROPOS: EACMph. Dept.	Max Planck Institute for Chemistry, Mainz; Goethe University Frankfurt am Main; TU Darmstadt, Germany
IOPRAO 2014 Pyranometer Intensive Measurement Campaign Lindenberg Falkenberg TROPOS: Remote Sensing Dept.	Meteorological Observatory Lindenberg of DWD (Deutscher Wetterdienst), Germany

Appendices: International and national field campaigns / Memberships

Campaign	Project partner
SALTRACE Saharan Aerosol Long-range Transport and Aerosol-Cloud-Interaction Experiment Barbados TROPOS: all departments	Germany, Barbados, Spain, France, USA
SPIN comparison TROPOS: EACMph. Dept.	Massachusetts Institute of Technology, USA
TROPOS Dach (replacing Seiffen II) TROPOS: Chemistry Dept.	Aerosol d.o.o./ Slovenia
UAS Melpitz 2014 Unmanned aerial systems (UAS): Boundary layer measurements in Melpitz	TU Braunschweig; University of Tübingen, Germany
Low Emission Zone Leipzig TROPOS: EACMph. Dept.	Saxon State Ministry of the Environment and Agriculture, Dresden, Germany
Scientific and technical support during an international CEN-fieldcampaign at UBA- EMEP station Waldhof	Federal Environment Agency (UBA), Germany
Yangtze River Campaign 2015 International field campaign in China TROPOS: Chemistry Dept.	Fudan University, Shanghai, China

* Experimental Aerosol and Cloud Microphysics Department

[†] EMEP: Co-operative Programme for Monitoring and Evaluation of the Long-Range Transmission of Air Pollutants in Europe

Memberships

Name	Board
Althausen, D.	Commission on Air Pollution Prevention of VDI and DIN - Standards Committee KRdL, NA 134-02-01-22 UA "Ground-based remote sensing of meteorological parameters" Department II Environmental Meteorology
Hellmuth, O.	Membership in the International Association for the Properties of Water and Steam (IAPWS), Working Group Thermophysical Properties of Water and Steam (TPWS)
Hermann, M.	Scientific Steering Committee (WLA) HALO
	Member of the "Stratospheric Sulfur and its Role in Climate" (SSiRC) SPARC initiative planning committee
Herrmann, H.	Chairman of the working group "Atmospheric Chemistry" in the GDCh-division "Environmental Chemistry and Ecotoxicology (AKAC)"
	DECHEMA/GDCh/Bunsen Society, Gemeinschaftsausschuss „Chemie der Atmosphäre“

Appendices: Memberships

Name	Board
Herrmann, H.	DECHEMA/GDCh/KRdL Division "Particulate Matter" - Member of the Steering Committee
	IUPAC Task Group on Atmospheric Chemical Kinetic Data Evaluation
	Advisory Board Member of ProcessNet-Fachgemeinschaft SuPER
	Fellow of International Union of Pure and Applied Chemistry
Iinuma, Y.	Chair der Working Group "Aerosol Chemistry within the EAA (European Aerosol Assembly)"
	Editorial Board Member "Atmospheric Measurement Techniques"
Macke, A.	Member od the Scientific Advisory Board of „Meteorologische Zeitschrift“
	Member of the Scientific Advisory Board of the German Meteorological Service
	Member of the International Radiation Comission
	Member od the Scientific Advisory Board of the research program "KLIWAS"
	Member of the HALO Science Steering Comitee
	Member of the HALO Board of Trustees
	Member of the DFG Senate Commission Oceanography
	Member of the EU Steering Committee of the Leibniz Association
	Member of the DFG Topical Board 313 "Atmosphere and Ocean Research"
	Deputy chairman of Section E of the Leibniz Society
Müller, K.	VDI and DIN - Standards Committee KRdL, member of the working group "Measurement of aerosol particles in the outdoor air"
	Member of the KRdL working group „Spiegelgremium zu CEN/TC 264/WG 35 EC/OC in PM“
Schepanski, K.	Member of Executive Commitee Leibniz Research Alliance INFECTIONS'21
	Member of Steering Commitee Leibniz Research Alliance INFECTIONS'21
Stratmann, F.	Work Package (WP) Leader EU-Projekt EUROCHAMP 2

Appendices: Memberships

Name	Board
Stratmann, F.	Member of the EUROCHAMP 2 User Selection Panel (USP)
	Board-Member of the International Comission on Clouds and Precipitation (ICCP)
Tegen, I.	SDS-WAS (WMO Sand and Dust Storm Warning Advisory and Assessment System), Member of Steering Committee
	HAMMOZ Steering Committee Member
	Member of Science Europe Committee for Life, Environmental and Geo Sciences
Wandinger, U.	Member of the ESA-JAXA EarthCARE Joint Mission Advisory Group
	Member of the EARLINET Council
	Member Scientific Steering Committee and Work Package Leader EU Project ACTRIS
	Member Scientific Steering Committee and Work Package Leader EU Project ACTRIS-2
Wehner, B.	Member of the Leipzig Branche of DMG (German Meteorological Society)
	Chair of the Working Group "Atmospheric Aerosols" within the EAA (European Aerosol Assembly)
	Speaker of the Working Group Chairs within the EAA (European Aerosol Assembly)
	Chair of the Working Group "Atmospheric Aerosols" within the EAA (European Aerosol Assembly)
Wiedensohler, A.	"Scientific Advisory Group" for aerosols within the "Global Atmosphere Watch" program of the Meteorological Organization
	VDI-Commission "Particle Counting in the Atmosphere"
	Member Scientific Steering Committee (SSC) and Work Package (WP) Leader within the EU Project ACTRIS
	Guest Professor at "Peking University", Department of Environmental Science, China
	Head of the World Calibration Center WMO-GAW
	Head of the European Center for Aerosol Calibration

Appendices: Editorships / Reviews

Editorships

Name	Journal
Birmili, W.	Editorial Board Member "Atmospheric Chemistry and Physics"
Herrmann, H.	Editorial Board Member "Atmospheric Measurement Techniques"
	Editorial Board Member "Atmospheric Pollution Research"
Iinuma, Y.	Editorial Board Member "Atmospheric Measurement Techniques"
Macke, A.	Editorial Board Member "Atmospheric Measurement Techniques"
	Member of the Editorial Committee "promet"
Schepanski, K.	Associate Editor, Aeolian Research
Tegen, I.	Associate Editor, Journal of Geophysical Research, Atmospheres
Wandinger, U.	Editorial Board Member "Atmospheric Measurement Techniques"
Wiedensohler, A.	Editorial Board Member "Atmospheric Chemistry and Physics"
	Editorial Board Member "Atmospheric Measurement Techniques"
	Chief Editor Atmospheric Environment

Reviews

Reviews	Number	
	2014	2015
Journals	142	148
Projects	15	12
Others	6	25
Total	163	185

Cooperations

International cooperations

Research project	Cooperation partners
ACCEPT Analysis of the Composition of Clouds with Extended Polarization Techniques	Ludwig Maximilian University, Munich; Metek GmbH, Elmshorn, Germany; University of Technology, Delft; Royal Meteorological Institute of the Netherlands (KNMI), The Netherlands
ACRIDICON-CHUVA Aerosol, Cloud, Precipitation, and Radiation Interactions and Dynamics of Convective Cloud System - Cloud processes of the main precipitation systems in Brazil	Germany, USA, Brazil
ACTOS Airborne Cloud Turbulence Observation System - Interaction between turbulent mixing processes and cloud micro-physical characteristics in stratiform boundary layer clouds	Michigan Technological University, Department of Physics, Houghton, USA
ACTRIS Aerosols, Clouds, and Trace gases Research InfraStructure Network	>50 partners
AERONET Aerosol Robotic Network	National Aeronautics and Space Administration (NASA), USA
AIE Atmospheric Environmental Impacts of Aerosol in East Asia	30 partners
AMIS / IRSES (Fate and Impact of Atmospheric Pollutants / International research staff exchange scheme)	China, Denmark, Germany, France, Spain
Anthropogenic influence of Asian aerosol on tropical cirrus clouds	National Center for Atmospheric Research (NCAR), Boulder, Colorado, USA
APRIL Atmospheric Products from Imager and Lidar	Royal Netherlands Meteorological Institute (KNMI), The Netherlands; Institute for Space Science, Freie Universität Berlin (FUB), Germany
AQMEII Air Quality Model Evaluation International Initiative	Austria, Australia, Belgium, Canada, Switzerland, Cyprus, Germany, Denmark, Finland, France, Greece, Italy, Luxembourg, Malta, The Netherlands, Norway, Poland, Portugal, Sweden, UK, USA
Atmospheric Nucleation	Universities of Helsinki and Kuopio, Finland
ATTO (Amazonian Tall Tower Observatory)	Instituto Nacional de Pesquisas da Amazônia INPA, Manaus; Universidade do Estado de Amazonas, Manaus, Brazil; Max Planck Institute for Chemistry, Mainz, Germany

Appendices: Cooperations

Research project	Cooperation partners
BACCHUS Impact of Biogenic versus Anthropogenic emissions on Clouds and Climate: towards a Holistic UnderStanding	20 partners from Switzerland, Finland, Germany, UK, Norway, Greece, Italy, Ireland, Bulgaria, Israel, France, Cyprus
CADEX Central Asian Dust Experiment	S.U. Umarov Physical-Technical Institute, Dushanbe, Republic of Tajikistan
CAREBeijing-North China Plain Air Quality Research in Beijing	China, France, UK, USA, Germany
CARIBIC/AGOS Civil Aircraft for Remote Sensing and In situ measurement in Tropospheric and Lower Stratosphere based on the Instrumentation Container Concept	Germany, UK, France, The Netherlands, Switzerland, Sweden
CARRIBA Cloud, Aerosol, Radiation, and turbulence in the trade wind regime over Barbados	Caribbean Institute for Meteorology and Hydrology, Barbados; Meteo France, France; Max Planck Institute for Meteorology; Leipzig Institute for Meteorology (LIM), Leipzig University, Germany
Central European Air Quality Cooperation - Harmonization of aerosol sampling and measurement; exchange of measurement data; comparison of PM transport models	Poland, Czech Republic
ChArMEx / ADRIMED Chemistry-Aerosol Mediterranean Experiment / Aerosol Direct Radiative Impact on the regional climate in the Mediterranean region	France, Italy, Germany
CLOUD Cosmics Leaving Outdoor Droplets	Germany, Switzerland, Finland, Austria, Portugal, Russia, UK, USA
CLOUD – ITN Cosmics leaving Outdoor Droplets - International Training Network	Germany, Switzerland, Finland, Austria, UK
CLOUD – train Cosmics leaving Outdoor Droplets - International Training Network	Germany, Switzerland, Finland, Austria, UK
COMPoSE Characterization of phase-partitioning in mixed-phase clouds	Brookhaven National Laboratory (BNL), Upton, NY, USA; McGill University, Montréal, QC, Canada
Cooperation partners involved in research projects at the TROPOS Research Station Melpitz	Norway, UK, Italy, Switzerland, Czech Republic, Hungary, Ireland, Finland, Austria, Sweden, Bulgaria, Belgium, France, Greece, The Netherlands, Spain, Denmark, Latvia, Poland, Portugal
COST Chemistry transport model intercomparison	Germany, Denmark, Finland, France, Bulgaria, Estonia, Italy, Malta, Spain, The Netherlands, Norway, Poland, Switzerland, UK, Greece, Israel

Appendices: Cooperations

Research project	Cooperation partners
Development and evaluation of methods for the quantification of trace compounds produced by biomass burning	Academy of Science of Taipei, Taiwan
EARLINET European Aerosol Research Network	Germany, Italy, Spain, Greece, Switzerland, Sweden, Portugal, Poland, Belarus, France, Bulgaria, Romania, Norway, The Netherlands, Finland, Ireland, Cyprus
ESA-ADM European Space Agency, Atmospheric Dynamics Mission	European Space Research and Technology Center (ESTEC), The Netherlands
ESA-EarthCARE European Space Agency, Earth Clouds, Aerosol and Radiation Explorer	European Space Research and Technology Center (ESTEC), The Netherlands; Japan Aerospace Exploration Agency, Japan
HCCT 2010 Hill Cap Cloud Thuringia 2010	Germany, UK, France, USA, Switzerland
Heterogeneous ice and salt crystallisation in aqueous electrolyte and polymeric solutions	State University St. Petersburg, Russia; University of Rostock; Leibnitz Institute for Baltic Sea Research Warnemünde (IOW), Germany; Institute of Thermomechanics AS, Czech Republic; University of Odessa, Ukraine; Kharkov Institute of Technology, Ukraine
IAPOS Integration of routine Aircraft measurements into a Global Observing System	Germany, UK, France
ICON-HAMMOZ development Model development	Max Planck Institute for Meteorologie, Hamburg, Germany; ETH Zurich; Institute for Atmospheric and Climate Science, Zurich, Switzerland
IGAS IAPOS for the GMES Atmospheric Service, EU project	Germany, UK, France, The Netherlands, Hungary, Switzerland (WMO)
Intercomparison of Satellite Derived Wind Observations	EUMETSAT, Darmstadt, Germany
ITARS - ITN Initial Training for Atmospheric Remote Sensing - Marie Curie Initial Training Network	Germany, Spain, Italy, UK, The Netherlands, Romania, France
Laboratory investigations in the field of liquid phase chemistry	National Institute of Chemistry Ljubljana, Slovenia; Université de Lyon; Université de Marseilles, France; Semenov Institute of Chemical Physics, Moscow, Russia
LACCT Leipzig Aerosol Cloud Turbulence Tunnel	Ilmenau University of Technology, Germany; Michigan Technological University, Houghton, USA
LACIS Leipzig Aerosol Cloud Interaction Simulator	USA, UK, Denmark, Germany, Finland, Austria, Switzerland

Appendices: Cooperations

Research project	Cooperation partners
Lagrangian turbulence in clouds	Max Planck Institute for Dynamics and Self-Organization, Göttingen; Ilmenau University of Technology, Germany; Michigan Technological University, USA; University of Warsaw, Poland
LEAK Leipziger Aerosolkammer	University of British Columbia, Dept. of Chemistry, Canada; University College Cork, Ireland; Slovenia, Institute of Chemistry, Slovenia
LIVAS Lidar Climatology of Vertical Aerosol Structure for Space-Based Lidar Simulation Studies	Institute for Space Applications and Remote Sensing, National Observatory of Athens, Greece; Institute of Methodologies for Environmental Analysis of the National Research Council of Italy (IMAA-CNR), Potenza, Italy
MACE Manila Aerosol Characterization Experiment	De La Salle University, Manila, Philippines
Melpitz Column 2015: Charaterization of aerosol particles and their properties in the column above the research station Melpitz	Germany, Switzerland, Greece
Mobile Landstation Determining aerosol and cloud microphysical processes at distinct land-based sites	Meteorological Observatory Lindenberg of DWD (Deutscher Wetterdienst); University of Cologne, Germany; Delft University of Technology, Delft, The Netherlands
Mobile Seestation Autonomous measurement plattform for the determination of energy and material exchange between ocean and atmosphere	Helmholtz Centre for Ozean Research Kiel (GEOMAR); Alfred Wegener Institute for Polar and Marine Research (AWI), Bremerhaven; Leipzig Institute for Meteorology, University Leipzig (LIM); Max Planck Institute for Meteorology, Hamburg; University of Hamburg, Germany; Nationales Observatorium Athen, Greece
Ocean Science Center Mindelo (OSCM)	Instituto Nacional de Desenvolvimento das Pescas (INDP), Mindelo, S. Vicente, Republic of Cape Verde; Helmholtz Centre for Ozean Research Kiel (GEOMAR), Germany
PAREST PArtikel-REduktions-STrategien	Germany, The Netherlands
PEGASOS Pan-European Gas-AeroSOLIs-climate interaction Study	>20 partners
Pollynet Collaboration in the development and application of Polly systems	Finnish Meteorological Institute (FMI), Kuopio, Finland; Department of Applied Environmental Science (ITM), Stockholm University, Sweden; Institute of Geophysics, University of Warsaw, Poland; Universidade de Évora, Centro de Geofísica de Évora, Portugal; National Institute of Environmental Research, Air Quality Research Division, Korea; National Observatory of Athens, Greece

Appendices: Cooperations

Research project	Cooperation partners
PRADACS Puerto Rico African Dust And Cloud Study	Germany, Puerto Rico, USA, Switzerland, Mexico, Brazil
Relations between directly emitted wood burning emissions and ambient particle concentration in the Melbourne region	Commonwealth Scientific and Industrial Research Organization (CSIRO), Melbourne, Australia
SOPRAN Surface Ocean Processes in the Anthropocene Cape Verde	Instituto Nacional de Desenvolvimento das Pescas (INDP); National Institute for Meteorology and Geophysics (INMG), Mindelo, S. Vicente, Republic of Cape Verde; University of York, UK; Hebrew University of Jerusalem, Israel
Submicrometer particle size distribution processes across the European continent	National Centre for Atmospheric Science, University of Birmingham, UK; Institut de Ciències del Mar, Barcelona, Spain; Department of Physics, University of Helsinki, Finland
Theory of Ice and Salt Crystallization in Aqueous Electrolyte and Polymeric Solutions	Georgia Institute of Technology, Atlanta, Georgia; SUNY at Buffalo, Buffalo, NY, USA; IAWPS International Association for the Properties of Water and Steam; Institute for Thermal Physics, Ekaterinburg; Joint Institute for Nuclear Research Dubna; St. Petersburg State University, Saint Petersburg, Russia
Twinning Partnership with GAW-Stations	Korean Meteorological Service; Global Atmosphere Watch (GAW), Anmyeon, Republic of Korea; Malaysian Meteorological Service, Danum Valley, Malaysia; Bulgarian Academy of Sciences, BEO-Moussala, Bulgaria
UFIREG - ultrafine particles & health	Germany, Czech Republic, Slovenia, Ukraine
Ultraschwarz - ultrafine particle exposure	Germany, Czech Republic

National cooperations

Research project	cooperation partners
Absorption efficiency of Black Carbon: determining representative atmospheric values and implications for radiative transfer	Max Planck Institute for Chemistry, Mainz
ACRIDICON Aerosol, Cloud, Precipitation, and Radiation Interactions and Dynamics of Convective Cloud System	11 partners
ACTRIS-D Aerosols, Clouds, and Trace gases Research InfraStructure Network	13 partners

Appendices: Cooperations

Research project	cooperation partners
AirShield (BMBF joint project) Airborne remote sensing for hazard inspection by network enabled lightweight drones	8 partners
ALADINA Investigating the Small-Scale Vertical and Horizontal Variability of the Atmospheric Boundary Layer Aerosol using Unmanned Aerial Vehicles	TU Braunschweig; University of Tübingen
CARIBIC-AMS (An Automated Aerosol Mass Spectrometer for the Regular Chemical Characterization of Aerosol Particles in the Upper Troposphere and Lowermost Stratosphere, DFG)	Max Planck Institute for Chemistry, Mainz
CLOUD-12 (BMBF-Project)	Goethe University Frankfurt am Main
Colrawi Combined Observations with Lidar Radar and WInd profiler	Deutscher Wetterdienst (DWD), Lindenberg
DFG-SPP HALO Conception and development of a HALO data base	World Data Center for Climate; Max Planck Institute for Meteorology, Hamburg; German Aerospace Center (DLR), Oberpfaffenhofen
DWD-Raman-Lidar	Deutscher Wetterdienst (DWD), Offenbach; Meteorological Observatory Lindenberg of DWD (Deutscher Wetterdienst); Loritus GmbH, Munich
Experimental verification of the charging of aerosol particles by X-ray radiation	Institute for Polymer Materials and Processes (PMP), University of Paderborn
Experimental characterization of agriculture dust emissions	Leibniz Centre for Agricultural Landscape Research (ZALF), Institute of Soil Landscape Research, Müncheberg; TU Braunschweig, Section of Climatology and Environmental Meteorology
F-Beach (Fichtelgebirge – Biogenic Emission and Aerosol Chemistry)	University of Bayreuth; Johannes Gutenberg University Mainz
GUAN German Ultrafine Aerosol Network	Federal Environment Agency (UBA), Dessau-Roßlau, Langen, Garmisch-Partenkirchen, Hofsgrund; Deutscher Wetterdienst (DWD), Hohenpeißenberg; IUTA Duisburg e. V.; Helmholtz Zentrum München - German Research Center for Environmental Health
Hans Ertel Zentrum for Weather Research	Deutscher Wetterdienst (DWD), Offenbach; University of Bonn
HD(CP)2 (BMBF) High definition clouds and precipitation for advancing climate prediction	16 partners

Appendices: Cooperations

Research project	cooperation partners
High-resolution modelling of clouds and gravity wavelengths: scale analysis, numerics, validation (Leibniz competition project)	Leibniz Institute of Atmospheric Physics, Rostock; Potsdam Institute for Climate Impact Research (PIK), Potsdam
IAGOS-D (In-situ Aircraft for a Global Observing System)	Forschungszentrum Jülich; Karlsruhe Institute of Technology (KIT); Max Planck Institutes for Chemistry and Biogeochemistry, Jena; German Aerospace Center (DLR); University of Heidelberg
ICOS (Integrating Cloud Observations from Ground and Space – a Way to Combine Time and Space Information)	University of Cologne; Freie Universität Berlin
INFECTIONS'21 (Leibniz) Transmission Control of Infections in the 21st Century	14 partners
INIUT (DFG Research Unit) Ice Nuclei Research Unit	Max Planck Institute for Chemistry, Mainz; Goethe University Frankfurt am Main; TU Darmstadt; Johannes Gutenberg University Mainz; University Bielefeld; Karlsruhe Institute of Technology (KIT)
Ion particle interactions during particle formation and growth above coniferous forest in Middle Europe	University of Bayreuth, BayCEER, Atmospheric Chemistry
Influence of domestic wood stoves on particulate concentrations in rural areas of Saxony	Saxon State Ministry of the Environment and Agriculture, Dresden
KLENOS Influence of a change of energy policy and climate on air quality as well as consequences for the compliance with limit values and examining further emissions	Federal Environment Agency (UBA), Dessau-Roßlau; TU Dresden, Institute of Hydrology and Meteorology
Leibniz Network “Mathematical Modeling and Simulation (MMS)”	24 partners
MARGA Physico-chemical characterization of the dynamic behaviour of ammonium salt in particulate matter aerosol particles - testing a new high-resolutions measurement method at EMEP-Level 3-Station Melpitz	Federal Environment Agency (UBA), Dessau-Roßlau
ML-CIRRUS Mid-Latitude Cirrus	10 partners
PalMod (BMBF) From the Last Interglacial to the Anthropocene: Modeling a Complete Glacial Cycle	17 partners

Appendices: Cooperations

Research project	cooperation partners
Parallel coupling framework and modern time integration methods for detailed cloud processes in atmospheric models	TU Dresden, Centre for Information Services and High Performance Computing (ZIH); Martin Luther University Halle-Wittenberg
Pollynet	Deutscher Wetterdienst (DWD), Hohenpeißenberg
Photocatalytic facades in cooperation with LWB (Leipzig housing cooperative)	MFPA Leipzig GmbH; Leipzig Institute for Materials Research and Testing; funded by the Leipziger Wohnungs- und Baugesellschaft (LWB)
Influence of soot on air quality and climate (pilot study)	Saxon State Agency for Environment, Agriculture and Geology (LfULG)
SALTRACE Saharan Aerosol Long-range Transport and Aerosol-Cloud-Interaction Experiment	German Aerospace Center (DLR) Oberpfaffenhofen; Ludwig Maximilian University, Munich; TU Darmstadt
SOPRAN (BMBF) Surface Ocean Processes in the Anthropocene	8 partners
Statistical modelling of aerosol particle size distribution in urban and rural environment	TU Braunschweig, Institute of Geoecology, Dept. of Climatology and Environmental Meteorology
Theory of ice and salt crystallisation in aqueous electrolyte and polymeric solutions	Polymer Physics, University of Rostock; Leibnitz Institute for Baltic Sea Research Warnemünde (IOW)
Deep analysis to verify the effectiveness of the Leipzig Low Emission Zone	Saxon State Agency for Environment, Agriculture and Geology (LfULG)
Improvement of data quality for the measurement of ultrafine particles in the outdoor air	Saxon State Agency for Environment, Agriculture and Geology (LfULG)

Boards

Boards of trustees

Name	Institution
RORin C. Liebner	Saxon State Ministry for Science and the Arts
RDin Dr. G. Helbig	Federal Ministry of Education and Research
Prof. Dr. S. Borrmann	Max Planck Institute for Chemistry (Otto Hahn Institute); Johannes Gutenberg University Mainz

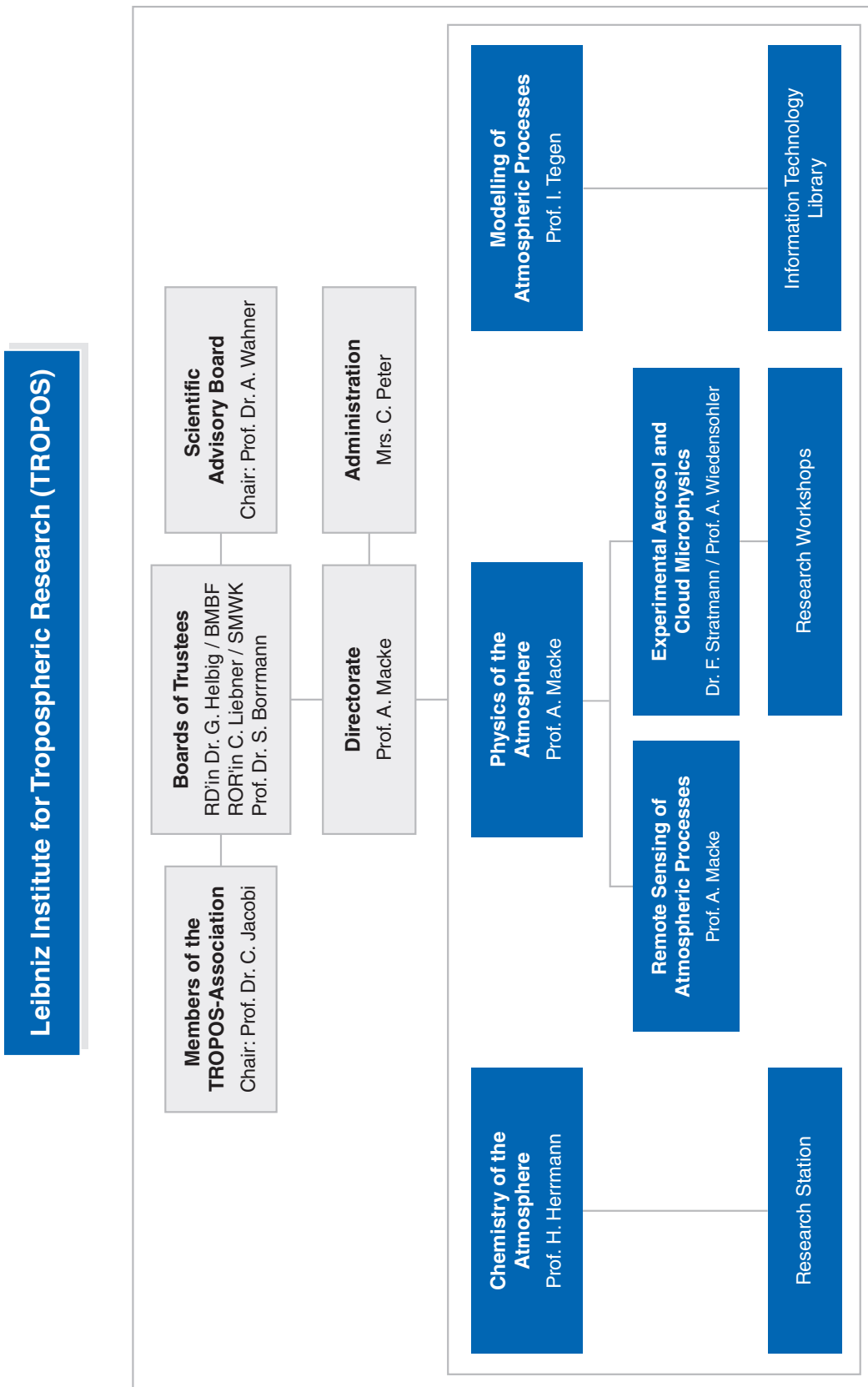
Scientific advisory board

Name	Institution
Prof. Dr. A. Wahner (Chairman)	Forschungszentrum Jülich GmbH; Institute for Energy and Climate Research, IEK-8: Troposphere
PD Mag. Dr. F. H. Berger	Deutscher Wetterdienst (DWD), Lindenberg Meteorological Observatory - Richard Aßmann Observatory
Prof. Dr. A. Bott	University of Bonn, Meteorological Institute
Dr. G. Ehret	German Aerospace Center (DLR), Institute of Atmospheric Physics, Lidar
Dr. C. George	IRCELYON - Institut de Recherches sur la Catalyse et l'Environnement de Lyon, University Claude Bernard
Prof. Dr. M. Kulmala	University of Helsinki, Department of Physics
Prof. Dr. J. Orphal	Karlsruhe Institute of Technology (KIT), Institute for Meteorology and Climate Research (IMK)
Prof. Dr. K. H. Schlünzen	University of Hamburg, Institute for Meteorology, KlimaCampus
Prof. Dr. R. Shaw	Michigan Technological University, Department of Physics
Prof. Dr. M. Wendisch	Leipzig University, Leipzig Institute for Meteorology (LIM)

Appendices: Boards

Members of the TROPOS association

Name	Institution
Prof. Dr. C. Jacobi (Chairman)	Leipzig University, Leipzig Institute for Meteorology (LIM)
Frau RORin C. Liebner	Saxon State Ministry for Science and the Arts
Frau RDin Dr. G. Helbig	Federal Ministry of Education and Research
Prof. Dr. P. Warneck	Professor emeritus
Prof. Dr. B. Brümmer	University of Hamburg, Institute for Meteorology
Prof. Dr. J. Quaas	Leipzig University, Leipzig Institute for Meteorology (LIM)
Dr. H.-H. Richnow	Helmholtz Centre for Environmental Research (UFZ)
Prof. Dr. B. Abel	Leipzig University, Wilhelm Ostwald Institute for Physical and Theoretical Chemistry
Prof. Dr. C. Simmer	Rhineland Friedrich Wilhelm University Bonn, Institute for Meteorology
Prof. Dr. W. Engewald	Leipzig University, Faculty for Chemistry and Mineralogy
Prof. Dr. E. Renner, honorary member	Professor emeritus
Prof. Dr. J. Heintzenberg, honorary member	Professor emeritus



TROPOS

Leibniz Institute for Tropospheric Research
Leibniz-Institut für Troposphärenforschung e.V. Leipzig
Member of the Leibniz Association (WGL)

Permoserstraße 15
04318 Leipzig
Germany

Phone: ++49 (341) 2717-7060
Fax: ++49 (341) 2717-99-7060
Email: info@tropos.de
Internet: <http://www.tropos.de>